

**Characterising metabolic deficits in sporadic and
familial Alzheimer's disease to identify new
therapeutic targets**

Simon Michael Bell

BSc(Hons), MB ChB, PG Dip(Health Research), MRCP

Department of Neuroscience

September 2020

A thesis submitted to the

University of Sheffield

for the degree of

Doctor of Philosophy

One never notices what has been done; one can only see what remains to be done.

Professor Marie Curie, November 7, 1867 - July 4, 1934

Contents

Acknowledgements.....	8
Abstract.....	9
Abbreviations.....	10
List of Figures.....	14
List of Tables.....	16
Chapter 1: Introduction.....	18
1.1 Alzheimer’s disease and Dementia.....	18
1.2 Alzheimer’s disease pathology.....	18
1.2.1 Amyloid Cascade Hypothesis.....	22
1.3 Clinical Features of Alzheimer’s disease and diagnosis.....	25
1.4 Diagnosis of Alzheimer’s disease.....	26
1.5 Treatment options for Alzheimer’s disease.....	27
1.6 Therapeutic challenges in AD.....	28
1.7 Metabolism and Alzheimer’s disease.....	29
1.8 Mitochondrial Structure and Function.....	29
1.8.1 Mitochondrial ATP generation and the electron transport chain.....	29
1.8.2 Mitochondrial control of Cellular Calcium.....	34
1.8.3 Reactive oxygen species and mitochondria.....	37
1.8.4 Mitophagy and cell death.....	39
1.9 Mitochondrial changes seen AD.....	41
1.9.1 Electron Transport Chain Disruption in AD.....	41
1.9.2 Mitochondrial Calcium Signaling in AD.....	46
1.9.3 Mitochondrial ROS production in AD.....	47
1.9.4 Mitophagy and cell death in AD.....	49
1.9.5 Mitochondrial Trafficking in AD.....	50
1.9.6 Mitochondrial abnormalities in AD Summary.....	51
1.10 Glycolysis.....	53
1.11 Glycolysis in AD.....	54
1.11.2 Changes to glycolysis in AD.....	54
1.11.3 Changes to the pentose phosphate shunt in AD.....	57
1.11.4 Glycolysis in AD summary.....	58
1.12 Other metabolic pathways affected in AD.....	58
1.12.1 Malate-Aspartate shunt.....	58
1.12.2 Fatty acid metabolism.....	58
1.13 Metabolic cooperation within the brain.....	59

1.14 The astrocyte in AD.....	61
1.14.1 The astrocyte and glucose storage in AD.....	64
1.14.2 Astrocyte AD summary	65
1.15 Inducible pluripotent stem cell models of Neurodegenerative disease.....	66
1.15.1 iPSC Models of Alzheimer’s Disease	67
1.15.2 iPSC AD Neurons	67
1.15.3 iPSCs AD Astrocytes	70
1.15.4 iPSC Summary and iNPC research.....	72
1.16 Introduction Summary	73
1.17 PhD Hypothesis, Aims and Objectives	74
1.17.1 Aims and Objectives:.....	74
Chapter 2: Methods	75
2.1 Materials	75
2.2 Methods.....	75
2.2.1 Patient selection and characterisation	75
2.2.2 Skin biopsy	76
2.2.3 Skin Biopsy set up and fibroblast culture.....	76
2.2.4 Freezing Down Fibroblasts/iNPCs	77
2.2.5 Fibroblast reprogramming	77
2.2.6 iNPC differentiation into Astrocytes	78
2.2.7 Immunohistochemistry	79
2.2.8 ATP Assay	80
2.2.9 Mitochondrial Membrane Potential Assay	80
2.2.10 Lactate Assay.....	81
2.2.11 Mitochondrial Stress Test Assay	82
2.2.12 Glycolysis Assay.....	82
2.2.13 ATP Substrate Assay.....	83
2.2.14 Bradford Assay	84
2.2.15 Glutamine/Glutamate Assay.....	84
2.2.16 Quantitative Polymerase Chain Reaction (qPCR)	85
2.2.17 Glucose Uptake Assay	85
2.2.18 Glutamate Uptake Assays	86
2.2.19 Drug Treatment Assays	87
2.2.20 MRI Acquisition	87
2.2.21 Neuropsychology testing	87
2.3 Statistical analysis	88

2.4 Media Constituents.....	89
Chapter 3: Ursodeoxycholic Acid improves mitochondrial function and redistributes Drp1 in fibroblasts from patients with either sporadic or familial Alzheimer's disease	94
3.1 Introduction	94
3.1.2 Mitochondrial Fission and Fusion	94
3.1.3 Apoε gene and its effect on metabolism in AD.....	95
3.1.4 Assessment of oxidative phosphorylation using the seahorse XF analyser	96
3.1.5 Reason for presenting additional results.....	97
3.1.6 Published Paper contributions by PhD Candidate	98
3.2 Published Paper	99
3.3 Additional results	100
3.3.1 Mitochondrial fusion mRNA is not changed in sporadic or familial AD fibroblasts.....	101
3.3.2 Fibroblasts with the ApoE ε4/4 genotype have a more severe mitochondrial morphology disease phenotype	102
3.3.3 Fibroblasts with the ApoE ε4/4 have reduced levels of ATP which can be corrected with the application of UDCA.....	107
3.3.4 All sporadic AD fibroblasts independent of ApoE genotype have a deficit in mitochondrial spare respiratory capacity.....	107
3.3.5 Mitochondrial Spare Respiratory Capacity was the only element of the Mito Stress test to show differences between AD and control fibroblasts	111
3.4 Discussion.....	112
3.4.1 Mitochondrial morphology is altered in AD.....	112
3.4.2 Fibroblasts with ApoE ε4/4 genotype produce less ATP and have altered mitochondrial morphology.....	113
3.4.3 All Fibroblasts independent of ApoE genotype have a decreased mitochondrial spare respiratory capacity	114
3.4.4 Study limitations	115
3.5 Chapter Conclusions	116
Chapter 4: Deficits in Mitochondrial Spare Respiratory Capacity Contribute to the Neuropsychological Changes of Alzheimer’s Disease.....	117
4.1 Introduction	117
4.1.1 Structural Neuroimaging changes in AD	117
4.1.2 Neuropsychological changes in early AD	118
4.1.3 The Default Mode Network	119
4.1.4 Assessment of glycolysis using the Agilent XF seahorse analyser	120
4.1.4 Reasoning for additional results	121
4.1.5 Published Paper contributions by PhD Candidate	122
4.2 Published Paper	123

4.3 Additional results	124
4.3.1 No significant difference was seen in glycolytic parameters based on fibroblast ApoE genotype	125
4.3.2 Sporadic AD fibroblasts use OxPHOS more than glycolysis in a glucose starved state	125
4.3.3 Extracellular Lactate levels are not different in sporadic AD fibroblasts based on ApoE genotype	129
4.3.4 The connectivity of the default mode network is altered in sporadic AD	130
4.3.5 Fibroblast spare capacity correlates with Bilateral pre-frontal cortex connectivity	132
4.3.6 Fibroblast MMP correlates with Bilateral Posterior Cortex Connectivity.....	134
4.4 Discussion.....	136
4.4.1 Fibroblasts from sporadic AD patients have reductions in glycolytic capacity and extracellular lactate independent of ApoE genotype.	136
4.4.2 Connectivity of the DMN is altered in sporadic AD	137
4.4.3 Fibroblast spare capacity and MMP correlates with elements of DMN connectivity	138
4.4.4 Chapter Limitations.....	139
4.5 Chapter Conclusions	139
Chapter 5 Astrocytes derived from human fibroblasts show deficits in both mitochondrial function and glucose metabolism in sporadic and familial Alzheimer’s disease	141
5.1 Introduction	141
5.1.2 Induced neuronal progenitor cell (iNPC) reprogramming	141
5.1.3 Selection of drugs assessed in chapter paper.....	142
5.1.4 Reasoning for additional results	143
5.1.5 Candidates paper contributions.....	143
5.2 Paper in preparation for submission	144
5.2.1 Abstract.....	145
5.2.2 Highlights	145
5.2.3 Research In Context.....	145
5.2.4 Background	146
5.2.5 Methods.....	148
5.2.6 Results.....	155
5.2.6 Discussion.....	182
5.2.1 The AD astrocyte metabolic phenotype	182
5.2.2 Astrocyte metabolism correlations with neuropsychological changes	185
5.2.3 Small molecule compounds correct astrocyte metabolic deficits.....	186
5.2.7 Conclusions	187
5.2.8 Supplementary figures.....	187
5.3 Additional results	192

5.3.1 Total cellular ATP levels are lower in ApoE ϵ 4/4 genotype astrocytes.....	192
5.3.2 Astrocyte glycolytic and mitochondrial abnormalities are independent of ApoE genotype	192
5.3.3 Extracellular lactate levels correlate with DMN connectivity changes.....	196
5.3.4 Astrocytes derived using the iNPC method maintain an aged phenotype	198
5.4 Discussion.....	200
5.4.1 ApoE genotype does not differentiate all metabolic abnormalities in AD sporadic Astrocytes, but may influence ATP levels	200
5.4.2 Extracellular lactate levels correlate with connectivity of the DMN	201
5.4.3 Astrocyte deficits are more pronounced in galactose-based media	201
5.4.4 Astrocytes have an aged phenotype based on RNA expression.....	202
5.5 Chapter limitations	202
5.6 Chapter Conclusions	203
Chapter 6 Discussion.....	205
6.1 Fibroblasts and Astrocytes have similar mitochondrial and glycolytic abnormalities in sporadic and familial AD.....	205
6.2 Astrocyte changes seen in other iNPC/iPSC models of neurodegenerative disease.....	208
6.3 Mitochondrial dysfunction and its importance to AD	209
6.4 Glycolytic dysfunction and its importance to AD.....	211
6.5 ApoE genotype may contribute to mitochondrial and glycolytic impairment in AD.....	213
6.6 Developing a metabolic biomarker for AD	213
6.7 Metabolism as a target for therapeutic intervention in AD	215
6.8 Further Directions	217
6.9 Final Conclusion	218
References	219

Acknowledgements

Over the past 4 years I have been supported by several research charities to which I am eternally grateful. The charities are the Wellcome 4ward North Research Academy (Grant Number: 216340/Z/19/Z), The National Institute of Health Research Sheffield Biomedical Research Centre, and Alzheimer's Research UK Yorkshire Network Centre Small Grant Scheme (Ref: ARUK-PCRF2016A-1). I have also been supported by an Alzheimer Research UK preparatory grant in the work that led up to the development of this PhD thesis.

I wanted to start this thesis with a quote from Professor Curie who was a visionary scientist, mother, and wife who changed our understanding of the world on multiple levels. I have been fortunate enough throughout my life to have been influenced by many women who have similarities with Professor Curie. My supervisors, Dr Heather Mortiboys, Dr Laura Ferraiuolo and Professor Dame Pamela Shaw have given me the scientific skills needed to perform, critic and analyse the data needed to complete this PhD. Professor Annalena Venneri has been both a trusted advisor for my research and fundamental influence in my understanding of Alzheimer's disease. Without their many hours of support I would not be the researcher I am today. My mother Marjorie Bell who has given me the determination and perseverance skills needed to be a clinical academic, My sister Katie Bell who has often prevented episodes of doubt with well-placed jibes. My wife Dr Sarah Jones who has had to listen to multiple research presentations, read many a first draft and pick me up when things haven't gone to plan in the lab, and my daughter Grace Bell, who has been a smiling loving presence in my life, and always forgives me for missed times at the park while I work on my research.

I will always be in the debt of my supervisor Dr Daniel Blackburn who took me under his wing nearly 6 years ago. With his constant support and guidance both clinically and scientifically, he has guided me through the challenges of being a clinical academic. Dr Matteo De Marco has spent many hours developing my knowledge of both statistical methods and neuropsychological tests which has made me a better scientist, and I also need to acknowledge Professor Tim Chico, my pastoral supervisor, for his excellent advise both on funding, doing a PhD and life in general.

Finally, I would like to acknowledge my Great Aunt Jennie Watson and her husband Victor Watson, who represent the people and families of people with Alzheimer's disease. Watching her change whilst living AD, and how this effected both her and her husband, has made me want to devote my career to fighting dementia and stopping this disease effecting future generations. Hopefully, this PhD will help in some way to achieve this aim.

Abstract

Introduction: Alzheimer's disease (AD) is the most common form of dementia with amyloid and tau aggregation central to disease pathology. Mitochondrial function and glycolysis changes are seen early in the disease. Understanding metabolic changes in the nervous system and peripherally will help develop new AD therapies. This thesis investigates how metabolism in peripheral patient fibroblasts and astrocytes derived from these fibroblasts is affected in AD and its therapeutic and biomarker potential.

Methods: Fibroblasts were taken from sporadic or familial (Presenilin 1 mutation) AD patients and controls. Mitochondrial structure, function, and glycolysis was assessed. The same fibroblasts were reprogrammed into induced neuronal progenitor cells and subsequently astrocytes. Mitochondrial and glycolytic function was assessed in the astrocytes. Metabolic changes were correlated with clinical features of AD and astrocytes were treated with drugs known to improve mitochondrial function.

Results: Sporadic fibroblasts had a more interconnected mitochondrial network, lower mitochondrial membrane potential and lower mitochondria spare respiratory capacity (MSRC). Similar changes were seen in familial fibroblasts but MSRC was not reduced. Sporadic and familial AD astrocytes had reductions in total ATP, reduced MSRC, and a more interconnected mitochondrial network. Apo ϵ 4/4 phenotype worsened ATP deficits in sporadic fibroblasts and astrocytes. MSRC correlated with clinical markers of AD in both sporadic astrocytes and fibroblasts. Deficits in total ATP and mitochondrial structure were partially corrected by treatment with known mitochondrial enhancers.

Discussion: This thesis is one of the first to show that metabolic deficits in both astrocytes and fibroblasts correlate with clinical features of AD. It highlights that astrocytes from sporadic and familial AD patients have impaired metabolism, which can be corrected, and potentially used as a biomarker of the future. This thesis has shown the importance of studying metabolism in AD, and further highlights astrocyte metabolism as potentially a key factor in the development of AD.

Abbreviations

Abeta-binding alcohol dehydrogenase	ABAD
Adenine Nucleotide Translocator	ANT
Adenosine Diphosphate	ADP
Adenosine Triphosphate	ATP
Alzheimer's disease	AD
Amyloid Beta Protein	A β
Amyloid Plaques	AP
Amyloid Precursor Protein	APP
Astrocyte neuron lactate shuttle	ANSL
Blood Brain Barrier	BBB
Blood Oxygenation Level Dependent	BOLD
Bridging integrator 1	B1N1
Carbonyl cyanide-4-(trifluoromethoxy) phenylhydrazone	FCCP
Central nervous system	CNS
Cerebro-Spinal Fluid	CSF
Clustered Regularly Interspaced Short Palindromic Repeats	CRISPR
Clusterin	CLU
Complement receptor 1	CRI
Computed Tomography	CT
Cyclophilin D	CypD
Default Mode Network	DMN
Deoxyribonucleic Acid	DNA
Down's Syndrome	DS
Dimethyl sulfoxide	DMSO
Dulbecco's Modified Eagle Medium	DMEM
Dynamin-related protein	Drp1
Eagle's Minimum Essential Medium	EMEM
Electron Transport Chain	ETC
Endoplasmic Reticulum	ER

Epidermal growth factor	EGF
Ephrin type-A receptor 1	EPHA1
Extracellular acidification rate	ECAR
Fibroblast growth factor beta	FGF-b
Flavin mononucleotide	FMN
Fluoro-2-Deoxy-D-glucose	FDG
Genome Wide Association Studies	GWAS
Glial fibrillary acidic protein	GFAP
Glucose transporters 1 and 2	GLUT1 & 3
Glyceraldehyde-3-phosphate dehydrogenase	G3PDH
Hanks' Balanced Salt solution	HBSS
Hexokinase	HK
Hypoxia-inducible factor-1alpha	HIF-1alpha
Induced neuronal progenitor cell	iNPC
induced pluripotent stem cell models	iPSC
inositol-1,4,5-triphosphate receptor-voltage-dependent anion channel	IP3R3-VDAC
Lactate dehydrogenase	LDH
Laminin subunit alpha 3A	LAMA3A
Long-term depression	LTD
Long-term potentiation	LTP
Malate-aspartate shunt	MAS
Magnetic Resonance imaging	MRI
Membrane-spanning 4-domains, subfamily A	MS4A
Mild Cognitive Impairment	MCI
Mini Mental State Examination	MMSE
Mitochondrial calcium uniporter	MCU
Mitochondrial Deoxyribonucleic acid	mtDNA
Mitochondrial dynamics protein 49	MiD49
Mitochondrial dynamics protein 51	MiD51
Mitochondrial fission factor	Mff
Mitochondrial fission 1 protein	Fis1

Mitochondrial Membrane Potential	MMP
Mitochondrial Permeability Transition Pore	MPTP
Mitochondrial Spare Respiratory Capacity	MSRC
Mitofusin 1	Mfn1
Mitofusin 2	Mfn2
Monoclonal Antibody	MAB
Motor Neuron Disease	MND
Neurofibrillary Tangles	NFT
Nicotinamide Adenine Dinucleotide	NAD
Nicotinamide adenine dinucleotide phosphate	NADPH
Non-Steroidal Anti-inflammatory Drugs	NSAIDs
Optic atrophy 1	Opa1
Oxidative phosphorylation	OxPHOS
Oxygen Consumption Rate	OCR
P1 P5-di(adenosine) pentaphosphate	PPAP
Parkinson's disease	PD
PBS and TWEEN20	PBST
Pentose phosphate shunt	PPS
Phosphate Buffered Saline	PBS
Phosphatidylinositol binding clathrin assembly protein	PICALM
Phosphofructokinase	PFK
Polyglucosan bodies	PGB
Positron-emission tomography	PET
Post-mortem	PM
Presenilin 1	PSEN1
PTEN-induced kinase 1	PINK1
Pyruvate dehydrogenase kinase	PDK
Pyruvate kinase	PK
Quantitative Polymerase Chain Reaction	qPCR
RAN binding protein 17	RanBP17
Reactive Oxygen Species	ROS

Single Nucleotide Polymorphisms	SNP
Sodium/calcium exchanger	NCX
Sporadic Alzheimer's disease	sAD
Superoxide ion	$O_2^{\bullet-}$
Telomeric repeat-binding factor 2	TERF2
Tetramethylrhodamine	TMRM
Tricarboxylic acid enzymes	TCA
Triggering receptor expressed on myeloid cells 2	TREM2
United Kingdom	UK
Ursodeoxycholic acid	UDCA
Voltage dependent anion-selective channels	VDAC

List of Figures

Figure 1.1 | The cleavage of the APP protein

Figure 1.2 | The Amyloid Cascade Hypothesis

Figure 1.3 | Mitochondrial structure and ETC changes in the brain in AD

Figure 1.4 | Mitochondrial Calcium Homeostasis

Figure 1.5 | Mitochondrial ROS Production

Figure 1.6 | Mitophagy

Figure 1.7 | Changes to mitochondrial function seen in AD

Figure 1.8 | Glycolysis and other glucose metabolic pathways

Figure 1.9 | Astrocyte neuronal co-operation

Figure 2.1 | Fibroblast Set Up

Figure 2.2 | Fibroblast Reprogramming

Figure 2.3 | ATPlite kit reaction

Figure 3.1 | Mitochondrial Stress Test Seahorse Trace graph

Figure 3.2 | Mitochondrial Fusion protein RNA qPCR results

Figure 3.3 | Mitochondrial morphology results split by sporadic AD fibroblast Apoε genotype

Figure 3.4 | Variance in mitochondrial morphology of control fibroblast based on ApoE genotype

Figure 3.5 | Total cellular ATP and Mitochondrial Spare Respiratory Capacity split by AD fibroblast Apoε genotype

Figure 4.1 | Glycolysis Assessment using the Agilent Glycolysis Stress Test

Figure 4.2 | Fibroblast glycolytic function split based on Apoε genotype and OCAR/ECAR ratios

Figure 4.3 | Glycolytic parameters for sporadic fibroblast controls split based on ApoE genotype

Figure 4.4 | Fibroblast extracellular lactate split on Apoε genotype

Figure 4.5 | DMN connectivity after network compartmentalization

Figure 4.6 | DMN connectivity correlations with MSRC

Figure 4.7 | DMN connectivity correlations with MMP

Figure 5.1 | Astrocyte characterization

Figure 5.2 | Astrocyte and iNPC total cellular ATP |

Figure 5.3 | Astrocyte Mitochondrial Function and Morphology

Figure 5.4 | Astrocyte Oxidative Phosphorylation Assessment

Figure 5.5 | Astrocyte glycolysis assessment

Figure 5.6 | Astrocyte Lactate excretion and Glucose uptake

Figure 5.7 | MSRC and MMP correlations with Neuropsychological tests

Figure 5.8 | Glycolytic reserve and extracellular lactate correlations with Neuropsychological tests

Figure 5.9 | Compound A & B treatment of control, sporadic and familial AD astrocytes

Figure 5.10 | Compound C & D treatment of control, sporadic and familial AD astrocytes

Figure 5.11 | Compound E & F treatment of control, sporadic and familial AD astrocytes

Figure 5.12 | Compound G & H treatment of control, sporadic and familial AD astrocytes

Supplementary Figure 1 | Glucose media Total Cellular ATP

Supplementary Figure 2 | Mitochondrial Morphology Glucose Media

Supplementary Figure 3 | Astrocyte Oxidative Phosphorylation in glucose media

Supplementary Figure 4 | Astrocyte Glycolysis in glucose media

Figure 5.13 | Astrocyte metabolic parameter split via sporadic Apoε genotype

Figure 5.14 | Control Astrocytes separated based on ApoE status

Figure 5.15 | Metabolic DMN correlations

Figure 5.16 | qPCR data for aging related gene expression

List of Tables

Table 1.1| ATN Classification criteria

Table 2.1| DMEM Media

Table 2.2| EMEM Media

Table 2.3| PBS

Table 2.4| iNPC Media

Table 2.5| Astrocyte Media

Table 2.6| Antibodies used for Immunocytochemistry

Table 2.7| Galactose Media

Table 2.8| Seahorse XF media

Table 2.9| Seahorse experiments drug locations

Table 2.10| ATP Substrate Assay Buffer A

Table 2.11| ATP Substrate Assay Complex Mixtures

Table 2.12| qPCR forward and reverse primers

Table 2.13| Glutamate Detection Reagent

Table 2.14| Krebs-Ringer-Phosphate-Hepes (KRPH) buffer (pH 7.4)

Table 2.15| Drugs used in drug treatment assays

Table 3.1| Fibroblast line demographics

Table 3.2| Mitochondrial Stress Test parameters

Table 4.1| Fibroblast line demographics

Table 5.1| Drugs used in chapter and mechanisms of action

Table 5.2| Antibodies used for Immunocytochemistry

Table 5.3| Patient Demographic Information and contemporary treatment status

Table 5.4| Patient demographics for Familial AD presenilin 1 lines and associated controls

Table 5.5| Astrocyte neuropsychological metabolic correlations

Table 5.6| Effects of drug compounds of ATP and mitochondrial morphology

Table 5.7| Aging qPCR cell lines

Chapter 1: Introduction

1.1 Alzheimer's disease and Dementia

Alzheimer's disease (AD) is both the most common neurodegenerative disease and most prevalent form of dementia worldwide[1]. It is calculated that around 50 million people globally have dementia [2, 3], with between 60-80% of cases thought to be due to AD [4]. In 2016 Dementia was the fifth leading cause of death worldwide[1], and in 2018 it was estimated that the total cost of dementia care to the world economy was \$1 Trillion dollars [3].

Two thirds of the people that have dementia live in low and middle income countries [5], which have less developed healthcare systems [6]. This is a particular problem for the future due to the lack of disease modifiable therapies and the high care costs for people with dementia [7].

Increasing age is the biggest risk factor for developing both AD and dementia, but low educational attainment, cardiovascular disease, obesity and diabetes have all been associated with an increased risk of developing dementia[8]. Interestingly, it has been suggested that up to a third of dementia cases could be prevented by amelioration of modifiable risk factors [8].

As AD is by far the most common form of dementia, the vast majority of dementia research has focused on developing treatments for and understanding the underlying mechanisms that lead to people developing this condition.

1.2 Alzheimer's disease pathology

The condition was originally identified in 1906 by the German pathologist and psychiatrist Dr Alois Alzheimer [9, 10]. In his original paper, Alzheimer offered the first description for both extracellular plaques (AP) comprising mainly of the amyloid beta protein (A β); and intracellular neurofibrillary tangles (NFT) made mainly of the cytoskeletal protein tau [11].

A β that contributes to the AP is cleaved by the secretase enzymes from the amyloid precursor protein (APP) in a sequential way. Beta and gamma secretase cleave APP to produce A β (amyloidogenic pathway) and alpha and gamma secretase cleave the protein to produce P3 (non-amyloidogenic pathway). The amyloidogenic pathway can produce several different isoforms of the A β protein, with the most common form found in AP being A β ₁₋₄₂. What causes the AP to develop in AD is unknown. At some point prior to the development of the clinical syndrome the balance between the production of A β and its removal from the brain is altered. Deposition of amyloid within the brain is the leading theory for what is likely to be the key pathological mechanism that leads to the development of AD, and is referred to as the amyloid cascade hypothesis [12-15]. The amyloid cascade hypothesis though has been challenged, as several aspects of the AD clinical

syndrome do not appear to be causally linked with amyloid deposition. It has been shown that the pattern of deposition of AP through the brain does not correlate well with clinical disease severity [16, 17], and several studies have shown that advancing age can often be a better predictor of the AP density than having a diagnosis of AD [18, 19]. Clinical trials of therapeutics that remove amyloid from the brain have not been able to reverse the progression of the disease, which has further questioned if amyloid deposition is the key pathological step in the development of AD [20-22]. Figure 1.1 shows the sequential cleavage pattern and cellular location of APP and its breakdown products. The amyloid cascade hypothesis is discussed in more detail in section 1.2.1

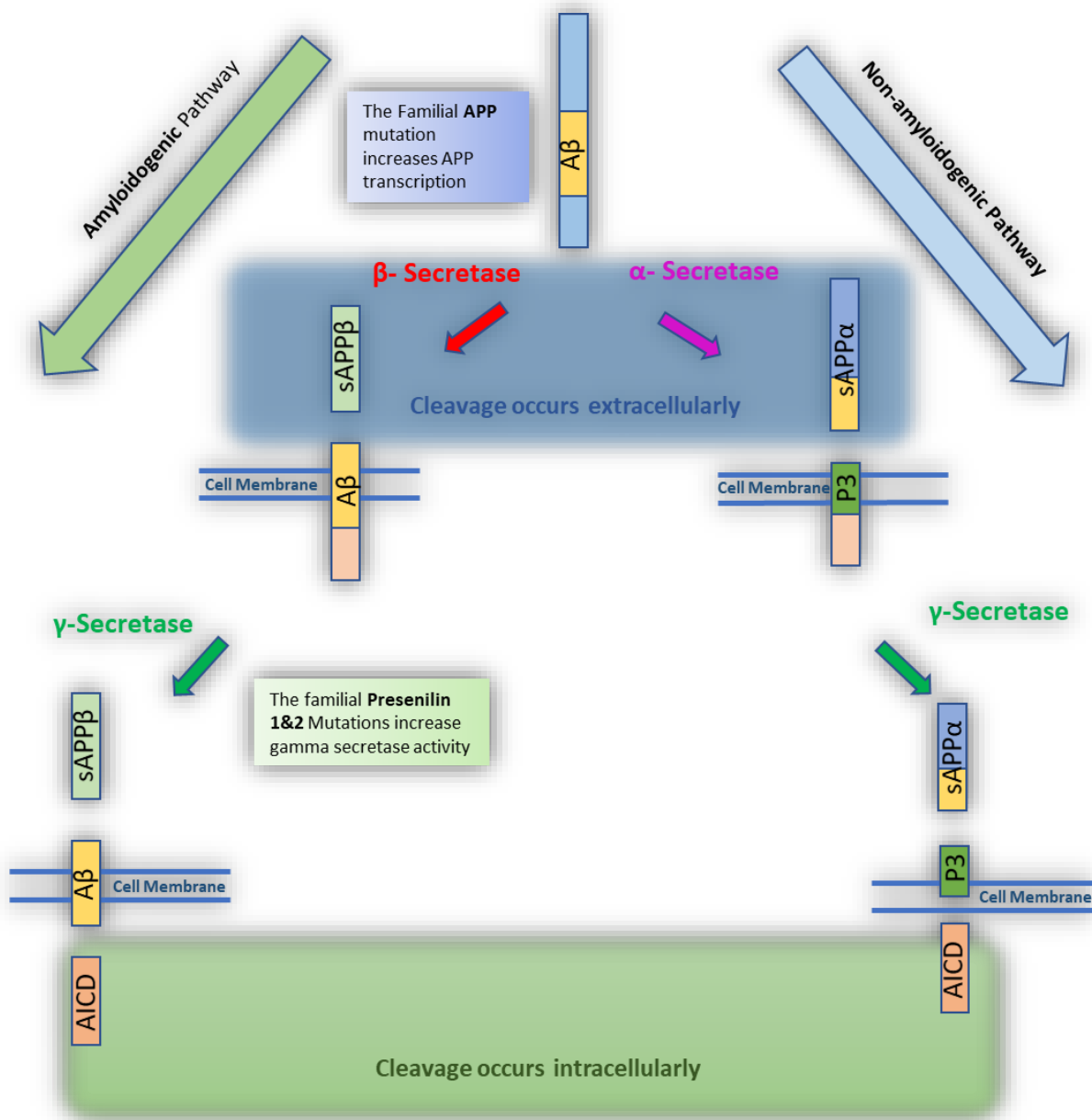


Figure 1.1| The cleavage of the APP protein APP is cleaved via two pathways. Initially the protein is cut by either beta-secretase (amyloidogenic pathway) or alpha-secretase (non-amyloidogenic pathway) and then moves to the cell membrane to be cleaved by gamma-secretase in both pathways. The amyloidogenic pathway generates sAPP α , amyloid-beta (A β) and amyloid precursor protein intracellular domain (AICD). The non-amyloidogenic pathway generates sAPP β , P3 and AICD. Familial forms of AD are caused by either an increase in the production of the APP protein or by increased efficacy of gamma-secretase to cleave the APP protein.

NFT mainly consist of the microtubule-associated protein (MAP) tau [23-25]. NFT development occurs when the tau protein goes through a conformational change in shape caused by either hyperphosphorylation [24], protein C/N-terminal truncation[26], or a combination of both. Unlike the AP deposition, NFT deposition follows a characteristic pattern throughout the brain during the course of AD [16]. The progression of NFT deposits through the brain starts in the medial temporal lobe, and then moves to include the lateral temporal lobes, parietal lobes, frontal lobes and then finally the occipital lobes [16]. This spread of NFT through the brain corresponds to a degree with the neuropsychological manifestations and clinical disease course [27-29]. It is unknown what causes the MAP tau to become hyperphosphorylated, but evidence points towards tau deposition following the development of AP, suggesting that in AD, unlike in other tau mediated neurodegenerative diseases, amyloid deposition is key for tau dysfunction and NFT formation [30].

As well as the accumulation of both NFT and AP another key pathological hallmark of AD is synaptic loss [31-34]. Synaptic loss correlates very closely with the clinical progression of AD, more so than the deposition of AP or NFT [35, 36]. Synaptic loss is not fully explained by the accumulation of NFT and AP [36], but several animal models in which amyloid protein is over expressed show synaptic loss prior to plaque formation [37-40], potentially suggesting a causal link. Interestingly, areas of the AD brain with early synaptic loss correlate with brain areas where a change in metabolic function is seen early in the course of the disease [41]. These brain areas are also the sites of early amyloid and tau deposition [41, 42], suggesting a complex relationship between, synaptic loss, amyloid/tau deposition and metabolic function. It is worth noting that the vast majority of energy consumed by the brain is through synaptic activity [43], therefore making deficits in metabolic function a potential key trigger for synaptic disruption.

Inflammation has been shown to contribute to the pathology of AD. Both AP and NFT can effect a local inflammatory response which can lead to further destruction of neurons and other brain cells [44]. Microglia, the macrophages of the brain, have been shown to have abnormal function in AD, with both protective and damaging properties identified. Microglia can both remove AP from the brain but also become activated by the A β protein which causes the release of cytokines and other inflammatory markers that can damage the brain [45]. There is also evidence from clinical studies to suggest that the use of Non-Steroidal Anti-inflammatory Drugs (NSAIDs) reduces the incidence of AD, further adding to the idea that inflammation has a key role in the development of AD [46].

One theory that tries to unify the complex relationship between protein aggregation, synaptic loss, metabolism and inflammation within the brain is the neuroplasticity theory of AD [47].

Neuroplasticity refers to how the brain modulates connections between neurons via synapses. This physiological process is integral to memory formation. When connections are increased in strength between 2 neurons, thought to be fundamental in the development of memories, this is described as long-term potentiation (LTP) [48]. When the connections between 2 neurons are weakened or lost this is referred to as long term depression (LTD) [49]. The brain constantly modulates the connections between neurons via LTP and LTD which in turn allows for the development of functional networks within the brain. The neuroplasticity theory for AD suggests that memory impairment develops in AD because the brain can no longer meet the energetic of neuroplastic process in the brain. Inflammation, protein aggregation, metabolism failure and synaptic loss all contribute to impairments in synaptic plasticity, and therefore AD develops because the fine balance between LTP/LTD is lost and neuronal connections start to breakdown [50].

Other pathological aggregates are seen in the AD brain such as Hirano bodies, Granulovacuolar Degeneration [11], and the choroid plexus inclusion called the Biondi body [51]. The contribution to the pathophysiological cause of each of these lesions is as yet not well understood in AD. Amyloid can also become deposited in the blood vessel walls of the brain leading to several different pathological processes such as microhaemorrhages and big lobar haemorrhages [11].

1.2.1 Amyloid Cascade Hypothesis

As already discussed in the above section the amyloid cascade hypothesis was originally proposed predominantly by Professors John Hardy and Dennis Selkoe in the early 1990's [12-15]. Although this has been the main theory for the cause of AD, it is not without its caveats, and criticisms. To understand both the reasoning behind the hypothesis and criticisms that have been made of this proposal a discussion is first needed around both the production of A β and AP from the APP protein, and the processes that lead to the accumulation of tau as NFT throughout the brain.

The APP protein is cleaved by 3 secretase enzymes. β and γ -secretase cleave the APP protein to produce A β . α and γ -secretase cleave APP to produce a protein called sAPP α , which is thought to have roles in protecting neurons from glucose and oxygen deficit by stabilising membrane potentials, synaptogenesis, neurite outgrowth and cell adhesion. The exact identity of both β and α -secretase enzymes is not completely known [52]. There is evidence that α -secretase is a member of the A Disintegrin and metalloproteinase (ADAM) family of enzymes with ADAM's 9, 10, 17, and 19 all suggested [53, 54]. The identity of β -secretase is also unknown, but Beta-site APP cleaving enzyme 1 (BACE1) is major secretase found within the brain and thought to be the most likely candidate enzyme that leads to amyloidogenic processing [55]. Cathepsin B also has β -secretase [56], but

BACE1 is by far the strongest candidate to cause the APP enzymatic processing that leads to AP formation. γ -secretase is a collection of 4 enzyme subunits called Presenilin 1 & 2, Nicastrin and Aph1 [57]. All four subunits are needed for γ -secretase activity. It has been shown that Nicastrin and Aph1 come together first in the cell membrane and then attract presenilin 1 and then presenilin 2. The cleavage of APP is performed by the presenilin proteins, with presenilin 1 the dominant aspartyl protease in the human neurons [57]. All three enzymes have multiple substrates as well as the APP protein, making therapeutic targeting of these enzymes difficult.

NFT are mainly composed of the cytoskeletal protein tau which has become hyperphosphorylated. The tau protein is a microtubule binding protein, which to a certain extent, can control microtubule assembly based on its phosphorylation status. Several enzymes can phosphorylate tau in the human cells. The most important when considering the amyloid cascade hypothesis are glycogen synthase kinase 3 β (GSK3 β), cyclin-dependent kinase 5 (Cdk5), and c-Jun amino terminal kinases (JNKs) (JNK). GSK3 β is constitutively active within a cell and inhibitory phosphorylation is used as a method of controlling this activity [58]. Insulin dependent phosphorylation via the action of the proto-oncogene protein kinase B (PKB, also known as Akt/RAC) at serine-9 [59], and wnt signaling dependent phosphorylation are thought to be the main inhibitory phosphorylation pathways [60]. Cdk5 is a kinase that is activated by its regulatory subunit p35 which allows phosphorylation. P35 can be metabolized by calpain to another protein called p25. This protein can constitutively activate Cdk5, which can increase its ability to phosphorylate proteins [61]. JNK can phosphorylate tau, and has been shown to have increased activity with increased levels of A β induced ROS stress [62].

The amyloid cascade hypothesis states that the deposition of amyloid within the brain is the key step in the development of AD and that synaptic loss, NFT formation and vascular damage occur as a consequence of this [13]. The evidence that supports this hypothesis comes from several sources. Firstly, familial forms of AD are caused by mutations in one of three proteins (APP, Presenilin 1&2) which lead to an increase in the production of the longer aggregatory forms of A β such as A β ₁₋₄₂ [63]. This produces in familial AD patients a form of pathology that is almost identical to that seen in sporadic forms of the disease. Secondly, amyloid itself has been shown to be toxic to synapses in its oligomeric form, leading to synapse loss in multiple animal models of AD [34]. Thirdly, accumulation of A β leads to tau hyperphosphorylation through the increased activation of the above-mentioned kinases. GSK3 β can lose its wnt mediated inhibitory phosphorylation via the actions of A β on the wnt inhibitor Dickkopf-1 (Dkk1) allowing the GSK3 β to hyperphosphorylate tau [64]. A β also increases intracellular calcium levels which activates calpain therefore increasing the production of p25 increasing Cdk5 tau phosphorylating ability [65]. Furthermore, AD is common in people with Down's

syndrome a condition which results for trisomy of chromosome 21, leading to an over expression of the APP protein [66]. Figure 1.2 shows the main steps in the amyloid cascade hypothesis.

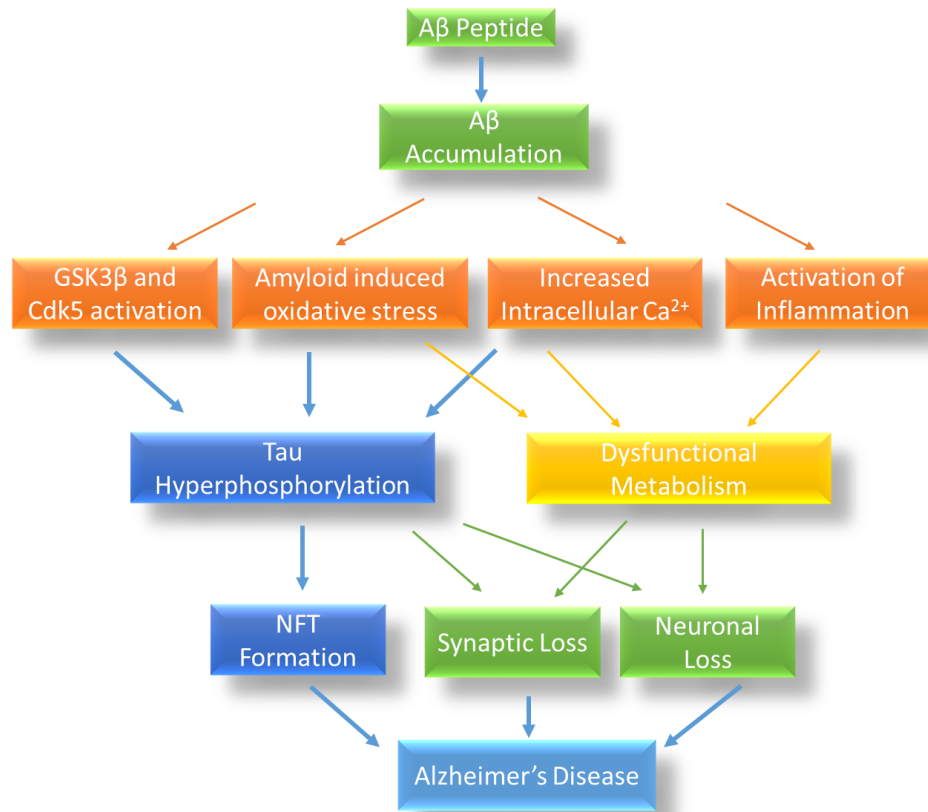


Figure 1.2 | The Amyloid Cascade Hypothesis This figure displays the main steps in the development of Alzheimer's disease based on the amyloid cascade hypothesis.

Although evidence supporting the amyloid hypothesis is compelling there are several problems with this hypothesis. Firstly, all drugs that have been developed to either remove amyloid from the brain or stop its production have failed to stop or reduce progression of the disease. In some cases, such as the drugs developed to inhibit the BACE-1 enzyme, the progression of disease has been made worse [67]. Secondly, the number of amyloid plaques within the brain does not correlate with the severity of the clinical syndrome in patients diagnosed with AD, with the tau progression through the brain showing a much closer relationship with clinical symptoms and pathological disease progression [18, 68]. Thirdly, when the mutations causing the familial forms of AD are studied in cell culture systems it has shown that the rate of increased amyloid production by a particular mutation does not have a linear relationship with the age of onset of the disease, which again suggests that amyloid volume is not a key determinant of disease progression [69]. Animal models

have also suggested that amyloid is not necessary for the development of NFT, again suggesting that amyloid accumulation maybe one of several pathological steps needed to develop AD [70].

1.3 Clinical Features of Alzheimer's disease and diagnosis

Clinically, AD presents with cognitive symptoms that effect a person's ability to perform the usual functions of daily life [71]. Classically, episodic memory (the ability to remember dates, and events) is the cognitive process affected earliest in AD. Semantic fluency (the ability to remember lists of objects) is another area of cognition affected very early in the course of AD [72]. More and more cognitive domains are affected as AD progresses. As described above, clinically the disease affects the medial temporal lobe structures first then moves to involve parietal, frontal and occipital lobes. The patterns in neuropsychological performance reflect this progression [73].

The disease progresses with a person's cognitive functions becoming gradually worse, until almost inevitably institutionalised care is needed [74]. During the course of the illness it is common for patients to lose the ability to talk, become incontinent, lose the desire to eat and drink and in the later stages the ability to swallow [75]. The average life expectancy after diagnosis is between 3-9 years depending mainly on the age at onset of symptoms [76].

Prior to the development of deficits in cognitive performance that would be severe enough to diagnose a person with AD, a pre-Alzheimer or mild cognitive impairment (MCI) stage of the disease is described [77]. The group of people that would be described as having MCI are more heterogenous than the people who have a diagnosis of AD. This is in part due to the fact the term encompasses both people who will eventually develop a diagnosis of dementia, and also people that will remain with MCI or even have an improvement in cognitive performance [78]. This makes prediction of transition from the MCI state to AD difficult. If a person presents with a more amnesic form of MCI, they are more likely to progress to AD [79]. People with a diagnosis of MCI who are positive of certain biomarkers of AD pathology such as increased brain amyloid, increased brain tau and signs of neuronal injury on brain imaging are also at an increased risk of developing AD from the MCI state [80].

AD has both sporadic (95%) and familial forms (5%) [81]. The familial forms are caused by mutations in the genes that encode APP [82-86], or the presenilin (PSEN) 1&2 protein subunits of the gamma secretase enzyme [83, 87, 88]. In general, patients with familial forms of AD develop cognitive symptoms much earlier than sporadic cases. Patients with familial mutations can develop cognitive impairment from the age of 30 years, whereas sporadic cases of AD typically present after the age of

60 [81]. Apart from age of onset, the disease course for both familial and sporadic AD is very similar. Animal models show that the mutations causing familial AD lead to an increased production in the A β , and AP pathology [89].

Sporadic forms of AD have gene alleles associated with an increased risk of developing the condition. The gene allele most strongly associated with an increased risk of developing sporadic AD is the Apo ϵ 4 allele [90]. Having two copies of the Apo ϵ 4 gene increases the risk of developing AD 10 fold for males, and 12-fold for females above the general population risk [91]. This Apo ϵ gene is a cholesterol transport gene with roles in both lipid transport and cell repair [92]. Genome wide association studies (GWAS) have identified ten other genes which have single nucleotide polymorphisms (SNP) associated with an increased risk of developing sporadic AD. These genes are ABCA7, bridging integrator 1(B1N1), triggering receptor expressed on myeloid cells 2 (TREM2), CD33, clusterin (CLU), complement receptor 1 (CRI), ephrin type-A receptor 1 (EPHA1), membrane-spanning 4-domains, subfamily A (MS4A) and phosphatidylinositol binding clathrin assembly protein (PICALM) [93]. These extra ten genes have functions in lipid metabolism, cellular endocytosis and immune response. None of the genes confers as great a risk of developing AD as the Apo ϵ 4 gene allele.

1.4 Diagnosis of Alzheimer's disease

A clinical diagnosis of AD is made based on characteristic changes in neuropsychological tests that suggest a pathology that starts by affecting the medial temporal lobe structures, and then spreads to involve other brain regions [73]. The neuropsychological diagnosis of AD is further supported by structural brain imaging abnormalities, which include atrophy of the medial temporal lobe structures, specifically the hippocampus [94] and changes in the expression of tau and amyloid proteins. Cerebrospinal fluid (CSF) analysis in AD shows a reduction in A β levels and an increase in hyperphosphorylated tau as compared to neurologically healthy controls [95]. Amyloid-PET brain imaging can also be used to identify increased deposition of amyloid within the brain, in characteristic patterns suggestive of AD [71, 96].

Several of these biomarkers have been incorporated into a binary AD biomarker classification system which is likely to be used more often in clinical practice in the coming years [97]. This biomarker system referred to as "ATN" (see table 1.1) is used to subcategorise patients with neuropsychological profiles consistent with AD. As already explained in the above sections when a patient develops a neuropsychological profile consistent with AD this does not always correlate with presence of amyloid and tau pathology [18]. Therefore, the aim of the ATN classification system is to deepen the understanding of other factors that may contribute to the development of AD. When the

classification system is applied to patients with MCI who are positive for all elements of the ATN (A+T+N+), a greater proportion of patients develop AD at 5 years (85%) than MCI patients with two negative categories (50%, A-T-N+) [98]. This further highlights that although increased amyloid and tau production within the brain increases the risk of developing AD, other aspects of cellular function must be important in those patients negative for the classical AD biomarkers but develop the disease clinically. Understanding how cellular metabolism changes in AD would help to develop and subcategorise patients who develop AD further.

Biomarker element	What positive means	How investigated
Amyloid (A)	If CSF A β 42 is low or the is high levels of A β on PET brain imaging	PET amyloid imaging CSF Amyloid
Tau (T)	If CSF or PET phosphorylated tau is recorded as high	PET phosphorylated Tau CSF Tau
Neurodegeneration	Signs of neuronal injury on structural brain imaging such as classical medial temporal lobe atrophy, a FDG-PET pattern of glucose uptake that fits with an AD pattern or total CSF tau is high	PET-FDG CSF Total Tau Structural Brain MRI

Table 1.1| ATN Classification criteria: This table highlights the elements of the ATN criteria used in the classification of AD.

1.5 Treatment options for Alzheimer’s disease

Few treatments exist for people with AD. Currently licenced therapies include the anticholinesterase inhibitors (donepezil, rivastigmine and galantamine). This group of drugs aim to restore levels of acetylcholine within the basal forebrain, as research has suggested that loss of acetylcholine transmission in this area of the brain leads to the characteristic pattern of memory loss seen in AD “The *Cholinergic Hypothesis*” [99]. The other main therapeutic option for people with AD is the N-methyl-D-aspartate (NMDA) antagonist, memantine, thought to reduce brain cell damage by decreasing levels of brain excitotoxicity [100]. Both these classes of drugs can be used in combination, as well as alone, but only moderate reductions in the rate of cognitive decline have been reported in AD patients treated with these drugs [100, 101].

As the build-up of both AP and NFT is a classical neuropathological finding in AD. Clearance of both proteins via the use of mono-clonal antibodies (MAB) has been performed in clinical trials, but no monoclonal antibody as yet has been successful in halting the progression of AD [20-22].

Interestingly, MAB have been shown to be successful at clearing the amyloid protein from the brain,

but this has not led to a reduction in disease progression, or symptom improvement [102, 103]. The most recent trials on the MAB Aducanumab suggest a possible benefit on cognitive function in a specific subset of patients, but original trials on this drug were stopped early due to primary trial endpoints not being achieved [104].

1.6 Therapeutic challenges in AD

AD has proven difficult to treat for many reasons. Most therapies are given to patients when the disease is well established both clinically and pathologically [105]. There is evidence that the pathological processes that lead to the development of AP occur many decades before any clinical features of AD are seen [106, 107]. This means that any anti-amyloid therapy potentially would need to correct many years of pathological changes before any benefits are seen. Another factor that potentially plays a role in why current therapeutic strategies have failed to control AD, is that AP accumulation does not correlate with the neuropsychological manifestations that define the disease well [16, 18]. NFT do follow a course of deposition within the brain that corresponds to the neuropsychological deficits seen, but tau accumulation alone cannot account for the clinical features of the disease. It is very likely that earlier diagnosis, perhaps even at the preclinical stage, and identification of other key pathophysiological processes is needed in AD before effective disease modifying therapeutics can be developed.

Developing therapeutic strategies for AD is further hampered by the fact that there is a relatively low concordance between pathological and clinical diagnoses of AD. Of the patients that receive a clinical diagnosis of AD concordance with a confirmed pathological AD ranges from 62-90% [108-113]. This suggests that in some patient cohorts nearly a third of patients with a clinical diagnosis of AD do not have the pathological hallmarks, therefore making therapies targeted at amyloid and tau pathology unlikely to have an effect. The problem of targeting pathological aggregates as a treatment option in AD is further compounded by the fact the cognitively normal individuals can have a pathological diagnosis of AD [113-115], suggesting that in this group at least the memory impairment is not caused by amyloid and tau aggregates. Pathologically the presence of pure AD in PM specimens is rare, with one study suggesting that only 36% of pathologically confirmed AD cases have purely AD pathology [111], with both vascular disease and Lewy body pathology common additional findings in patients diagnosed with AD [108, 109, 111].

Together this pathological/clinical discordance suggests either the clinical diagnosis of AD is not accurate enough to truly diagnose the condition, or that the clinical entity that we think of as AD is actually a group of diseases which have a combination of pathological substrates and pathophysiological drivers that lead to the disease.

To aid early diagnosis of AD looking at processes other than protein accumulation is potentially beneficial. As already stated, changes in brain metabolism occur in areas of the brain where both synaptic loss and AP build up is seen early. Having a deeper understanding of the pathophysiological changes in metabolism within the brain, is therefore likely to aid both early diagnosis and future therapeutic development. This may also allow for subcategories of clinical AD to be developed, which is very likely to improved targeted therapies.

1.7 Metabolism and Alzheimer's disease

Cellular metabolic changes within the brains of people with AD are seen very early in the condition, and often precede the development of both amyloid plaques and NFT. Abnormalities have been shown in many metabolic pathways in AD [116]. Mounting evidence suggests that deficits in the function of mitochondria, specifically how they control oxidative phosphorylation (OxPHOS) and changes in the process of glycolysis [117], are likely to be key in the development and establishment of AD. In fact, an alternative mitochondrial hypothesis for the aetiology of AD states that people who inherit mitochondrial genes that predispose them to lower mitochondrial respiration rates are more likely to develop the condition [118]. The following sections will first describe the structure, function of mitochondria and the glycolytic pathway, and then focus on how AD has been shown to affect mitochondrial function and glycolysis.

1.8 Mitochondrial Structure and Function

Mitochondria are double membraned organelles abundant in almost all types of mammalian cells [119]. They are very dynamic organelles and are transported throughout the cell. Mitochondria are in a constant state of flux; altering morphology and localization depending on energy demands or metabolic stresses within the cell [120]. Mitochondria have multiple biochemical roles within a cell, which are detailed in the next sections.

1.8.1 Mitochondrial ATP generation and the electron transport chain

The main pathway by which mitochondria generate ATP is OxPHOS. This process occurs in the inner mitochondrial membrane via the reduction of oxygen. Electrons move down an electrochemical gradient via four proteins complexes that form the electron transport chain (ETC), the final step in this chain is the reduction of oxygen. Electrons are transported to the ETC via the universal cofactor Nicotinamide Adenine Dinucleotide (NAD). NAD gains 2 electrons and a proton from different enzymatic steps of the tricarboxylic acid cycle (TCA) to become NADH. The NADH molecule is oxidized by complex I, releasing the electrons into the ETC [121]. Electrons are then passed between the four complexes of the ETC which allows complexes I, III and IV to move protons from the mitochondrial matrix into the intermembrane space. Protons then flow back into the mitochondrial

matrix via a fifth complex (complex V or, FOF1-ATP Synthase). This flow of protons through complex V causes a conformational change in shape that generates ATP from a phosphate molecule and adenosine diphosphate. The rate at which ATP can be produced by mitochondria is determined by the electrochemical gradient established across the inner mitochondrial membrane via the movement of protons. The movement of protons is in turn dependent on the number of electrons available to the ETC to reduce, therefore the NAD/NADH ratio is key to the level of ATP that can be produced by mitochondria. The 5 complexes that form the ETC are comprised of 97 different genes (84 nuclear genes and 13 mitochondrial) [122]. The process of OxPHOS is detailed in figure 2.1. The citric acid cycle generates the majority of the substrates for OxPHOS within the mitochondrial matrix [123]. Glycolysis occurs in the cytoplasm, and feeds substrates into the citric acid cycle for OxPHOS [124]. Figure 2.1 shows the gross morphological structure of mitochondria, and how ATP is generated.

The ETC complexes are very mobile within the inner membrane of the mitochondria. The movement of electrons through the complexes is improved by different complexes joining together to form super-complexes [125], although they can function separately within the phospholipid membrane. The stability of complex I has been shown to be improved by forming super-complexes with complex III [126]. Evidence from animal models suggests that as the cortex ages there is an increase in reactive oxygen species (ROS) produced, and a reduction in super-complex formation [127]. From this observation it has been suggested that a reduction in super-complex formation increases the tendency of the ETC to produce ROS, as the reducing ability of the mitochondria becomes impaired [127]. A decrease in the reductive capacity of the mitochondria leads to increased oxidative damage to the organelle. The oxidative damage can lead to dysfunction of the ETC proteins which can decrease the OxPHOS capability of the mitochondria [125].

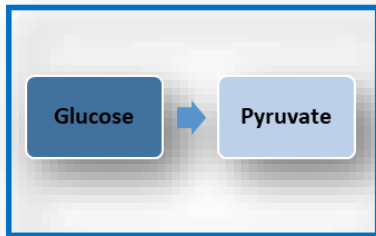
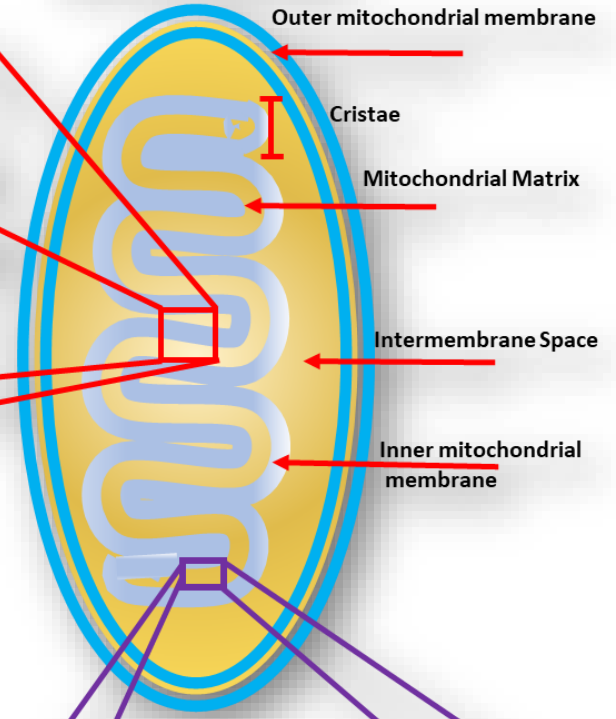
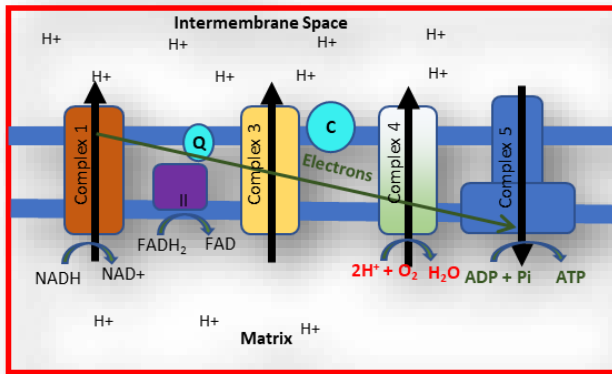
Depending on the ATP demands of the cell, mitochondria can undergo both fission and fusion events to control ATP production. Mitochondria will often fuse together within a cell in times of increased energy demand, or metabolic stress [119]. An example of metabolic stress would be stress induced mitochondrial hyperfusion (SIMH) [128]. In SIMH mitochondria fuse together to increase ATP production as a mechanism to combat cellular stress induced by such factors as UV radiation. Mitochondrial fusion allows the transfer of ETC complexes between mitochondria, which can enhance ATP production. Mitochondrial fission is less directly linked to managing the ATP demands of the cell, but is used as a way of identifying defective mitochondria that need to be removed and destroyed to protect the whole mitochondrial cell network [129]. Mitochondrial fission is also important in the trafficking of mitochondria to the correct cellular location [130], and therefore allowing mitochondria to meet the local energy demands of a cell. A complex cascade of protein

interactions controls both mitochondrial fission and fusion, but 4 key proteins are essential for mitochondrial remodelling. Mitochondrial fusion is controlled by 3 proteins: mitofusin 1 & 2 (MFN1 & 2) and optic atrophy protein 1 (OPA1). Mitochondrial fission is mainly controlled by dynamin related peptide-1 (DRP1) [131]. Mitochondrial fission and fusion dynamics have been reviewed extensively by Chan (2020) [132].

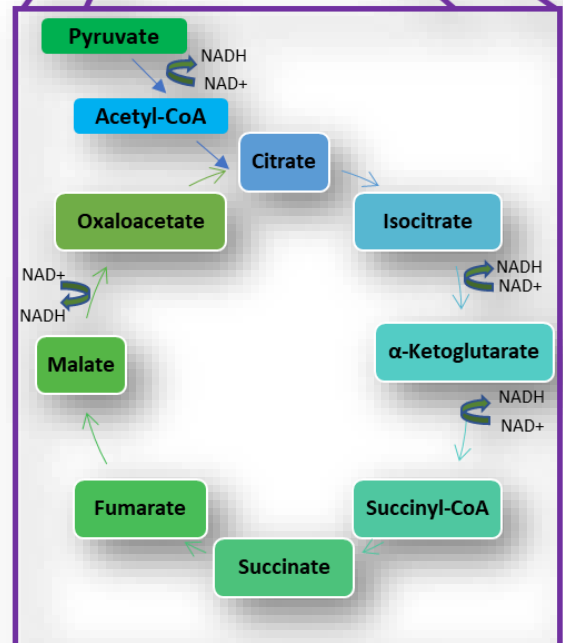
Mitochondrial density within many different cell types is not uniform which is thought to be caused by the differing ATP demands in different cellular localities. An example of how the density of mitochondria can differ in one cell type would be the neuron, where synaptic terminals are generally enriched in mitochondria compared to the rest of the cell. Studies have shown that mitochondria within the synapse of a neuron have increased DNA mutations, reduced bioenergetic function [133], and decreased complex activity [134], when compared to mitochondria closer to the cell nucleus. Potentially, differences in metabolic function seen in different brain regions in neurodegenerative diseases such as AD, are explained by the heterogeneity of mitochondrial distribution within different brain cell types [135]. Mitochondrial heterogeneity is difficult to study in human neurodegenerative disease without using model systems that have human mitochondria.

MITOCHONDRIA

ETC (Inner Membrane)



Glycolysis (Cytosol)



Citric Acid Cycle (Mitochondrial Matrix)

Figure 1.3 | Mitochondrial structure and ETC changes in the brain in AD The overall structure of mitochondria is shown in the top part of the diagram. In the panel labelled **Normal ETC** the process of ATP generation via the electron transport chain is displayed. Electrons are donated from electron donors such as NADH and FADH. These electrons pass down an electron gradient via the 4 complexes of the electron transport chain. This process is aided by the 2 electron transporters Cytochrome C (**C**) and Ubiquinone (**Q**). The process of electron transfer allows complexes 1,3 & 4 to pump protons from the matrix into the inner membrane space. The movement of protons in this way generates the **Mitochondrial Membrane Potential (MMP)**. The protons then pass through complex five down an electrochemical gradient. This causes a change in shape of complex V which leads to ATP generation. The panel labelled **Citric Acid Cycle** shows the process by which most of the substrates for complex I & II are generated. In the panel labelled **Glycolysis**, the breakdown product of glucose is described, further detail of this process is described in figure 1.7. Each panel in brackets identifies the place in which the metabolic process occurs.

1.8.2 Mitochondrial control of Cellular Calcium

All human cells rely on calcium currents within the cell to affect different biological processes. Cellular calcium signalling is very diverse and has the potential to lead to both cell proliferation and death [136]. The concentration of cytosolic calcium is under tight control by many different cellular organelles, with mitochondria having a fundamental role in this process. Rises in cytosolic calcium lead to movement of calcium into the mitochondrial matrix via the mitochondrial calcium uniporter (MCU) on the inner mitochondrial membrane [137, 138]. Calcium can freely diffuse through the outer mitochondrial membrane, and can also move through the voltage dependent anion-selective channels (VDAC), but the inner membrane is impermeable to this ion [139]. If the cytosolic calcium concentration exceeds 1mM then the MCU is opened by two proteins activated by the increased calcium concentration called MICU 1&2. Usually the cytosolic calcium would not reach a concentration of 1mM as this would be toxic, but this can occur in small areas adjacent to the endoplasmic reticulum (ER) when it releases calcium. MICU1 also has a role in controlling the influx of calcium into the mitochondrial matrix at low cytosolic calcium concentrations [140]. Due to the large negative electrical potential within the mitochondrial matrix generated by the complexes of the ETC even at low cytosolic calcium concentrations, the continual movement of calcium down its electrochemical gradient could lead to mitochondrial calcium overload. The MICU proteins work as “gate keepers” for the MCU allowing the regulation of matrix calcium influx [141]. This in turn ensures that a wide range of cellular cytoplasmic calcium concentrations can be buffered by the mitochondria.

The flow of calcium into the mitochondrial matrix down an electrochemical gradient highlight how the mitochondrial membrane potential is important in setting the amount of calcium that can enter the organelle. Potentially, in disease states, where membrane potential is low, cellular calcium homeostasis could be significantly affected. Once calcium has entered the matrix it can act as a signalling molecule activating the mitochondrial dehydrogenases; pyruvate dehydrogenase, α -ketoglutarate and isocitrate dehydrogenase [142]. This has the effect of increasing ATP generation by the mitochondria, and also highlights how increased cytosolic calcium concentrations caused by increased calcium signalling within the cell can upregulate ATP production when the calcium eventually enters the mitochondria. ATP production in this sense, could be seen as a positive feedback loop as entry of calcium into the cell requires the activation of certain ATP dependent ion pumps to return cytosolic calcium to a normal concentration. The actions of these ATP dependent pumps are particularly important at neuronal synapses, as they allow the synapse to maintain ion gradients that are essential for transmission across the synaptic cleft. This also highlights how important optimal mitochondrial ETC function is in maintaining synaptic function.

Export of calcium from the mitochondrial matrix is controlled by a sodium/calcium exchanger (NCX), and potentially a transporter that can move both hydrogen ions and calcium. This allows the mitochondria to keep a steady state concentration of calcium within the matrix of 0.25-1.0 μ m [143]. The mitochondrial permeability transition pore (MPTP) can also aid with the efflux of calcium, but this is usually when the mitochondria has become overloaded with calcium [144]. The MPTP is a complex ion pore that is made of a combination of proteins found in the matrix, inner mitochondrial membrane and outer mitochondria membrane. The identity of the proteins that come together to form the MPTP, to a certain extent, is still debated but are very likely to include Cyclophilin D (CypD), Adenine Nucleotide Translocator (ANT) and VDAC [145]. In response to increase ROS production or high calcium concentrations, CypD moves from the matrix to the inner mitochondrial membrane and binds with ANT to form a pore that allows the movement of calcium and other ions/proteins from the matrix to the intermembrane space. Calcium can then flow out of the mitochondria via VDAC. MPTP opening can be the first stage in the development of cellular death cascades as described below, but the pore also has roles in cellular signalling pathways. Figure 1.3 highlights the proteins involved in calcium homeostasis in mitochondria.

Mitochondrial Calcium Homeostasis

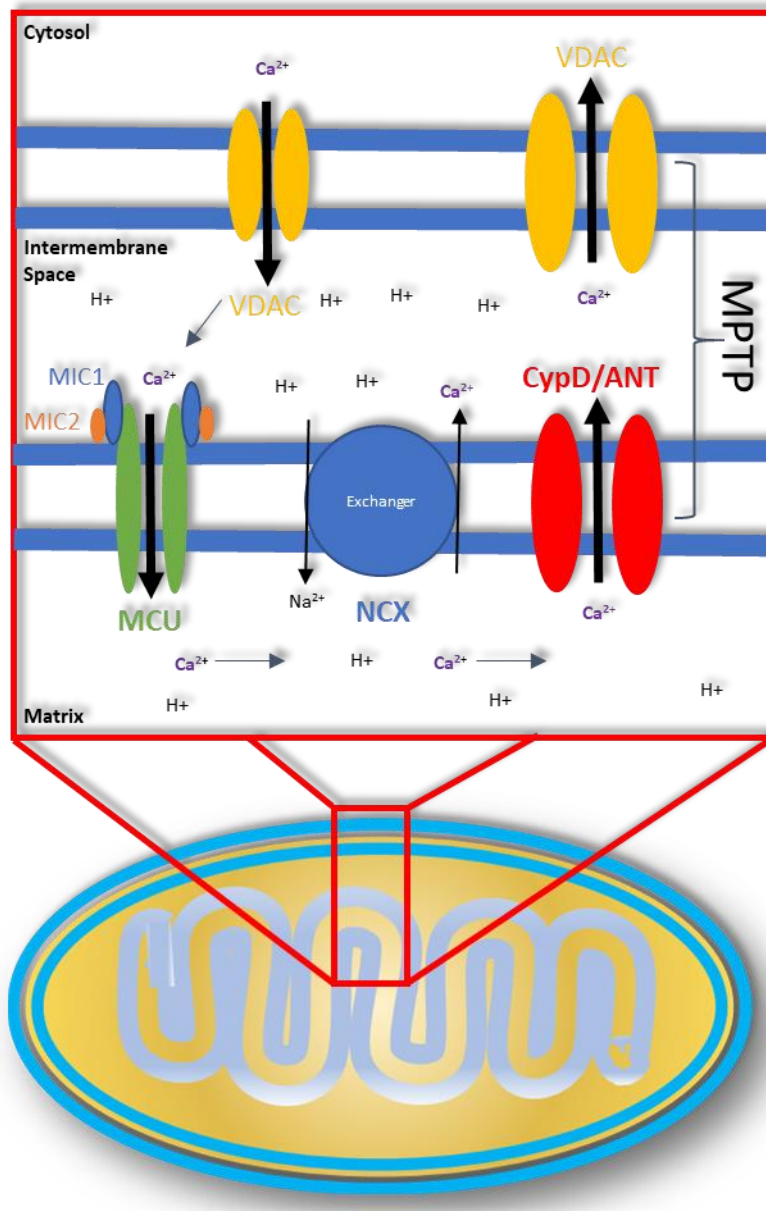


Figure 1.4| Mitochondrial Calcium Homeostasis As cytosolic calcium increases it moves into the mitochondrial intermembrane space via the **Voltage dependent anion channel (VDAC)**. Once in the intermembrane space calcium can be transported into the mitochondrial matrix via the mitochondrial **calcium uniporter (MCU)**. To maintain the mitochondrial calcium concentration the **sodium calcium exchanger (NCX)** can move calcium back into the intermembrane space. If mitochondrial calcium exceeds a certain concentration the **Mitochondrial Permeability Transition Pore (MPTP)** can also allow calcium exit from the mitochondria.

1.8.3 Reactive oxygen species and mitochondria

Mitochondria are one of the major sites within a cell for the production of ROS. Initially ROS were thought of as a necessary by-product of processes such as OxPHOS, but recently research has revealed that these molecules are active in cellular signalling pathways. The main ROS produced by the mitochondria is the superoxide ion ($O_2^{\bullet-}$). The main site of $O_2^{\bullet-}$ production within the mitochondria is complex I of the ETC, but complex III, α -ketoglutarate dehydrogenase and α -glycerol-3-phosphate dehydrogenase can all produce $O_2^{\bullet-}$, to a lesser extent [146]. Complex II is also a suggested site of ROS generation, but is currently debated as to whether complex II ROS has significant biological effects [147].

The $O_2^{\bullet-}$ ion is produced by the addition of an electron to a molecule of O_2 . The site for this reaction within complex I is thought to be the Flavin mononucleotide (FMN) motive. The protein is the site at which NADH passes electrons to complex I to be used in the active process of proton pumping across the inner mitochondrial membrane. $O_2^{\bullet-}$ ions are generally produced by complex I in one of 3 ways i) when the NADH/NAD ratio is high, ii) when Co-Enzyme Q is fully reduced or, iii) when the mitochondria are synthesizing ATP [146]. States 1 and 2 produce far more $O_2^{\bullet-}$ than ATP synthesis. As mitochondria are generally in a state of ATP production, this pathway for generating $O_2^{\bullet-}$ is likely to be the most important in determining the superoxide production by the mitochondria [146].

Other ROS include hydrogen peroxide and the hydroxyl radical, both of which can also be produced in the mitochondria. Hydrogen peroxide is produced by the dismutation of the $O_2^{\bullet-}$ ion either spontaneously or through the action of the superoxide dismutase enzymes [147]. The hydroxyl radical is produced via the breakdown of the hydrogen peroxide and $O_2^{\bullet-}$ ROS, or via ultra-violet radiation's effect on water molecules. The hydroxyl radical is the ROS mostly likely to cause oxidative damage to DNA structures [148].

Mitochondrial ROS have a role in adapting the cell response to certain stressors such as hypoxia, starvation and pathogen infection. Certain ROS molecules, such as hydrogen peroxide, have been shown to have a role in many different signalling pathways including autophagy, immune response (pathogen neutralization), cell differentiation, cell aging and adaptation to hypoxia [149]. Although often the exact site of ROS action in a metabolic pathway is not fully understood. Of note, when considering the cellular response to hypoxia ROS increase the stabilization of hypoxia-inducible factor-1alpha (HIF-1alpha), which has been shown to upregulate glycolytic pathway enzymes including hexokinase and 6-phosphofructokinase in tumour cells [150]. This shows how intricately linked OxPHOS, glycolysis and hypoxia are within a cell, and how changes in one pathway are likely to affect cellular metabolism in multiple ways. This biochemical pathway link also highlights how

different cell stressors can affect change in metabolism both directly and indirectly. Figure 1.4 displays the most common site of ROS production in mitochondria, and how they are released into the rest of the cell.

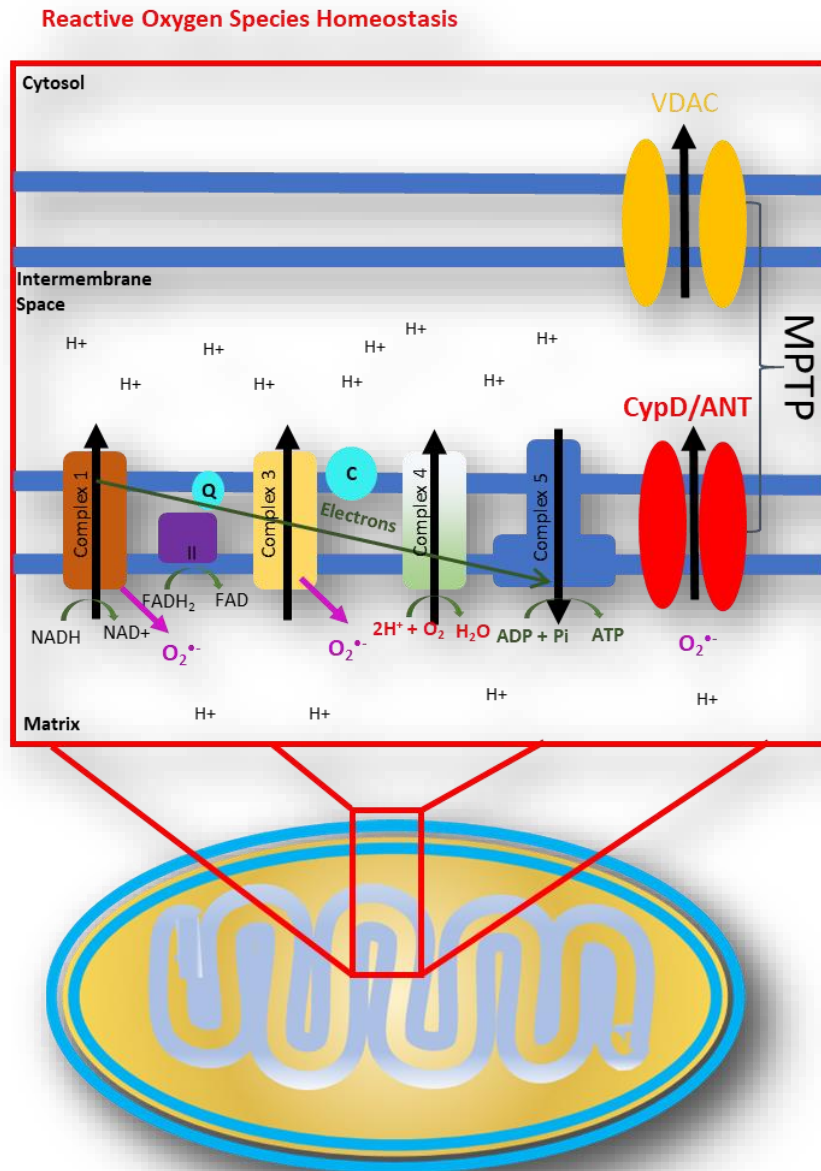


Figure 1.5| Mitochondrial ROS Production The main sources of mitochondrial ROS production are complex I and III of the ETC. Sites of ROS production are highlighted in pink ($O_2^{\bullet-}$). ROS production can open the MPTP which allows ROS to be used as a signalling molecule or in times of excess lead to oxidative damage in other cellular organelles.

1.8.4 Mitophagy and cell death

Mitophagy is a type of autophagy that refers specifically to the removal and destruction of defective mitochondria from a cell. Mitophagy is a method by which a cell can perform quality control of its own mitochondrial pool. This is an extremely important biological process, as defective mitochondria can lead to global cell dysfunction, and have a key role in the development of certain neurodegenerative diseases such as Parkinson's disease [151]. Like all autophagic processes, mitophagy involves the envelopment of a damaged or defective mitochondria by a double membraned organelle (an autophagosome) which then fuses with a lysosome allowing the breakdown of the autophagosome content [152-154]. Mitophagy can be stimulated by depolarization of the MMP, oxidative stress secondary to ROS production, mitochondrial DNA mutations, or when a cell is exposed to starvation, hypoxia or nutrition poor environments [154]. Mitochondrial fragmentation has also been shown to play an important role in initiating mitophagy. Mitochondrial fragmentation allows for the separation of defective mitochondria from the cellular mitochondria network [155, 156]. Experiments in which the mitochondrial fission protein Drp1 has been knocked down show impairment of mitophagy [156]. Interestingly at times in which cellular autophagy is happening on a wider scale from metabolic insults such as starvation, mitochondria can become elongated to prevent them undergoing the autophagic process, and therefore maintaining cellular ATP production [157, 158]. The elongation of mitochondria occurs because the Drp1 fission protein is phosphorylated stopping it binding to mitochondria.

The PINK1-Parkin pathway is the best understood signalling cascade that initiates mitophagy. Parkin is a protein normally found in the cytoplasm of a cell. It has been shown that dissipation of the mitochondrial membrane potential can recruit Parkin to the mitochondrial outer membrane [159]. Parkin has to bind to PTEN-induced kinase 1 (PINK1) on the mitochondrial outer membrane to have its action. The expression of PINK1 on the outer mitochondrial membrane becomes more stable when mitochondrial membrane potential is dissipated, suggesting that both PINK1 and Parkin recruitment is dependent on mitochondrial functionality. Once Parkin has become stable on the mitochondrial outer membrane it has the ability, through its E3 ligase activity, to perform ubiquitination of the outer membrane proteins, which include DRP1, MFN1/2, and VDAC [160]. The ubiquitination of the outer mitochondrial membrane proteins increases the binding of the p62 protein, which recruits the mitophagy promotor LC3, which can start the autophagosomal degradation of the mitochondria [161]. Figure 1.5 displays the process of Parkin-PINK1 mediated mitophagy

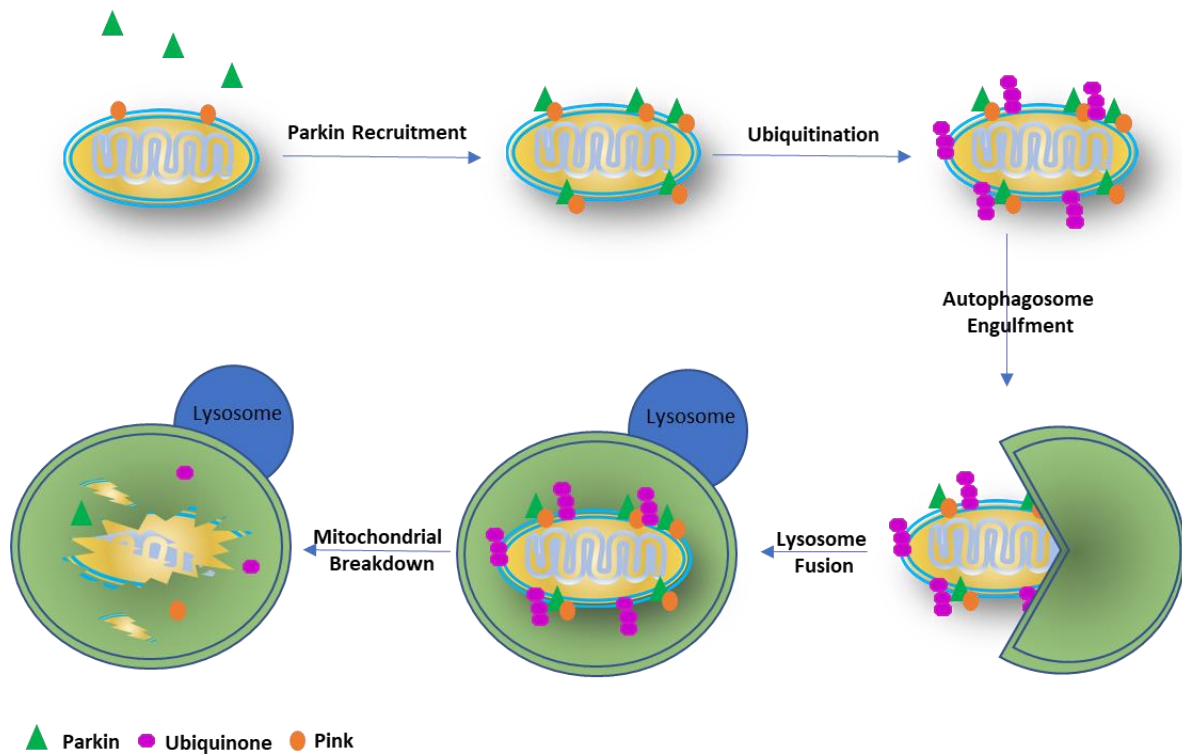


Figure 1.6| Mitophagy When a mitochondrion has become defective, often secondary to oxidative damage or membrane potential dissipation mitophagy is initiated. The main pathway for mitophagy includes the recruitment of parkin from the cytosol to the outer mitochondrial membrane. Here it binds with Pink and initiates the ubiquitination of the mitochondria. This signals an autophagosome to engulf the mitochondria where it is broken down via the action of lysosomal enzymes.

Mitochondrial quality has an important role in determining cell fate. As described above, mitochondria have the ability to generate ROS, but this can increase the oxidative stress the organelle is exposed to. If the oxidative stress a mitochondria is exposed to reaches a certain level this can lead to permanent opening of the MPTP, which ultimately can lead to cell death via necrosis [162]. Mitophagy is an important regulator of mitochondrial oxidative stress, and therefore a key signalling pathway that can prevent MPTP opening, and cell death. Opening of the MPTP can also lead to apoptotic cell death via the release of cytochrome c into the cytoplasm. If the MPTP remains open, it allows the passage of small proteins (<1.5kDa) into the matrix of the mitochondria, which in turn leads to mitochondrial swelling via osmotic forces [163]. This swelling of mitochondria leads to the loss of the outer mitochondrial membrane integrity which causes the release of cytochrome c into the cytoplasm. It is theorised that rapid opening and closing of the MPTP may be a way the mitochondria can control both mitochondria matrix calcium concentration and ROS signalling.

1.9 Mitochondrial changes seen AD

Multiple mitochondrial abnormalities have been described in AD [164-167]. Detailed below is evidence for what effects AD has on the biological roles of mitochondria as described above.

1.9.1 Electron Transport Chain Disruption in AD

Much of our knowledge of AD mitochondrial dysfunction in human tissue comes from *post-mortem* (PM) brain samples from patients with the condition. Studies investigating the expression of OxPHOS proteins and mitochondrial DNA have revealed potentially conflicted results. Gene expression micro-array analysis of PM frozen hippocampal samples has revealed a global decrease in nuclear encoded OxPHOS protein subunits and no change in mitochondrial DNA (mtDNA) encoded subunits when total RNA from AD brains was compared to both aged-matched controls and patients with MCI [168]. A study investigating RNA levels in the mid temporal gyrus has revealed a decrease in the RNA that encodes subunits 1&2 of complex IV within the mid-temporal lobe [169]. A similar reduction in RNA of subunit 3 of complex IV has been shown in the same brain areas by a different group [170]. These subunits are all mitochondrially encoded [171], but do not appear to be associated with a loss in mitochondrial number, or correlate with amyloid brain levels [172, 173]. RNA from subunit 2 of complex IV has also been shown to be decreased in the hippocampus of the AD brain, but in the same study no change was seen in the RNA of nuclear encoded subunits of the complex IV [173]. In contrast, both total cellular mtDNA and complex IV protein levels in the AD hippocampus, frontal and temporal lobes has been shown to be increased in AD [174]. This study reports that the majority of the mtDNA and complex IV protein is not found within the mitochondria but in the cytoplasm, suggesting a greater turnover of mitochondria or a decrease in their proteolytic breakdown [174]. This study does not mention if the mtDNA that encodes OxPHOS complexes has a change in expression level, and reports no difference in mtDNA expression in glial cells or neurons in areas of the brain not classically affected by AD. Further studies have suggested that the RNA for the mitochondrially encoded subunits of complexes III and IV is increased in the AD brain whereas the mitochondrially encoded subunits for complex I are decreased [175, 176]. Together these reports suggest that the turnover of mitochondria is altered in the AD brain, and that the expression of ETC proteins is potentially altered.

The apparent conflicting nature of the results across the papers described above may be explained by the fact that each study has small numbers of participants and uses different techniques to preserve the brain samples used for analysis. RNA is known to be unstable when being prepared from tissue samples, which potentially may also affect results. It has been shown that the AD brain has a higher load of both mtDNA and nuclear DNA mutations, which may also help to explain the

differences in results seen here [177-179]. The increased mutation frequency is likely to mean the changes in RNA and protein expression could occur by chance meaning results between studies could vary. Changes seen in these studies are not specific to AD, with similar changes also seen in the brains of people with autism [180]. The fact that differing expression profiles of the ETC RNA and protein subunits differs between these studies may also highlight the heterogeneity of AD, and how in sporadic AD there are likely to be multiple factors that affect the expression of ETC proteins. These studies focus on cases that are towards the end of the disease process, and therefore changes may not be triggers of AD but more consequences of the progression of the disease. The changes seen in PM studies may be a consequence of disease progression and may not be present at the start of disease. This would potentially make these changes unsuitable of biomarker and therapeutic development. The hippocampal mitochondrial changes are reported more in AD than the other conditions suggesting disease selectivity, but mitochondrial ETC complex expression abnormalities are present in multiple neurodegenerative diseases suggesting a common pathological site across this disease group.

Functional assessment of human nervous system mitochondria is difficult when using PM tissue as the cells are no longer active. But several studies on frozen PM brain samples from patients with sporadic AD have shown a decrease in the activity of complex IV [181-186]. The frontal, temporal and parietal lobes in certain studies show selective reduction in the activity of complex IV [181, 182], but this finding is not consistent across the whole body of evidence, with studies using very similar techniques showing deficits in complex IV activity throughout the whole brain [183, 184, 186]. The reason for the reduction in complex IV activity seen in the AD brain is not known but the structure of the complex IV protein is changed in AD, potentially as a result of oxidative stress [185]. The loss of neurons seen as AD progresses has also be suggested as a cause for the apparent reduction in complex IV activity[186]. A theory corroborated by evidence from animal models show complex IV activity reduction as a consequence of loss of neuronal activation [187-189]. A loss of neuron/synaptic number though, would not fully account for the selective loss of activity of complex IV over the other ETC complexes reported in these studies, although it puts forward the hypothesis that OxPHOS demand may modulate ETC activity and expression [190]. Interestingly, the activity of the other ETC complexes has been reported to be reduced in AD PM brain samples [183, 184], but this finding is not repeated across all studies. Through PM brain samples it is difficult to ascertain if the changes seen in complex IV activity are present from birth or are the consequence of another pathological process in AD such as protein aggregation, or synapse loss.

Study of blood cells in AD patients has revealed functional changes in the OxPHOS pathway.

Peripheral blood mononuclear cells (PBMCs) show decreased basal oxygen consumption rates (OCR)

and proton leak in AD but no change in mitochondrial maximum respiratory capacity when compared to age matched controls [191]. This work is complemented by work specifically in lymphocytes (a type of PBMC) which shows a reduction in basal OCR, but also a reduction in maximum respiratory capacity [192]. Lymphoblastic-cell-lines (LCL) from AD and Down's Syndrome (DS) patients have a low MMP in both old and young DS patients, but ATP loss is not seen until later in the disease, when AD had developed [193]. This suggests that the loss of ATP maintenance is developed through the course of AD as opposed to blood cells having a lower level of cellular ATP prior to disease onset. In whole blood samples from people with AD or MCI the OxPHOS genes that are nuclear encoded are down regulated and those that are mitochondrially encoded are upregulated [194]. It is unclear if this affects the function of the ETC, but it is interesting that differences in the expression of mtDNA genes are seen between peripheral and CNS tissue samples. This may suggest different mechanisms are present in a particular cell type to combat the effects of altered OxPHOS gene expression and may go some way to explaining why AD does not manifest itself in non-CNS tissues. These changes in OxPHOS seen in AD blood cells may be the cause of the decreased MMP and reduction in total cellular ATP levels that have also been reported in PBMCs [192, 195].

Platelets have also been shown to have abnormalities in the ETC in AD, and are often suggested to be a good peripheral cell model for the disease [196]. Platelets contain the enzymatic pathways needed to produce A β from the APP protein, and have been shown to secrete A β into the blood stream [197, 198]. The basal OCR for platelets from patients with AD is similar to controls, until platelets become activated through exposure to substances such as collagen, thromboxane or monoamine neurotransmitters [198, 199]. Reductions in basal and maximum OxPHOS capacity thought to be due to a combination of reductions in complex I substrates, lower activities of complex IV, increased activities of complex I and reduced concentrations of Ubiquinone, have been reported in platelets from AD patients once activated [195]. The evidence that platelets only start to show deficits in ETC function when activated suggests capacity deficits in the ETC function in AD that may only be measurable at times of physiological stress. Several studies have shown both a decrease in the activity and the expression of the complex IV enzyme and its subunits in the platelets of patients with AD [199-201]. The changes seen in the metabolism of blood cells in AD could be an example of inherent deficits in mitochondrial function, but some evidence from animal models suggests that the changes in blood cell ETC function may be precipitated by the development of the pathological aggregates of AD within the brain [199]. A proinflammatory environment within the brain is established which then activates platelets leading to the OxPHOS deficits [199]. The changes in

metabolic function seen in PMBCs may also be a direct consequence of the changes seen within the brain, but this has not yet been shown.

Fibroblasts from patients with both sporadic and familial AD have been extensively studied for both functional and structural abnormalities in AD. Like platelets, fibroblasts can produce A β , and this is increased in fibroblasts from patients with AD [173, 202]. The function of the ETC of fibroblasts from patients with AD shows more variable results than those from blood cells. ATP and MMP levels have been shown to be low in some studies of both sporadic and familial AD fibroblasts [203-205]. But normal and higher than control levels have also been seen in AD fibroblasts [206, 207]. Alterations in the NAD/NADH ratio, and how this is maintained is seen in fibroblasts from patients with sporadic AD who have high OCR and MMP compared to controls [207]. This suggests that the functional changes seen in the mitochondria of AD fibroblasts may not be a direct consequence of ETC activity but caused by the substrates that interact with the different complexes. The design of each of these studies on AD fibroblasts is quite different, with control group comparators ranging from being completely disease free to having other forms of dementia and neurological illness. This may explain why fibroblast studies reach less of a consensus about the functional mitochondrial alterations seen in AD. All these studies agree that there are deficits in the function of the ETC, which may not necessarily affect mitochondrial function until a stressor is added [206]. As with PM samples and blood cells inhibition of the complex IV enzyme in fibroblasts is also stipulated to cause the changes in ETC function [206].

It remains unclear if the functional and structural changes to the ETC seen in AD are a result of a primary mitochondrial change, as suggested in the mitochondrial hypothesis of AD [208], or as a consequence of the build up of amyloid within the brain and body of AD patients. Evidence from animal and cell models suggests that both amyloid and tau have a direct effect on the function of the ETC. In triple transgenic 3xTg-AD mice (human APPSWE, TauP301L, and PS1M146V genes) abnormalities in mitochondrial function are seen in the embryonic stage and in young mice long before the build up of amyloid [209]. In this AD mouse model most of the subunits of complexes I & IV are down regulated and complexes III & V are up regulated when the mitochondria are isolated and examined at 6 months [210]. Interestingly in the APP23 mouse upregulation of both glycolysis and OxPHOS is seen before amyloid deposition, and this seems to increase the oxidative stress within cells [211]. This appears to be opposite to the metabolic changes that are seen in the transgenic 3xTg-AD mice. PSEN2 plays a role in maintaining MMP, as knock down of PSEN2 in mouse embryos reduces MMP [212, 213]. Showing that 2 of the key mutations that cause familial AD may have a link to the altered metabolism seen in AD models. This is also a reason for studying both familial and sporadic disease when investigating mitochondrial function in AD. Other studies using

triple transgenic mice that have mutations in the APP gene and an increased propensity to develop tau pathology (human APPSWE, TauP301L, and PS1N141) have shown deficits in MMP, total cellular ATP, mitochondrial spare respiratory capacity and OCR. This paper shows that the tau preferentially disrupts complex I of the ETC whereas amyloid preferentially disrupts complex IV [214]. The effect tau has on complex I has also been highlighted in studies looking at the effects of the plant poison Annonacin, which has a structure very similar to tau and can also cause complex I deficits [215]. This study shows that reduced complex I activity leads to a redistribution of tau towards the cell stoma, which can potentiate the development of NFT and cell death, suggesting that tau pathology can also be exacerbated by poor mitochondrial function. The tau and amyloid effects on the ETC have also been shown to work synergistically to increase the speed at which mitochondrial dysfunction happens in animal models [216]. It has been shown the tau's effects on the function of the ETC are propagated by the addition of amyloid [217].

Multiple cell line experiments have shown that over expression of the APP protein affects the activity and structure of mitochondria. APP over expression has revealed that complexes I,II & IV all have reduced expression in the presence of A β [218, 219] leading to reduced MMP and ATP production. The trafficking around the cell and structure of mitochondria is also affected by A β [166], with mitochondria shown to be more fragmented and to have a reduced MMP [167]. Removal of the mitochondria from a cell line has also been shown to stop the toxic effect of A β on the cell line [219], again linking metabolism to A β pathology.

Limited evidence for a definitive primary mitochondrial OxPHOS pathology has been identified so far in AD, but a recent study has shown that a point mutation in the PTC1 protein, encoded by nuclear DNA, is much more prevalent in people with AD [220]. This protein is essential for the normal assembly of mitochondria and this mutation has been shown to cause deficits in OxPHOS.

Interestingly, cybrids (SH-SY5Y cell line with mtDNA removed and human platelet mtDNA added) created from patients with AD and controls also reveal reductions in the activities of complexes I, II & IV, an increase in reactive oxygen species production, and a 40-50% reduction in ATP generation [221]. Changes in mitochondrial structure including shorter length, increased fragmentation, and a collapse of the mitochondrial network were also seen. This is without the presence of APP suggesting that the A β protein may exacerbate a mitochondrial phenotype that already exists in AD.

Research into mitochondrial ETC deficits seen in AD reveals mixed results depending on the situation in which the mitochondria are observed or the tissue in which they are studied (e.g. PM brain, peripheral blood cells in people living with AD or animal models). Interestingly the changes to ETC gene expression in peripheral cells are often associated with a reduction in ATP production,

suggesting a reliance on OxPHOS for ATP production in the periphery, but in most studies glycolysis and other metabolic pathways are not investigated therefore the contribution to ATP deficits is not known. Inconsistency in findings could be explained by differences in experimental techniques. Constituents of media, such as concentration of metabolic substrates, can affect mitochondrial function and may explain differences among studies. The dynamic nature of mitochondria will also contribute to the conflicting results, and highlights the need to study mitochondrial functional dynamics in a human CNS model of sporadic as well as familial AD. This type of model system would enable observations of the interaction of different CNS cell types in order to highlight which mitochondrial abnormalities potentially contribute to AD.

1.9.2 Mitochondrial Calcium Signaling in AD

The tight control of both intracellular calcium and intramitochondrial calcium has been shown to be affected in AD. PM samples from AD patient frontal cortex tissue show that the Na/Ca exchanger that maintains mitochondria matrix calcium is remodelled, and has reduced expression [222]. This leads to an increase in the matrix calcium concentration. In the same paper a transgenic mouse (3xTg-AD) with the Na/Ca exchanger deleted is shown to have an accelerated amyloid and tau pathology as well as increased memory loss. The cognitive deficit seen in the mouse model can be corrected by the normal expression of the Na/Ca exchanger, suggesting that high levels of mitochondrial matrix calcium are essential to the development of the pathology of AD. A β has also been shown to increase intracellular calcium levels, which can increase cellular vulnerability to excitotoxicity [223]. This will also influence mitochondrial function as the calcium buffering capacity of the mitochondria is challenged by an increased intracellular calcium. A recent study using an animal model of AD (the APP^{swe}/PSEN1 Δ E9 (APP/PS1) Tg mouse) has suggested that A β increases mitochondrial calcium levels via its actions on the mitochondrial calcium uniporter [224]. The same study shows that in the PM AD brain, the expression of influx calcium transporters is reduced, and efflux transporters increased suggesting an adaptive mechanism by neuronal cells to manage the increased mitochondrial calcium load caused by A β . The efflux of calcium from mitochondria has been shown to be further impaired by the presence of misfolded tau [225, 226], giving further evidence of the synergistic effect that both tau and amyloid aggregates have on the dysfunction of mitochondria in AD.

The buffering of calcium by the mitochondria and endoplasmic reticulum is particularly affected by mutations in the PSEN 1&2 genes that are seen in AD, with an increase in mitochondrial calcium seen in PSEN1&2 gene mutations that cause AD [227-229]. The presenilin proteins have a role in regulating ER calcium release and maintaining cytosolic calcium concentrations [230]. The presenilin mediated release of calcium has been shown to have a direct effect on reducing MMP, which in turn

can predispose cells to increased autophagy [227]. The presenilin-1&2 proteins are enriched in a specialized part of the ER called the mitochondrial associated ER membrane (MAM). The MAM sites are where the mitochondria and ER directly interact, and as they are enriched in presenilin proteins, the catalytic core of the γ -secretase enzyme, this may explain why mitochondria accumulate A β and why presenilin mediated calcium release leads to reduced MMP [231]. Presenilin mediated calcium release by the ER may lead to an increase in amyloid entering the mitochondria, which subsequently effects MMP. In cell models, application of A β to neurons has been shown to increase mitochondrial calcium levels via upregulating the inositol-1,4,5-triphosphate receptor-voltage-dependent anion channel (IP3R3-VDAC) contacts, also part of MAMs, [232]. This same paper showed that the IP3R3-VDAC contacts are increased in PM AD brain samples, although it is not stated if the PM samples come from patients with the familial or sporadic forms of the disease.

The fact the presenilin proteins are a key part of the MAMs highlights what is very likely to be an important difference in what determines the pathogenesis of the mitochondrial dysfunction in familial and sporadic forms of AD. Currently literature appears to suggest that the abnormal mitochondrial calcium concentration and signalling seen in AD is a direct effect of the A β and Tau proteins or caused by the presence of mutations with the PSEN1 & 2 genes associated with familial AD. Evidence of an inherent change in calcium concentration, or signalling abnormality is yet to be found, although as most models that investigate calcium signalling in AD rely on the pre-exposure to A β , then inherent calcium changes would be difficult to identify. It has been shown that MMP is reduced in both sporadic and familial AD patient cells, therefore as mitochondrial calcium concentration is dependent on MMP this may indicate that mitochondrial calcium concentrations are affected independently of the effect of amyloid and tau.

1.9.3 Mitochondrial ROS production in AD

Mitochondria are the main source of ROS production within a cell accounting for 90% of all ROS production [233]. As mentioned previously, ROS are used by cells as signalling molecules, but in AD the tight balance between production of ROS and breakdown is altered. As ROS molecules are difficult to study directly, often evidence of ROS activity is identified via the oxidization of biological molecules. In AD there is evidence of increased lipid, protein, DNA and RNA oxidation both centrally [234-237] and peripherally [238, 239] suggesting an increase in ROS production associated with the disease. As a result of the increased oxidation, cell physiology in AD is put under strain as the oxidized molecules either cease to function or develop abnormal function.

Studying patients with DS has shown that oxidative stress in AD is an early event. The brains of patients with DS develop oxidative damage years prior to the build up of the amyloid and tau

aggregates [240, 241]. This finding is also replicated in animal and cell models of AD which show increased oxidative damage prior to amyloid deposition [167, 242, 243]. In human PM brain tissue a greater level of oxidative stress is seen when compared to controls, but as the disease progresses and the build up of both amyloid and tau aggregates increases, the level of oxidative damage appears to reduce [236, 244, 245]. This has led researchers to suggest that the amyloid protein may have an increased expression in AD because it acts as an antioxidant against mitochondrially induced oxidative stress [234-236, 246]. This is an interesting theory, as it links several aspects of AD pathology together (mitochondrial dysfunction, oxidative stress, and protein aggregation) and also gives a physiological role to the amyloid protein, which has to a certain extent remained elusive.

Conversely, oxidative stress has been shown to be highest around AP within the brain of a mouse model of AD [243], although this does potentially contradict the findings from PM human brain studies showing less oxidative damage in brain areas with high amyloid load [235]. Fragments of the A β protein have been shown to have the ability to cause ROS production [247], and both β secretase activity and tau hyperphosphorylation have been shown to be increased by the activity of ROS [245, 247]. This suggests that mitochondrial ROS production may actually exacerbate the accumulation of amyloid and tau aggregates, as opposed to these proteins being produced as antioxidants. The A β protein can also interact with A beta-binding alcohol dehydrogenase (ABAD), a dehydrogenase which has roles in controlling mitochondrial exposure to oxidative stress [248]. Binding of A β to ABAD distorts the dehydrogenase's shape stopping the binding of NAD and increasing mitochondrial oxidative stress in both mouse models and human neuronal tissue. ABAD would normally bind to CypD, but in the presence of A β this reaction is impaired which can also lead to increased MPTP opening in AD neurons, and therefore increased risk of cellular death cascades being initiated [248, 249].

Mitochondrial efficiency in AD is likely to significantly affected by the increased damage seen by the production of ROS. It could be postulated that the AD brain expresses less dismutase enzymes, which are involved in the reduction of ROS. However, work on PM specimens has shown that the expression of these enzymes in AD brains is the same as found in control samples, with differential expression occurring in places of higher oxidative stress [244]. The ETC is the main site of ROS production in the mitochondria, which links the production of ATP with the production of ROS. The altered balance of ROS and oxidative stress within the AD brain further highlights the importance of understanding how the function of the ETC changes in AD. As the A β protein has been shown to potentially have both positive and negative effects on the level of ROS production in AD, this could be another example of how the capacity of mitochondrial function is key to the development of AD pathology. The A β protein may have an antioxidant role at the start of the disease but as the

capacity of mitochondrial function is already impaired, the antioxidant role of A β may not be able to rescue the established mitochondrial AD phenotype, leading to increased A β accumulation and to the development of more ROS.

1.9.4 Mitophagy and cell death in AD

There is a significant body of literature showing that the dynamics of mitophagy are altered in AD [250-258]. Most of these reports focus on the Pink-Parkin mitophagy pathway, but abnormalities in cardiolipin induced mitophagy have also been reported in AD mouse models [257]. It has been shown in several studies that there is an increased recruitment of Parkin to defective mitochondria in both CNS and peripheral cells in AD, but the mitophagic destruction of these mitochondria is impaired [255, 256, 259]. As the disease progresses, markers of mitophagy are shown to increase in both animal models and PM brain tissue, but the amount of Parkin available for mitophagy is reduced in the cytosol [259]. The reason for the build up of mitochondria signalled for mitophagy is not fully understood in the current literature, but there is evidence of lysosomal dysfunction (a key part of mitochondrial clearance) in cells that have either the PSEN1 mutations that cause AD [260], or express the ApoE ϵ 4 allele [261]. The cause for the increased recruitment of Parkin to the mitochondria is not fully understood but is very dependent on the depolarization of the MMP which, as described above, can be caused by amyloid interacting with the mitochondria. Amyloid also has a propensity to increase ROS production, which may also lead to increased Parkin recruitment, as a further signal to initiate mitophagy. Tau has an effect on mitophagy but experiments from animal and cell models have shown that tau can both increase Parkin recruitment to mitochondria [251] or stop its translocation from the cytoplasm [252, 253].

The literature on mitophagy in AD depends on research from PM brain samples or animal and mouse models which overexpress either the amyloid or tau protein. This means that understanding the changes in mitophagy that happen at the start of the disease, or if deficits in mitophagy occur prior to the onset of symptoms of AD is difficult. This is an important shortfall in the literature that is starting to be answered by using induced pluripotent stem cell models (iPSC) of AD.

As both ROS production and the dissipation of MMP can be key factors in determining whether a mitochondrion should undergo mitophagy, the function of the MPTP also has a key role in determining both the level of cellular mitophagy and cellular death. The function of the MPTP has been shown to be altered in AD with some studies showing a more constant activation of the pore in AD fibroblasts when compared to controls [262]. Constant opening of the MPTP exposes the cytoplasm to increased ROS and calcium release which can be signals for mitophagy and cell death. The A β protein has been shown to directly interact with CypD which increases the activation of the

MPTP [263, 264]. There is also evidence that the increased calcium concentration mitochondria are exposed to in AD, due to the increased number of MAM contacts, causes the MPTP to open more frequently to normalize matrix calcium concentration [262]. Inhibiting or knocking down the CypD protein in mouse and cell models, which essentially stops the formation of the MPTP, removes the toxic effect that A β has on the mitochondria [263]. This has led to the suggestion that blockage of the MPTP could be used as a therapeutic target in AD, but this negates the fact that MPTP has a physiological role. It is interesting that blocking of the MPTP stops the effect amyloid has on the mitochondria, but this work has only been performed in mouse models of a relatively young age. It is reasonable to conclude that blockage of the MPTP does not take into account any potential effects that minor changes in mitochondrial function may have on the development of AD, and also does not account for the other effects outside of the mitochondria that the amyloid has on many different cell organelles. Cell death can be mediated in many ways in AD via the actions of A β . As well as MPTP mediated cell death, A β has a direct effect on caspase signalling highlighting the complex nature of the disease [265].

1.9.5 Mitochondrial Trafficking in AD

As well as the described changes to both mitochondrial structure and function mentioned above, the trafficking of mitochondria within AD is affected [266]. Mitochondrial movement throughout the cell is performed by a specialized group of molecular motor proteins that use the cellular network of microtubules. The 2 major protein that perform this mitochondrial trafficking are Kinesin 1 and Dynein [267]. In general Kinesin 1 traffics proteins and organelles in an anterograde motion. In neurons this means movement away from the cell body and towards the synapse. Dynein in general moves cargos in a retrograde motion (towards the cell body) [268]. This movement of cargos via these molecular motors is ATP dependent, and sensitive to cellular calcium concentrations .

In AD the trafficking of mitochondria is affected in several ways. Oligomeric forms of A β have been shown to reduce both the anterior and retrograde movement of mitochondrial in neuronal cells, with anterograde movement effected to a greater extent than retrograde [266]. This has the effect of decreasing the number of mitochondria at neuronal synapses, which is thought to be one of the reasons for synaptic loss in AD. Mutations in the presenilin 1 gene which lead to the development of familial AD have been shown to impair axonal transport of mitochondria via increased phosphorylation of Kinesin 1 [269]. Tau hyperphosphorylation has also been shown to effect intracellular trafficking as increase phosphorylation and increased tau recruitment to the microtubule network affects the binding of the molecular motor proteins which again has the effect of reducing the movement of mitochondria through cells [270]. Increased calcium concentrations

also can stop mitochondrial axonal transport, which as this is another intracellular biochemical change seen in AD, may also contribute to altered cellular trafficking [271].

Disrupted mitochondrial transport through the cell will clearly have negative effects on cellular function. The obvious example of this being the effect that reduced mitochondrial trafficking to synapses has on synaptic function. Both tau and amyloid have an effect on this process, but clearly the effect of defective trafficking will be compounded by the altered ETC function and calcium homeostasis seen in AD. Cellular mitochondrial transport is an area of cellular function where several abnormal mitochondrial processes likely work together to cause a pathological effect.

1.9.6 Mitochondrial abnormalities in AD Summary

The research in the above sections highlights the key role that mitochondrial function and homeostasis has in the development and progression of AD. Functional deficits in the ETC lead to reduction in MMP and ATP generation, which affect the ability of mitochondria to meet the active demands of the cell in AD. Complex IV has been shown in multiple studies and in multiple cell types to have a reduced activity in AD, but functions of the other ETC proteins are also impaired. The pathological process of AD affects the ability of the mitochondria to store and buffer calcium, but it is not yet known if mitochondria have inherent calcium homeostasis deficits independent of the actions of tau and amyloid. AD mitochondria are more likely to produce ROS which leads to higher levels of cellular and mitochondrial oxidative stress, which as the disease progresses further disrupts the functions of the ETC. Mitophagy is increased in both the AD brain and peripheral cells, at the start of the condition, and becomes more affected as the disease progresses.

Much research has focused on how mitochondria function abnormally in the presence of either amyloid or tau. Less research focuses on whether deficits in the function of mitochondria are present within a cell without the addition of these pathological aggregates. Having a full understanding of the function of the ETC changes in AD that are independent of the build of amyloid or tau may help to identify a group of patients that have a mitochondrial phenotype to the disease. The function of the ETC is fundamental in maintaining calcium, ROS, and mitophagy homeostasis, so a complete understanding of any deficits that occur in ETC function would help to develop our understanding of how these mitochondrial functions are altered when amyloid and tau start to aggregate. Identifying changes in mitochondrial ETC function that are independent of amyloid or tau aggregation requires models of AD that source mitochondria from humans with the condition, and uses model paradigms in which the mitochondria are maintained in a system that is as close to what is seen *in vivo* as possible. Mitochondrial deficits are seen very early in the course of AD so a better understanding of how the mitochondrial ETC function predisposes people to the condition may open

a pathway to earlier diagnosis and treatment. Figure 1.6 summarises the changes seen in mitochondria in AD.

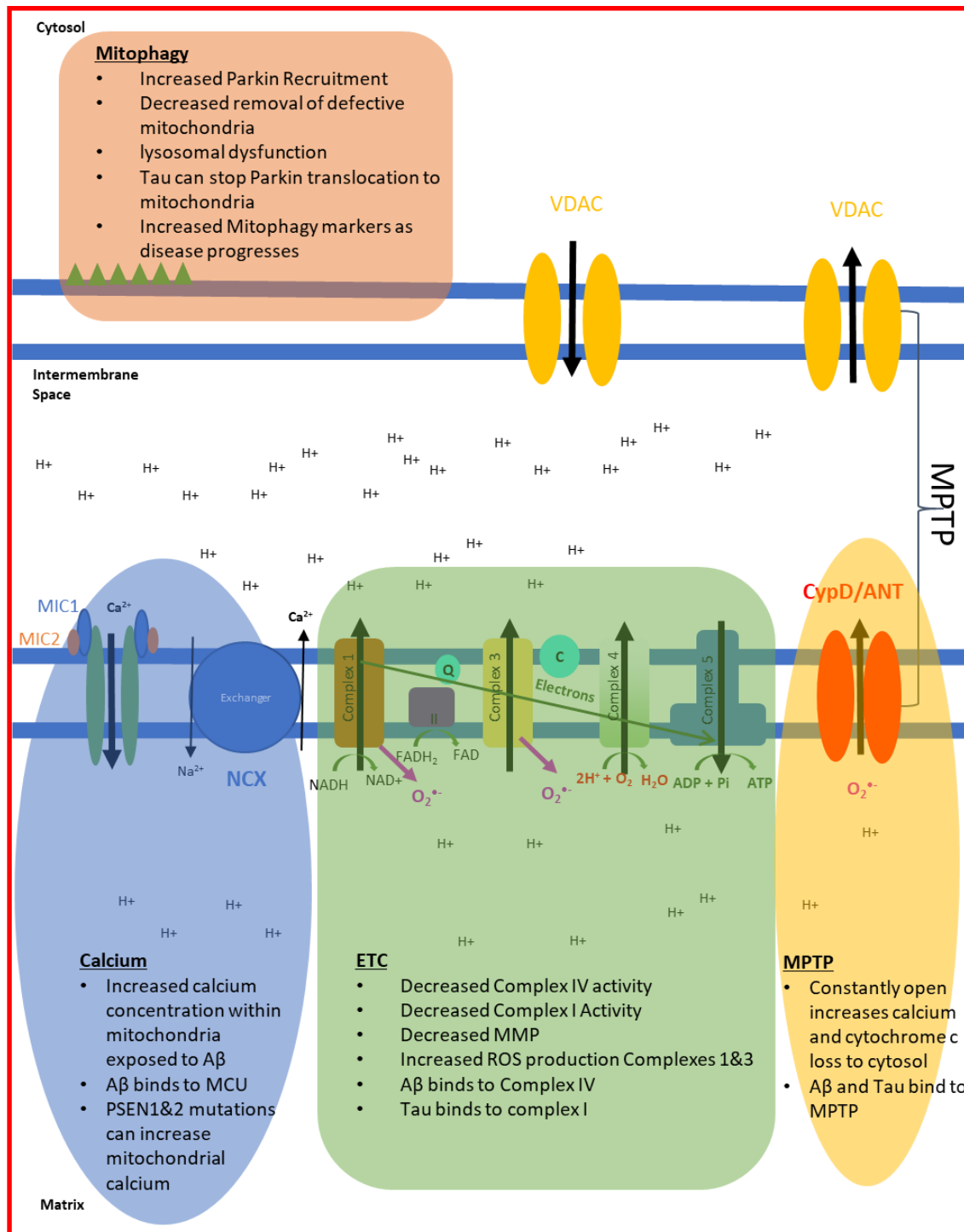


Figure 1.7| Changes to mitochondrial function seen in AD Highlighted in this figure are the different pathological changes that occur to the mitochondria through the course of AD. **Mitophagy** changes are highlighted in orange, **calcium** metabolism in blue, **electron transport chain (ETC)** changes in green and changes to **the Mitochondrial Permeability Transition Pore (MPTP)** in yellow.

1.10 Glycolysis

Glycolysis is the conversion of glucose to pyruvate or lactate which results in the generation of ATP and metabolites for metabolic pathways including the citric acid cycle and fatty acid metabolism [124]. This process is common to all cells within the human body and allows for a more rapid generation of ATP than OxPHOS. Conversion of glucose to pyruvate generates ATP via the actions of the phosphoglycerate kinase (PGK) and pyruvate kinase (PK) and consumes ATP via the action of hexokinase (HK) and phosphofructokinase (PFK). NADH is created in the glycolytic pathway via the action of glyceraldehyde-3-phosphate dehydrogenase (GA3PDH), and consumed by lactate dehydrogenase [272]. Glucose-6-phosphate, the product of the action of HK on glucose and the first step in the glycolytic pathway, can be utilized by other metabolic pathways including the pentose phosphate shunt (PPS) and gluconeogenesis. Figure 1.7 shows the glycolytic metabolic pathway and the fates of the different products of glucose metabolism. The following sections will discuss how glycolysis and its associated metabolic pathways are affected in AD.

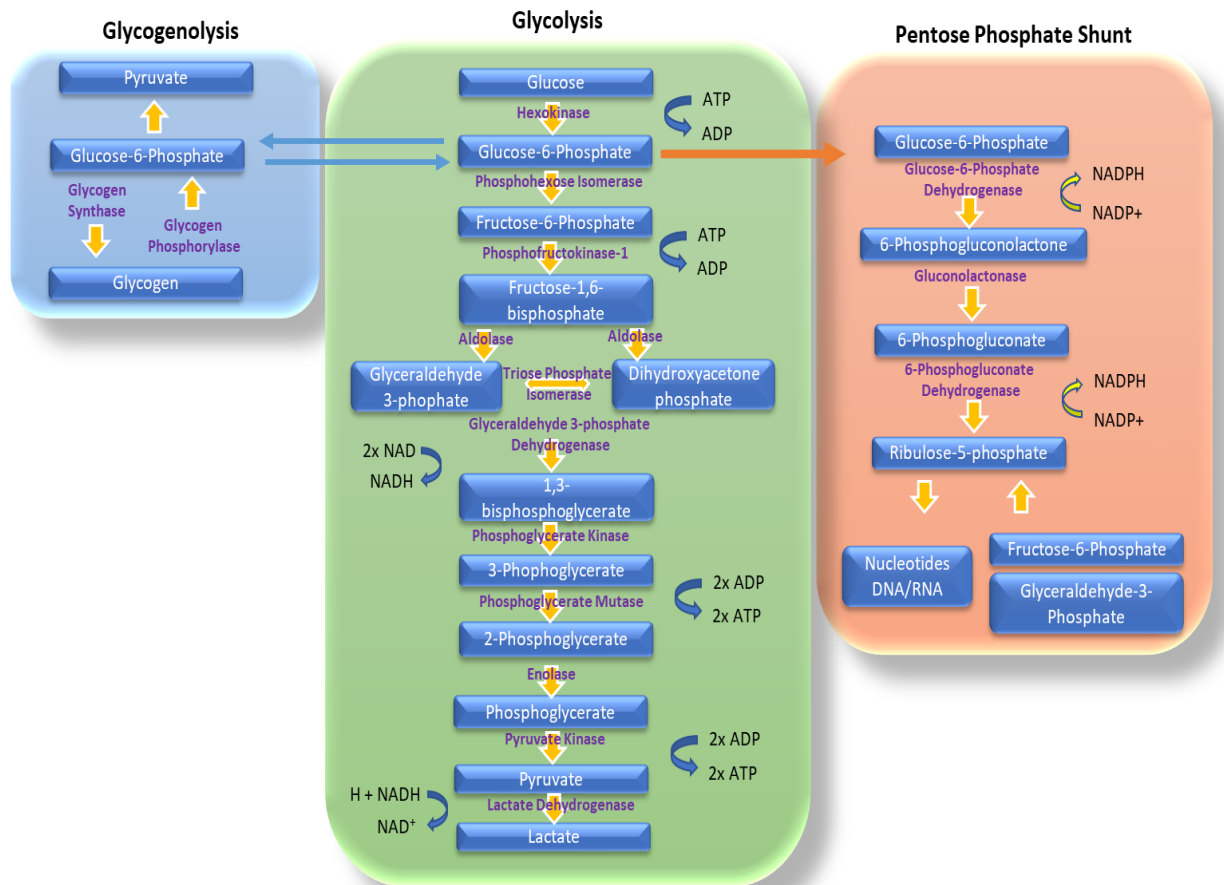


Figure 1.8| Glycolysis and other glucose metabolic pathways Highlighted in this figure are the different enzymes and substrates involved in the metabolism of glucose via, **glycolysis** (green box), **glycogenolysis** (blue box) and in the **pentose phosphate shunt** (orange box). Sites of ATP, NADPH, NADH, and ADP generation are shown. Sites of transfer of glucose products between metabolic pathways are highlighted with blue arrows for movement into glycogenolysis and orange for movement through the pentose phosphate shunt.

1.11 Glycolysis in AD

1.11.2 Changes to glycolysis in AD

Glycolysis is a metabolic pathway utilized to great effect by the brain. At times of increased brain activity glycolysis can offer a rapid supply of ATP, even though glycolysis produces less molecules of ATP per glucose molecule consumed when compared to OXPHOS [273]. Unlike OXPHOS, glycolysis can be directly observed in the human brain using radioactive forms of glucose such as 2-[18F] fluoro-2-Deoxy-D-glucose (FDG). Using -[18F]fluoro-2-Deoxy-D-glucose positron emission tomography (FDG-PET) a reduction in glucose metabolism has been seen in both ageing and AD [274], although this shift accounts for glucose consumed in both glycolysis and other metabolic

pathways [41]. Aerobic glycolysis can be imaged within the brain also, which has also shown that as the brain ages aerobic glycolysis decreases [275]. In AD there is a reduction in aerobic glycolysis in brain areas susceptible to amyloid deposition [41], and in brain areas where high levels of tau accumulation is seen [42]. The change in brain glucose metabolism seen on FDG-PET imaging in AD is relatively specific, and reveals a temporal-parietal pattern of low glucose metabolism, which can be used to diagnose AD clinically [276]. Whole brain imaging of glucose is a useful tool to identify regional changes in glycolysis, but the resolution is not high enough to allow for understanding of which particular brain cell type is affected by the change in glycolysis, and to what extent. Brain imaging can also not identify specific changes in the functions of enzymes of glycolysis, nor identify if certain brain glucose receptors are up or down regulated in AD.

PM brain samples have been able to identify changes in key glycolytic enzymes in AD.

Phosphofructokinase (PFK) has been shown to be elevated in the temporal and frontal lobes of patients with sporadic AD [277], and potentially these changes in PFK function occur in glial cells, as PFK enzyme colocalizes with glial fibrillary acidic protein (GFAP) [278]. Lactate dehydrogenase (LDH) and pyruvate kinase (PK) enzymes involved in the generation of both lactate and pyruvate have both been shown to be significantly increased in the temporal and frontal lobes [278] of PM AD brain specimens. One study looking at neurons from PM samples using mass spectroscopy quantified glycolytic enzyme protein expression in AD showing a down regulation of PK, enolase, aldolase A, aldolase C, and up regulation of glyceraldehyde-3-phosphate dehydrogenase (G3PDH) [279].

Interestingly, most PM studies show a general upregulation in glycolytic enzyme protein, but brain imaging studies suggest a low glucose uptake by the brain in AD which is potentially an area of contradiction between the two research techniques. These differences might be explained by the reduction of glucose transporters (GLUT1 & 3) seen within the brain as the disease progresses [280]. Increased enzyme expression may be a response to reduced glucose availability caused by a reduction in the GLUT1 & 3 receptors. Increased glycolytic enzyme protein may also be a compensatory response to the deficits in mitochondrial function seen in AD as the disease progresses.

These imaging and PM studies are both limited by the fact that they have participants with either established AD or end-stage AD. For this reason, it is difficult to ascertain whether the detected changes in glycolysis occur at an early stage of disease or as a result of another pathological mechanism such as amyloid deposition.

Glycolytic enzyme activity changes are also seen in non-CNS cell types. Familial AD fibroblasts and leukocytes have reductions in hexokinase (HK) activity, but no changes in LDH or PFK activity [281].

In the same paper, differences between sporadic and familial AD are reported, as sporadic AD leukocytes do not have reductions in glycolytic enzyme activity. Fibroblasts from patients with sporadic AD rely more on glycolysis as the disease progresses, but cannot increase their glucose intake [282]. Kaminsky and colleagues (2013) have shown that red blood cells (RBC) have increased HK, and PFK activity, compared to aged-matched controls, but not to younger controls, which have similar levels of activity to the AD RBC [283]. It is worth mentioning that peripheral cell glycolysis in AD has been investigated much less than peripheral mitochondrial function.

Differences in neuronal and astrocyte metabolism have been shown in various animal models of AD. In the Tg2576 mouse at 24 months of age reduced PFK activity is seen in neurons, but not astrocytes [284]. In an APP/PSEN1 mouse model lactate levels are higher when compared to control mice of the same age and this is detrimental to learning tasks [285]. Interestingly, in wild type mice lactate levels in the brain decrease with age and, by increasing the expression of lactate producing enzymes (pyruvate dehydrogenase kinase [PDK] and LDH), mouse memory can be improved. This is not the case in the APP/PSEN1 mice, where overexpressing the enzymes is actually detrimental [285]. These enzymes are expressed in the soma of neurons in control mice, but in both the soma and around AP plaques in APP/PSEN1 mice astrocytes. This data suggests that the amyloid build up affects glycolysis in different ways depending on CNS cell type. This is also further evidence to support the need to study astrocyte glycolytic function specifically, as enzyme changes in astrocytes seem to be detrimental to learning generally and more specifically in the context of AD. In a different APP/PSEN1 mouse model, increased glucose metabolism via glycolysis is seen before amyloid plaque deposition [286]. These authors suggested that these changes to metabolism are neuron specific as they detected no increase in glial acetate metabolism.

In many cell model systems of AD the addition of amyloid to the cells shows an increase in glycolysis and suggests that the cells undergo the Warburg Effect, by which cells upregulate glycolysis and start to depend on it more than OxPHOS for energy production [287]. This is often seen in tumour cells from cancer patients and is thought to be a way the cell manages the generation of ROS produced by the OxPHOS in mitochondria. In a paper by Soucek and colleagues (2003), the cell lines B12 and PC12 were grown in a media containing amyloid until the cells became resistant to its effects [288]. As the cells became resistant to amyloid, they up regulated glycolysis enzymes. The authors suggest that this might explain why brain homogenate samples taken at the end of disease have raised glycolysis enzymes. The suggestion being that the cells that survive to the end of the AD pathological process have a greater ability to utilize glycolysis than those that succumb to the progression of pathology. The findings are also in line with research from mouse models suggesting that astrocytes can upregulate glycolysis in response to amyloid. B12 cell lines are not naturally resistant to A β and

normally show a reduction in ATP production thought to be due to a reduction in glycolysis activity from ROS inhibiting enzyme function [289].

Very few studies exploring the changes in glycolysis in AD cells in all model types do this without first exposing a cell or animal model to A β . As a result of this little is known about what changes happen in the glycolysis pathway before the deposition of amyloid. This highlights another important question that has been difficult to answer to date due to model systems available.

1.11.3 Changes to the pentose phosphate shunt in AD

The pentose phosphate shunt (PPS) is a branch of glycolysis where glucose-6-phosphate can be converted to ribose 5-phosphate, and via this conversion produces 2 molecules of Nicotinamide adenine dinucleotide phosphate (NADPH). Ribose 5-phosphate is a sugar that can be used in the synthesis of nucleic acids, whereas NADPH is an important reducing equivalent that helps to protect the cell from oxidative stress [290]. It is estimated that 10-20% of glucose consumed by a cell is metabolized via the PPS. Fructose-6-Phosphate and glyceraldehyde-3-phosphate, both intermediate products of glycolysis, can also be metabolized in the PPS, but their metabolism to Ribose 5-phosphate does not lead to NADPH production. Figure 1.7 highlights the major steps in the PPS.

Evidence from both PM brain tissue and animal models suggests that the PPS enzymes glucose-6-phosphate dehydrogenase and 6-phosphogluconate dehydrogenase have increased activity in AD [288, 291, 292]. These enzymes are the sites of NADPH reduction, and it is believed that the upregulation of these enzymes is a direct consequence of the increased oxidative stress seen in AD. Metabolomic studies of the blood from patients with AD has shown that the whole PPS pathway is upregulated in AD [293], suggesting that the oxidative stress of AD is not just seen within the CNS. The protection from oxidative stress offered by the PPS is also thought to contribute to the survival of neurons when subjected to A β . B12 and PC12 cell line experiments have shown that increased flux of glucose through glycolysis and the PPS increases the likelihood of survival when toxic concentrations of A β are added to the cells [288]. As the brain's ability to uptake glucose diminishes both with age and the progression of AD, it is likely that the protective effect of the PPS system is impaired, which will further exacerbate the unfavourable metabolic environment the brain is exposed to through the course of AD. This hypothesis is evidenced by a study that investigates NMR spectroscopy in a mouse model of AD which shows as the disease progresses, glucose products move less through glycolysis and the PPS [294]. Targeting the PPS as a way to improve oxidative stress within the AD brain has potential as a therapeutic strategy, but consideration has to be taken about the capacity for glucose uptake by different types of CNS cell as this will be a key limiting factor.

1.11.4 Glycolysis in AD summary

Glucose is a key energy metabolite for the brain and several elements of its metabolism and storage appear to be affected in AD. The AD brain is less sensitive to glucose, but interestingly appears to have increased levels of glycolytic enzymes. This potentially is a combination of reduced uptake and abnormalities in mitochondrial function leading to an increased reliance on glycolysis. The branch metabolic pathways for glycolysis also appear to be affected in AD with PPS upregulation seen as a likely response to increased oxidative stress.

Research to date indicates that amyloid can increase glycolysis, and likely PPS function in AD directly, but evidence is more limited as to if the AD brain has glucose metabolism defects that are independent of amyloid build up. The above papers also show the pivotal role the astrocyte has in glucose brain management. Further research is needed to develop our understanding of inherent brain glycolytic deficits and what role the astrocyte plays in these.

1.12 Other metabolic pathways affected in AD

Several other metabolic pathways have been shown to have abnormalities in AD:

1.12.1 Malate-Aspartate shunt

The malate-aspartate shunt (MAS) is a metabolic pathway that allows NADH generated via glycolysis to cross the inner mitochondrial membrane. This NADH can then be used by the ETC, and also helps to maintain the NADH/NAD⁺ ratio of the cytoplasm [295]. PSEN1 mouse models have shown that as the mouse ages, key enzymes in the MAS (malate dehydrogenase, aspartate aminotransferase, and glutamate aspartate transporter) have increased expression, potentially related to altered cytosolic calcium concentrations [296]. PM AD hippocampal and entorhinal cortex samples have suggested inhibition of MAS activity evidenced by low aspartate and high malate levels, thought secondary to increased ammonia concentrations [297]. There is debate over the significance of the MAS function within the brain though, and it is thought that neurons are the only site of MAS activity [298].

1.12.2 Fatty acid metabolism

Fatty acid metabolism has been shown to be extensively altered in AD in both the CNS [299] and non-nervous system cells [300]. The diverse nature of fatty acids has led to the suggestion that the alteration in their metabolism, leading to different proportions of certain fatty acids, could be developed into an AD biomarker [299, 301]. There is evidence that their abnormal metabolism seems to be linked to the deposition of amyloid and tau [299]. A full review of fatty acid metabolism changes seen in AD is outside the scope of this thesis.

1.13 Metabolic cooperation within the brain

Neurons as a cell type are highly dependent on OxPHOS to meet their energy needs. Originally it was believed that the vast majority of energy consumption by neurons was as a result of action potential transmission. It has since been shown that the vast majority of energy expenditure for neurons and the brain as a whole is to maintain ion gradients within cells, and also to recycle neurotransmitters [302]. In order to be able to maintain these crucial functions, the brain relies on the metabolic function of astrocytes. The primary example of this co-operative metabolic relationship is at glutamatergic synapses [303].

Glutamatergic synapses are the major excitatory synapse found within the brain and account for 80% of all synapses [304]. A synapse in its most basic form is a connection between 2 neurons, which is extensively covered by the end feet processes of an astrocyte “the tri-partite synapse”. When glutamate is released into the synapse, this causes an increase in the concentration of potassium at the synapse. To maintain the potassium and glutamate synaptic concentrations, astrocytes take up both substances in exchange for a sodium ion [303]. When a neurotransmitter such as glutamate is released from a neuron, this activates a calcium wave within the surrounding astrocyte, which via gap junctions, can be propagated through many astrocytes. The process of glutamate uptake by astrocytes is ATP dependent and the calcium influx into the cell may stimulate ATP generation for this uptake. The rate of glutamate uptake by the astrocyte controls the rate of post synaptic signalling, so has a direct effect on LTP and LTD.

Once inside the astrocyte, the glutamate has several potential fates. It can be converted to glutamine, at the expense of another molecule of ATP and then transported back to neurons to replenish glutamate and γ -aminobutyric acid (GABA) stores. The glutamate can be also converted into alpha-ketoglutarate, and metabolized via the TCA cycle to produce ATP for the astrocyte [305]. The ATP used in the metabolism of glutamate has been shown to come from glycolysis, with an estimated 80-90% of all brain glycolysis utilized to maintain glutamate synaptic balance [306]. The glucose used by the astrocyte for glycolysis comes from the blood stream, with several studies showing that as brain activity increases, blood flow is diverted by astrocytes to the active brain regions [307]. This research has shown that FDG-PET signalling is directly measuring the function of glutamatergic synapses.

As stated, neurons are very OxPHOS dependent, and in fact if glycolysis is increased in neurons, they develop increased oxidative stress from lack of PPS usage. At times when neurons need to increase their energy expenditure instead of increasing the utilization of glycolysis, TCA substrates are generated from lactate, which allows glucose consumed by the neuron to be used for PPS pathway

metabolism and antioxidant production [308]. The main source of lactate within the brain has been shown to be the astrocyte, with a large body of evidence now suggesting that lactate made by the astrocyte is shuttled to neurons via an astrocyte neuron lactate shuttle (ANSL) [309, 310], allowing the neuron to maintain physiological function at times of increased energy demand, without upregulating neuronal glycolysis. Glycogen is a source of glucose for astrocytic glycolysis and lactate for potential neuronal usage. As described above astrocytic glycogen has been shown to be a necessity for LTP and memory formation [311, 312]. The role the astrocyte has in maintaining neuronal synaptic homeostasis is likely to be the reason glycogen is critical to memory formation. Figure 1.8 shows the metabolic cooperation that exists between the astrocyte and neuron at a glutamatergic synapse.

As the astrocyte has a key role in maintaining neuronal metabolism at glutamatergic synapses any deficits in its metabolic function are likely to precipitate brain disease states. The astrocyte has been shown to be extensively altered in AD, however its metabolic function has been difficult to investigate due to the limitation of animal and PM models. The next section will describe the role of the astrocyte in AD and how astrocytic metabolism could be investigated in a human cell model system.

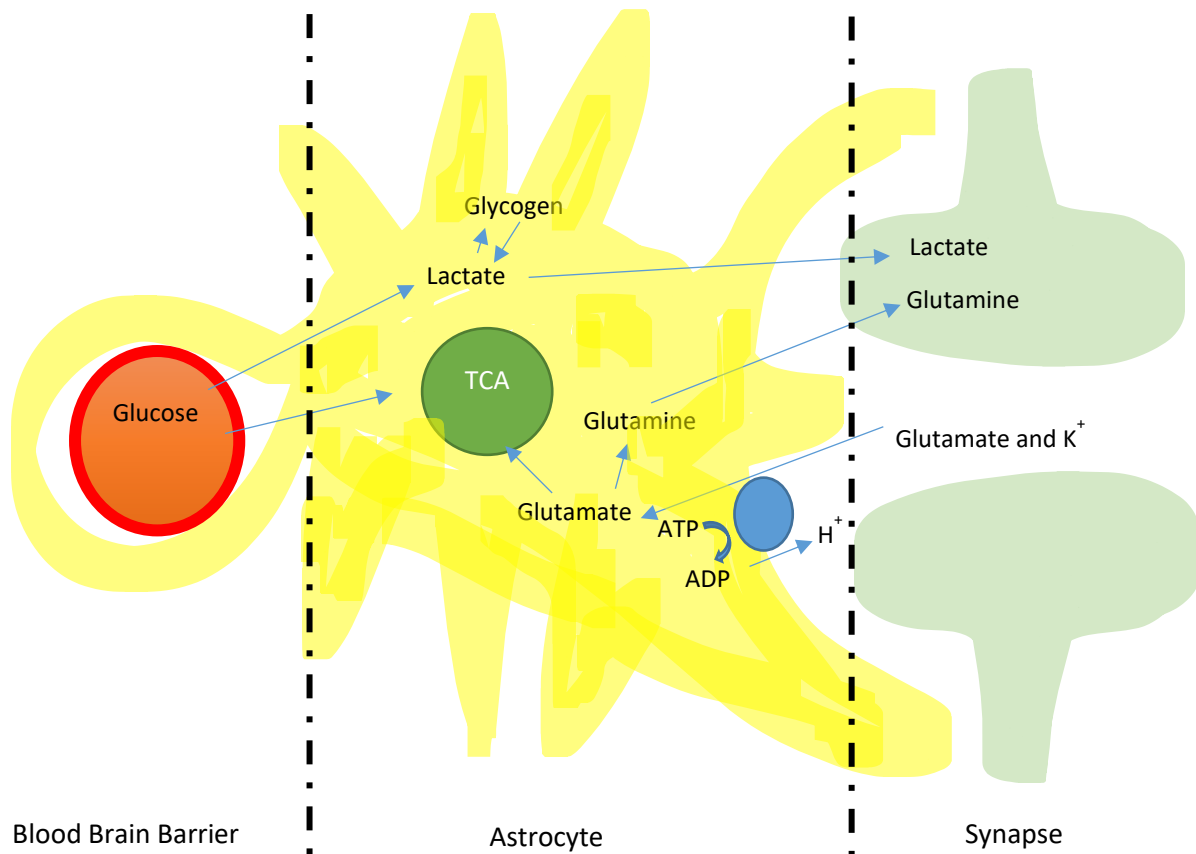


Figure 1.9 | Astrocyte neuronal co-operation This figure highlights how that glutamatergic synapse is dependent on the function of the astrocyte for its maintenance. The astrocytes removes glutamate and potassium from the synaptic cleft and can supply the neuron with both lactate and glutamine to maintain metabolism and neurotransmitter concentrations. Lactate can come from many sources including glutamate breakdown, blood glucose and astrocyte glycogen. The astrocyte is able to modulate blood flow to specific brain areas dependant on glucose demand and glutamatergic synapse activity.

1.14 The astrocyte in AD

Astrocytes are the most abundant cell-type within the brain and have a critical role in maintaining the homeostasis of this organ [313]. In particular, they function as a life support system for neurons providing them with metabolic support in times of increased energy expenditure. One example of this is the provision of lactate to neurons via the lactate shuttle [314], as described above.

The astrocyte maintains synaptic homeostasis, synthesizes cholesterol, and removes waste products produced by neuronal cells. The homeostatic maintenance role the astrocyte performs relies on the cell being extensively linked, via gap junctions, to other astrocytes and ependymocytes, so they can

deposit unwanted neurotransmitters, and ions to distant sites outside of the central nervous system [315]. Astrocytes can have a wide variety of shapes, with some processes that surround neuronal synapses being so narrow in diameter that mitochondria cannot pass into them [305]. This clearly will have consequences with regard to metabolic processes that can function in this specialized area of the cell. As described above, astrocytes are particularly important in processes such as maintaining synaptic function and form [316-318]. The astrocyte also has a key role in recycling synaptic content and provides multiple metabolic substrates for neuronal use. This functionally diverse cell also forms part of the Blood Brain Barrier (BBB) and regulates the immune response [319].

In vitro studies have shown that the astrocyte has a role in Amyloid Precursor Protein (APP) metabolism [320], and removal of A β [321]. When astrocytes are treated with amyloid beta this up regulates glucose uptake, glycolysis and tricarboxylic acid cycle activity [322]. In mouse AD models it has been shown that increased astrocyte A β uptake effects the astrocytes ability to support neuronal survival in co-culture, which is thought in part to be due to the observed increase in glycolysis [322]. It appears that when the astrocyte uptakes A β this increases the astrocyte oxidative stress, which it then employs glycolytic pathways which generate NADH reducing equivalents to protect itself. This leads to an increase in astrocyte glucose utilization which is at the expense of passage of glycolytic substrates to the neuron. Uptake of A β by astrocytes also makes them develop an inflammatory/activated phenotype which correlates better with memory impairment in mouse models of AD than the deposition of A β alone [323]. A proinflammatory phenotype for an astrocyte also increases its glycolytic pathway usage as the intracellular proinflammatory environment within the cell leads again to increased ROS production and deploying of mechanisms to control this [324]. Transgenic mice studies suggest defects in astrocyte metabolism as an initiating factor in AD [325]. In this study the astrocytes from an AD mouse model are shown to have reduced glycogen stores, which may be as a result of the increased glycolysis seen in AD mouse astrocyte models described above. By replenishing this glycogen, the AD mice do not develop elements of the pathology induced by over expression of A β . These *in vitro* studies highlight how two key pathological markers of AD, that of amyloid build up and increased brain inflammation have potential to affect key metabolic pathways within astrocytes, which then lead to an inability to support neuronal function.

Consideration has to be made for the fact that these studies are performed in mice, which have very functionally different astrocytes to those found in humans, which may affect result interpretation. The implementation of these results in describing how sporadic AD affects astrocyte function in the human brain may not be appropriate as these models depend on a starting point of increased amyloid expression. Studies on human astrocytes would help to confirm that these *in vitro* findings

are applicable to the human disease. To understand if the *in vitro* findings for changes in glycolysis are seen in human astrocytes living human astrocytes need to be studied.

There are examples of astrocyte abnormalities found in AD mouse models being replicated in human AD astrocytes. A recent study has even suggested that a specific sub-type of astrocyte is seen in the AD brain and mouse models, dubbed the “AD astrocyte” [326]. This particular astrocyte has an inflammatory gene transcription phenotype, with upregulation of genes also involved in endocytosis, the complement cascade, ageing and amyloid accumulation. The AD astrocyte is seen in the aged human brain as well but presents itself much earlier in the AD brain. It is unknown if this particular astrocyte subtype occurs as a consequence of amyloid production or is always present in the AD brain.

Research on human PM brain tissue from patients with AD has also revealed that the astrocyte is changed through the course of AD. Human astrocytes taken from PM AD brains show multiple biochemical abnormalities in AD including perturbations of insulin signalling [327, 328], cellular calcium homeostasis [329], glutamate synaptic homeostasis [235] and oxidative stress response [330]. Insulin signalling in astrocytes is involved in several different biological processes including cell growth and proliferation, autophagy, and protein translation. PM astrocyte specimens from AD brains show a down regulation in this signalling cascade, which potentially could affect these vital cellular processes. Interestingly, down regulation of the insulin and insulin-like growth factor 1 signalling pathways in astrocytes has been shown to be associated with decreased complex I activity of the mitochondrial ETC [331]. Complex I gene expression down regulation has also been shown in astrocytes from the precuneus in AD PM brain specimens [332]. The reason for down regulation of complex I in both scenarios may be due to astrocyte exposure to increased oxidative stress. Complex I could be down regulated in this situation to reduce the rate of OxPHOS, and therefore decrease further ROS release. This potentially would put further pressure on the glycolytic pathway in the AD astrocyte, which as described above is already affected by both amyloid build up and inflammation.

The abnormalities in calcium signalling in AD astrocytes seen in PM specimens may also affect mitochondrial function. Calpain-10, a calcium signalling protein known to cause calcium induced mitochondrial dysfunction, has been shown to have increased expression in astrocytes which have higher Braak AD tau scores in PM brains [333]. The expression of glutamate receptors on astrocytes changes as AD pathology progresses, with reductions in the glutamate excitatory amino acid transporter 2 (EAAT2) seen later in disease [235]. The increased oxidative stress response seen in AD astrocytes is likely to be caused by a combination of factors including the changes to glutamate receptors, calcium signalling, amyloid uptake and development of an inflammatory phenotype.

Work on PM AD astrocytes from the Cognitive Function and Ageing (CFAS) study has defined the cellular pathology of astrocytes occurring early in AD progression. This includes: the development of gliosis [235, 334], which is a process astrocytes can undergo which changes their morphological structure and protein expression profile, that can be a response to inflammation, protein build up or physical trauma [335]. The ability of the astrocyte to respond to damage caused to its own DNA or the “DNA damage response” is also effected early in the course of AD [336]. DNA damage response changes are thought to lead to changes in insulin and Wnt signalling, which in turn leads to increased activity of the Glycogen synthase kinase 3 β (GSK3 β) enzyme which causes the hyperphosphorylation of tau [329, 337]. The DNA damage response may also be linked to the increased ROS production that occurs in astrocytes as a result of the increased amyloid exposure and the pro-inflammatory environment. Changes to both astrocyte morphology such as that seen in gliosis, and unopposed alterations to the astrocyte DNA, will also have an effect on the metabolic and homeostatic roles that the cell performs for itself and neurons.

Work investigating the astrocyte in AD PM samples have described changes to protein expression and cellular stress that altered metabolism observed in animal AD models may explain. Where a gap exists in the research literature is a causal link between changes seen in animal models of AD exposed to amyloid and tau, and the PM changes seen in the AD human astrocytes. Systems that are able to replicate the findings of animal models in living human AD astrocytes would help to identify what the causal link might be. Reviewing the literature from PM AD astrocyte studies also reveals that the majority of changes seen in the astrocytes are potentially linked to the metabolism of this cell type, and potentially increased ROS production. Astrocytes have been shown to be very glycolytic cells, and therefore in the next section changes to glucose, storage and breakdown will be discussed as this will affect both astrocyte metabolism and ability to respond to ROS induced stress.

1.14.1 The astrocyte and glucose storage in AD

Astrocytes are the main site within the brain that glucose can be stored as other molecules [338]. Glucose through its conversion to glucose-6-phosphate can be stored within the brain as glycogen [339]. Astrocytic glycogen has been shown to be a key metabolic substrate of learning and memory [311, 312, 340]. Astrocytic glycogen breakdown has also been shown to be important in the astrocyte’s ability to maintain potassium concentrations in the extracellular space after prolonged neuronal transmission [341, 342], and has a role in maintaining glutamate homeostasis via its actions on the enzyme carbonic anhydrase [341]. Interestingly, several of the above glycogen dependent processes in astrocytes actually use glucose or lactate as the effector molecule. The amount of glucose required for each of the above processes is available within the brain without the need to breakdown glycogen and so it remains to be discovered why the brain is organized to need

glycogenolysis to maintain these metabolic processes. Figure 1.7 highlights the major steps in Glycogenolysis and Glycogenesis

In AD it has been shown that the amylose glucose storage molecule is increased in astrocytes from AD brain and mouse models [343]. Amylose is resistant to glycolytic enzymes so effectively takes a proportion of stored glucose out of metabolic circulation. An abnormal form of glycogen called polyglucosan accumulates in the brains of people with AD in the form of polyglucosan bodies (PGB) [344]. This molecule does not have the same branch points as glycogen and again cannot be metabolized by normal glycolytic enzymes. The amount of glucose within the AD brain has been reported as being 3 times as high as that seen in controls, which may be because the amylose molecule is more abundant, decreasing the useable glucose proportion.

An enzyme that can metabolise glycogen back into glucose, α -amylase, has been shown to have both increased activity and increased protein expression in the AD brain [344, 345]. Upregulation of this enzyme may be because of the increased abnormal forms of glycogen stored in the AD brain which lead to an effective glycogen deficit. The data from the above studies suggests that significant quantities of glucose taken up by the brain may not be able to participate in glycolysis due to the abnormal storage of glucose as either amylose or PGD. This will almost certainly have repercussions for maintaining ion gradients within the brain and the effectiveness of learning and memory. These studies also highlight the key role the astrocyte has in maintaining the glucose homeostasis of the brain.

Gluconeogenesis is the process by which glucose can be generated from non-carbohydrate carbon sources such as proteins, and pyruvate. Gluconeogenesis was classically thought not to be seen within the brain, but recent studies have shown astrocytes have the key enzymes needed for this pathway [346]. Systematically it has been shown in metabolomic mouse AD models that gluconeogenesis is impaired in the liver and kidneys (traditional sites of gluconeogenesis) [347], but data on astrocytic gluconeogenesis changes has not yet been identified. Gluconeogenesis has common steps with glycolysis and has potential to contribute to the metabolic changes in AD astrocytes.

1.14.2 Astrocyte AD summary

Although post-mortem evidence suggests that astrocytes an abnormal structure in AD, and animal models suggest a role for altered astrocyte metabolism [322], limited data exists on whether astrocytes have deficits in OxPHOS or glycolysis in AD. Disruption of these pathways would have a profound effect on the astrocyte's ability to perform roles that have a high energy demand and could contribute to the astrocyte abnormalities seen in AD described above. Any defect of astrocytic

energy utilization and/or provision could result in failure of brain homeostasis and lead to synaptic loss and impaired neuronal survival. Developing compounds to correct abnormalities in mitochondrial function or glycolysis in astrocytes might therefore provide a novel therapeutic approach for AD. Astrocyte function and gene expression is very different between animals such as mice and rats, often used to model AD, and humans [348]. Therefore, to understand mitochondrial function and astrocyte metabolism a living human cell model of astrocytes derived from people with AD is needed. The development of induced pluripotent stem cell technologies has allowed for this type of experimental model to be created.

1.15 Inducible pluripotent stem cell models of Neurodegenerative disease

The ability to reprogram a terminally differentiated cell into an induced stem cell was originally described by Yamanaka and Takahashi [349]. This cellular modelling method takes terminally differentiated cells such as fibroblasts, mesenchymal stem cells or leukocytes and transduces the cell with viruses, such as adenoviruses, that contain several pluripotency inducing genes (Oct3/4, Sox2, c-Myc, and Klf4). These genes are expressed in the host cell and this differentiated cell can then develop pluripotency again, becoming an induced pluripotent stem cell (iPSC). In the original paper by Yamanaka and Takahashi, 24 different genes were investigated for the abilities to induce pluripotency in terminally differentiated cells. Of these 24 different genes it was found that Oct3/4 and SOX2 are essential to maintain cell pluripotency, and that c-Myc and Klf4 were needed to maintain cell proliferation. Nanog also induces pluripotency in terminally differentiated cells, but is not essential for the process like SOX2 and Oct3/4 [349]. As this technology has developed further it has been shown that cells can be reprogrammed with using just c-Myc or Klf4 and both factors are not required [350].

The power of iPSC technology can be seen in the multitude of research fields these techniques have been applied to. In the field of human disease research, applications are seen in cardiovascular disease [351], liver disease [352], and respiratory illnesses [353]. The technology has increasingly been used to study and model neurodegenerative disorders; including motor neuron disease (MND) [354], Parkinson's disease [355], and AD [356]. In neurodegenerative research, this technology offers the opportunity to study nervous system cells from human subjects with the condition of interest. For research into metabolism in neurodegenerative disease, iPSC are living cells which allow for metabolic function to be studied directly. This is an important model system for AD research as it allows for the study of organelles such as the mitochondria to be investigated in a more physiological environment. This particular system is also important for understanding how different pathological elements of the AD process interact in a living system. iPSC technology allows for both glycolysis and mitochondrial function to be studied together without developing a system in which

only the presence of amyloid defines it as an AD model. The following sections will describe the use of iPSC technology in AD research.

1.15.1 iPSC Models of Alzheimer's Disease

1.15.2 iPSC AD Neurons

iPSC technology has been applied to AD research for at least the last 8 years. Several different types of neurons have been created from patients with both sporadic and familial forms of AD. Standard neuronal differentiation protocols have been used which generate cells positive for the neuronal markers β 3-tubulin and Microtubule-associated protein 2 (MAP2) [356-359], but protocols based on that described by Shi et al (2012) [360] have also been used to develop cortical neurons [361-363], and basal fore brain cholinergic neurons [364]. Both two dimensional [356-359] and three dimensional cultures have been created from AD iPSCs [361, 365, 366], and to try and understand how the passage of time effects the secretion of AD associated protein aggregates, cortical neurons have been created from patients with DS prior to the development of dementia [358, 367].

As this technique is relatively new the majority of early AD iPSC research focused on whether this cell model can recreate the pathology of AD in neurons. Multiple groups have shown that iPSCs used to generate neurons from AD patients can express the pathological proteins seen in AD, and have a similar gene expression profile to PM AD neurons [368, 369]. iPSC AD neurons have been shown to have an increased A β 42/40 ratio [356, 359, 361, 367, 370-372], show hyper phosphorylated tau molecules [356, 358, 360, 371, 373-376], have both beta-secretase and Glycogen synthase kinase 3 beta activity [358, 374, 377], and can secrete A β into the extracellular space [356, 360, 378]. Using iPSC derived neurons has developed our understanding of how tau might propagate in the AD brain. Mis-folded tau, as seen in AD and many other neurodegenerative diseases, has been shown to spread from one neuron to another through neuronal activity in iPSC neuronal models. Once in the new neuron the mis-folded tau can then cause the normally structured tau in the recipient neuron to become mis-folded, suggesting that tau spread through the brain may occur in a prion like way [379]. Although this work was not performed in neurons generated from patients with AD this work shows how the iPSC model system can be manipulated to understand the cause of pathological process seen at autopsy.

Although many elements of AD pathology are replicated in iPSC derived AD neurons, monolayer cell cultures of AD iPSC neurons have not been shown to develop AP or NFT. The reason for this is unknown, and is a potential limitation of the model system, but three dimensional neuronal cultures using the same technology have shown aggregates that would be consistent with AP and NFT [365, 366]. Three dimensional neuronal and organoid culture systems appear to reduce the diffusion

ability of A β and tau, which is thought to partly explain why these culture models develop the aggregated protein structures seen in AD. Using three dimensional cultures though also have drawbacks as to study single cell metabolism in these structures is difficult due to the difficulty with identifying the margins on a singular cell. Studying cellular organoids can also be difficult in three dimensional structures made of many cell types for the same reasons. Understanding how to attribute a particular metabolic change to a particular cell type can be difficult in this system. 2D cultures are more suitable for investigating changes to mitochondrial function and glycolysis, which can then be further explored in 3D systems which express aggregated forms of amyloid and tau.

The majority of AD iPSC studies have small numbers of cell lines, which is likely to be due to the fact that iPSC generation can be expensive. The factors needed to reprogram the donor cells, and the long differentiation times (sometimes >100 days) needed to develop cells that express neuronal markers and exhibit neuronal function are the main costs. The majority of the AD iPSC neuronal work has focused on familial AD mutations which has led to the observation that some APP mutants have increased efficacy for β -secretase activity due to a conformational change in the APP β -secretase active site [377]. AD iPSCs generated from Presenilin mutants have revealed that in multiple mutations of the PSEN1 or 2 genes, a loss of function of the γ -secretase enzyme is observed, which leads to a propensity for neurons to cleave APP to produce A β_{1-42} and not A β_{1-40} [361, 376, 380]. The mutations associated with developing AD lead to a reduced function of γ -secretase enzyme leading to a total reduction in A β , but also a more significant reduction A β_{1-40} which leads, in some mutations to an increase in the A $\beta_{42/40}$ ratio [381, 382]. These are clearly very important findings when trying to understand the mechanism of protein accumulation in familial AD, and may also suggest that different mechanisms precipitate protein accumulation in sporadic AD.

A more limited number of studies have created iPSC neurons from sporadic AD patients which have shown interesting findings with regards to A β ratios, and A β secretion. iPSC generated from sporadic AD patients have been shown in multiple studies to have either an increase in A β expression, or have levels similar to control cell lines [357, 362, 364, 374, 383]. This potentially highlights how in sporadic AD A β and tau accumulation may not be the first step in disease initiation in a proportion of patients. Exploring this further using iPSC technology has the potential to develop a personalized medicine approach to AD, as it will allow for a selective deconstruction of each of the separate pathophysiological processes that contribute to AD.

Several papers have investigated the mitochondrial functional change in iPSC derived AD neurons. One study has reported a reduction in cellular ATP levels in sporadic (n=1) and familial (n=1 APP

mutation) AD neurons [363]. Decreased MMP has also been reported in PSEN1 mutant neurons (n=1) [384]. Four studies have reported an increase in ROS production in both sporadic and familial AD iPSC neurons [362, 370, 384, 385], but numbers in these studies were relatively small. Study size is likely to be an important factor to consider when studying metabolism in any iPSC work devoted to sporadic AD as mitochondrial functional changes are likely to be part of a spectrum as seen when studying A β levels in these models. Larger sized sporadic AD iPSC studies are needed so a full understanding is gathered about what proportion of sporadic AD patients' neurons or astrocytes have mitochondrial deficits.

Interestingly it has been shown in sporadic AD iPSC neurons that increased ROS production is seen without the presence of increased amyloid or tau aggregates, suggesting a amyloid independent mechanism [362]. The increased ROS has been reported in PSEN1 iPSC derived neurons as well, but this is thought to be caused by amyloid accumulation within the mitochondria. PSEN1 neurons develop a stressed mitochondrial phenotype with mitochondria showing increased fission, increased Drp1 and reduced MFA1 and OPA1 [373]. These two papers further highlight how mitochondrial dysfunction in AD may have different or multiple precipitants in sporadic and familial disease. Mitophagy impairment in both sporadic and familial AD neurons has been reported [255, 363], as have abnormalities in lysosomal function [386] in PSEN1 lines. All these findings suggest altered mitochondrial function or structure in AD iPSC neurons. Several processes that lead to the elimination of amyloid and tau from the brain are active processes, therefore they depend on ATP. Dysfunctional mitochondria could lead to a reduction in ATP production which could affect protein clearance. Increased ROS production may also be a result of increased intracellular calcium concentration or ER stress, which has been seen in sporadic and PSEN1 iPSC neurons [370, 372, 387].

When considering the changes in mitochondrial function seen in AD iPSC lines it has to be remembered that the neurons developed often have a foetal phenotype. Although changes in mitochondrial function seen are consistent with work performed in aged cells from PM and animal models, further understanding is needed of how the reprogramming process affects both mitochondrial gene expression and cell reprogramming viability. As the reprogramming process can alter the dependency on different metabolic pathways in a cell, this may affect which cells complete the reprogramming process. Potentially cells with more abnormal mitochondria may never reach full pluripotency, and therefore are never selected for clonal expansion and study. The fact that the neurons developed have a foetal phenotype to start with may also effect the dominant metabolic pathway used by the cell, and may also mean that any mitochondrial or glycolytic changes that develop over time in AD may be reset, and so cannot be studied. It could also be the case that a particular mitochondrial pathological change effects the function of a cells to the extent that

pluripotency cannot be established. If this was the case, then certain mitochondrial abnormalities would never be seen in iPSC model systems. This particular problem could to a certain extent be controlled for by investigating changes seen in mitochondrial function in the donor cell types prior to reprogramming.

Although limited, the research on mitochondrial functional changes seen in AD iPSC derived neurons also highlights the complexity of the pathophysiology of the condition. Studies that have employed clustered regularly interspaced short palindromic repeat (CRISPR) genome editing show that removal of familial AD mutations in certain studies, corrects the mitochondrial abnormalities [372].

Therefore, even though mitochondrial abnormalities are seen without the presence of A β , A β may also be the cause of the mitochondrial and ROS abnormalities seen in neurons. Potentially sporadic AD mitochondria are already predisposed to have increased ROS production, which is then exacerbated by increased amyloid and tau expression. Deconstructing whether mitochondrial dysfunction or amyloid accumulation is the most important factor in generation of ROS in sporadic AD neurons is an ideal question to be answered by iPSC model systems.

The work on iPSC derived neurons from patients with AD has highlighted several new aspects of amyloid processing especially in familial derived neurons. Although the work is still in its infancy, the majority of findings related to AD pathology correlate with experiments performed in peripheral tissue, PM studies and animal experiments. Further work is needed to understand how metabolic pathways are affected by the reprogramming process, and to understand why monolayer cell cultures do not develop AD protein aggregates like three dimensional ones.

1.15.3 iPSCs AD Astrocytes

Astrocyte differentiation from iPSCs has been achieved, but in the majority of cases astrocytes are generated after a neuronal like cell colony has first been established. This can mean that astrocytes generated using iPSC can have very long differentiation times which can be expensive [388].

Originally deriving astrocytes using this technology led to poor yields of pure astrocytes, although more recent differentiation techniques have meant that purities above 90% have now been established [388, 389]. Importantly several studies have been able to show that iPSC derived astrocytes can uptake glutamate, an important functional property of astrocytes, and a key component of the astrocyte-neuronal relationship [388, 390].

The majority of literature for iPSC AD astrocyte work focuses on PSEN1 mutations. As with iPSC derived neurons, iPSC derived astrocytes express a gene profile very similar to astrocytes collected from PM AD brains [388, 390, 391]. Several studies have shown that astrocytes from patients with AD secrete more A β than controls [370, 389, 391], and one study has used iPSC derived astrocytes to

identify new genes that influence the increased A β levels, tau hyperphosphorylation and increased cytokine production seen in AD astrocytes. One of the genes identified, FERMT2, was shown to alter A β secretion in both neurons and astrocytes, but when knocked down in both cell types decreased tau phosphorylation in astrocytes, and increased the A β 42/40 ratio in neurons [391]. This work has shown how studying astrocytes specifically in AD can not only identify new therapeutic targets for the condition, but that consequences of gene expression in astrocytes and neurons are different meaning that to understand the pathology of AD better full characterization is need of all nervous system cells.

One study has looked at mitochondrial function in iPSC derived AD astrocytes with a PSEN1 mutation [389]. In this study astrocytes were created from 3 patients with a PSEN1 mutation. The study shows an increase in OCR in the PSEN lines and a trend towards an increase in mitochondrial spare respiratory capacity. The PSEN1 astrocytes have decreased calcium currents and increased calcium uptake, although it is not discussed, if these changes are due to mitochondrial functional changes. The increased mitochondrial function, evidenced by the high OCR, seen in the astrocytes in this study is thought to be a consequence of reduced capability for the astrocytes to perform glycolysis. Both glycolytic reserve and extracellular lactate levels are decreased in the PSEN1 astrocytes which suggests decreased glycolytic function. The study also highlights that in co-culture with neurons from control cell lines, these astrocytes do not support neuronal survival to the extent that control astrocytes can. Using CRIPSR techniques to remove the PSEN1 mutation alleviates the disease phenotype [389]. The fact that both changes in glycolysis and OxPHOS are seen in astrocytes in this study has developed a precedence for further work to understand not only how the two metabolic pathways interact, but specifically how they are affected in astrocytes in AD.

Sporadic AD astrocytes have been created using iPSC technology which have shown an increased A β excretion by the astrocytes from one of 2 lines created, again highlighting the potential heterogeneity of sporadic AD [370]. One study has created iPSC astrocytes from control subjects with apoE4/4 phenotype, showing that in co-culture these astrocytes support survival of neurons to a lesser extent than astrocytes with the apoE3/3 phenotype [392]. This finding clearly has implications for sporadic AD astrocyte function and may compound any underlying metabolic functional changes seen.

These studies show that iPSC technology can create astrocytes from AD patients, and changes in gene expression are similar to that seen in PM astrocytes. Research in this area has started to identify the potential possibilities of using iPSC derived astrocytes to study AD, but this research is still confined to a relatively small number of studies. There is clearly a need to develop the

understanding of metabolic functional changes seen in AD astrocytes created using this technology. The majority of iPSC astrocyte work has focused on familial AD, meaning that a gap in the understanding of how astrocytes are affected in sporadic AD needs to be addressed with iPSC research. Studies already performed using iPSC derived AD astrocytes all have relatively small sample sizes, which as mentioned in the above section, may affect result interpretation when considering sporadic AD. Studies would also benefit from comparing derived astrocyte function to the function of the donor cell type from the same person. This would help to develop the understanding of how the reprogramming process affects derived cell function, but also open up the opportunity to perform experiments in larger cohorts of cell types that have fewer financial constraints, if changes seen in iPSC derived cells mirror those seen in parent donor cells. Patient cell reprogramming has much potential in developing our understanding of how the astrocyte neuron relationship is affected in AD.

1.15.4 iPSC Summary and iNPC research

iPSC technology offers huge potential to develop our understanding of different brain cell interactions, but also the ability to test drugs identified through drug screening in a CNS setting. The fact that these cells come from human patients with the disease is critical as it allows for the study of AD cell homeostasis, without the need to over express the amyloid or tau proteins. This is a particular strength of this model system that can be exploited to study mitochondrial function in AD, as we can study mitochondria from patients with the condition in cell types that the disease affects. This, to a certain extent, is a unique feature of this model system when compared to others available to study mitochondrial and metabolic change in AD.

A limitation of using this model system is that the neurons and glia differentiated from iPSCs display a phenotype which most closely represents that seen in foetal neuronal cells. After prolonged differentiation of more than 200 days, the neurons can then become “aged”. Since the original development of this reprogramming technique, alterations have been made that allow cells generated from the reprogramming methods to maintain an aged phenotype and enable more direct reprogramming [393]. One such method is direct reprogramming which creates induced neuronal progenitor cells (iNPCs) that maintain an aged phenotype [350, 394]. Once iNPCs have been generated, iAstrocytes can be differentiated in 7 days, and neurons usually within a month. This reduces the time needed for differentiation when compared to iPSC techniques. As the body makes the transition to the adult state, the metabolic pathways relied upon to generate ATP also change. For this reason, it is important to study brain cellular metabolism in age appropriate cells and understand the contribution of each metabolic pathway in the model being used.

For this thesis, a similar direct reprogramming method is employed to that described by Mertens et al above [393]. Using this particular reprogramming technique iNPCs have been generated from patients with both sporadic and familial motor neuron disease (MND) [395-400] and sporadic and familial PD [396, 401], which have in turn been differentiated into astrocytes. Importantly it has been shown that this version of iNPC reprogramming generates neurons and astrocytes that have gene expression profiles similar to primary cells, and that diseased MND astrocytes can recapitulate motor neuron damage seen within the MND CNS [350]. iNPC models have identified that the pathological effect of astrocytes on neurons in MND is in part mediated via extravesical micro-RNA release leading to motor neuron network degeneration [400]. iNPC astrocytes have also been shown to modulate the expression of major histocompatibility complexes on neurons, which again has highlighted how MND astrocytes have pathological functions that affect neuronal survival [402]. Metabolic changes have also been reported in iNPC astrocytes generated from familial MND patients with decreased metabolic flexibility, and altered glycogen and fructose metabolism reported [396]. Deficits in mitochondrial capacity, and glycolytic function have also been reported in familial and sporadic MND iNPC astrocytes, without the need for the over expression of pathological protein aggregates [395]. This research is evidence that iNPC derived cells are a good model system to identify changes in cellular metabolic function.

This thesis is the first to describe the use of this particular iNPC reprogramming technique to create astrocytes from patients with sporadic and familial AD.

1.16 Introduction Summary

Data suggest that the process of OxPHOS in mitochondria is affected early in AD. Evidence from both animal and cell models of AD suggests that changes in oxidative metabolism occur long before the deposition of amyloid plaques. Very similar conclusions can be reached from the data presented in experiments interrogating the process of glycolysis in AD. Changes in OxPHOS and glycolysis occur in multiple cells outside the central nervous system, again without the build up of amyloid, suggesting that these changes may be of fundamental importance in the disease process. Non-CNS model systems though cannot reveal how these changes in metabolism affect processes unique to CNS cells such as synapse formation and electrochemical signal transmission. Data from PM tissue can show metabolic changes within the brain, but samples gained in this way are often at the end stage of the disease and therefore causality between different pathological events cannot be established. A model system allowing comparison between peripheral cell metabolic abnormalities and CNS cells derived from these peripheral cells would help the development of our understanding of the condition. This type of model system would also allow for the investigation of maximum capacity of

human OxPHOS and glycolysis within the CNS, and how this may affect cellular functions uniquely in these cells.

Limited research has been performed using iPSC astrocytes to study the astrocytic component to AD and to date no research has been published using iNPC derived astrocytes to study AD. This project describes the metabolic abnormalities seen in fibroblasts and astrocytes differentiated from iNPCs from patients with both sporadic and familial AD.

1.17 PhD Hypothesis, Aims and Objectives

Hypothesis: Fibroblasts and Astrocytes derived from patients with AD have impairments in glycolysis and mitochondrial function that can be corrected by repurposing FDA approved compounds.

1.17.1 Aims and Objectives:

Aims:

To characterise metabolic deficits in human derived astrocytes and their parental fibroblasts, which could be used as potential drug targets or biomarkers for AD in the future.

To correlate metabolic findings with established clinical markers of AD.

Objectives:

1. Characterise patient derived iAstrocyte and parental fibroblast impairments in glycolysis and mitochondrial structure and function.
2. Explore possible mechanisms that may be responsible for the altered glycolysis and mitochondrial structure and function.
3. Determine if pre-selected compounds, known to improve mitochondrial function, improve AD patient derived iAstrocyte mitochondria function.
4. Correlate iAstrocyte metabolic deficits against established clinical markers of AD.

Chapter 2: Methods

2.1 Materials

All materials used in this project were supplied by SIGMA-ALDRICH company Ltd, UK, unless otherwise stated.

2.2 Methods

2.2.1 Patient selection and characterisation

All sporadic patients and controls included in this study were collected as part of the Virtual Physiological Human – Dementia REsearch Enabled by IT (VPH-DARE@IT; <http://www.vph-dare.eu/>) initiative, a multicentre project funded by the EU (Framework Programme 7). A total of 10 patients with a clinical diagnosis of sporadic AD (the criteria by McKhann et al., 2011[403]) were selected. A diagnosis of Alzheimer dementia was made after assessment by both a consultant neurologist with a specialist interest in cognitive disorders, and a professor of neuropsychology had assessed the patients. The diagnosis was made on clinical grounds and did not incorporate amyloid or tau biomarkers. Each patient had undergone a brain MRI and cognitive profiling. The cognitive domains characterised by the tests were selected based on their susceptibility to neurodegeneration of the AD type. Patients were not eligible if there were the potential for a non-degenerative cause of their cognitive symptoms. Specific exclusion criteria were set as follows: medical diagnoses of clinical concern which could otherwise justify the potential presence of cognitive difficulties; MRI images showing abnormalities other than the effects of ageing and/or neurodegeneration; medical or radiological evidence of acute or chronic cerebrovascular disease; history of transient ischemic attacks, cardiovascular disease, uncontrolled seizures, peptic ulcer, sick sinus syndrome, or neuropathy with conduction defects; abnormal levels of folate, vitamin B12, or thyroid-stimulating hormone; treatments with medications for research purposes or with significant toxic effects on internal organs; evidence of a psychiatric or psychological cause of cognitive impairment.

A second cohort of sporadic patients, and a cohort of familial PSEN1 mutation patients, was selected from the Coriell cell repository. In sporadic AD patients a diagnosis was made using clinical criteria alone. For all PSEN1 patients included in the study, the PSEN1 gene was sequenced and PSEN1 mutation identified. Table 3.1 in chapter 3 highlights the demographic details for the patients included in this thesis.

2.2.2 Skin biopsy

Skin biopsies were taken from patients and controls recruited from the Sheffield young onset memory clinic, Sheffield, UK. Ethical approval for biopsy was gained from the NHS Yorkshire & The Humber - Bradford Leeds Research Ethics Committee (Reference: 16/YH/0155). Biopsies were taken from the non-dominant arm of all participants. The area for biopsy was cleaned with alcohol based cleaning solution, anaesthetised with 2% lidocaine (2mls), and then 2, 3mm diameter biopsies were taken with a punch biopsy (Stiefel). The biopsies were removed from the skin using a scalpel (Swann-Morton) and 1 was placed in Minimum Essential Medium (EMEM), the other in Dulbecco's Modified Eagle Medium (DMEM) based fibroblast culture media (See table 2.1&2.2 for media constituents). All patients biopsied had first been selected to be part of the VPH-DARE@IT project.

2.2.3 Skin Biopsy set up and fibroblast culture

Biopsies were dissected into 6 pieces and then placed into a T25cm² (Greiner bio-one) tissue culture flask containing 0.5mls of media that consisted of 50% EMEM or DMEM and 50% FBS (Biosera). 0.5mls of the same media was added to the T25cm² flasks on alternate days until the biopsies had grown epithelial and fibroblast cells. This was usually for 1 week from setting up the biopsy. Once biopsies had started to grow additional cells the media was changed to EMEM or DMEM only, without the extra FBS. Skin biopsies were grown in the T25cm² flasks until they became confluent with fibroblasts. At this stage the biopsies were washed in Phosphate Buffered Saline solution (PBS) (see table 2.3 for constituents) twice (2.5mls each wash) and then lifted from the biopsies using 1X Trypsin-Versene (Lonza) 2.5mls. The lifted fibroblasts were seeded in a new T25cm² flask. The biopsy was then re-fed with media and this process was repeated until the biopsy flask becomes confluent with fibroblasts again. The fibroblasts taken from the biopsies were then grown until confluent and split into a T75cm² tissue culture flask (Thermofisher). Once fibroblasts had become confluent they were trypsinised and early passages (up to passage 4) were then frozen down for future studies (see 2.2.3 for freezing down method). Subsequent fibroblasts are used for experimental work. Figure 2.1 show examples of skin biopsy cell growth and cultured fibroblasts.

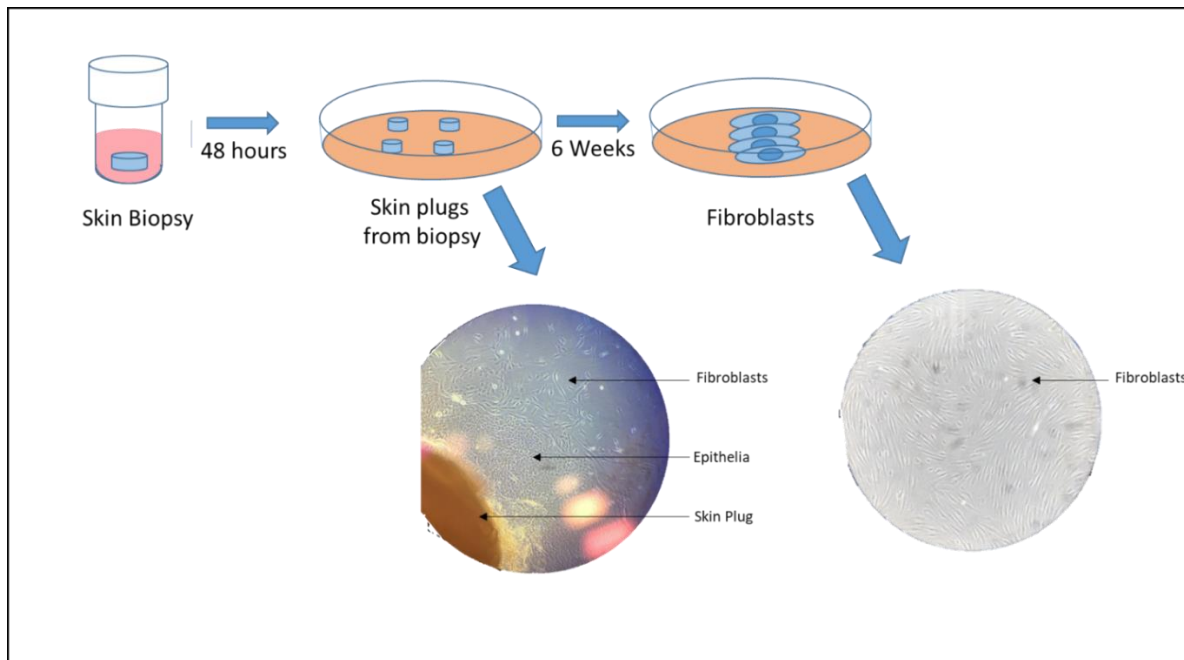


Figure 2.1| Fibroblast Set Up this diagram shows the process of generating fibroblasts from skin biopsies. Examples of epithelial and fibroblast growth from biopsy are shown.

2.2.4 Freezing Down Fibroblasts/iNPCs

When the T75cm² flask (Thermofisher) is confluent it was washed twice in PBS, then split using trypsin as described above. Cells were centrifuged at 1000g for 4 mins in a Harrier 15/80 (MSE) centrifuge and the pellet resuspended in Freezing Down Media (tissue culture media with an additional 10% FBS and 10% Dimethyl-sulfoxide [DMSO]). One T75cm² flask was split into 2 freezing down vials (Fisher Scientific). Cells were transferred to a CoolCell™ Cell Freezing Container (Biocision) and then placed in a -80°C freezer, these containers do not contain isopropanol. After 2 hours cells were transferred to a liquid nitrogen dewar for long term storage.

2.2.5 Fibroblast reprogramming

The fibroblast reprogramming regime was based on that described by Meyer et al (2014) [350]. Fibroblasts are plated in a 6 well plate (Greiner bio-one) at 100,000 cells per well in DMEM media. The next day the cells are transduced with adenoviruses containing the non-integrating vectors, OCT3/4, Sox2, KLF4, Lin28 and Nanog. A multiplicity of infection (MOI) of 10 was used for each viral vector. These viruses are added to the cells in DMEM media. 48 hours later the transduced fibroblasts are washed once in PBS and then the media is changed to iNPC media (see table 2.4). At this stage a conformational change in shape was seen in the fibroblasts as they start to shorten and develop larger nuclei. The fibroblasts remained in this well until they were completely confluent. Once confluent the cells were lifted by adding 600µl of Accutase (Gibco) to the well for 1 minute. The Accutase was then quenched with iNPC media and the cells were centrifuged for 4 minutes at 200g.

The cells were replated into 2 wells of a 6 well plate pre-coated with Fibronectin (Millipore) (concentration 1mg/ml diluted 1:200 in PBS). The reprogrammed cells were split into 3 wells of a six well plate and then a 10cm petri dish (Thermo Scientific). The 10cm dish split was repeated until the cells developed a morphology consistent with iNPC's. At this stage the cells were stained for PAX6 and Nestin (see table 6 for antibody concentrations, and section 2.2.6 for immunochemistry method) to establish iNPC conversion was successful. Once cells were confirmed to be iNPCs they were split at a ratio of 1:5 and frozen down until passage 4 was reached. At this point they can be used for experimental work. The freezing process uses media used for iNPC's culture with the addition of 10% DMSO. The process is the same as described above for fibroblasts, but without washing steps.

2.2.6 iNPC differentiation into Astrocytes

Once iNPCs become confluent they were split as described above and then plated in a 10cm petri dish (Thermo Scientific) coated with Fibronectin (Concentration 1mg/ml diluted 1:400 in PBS). For astrocyte differentiation 50,000-100,000 iNPCs were then plated into 10mls of Astrocyte growth medium (see table 5). The cells were cultured for four days in this media, with replacement of the media happening on day 4 after seeding. Day 5 post seeding the astrocytes were lifted using Accutase (1ml/ dish) and plated for experiments. Experimental work is done at day 7. Changes to galactose media were made at day 6. Figure 2.2 shows examples of iNPC's and astrocytes differentiated from fibroblasts.

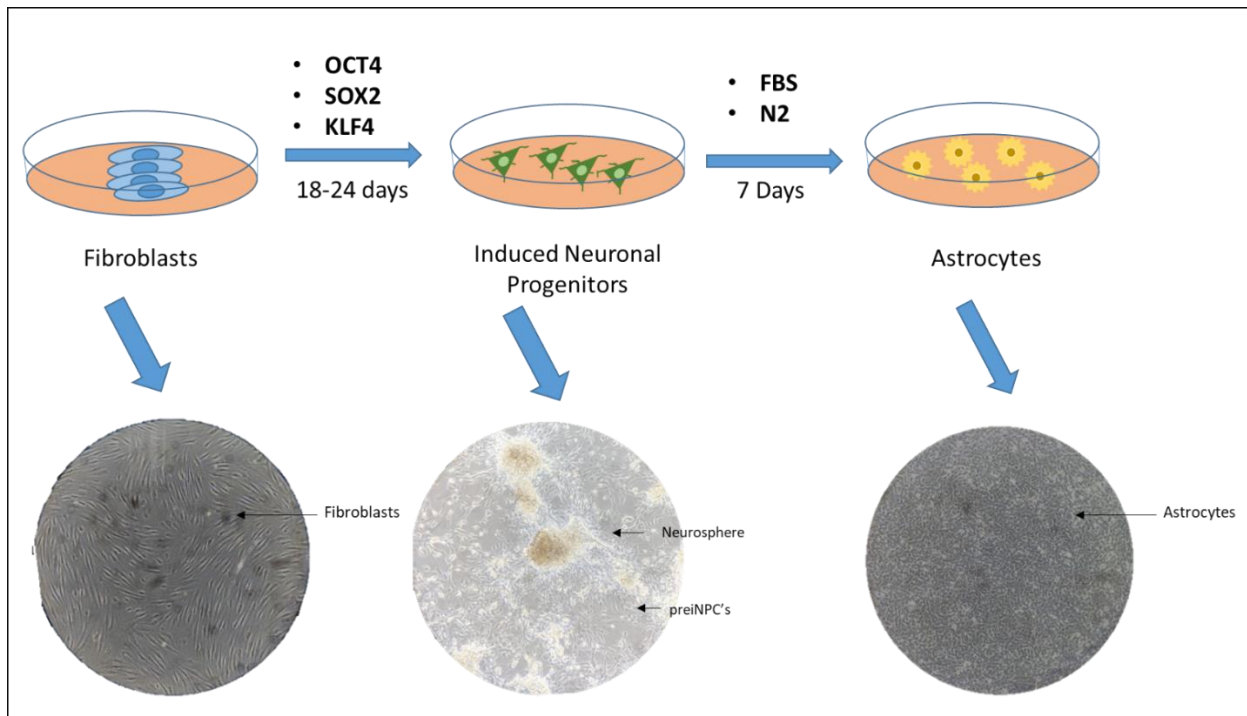


Figure 2.2| *Fibroblast Reprogramming* This figure highlights the major steps in the reprogramming of fibroblasts to iNPCs and then iNPCs differentiation into astrocytes. Factors used for iNPC reprogramming and astrocyte differentiation are shown. Bright field image examples are shown of the cell reprogramming process at each stage.

2.2.7 Immunohistochemistry

Fibroblasts, iNPCs, or astrocytes were plated in a black 96 well plate (Greiner bio-one) at a density of 2500 cells/well. After 24 hours cells were fixed with 4% paraformaldehyde (PFA) for 10 minutes. Cells were then permeabilised in a solution of 0.1% triton, PBS and TWEEN 20 (1:1000) (PBST) for 30 minutes. Following this, cells were washed with PBST twice. Cells were then blocked in PBST and horse serum (5%) for 60 minutes, to prevent any non-specific primary antibody binding. Primary antibodies at various concentrations (See table 2.6) were added to cells for an overnight incubation at 4°C. Cells were then washed in PBST three times and then secondary fluorescent antibodies (See table 2.6) were added at a concentration of 1:1000 in PBST for 1 hour to allow visualization. Cells were then washed a further 3 times in PBST. Hoechst dye (Life Technologies) at a concentration of 16.2mM was diluted 1:8000 in PBS and then added for 5 minutes to visualize the nucleus. Cells were washed a final time in PBST and then staining was visualised using an OPERA high content imager (Perkin Elmer) 10 fields per well where imaged and a z-stack consisting of 8 planes was taken, this equates to approximately 100cells imaged.

2.2.8 ATP Assay

Total cellular ATP measurements were done in white 96 well plates (Greiner bio-one) for both astrocytes and fibroblasts. The ATPlite kit (Perkin Elmer) was used to measure total cellular ATP. Cells were plated at a density of 5000 cells/well. 24 hours later media was changed if this was required. Media was changed to either a media that contained galactose as the primary sugar instead of glucose (see table 2.7), or cells were maintained in the glucose-based media depending on experiment. 24 hours after the media change cells were lysed using mammalian cell lysis solution. This increases the pH of the cell solution stopping the action of endogenous ATPases. 50µl of cell lysis solution was mixed with 100µl of PBS per well. Samples were then shaken on an orbital shaker (Grant Bio) at 700rpms for 5 minutes. The ATP substrate was then added to the cell solution (50ul/well). This solution contains d-Luciferin which reacts with ATP to release light see figure 2.3. The ATP substrate solution also reduces the pH of the solution allowing the reaction to occur.



Figure 2.3 | *ATPlite kit reaction* taken from (Luminescence ATP Detection Assay System methods document).

Samples were then dark adapted for 10 minutes and then measurements were taken using the PHERAstar plate reader (BMG Labtech) in luminescence mode. Once the experiment is completed quantification of DNA amount in each well is performed by adding cyquant to each well (1.1µl of cyquant is added to 1ml of Hanks' Balanced Salt solution (HBSS) then 50µl of this is added per well). Cyquant binds to double stranded DNA and its fluorescence is linear between 50-5000000 cells. The cyquant was incubated with cells for 60 minutes at a temperature of 37°C and then the plate was read using the PHERAstar plate reader (Excitation 485nm, emission 520nm). For the inhibitor assay oligomycin (100µM) and 2-deoxyglucose (50mM) were added to the cells for 30 minutes and incubated at 37°C during this time. The ATP assay was then performed as described above.

2.2.9 Mitochondrial Membrane Potential Assay

Mitochondrial membrane potential was measured using the potentiometric dye tetramethyl rhodamine (TMRM) (ThermoFischer Scientific). TMRM binds to the most negatively charged part of the cell. As the mitochondria are generally the most negatively charged part of the cell you can quantify their membrane potential using TMRM. As the dye binds to the mitochondria, structural and functional markers of mitochondria can also be quantified, although the measurement of structural elements of mitochondria is dependent on their membrane potential. If the mitochondrial

membrane potential is low, then it will be difficult to visualise structural elements of the mitochondria. The TMRM dye excess is washed off after one hour of incubation. This was done to stop the TMRM quenching its own fluorescence, and hence maintaining the linear relationship between fluorescence and membrane potential [404]. Prior to performing MMP experiments an assessment has to be made of whether the TMRM dye is being used in a quenched or de-quenched state. A quenched state refers to when a cationic dye becomes so concentrated in the mitochondrial matrix that molecules of the dye aggregate and stop fluorescing [405]. When a rapid loss of membrane potential occurs, such as that seen when FCCP is added to the cells then if the matrix is overloaded with dye “quenched” an increased TMRM signal is seen as in the quenched state the TMRM dye is released slower by the mitochondrial matrix. In the de-quenched state, the TMRM signal will be completely dissipated when FCCP is added to the cells [406]. Prior to performing MMP assessment of fibroblasts and astrocytes FCCP was added to the cells to show that the dye was being used in the de-quenched state.

Fibroblasts or astrocytes were plated in a black 96-well plate at a density of 2500 cells/well. 24 hours later media was changed as described in the ATP assay section. 24 hours after this incubation, media was replaced with phenol red-free media (ThermoFischer Scientific) containing TMRM (concentration 80nM) and hoescht (concentration 10nM) (Sigma Aldrich). The cells were then incubated for 1 hour at 37°C. After this, dyes were removed, and the cells were placed in phenol red-free media alone. The mitochondria were then visualised using an InCell 2000 high content imager, 25 fields with an average number of 500 cells were visualised. Collected images were then assessed for mitochondrial morphology parameters using the InCell Developer software and segmentation protocols [407]. Parameters assessed include mitochondrial form factor. This is a combined measurement of both a mitochondria’s perimeter length and area (Form Factor= $(\text{Perimeter}^2/4\pi \cdot \text{area})$). It is a measure of how round a mitochondrion appears to be, but also gives an indication of how interconnected the mitochondrial network is. The measurement is similar to the more commonly used aspect ratio.

2.2.10 Lactate Assay

Media lactate was measured when fibroblasts or astrocytes had reached confluency. An L-Lactate assay kit (abcam ab65331) protocol was followed whilst performing this experiment. In summary, total cellular lactate was measured by oxidising lactate through the actions of lactate dehydrogenase. This produces NAD⁺ which then reacts with formazan, a chromogenic dye, which produces a light signal.

1µl of fibroblasts or astrocyte media was added to 49µl of lactate assay buffer (LAB) Costar 3590, 96-well clear flat bottom plate (Corning). After this a further 46µl of LAB was added to each well with 2µl of substrate (formazan) and 2µl of enzyme (lactate dehydrogenase) from resuspended aliquots supplied with the assay kit. Samples were then gently mixed on an Orbital Shaker at 100rpm for 30 minutes at room temperature. The plate was then read on a PHERAstar Plate reader absorbance filter at 570nm. To measure the lactate a standard curve was created (2-10nmol range of lactate concentrations), and background lactate measurements were made. Disease samples were normalised to the controls of the day for lactate readings.

2.2.11 Mitochondrial Stress Test Assay

Cells were plated in a Seahorse XF24 Cell Culture Microplate (Aglient) at a density of 60,000 cells/well for fibroblasts and 10,000 cells/well for astrocytes. 24 hours later media was changed as described above in ATP sections. On the same day Seahorse XF Calibrant Solution at a volume of 1ml/well was added to each well of the Seahorse XF24 sensor cartridge plate (Aglient). This plate was then incubated at 37°C for 24 hours. 48 hours after plating cells the media was changed to Seahorse XF assay media (See table 2.8). This media change was done to increase measurement consistency, as the XF Media has a set buffering capacity allowing for inter-plate comparisons. The cells were then incubated for 60 minutes at 37°C in a CO₂ concentration found in air. Prior to running the assay oligomycin, FCCP and rotenone were then added to ports A, B, and C on the sensor cartridge plate respectively. Table 2.9 lists drug concentrations and ports. The Seahorse XF24 Cell Culture Microplates were then read in the Seahorse XF24 machine. The XF24 analyser first calibrates the culture plate and then mixes each well in the plate for 3 minutes, the machine then pauses for 2 minutes and a reading was taken for 3 minutes. This protocol was repeated three times and then the contents of port A were injected into the media. The same process was followed for 3 cycles and then port B was injected. Port C was injected into the media after a further 3 cycles. This is the same protocol as described by Mortiboys et al (2015) [408]. Measurements of the oxygen consumption rate (OCR), as a surrogate measure of OxPHOS, and extracellular acidification rate (ECAR), a surrogate measure of glycolysis, were taken at each reading point. Once readings were gathered a cell count for each plate was performed by first fixing the seahorse plate with 4% PFA and then adding hoescht (concentration 20mM diluted 1:8000) to each well. Cell count readings were performed on an INCELL2000 high content imager.

2.2.12 Glycolysis Assay

The glycolysis assay uses the same principals to measure cellular glycolysis as the mitochondrial stress test by measuring the change of pH (ECAR) in the cell media caused by lactate production as part of glycolysis. Cells were plated in a Seahorse XF24 Cell Culture Microplate (Aglient) at a density

of 60,000 cells/well for fibroblasts and 10,000 cells/well for astrocytes. The next 48 hours of the glycolysis experiment were identical to the mitochondrial stress test assay. When the media was replaced with Seahorse XF assay media, there was no glucose added to the media. Ports A, B and C on the sensor cartridge plate contained glucose, oligomycin and 2-deoxyglucose respectively (See table 2.9). The protocol for the running of the seahorse XF24 machine is the same as used for the mitochondrial stress test. Cell counts were performed in the same way as the mitochondrial stress test.

2.2.13 ATP Substrate Assay

The ATP substrate assay was used to investigate impairments in ETC complex function. 500,000 cells are collected at day 7 of astrocyte differentiation. Cells were suspended in 250µl buffer A (see table 2.10). Buffer A is used at a pH of 7.4. Cells were then permeabilised with histone 2ug/ml for 5 minutes. After permeabilization 5 volumes of buffer A (1250µl) are added to the cell suspension. The suspension was then centrifuged for 5 minutes at 10,000rpm. Cells were then resuspended in 150µl of Buffer A. 50µl of the resuspension was taken for Bradford assay (see section 2.2.14). 550µl of buffer A was then added to the remaining 100µl of suspension for use in the substrate assay. The assessment of complex linked ATP production at this stage must be performed with 15 minutes of adding the 550µl of buffer A to samples.

A PHERAstar plate reader (BMG Labtech) in luminescence mode was used to read ATP levels after addition of complex I or complex II substrates. The plate reader was set to perform an ATP kinetics assay. A background luminescence reading was made of each well on the assay plate containing 160µl of cell suspension and one of either the complex I, or II substrate mixture (see table 2.11). Both complex I&II conditions were repeated with the addition of 2µl of oligomycin (per well). This is done to confirm that the luminescence recorded was a production of ETC complex activity. Addition of oligomycin stopped any increase in luminescence above background, therefore the increased luminescence generated from addition of the ATP substrate was due to ETC complex activity. After baseline kinetics were measured the machine was paused and 5µl of Adenosine diphosphate (ADP) (0.1mM) and 10µl of The ATP substrate solution, described above in the ATP assay section (5.2.7) were added to each well. The kinetics assay was then resumed and measurements of substrate use were made every 30 seconds for 10 minutes. P₁ P₅-di(adenosine) pentaphosphate (PPAP) is added to wells before the measurement of substrate use to block the luminescence generated by adenylate kinase activity which occurs before luminescence is generated from OxPHOS [409]. Without the addition of PPAP the signal generated would not represent substrate usage by the ETC.

Once the assay is completed a kinetics curve is constructed and gradient was measured. Protein content estimation (via Bradford assay see section 2.2.14) was performed which gradient readings were then normalised to.

2.2.14 Bradford Assay

A Bradford assay was performed in certain experiments to estimate the amount of protein contained within a particular sample. A standard curve was created from a BSA standard (Curve protein concentrations 0ug/ml to 10 ug/ml). 5µl of each of the protein standards was plated on a Costar 3590 96-well clear flat bottom plate (Corning) well plate in triplicate. For the ATP substrate assay 1µl of sample was added to 4µl of deionized water and then place in separate wells in the 96-well plate in triplicate. 250µl of Comassie blue solution (Thermo Scientific) was then added to each well. Readings of protein concentration were then made using a PHERAstar plate reader, absorbance 595nm (BMG Labtech). A standard curve was created to calculate protein concentration.

2.2.15 Glutamine/Glutamate Assay

A Glutamine/Glutamate-Glo™ Assay (Promega) was used to measure intracellular concentrations of glutamine and glutamate. A 10cm dish of Astrocytes (≈ 2,000,000 cells) was washed 3 times in 5mls of PBS for 5 minutes per wash. Cells were then immersed in Inactivation solution (2mls of HCL 0.3N and 1ml PBS) for 5 minutes. After this the dish was scraped using a cell scraper (Corning) and 1ml of Tris solution (2-Amino-2-(hydroxymethyl)-1,3-propanediol, 450mM at pH 8.0) was added to the cells. 200µl of this solution was then added to 200µl of PBS. 25µl of this dilution was then placed in a well of a white 96-well greiner plate. For the assay 4 wells of cell solution were needed per astrocyte line. 2 wells had 25µl of glutaminase buffer (Promega) added only, and 2 wells had 25µl of glutaminase buffer with 0.125µl of glutaminase (100u/ml, Promega) added. A glutamate concentration curve was set up with glutamate concentrations starting at 0µM to 50µM. Glutamate for the concentration curve was sourced from Promega. 25µl of the glutamate standards were then added to wells on the 96-well plate. 25µl of glutaminase buffer was added to each of the glutamate standard wells. The plate was then shaken for 1 minute (700rpm) and samples were incubated at room temperature for 35 minutes.

After incubation 50µl of Glutamate Detection Reagent (See table 2.15) was added to each of the sample and concentration curve wells. The plate was shaken for another minute (700rpm) and then incubated at room temperature for one hour. Measurements of luminescence were then taken using a PHERAstar plate reader (Excitation 485nm, emission 520nm) (BMG Labtech). The ratio of glutamate to glutamine was calculated by subtracting the measurements of the wells with only glutaminase buffer in them from the wells that have glutaminase and glutaminase buffer in them.

The result of the subtraction gave the glutamine amount and the remainder was the glutamate measurement.

2.2.16 Quantitative Polymerase Chain Reaction (qPCR)

For qPCR approximately 750,000 fibroblast cells or 2,000,000 astrocytes were harvested. For fibroblast UDCA experiments, fibroblasts were treated with UDCA at a concentration of 10 μ M or 100nM 24 hours prior to harvest. The RNeasy Mini Kit (Qiagen) was used to extract RNA from samples. RNA extraction was performed as described in the kit protocol. 350 μ l of RLT buffer was added to the collected cells and then using a needle and syringe the sample was homogenised. 350 μ l of 70% ethanol was then added to the sample and mixed by pipetting the sample up and down. 700 μ l of the prepared sample was then placed in a RNeasy spin column (Qiagen) and placed in a 2ml collection tube. The spin column was then spun for 15 seconds at 8000g using a Sigma 1K15 centrifuge. 700 μ l of RW1 buffer is then added to the spin column and the sample is then spun again for 15 seconds at 8000g. The same process is then repeated with 2 volumes of 500 μ l of RPE buffer discarding the column flow through at each step. The spin column was then transferred to a new collection tube and 30 μ l of RNase-free water is added before the column was spun for 1 minute at 8000g to elute RNA. RNA mass and purity were then measured using a spectrophotometer (NanoDrop ND-1000 machine). RNA purity was calculated using the 260/280nm absorbance ratio. Only samples that had a ratio reading of 2 or above were accepted for qPCR. A ratio of less than 2 suggests protein contamination from the isolation procedure.

After calculating RNA purity and mass, RNA levels were measured using a Stratgene PCR machine. A High-Capacity cDNA Reverse Transcription Kit (Thermofisher scientific) was used to prepare samples for qPCR. Samples were loaded on to a PCR plate (Bio-Rad) at 12.5ng/ μ l. 10 μ l of sample, 2 μ l of 10Xrt Buffer, 0.8 μ l of 25xdNTP Mix(100nM), 2 μ l of 10xRT random primers, 10 μ l Sybr Green detection dye (Thermo Scientific) and 4.2 μ l RNase-free water was added to each well. The plate was spun on an ALC PK1200 centrifuge at 3000rpm for 2 minutes prior to starting qPCR. Samples were prepared on ice. The PCR machine was set to run a cycle that had 3 steps. Step 1 was 10 minutes long at a temperature of 25 $^{\circ}$ C, step 2 120 minutes at 37 $^{\circ}$ C and step 3, 5 minutes at 85 $^{\circ}$ C. 40 amplification cycles were performed. Table 2.12 displays the forward and reverse primer sequences used for each gene assessed. Disease samples were normalised to the controls of the day.

2.2.17 Glucose Uptake Assay

Glucose uptake of astrocytes was measured using the Glucose Uptake Assay Kit (Fluorometric) (Abcam, ab136956). For this assay cells were treated with 2-deoxyglucose a molecule identical to glucose, except 2 hydroxyl groups have been replaced by hydrogen atoms. This prevents the sugar

from being metabolised when it is taken up by cells. 2-Deoxyglucose is transported into cells using the same transporters as glucose. It has an identical uptake pathway into cells and therefore measurement of 2-deoxyglucose is equivalent to measuring cell glucose uptake.

Astrocytes were plated at a density of 2500 cells per well in a 96 well black griener plate. At day 7 after differentiation the astrocytes were washed 3 times in PBS and then incubated for 40 minutes in a 100µl of Krebs-Ringer-Phosphate-Hepes (KRPH) buffer with 2% bovine serum albumen added pH 7.4 (see table 2.14). After this the astrocytes were washed again 3 times in PBS and then 2-deoxyglucose at a concentration of 50mM was added to the cells for 20minutes suspended in KRPH (volume 100µl per well). Cells were then washed again 3 times in PBS and then 90µl of Extraction buffer (Abcam) was added. Astrocytes were pipetted up and down in the well and then snap frozen in liquid nitrogen. After freezing samples were left to thaw on ice.

Once samples have been warmed 10µl of Neutralisation buffer (Abcam) was added to each sample. Samples were then mixed in a centrifuge at 500rpm for 2 minutes. 25µl of sample was then placed in a black 96-well plate, with the volume made up to 50µl with glucose uptake assay buffer (Abcam). Using the 2-deoxyglucose standard a standard curve was created with concentrations between 0µM-20µM of 2-Deoxyglucose. 50µl of each standard was plated on the black 96-well plate. 50µl of reaction mix (47µl Glucose uptake assay buffer, 2µl of enzyme mix and 1µl of PicoProbe, all supplied by Abcam) was added to each sample and standard well. Samples were then incubated in an incubator for 40 minutes at 37°C. measurements of Fluorescence at Ex/Em=535/587nm were then taken using PHERAstar plate reader (Excitation 485nm, emission 520nm) (BMG Labtech).

2.2.18 Glutamate Uptake Assays

An Abcam colorimetric Glutamate Assay kit (ab83389) was used to measure astrocyte glutamate uptake. Assay was performed as per manufacturers guidance. Astrocytes were plated on a black 96 well plate (Griener) at a density of 10,000 cells/well at day 5 of differentiation. On day 7 of differentiation the astrocyte media was changed to HBSS (Gibco), without calcium or magnesium for 30 minutes. This media was then changed to HBSS containing magnesium and calcium for 3 hours which also contained 100µl of glutamate at a concentration of 1:1000. After this the cells were washed in PBS and resuspended in glutamate assay buffer (100µl/well). Samples were homogenised by pipetting the sample quickly up and down and then snap frozen in liquid nitrogen. Samples were either then stored or defrosted on ice. After the samples had defrosted, they were centrifuged for 5 minutes at 17000G at a temperature of 4°C, supernatant was collected and for each samples 50µl was added to a black 96-well plate (Griener). To each sample 100µl of reaction mix was added (Glutamate assay buffer 90µl, Glutamate developer 8µl and Glutamate enzyme mix

2µl). A glutamate concentration curve was created, and background sample wells containing 50µl of sample plus background reaction mix (Glutamate assay buffer 92µl, and Glutamate developer 8µl) were added to the plate. The plate was then incubated for 30 minutes at a temperature of 37°C and output was measured using a PHERAstar plate reader (BMG Labtech) OD450nm.

2.2.19 Drug Treatment Assays

ATP and MMP assays as described above were performed after the treatment of astrocytes for 24 hours with 8 different compounds known to improve mitochondrial function (See table 2.15). These compounds are all drugs already accredited for use in humans, but not to treat Alzheimer's disease. Drugs were diluted in astrocyte media (see table 2.5) and astrocytes were treated at drug concentrations of 1µM, 10µM and 100µM. To perform the drug treatment assays astrocytes were plated at 1000 cells per well in a white 384 greiner plate for ATP assays or a black greiner 384 well plate at a density of 500 cells per well. Astrocytes were treated at day 6 of differentiation using an ECHO 550 Liquid Handler (Labcyte). After drug application astrocytes were incubated at 37°C for 24 hours. ATP and MMP measurements were performed and analysed as described above (Sections 2.2.7 and 2.2.8 respectively).

2.2.20 MRI Acquisition

All MRI sequences were acquired as part of the VPH-DARE research project. MRI images were acquired using 3T scanner (Philips Achieva system). For this project functional MRI (fMRI) sequences were reviewed by experts in the field and the default mode network (DMN) was extracted for both controls and patients with AD from these fMRI sequences.

The DMN is a group of functionally connected neuroanatomical brain regions that show synchronised activity when a person is not focusing on any specific externally driven task [410]. This network has been shown to be disrupted early in the course of AD [411]. The DMN was split into several regions of activity, and then each region was correlated with fibroblast/astrocyte spare capacity, extracellular lactate, MMP and glycolytic reserve readings. MRI acquisition and DMN function are described in more detail in chapter 4.

2.2.21 Neuropsychology testing

Patients from the Sheffield cohort were recruited due to participation in the VPH-DARE research study. This study includes neuropsychological profiling which was performed by expert neuropsychologists. As part of this neuropsychological testing measurements of phonemic (the letter fluency test) and semantic (the category fluency test) fluency were made. In brief these tests are performed by asking patients to list all the words that they can think of that begin with a certain letter in 1 minute (phonemic fluency) or to list objects from a certain category (semantic fluency)

this includes listing animals, fruits and cities. Immediate and delayed memory (via the prose memory test) was also chosen to be correlated with mitochondrial spare capacity.

These tests were chosen as 3 of the neuropsychological measures (semantic, immediate and delayed recall) are shown to be affected early in AD [412]. The final test, phonemic fluency, was chosen as a test that is not affected early in the course of AD [413]. For these 4 tasks a score was generated which was then compared with mitochondrial functional markers or glycolytic markers listed in the MRI section. Further details on neuropsychological assessment in AD are described in chapter 4.

2.3 Statistical analysis

For comparing disease groups to controls for mitochondrial and glycolysis experiments a Student's t-test was used. For correlations between fibroblast spare capacity readings and neuropsychological and neuroimaging data a Spearman's Rank correlation coefficient was used as the data were not normally distributed.

2.4 Media Constituents

Table 2.1| DMEM Media

Media Constituent	Concentration/Volume	Supplier
Dulbecco's Modified Eagle's Medium with L-Glutamine and 4.5g/L Glucose	500mls	Lonza
Fetal Bovine Serum	50mls in 500mls of media	Biosera
Penicillin	100IU/ml in 500mls of media	Sigma Aldrich
Streptomycin	100IU/ml in 500mls of media	Sigma Aldrich
Sodium Pyruvate	5mls of 1mM stock in 500mls of media	Sigma life sciences

Table 2.2| EMEM Media

Media Constituent	Concentration/Volume	Supplier
Minimum Essential Medium with Earle's essential salts and L-glutamine	500mls	Corning, USA
Fetal Bovine Serum	50mls in 500mls of media	Biosera
Penicillin	100IU/ml in 500mls of media	Sigma Aldrich
Streptomycin	100IU/ml in 500mls of media	Sigma Aldrich
Sodium Pyruvate	5mls of 1mM stock in 500mls of media	Sigma life sciences
Non-essential Amino Acids	5mls of 0.1mM stock in 500mls of media	Lonza
Multi-vitamins	5mls in 500mls of media	Lonza
Uridine	50ug/ml in 500mls of media	Sigma

Table 2.3| Phosphate Buffered Saline

Media Constituent	Concentration/Volume	Supplier
Phosphate Buffered Saline Tablets	1 tablet	ThermoFischer
Deionised Water	100mls	NA

Table 2.4 | iNPC Media

Media Constituent	Concentration/Volume	Supplier
DMEM/F12 Glutamax	500mls	Gibco
B27	5mls	Gibco
N2 Supplement (100X)	5mls	Gibco
FGF	5µl of 1mg/ml stock	Gibco
Streptomycin	100IU/ml	Sigma Aldrich
Penicillin	100IU/ml	Sigma Aldrich

Table 2.5| Astrocyte Media

Media Constituent	Concentration/Volume	Supplier
Dulbecco's Modified Eagle's Medium with L-Glutamine and 4.5g/L Glucose	500mls	Lonza
Fetal Bovine Serum	50mls	Biosera
Penicillin	100IU/ml	Sigma Aldrich
Streptomycin	100IU/ml	Sigma Aldrich
N2 Supplement (100X)	5mls	Gibco

Table 2.6| Antibodies used for Immunochemistry

Antibody	Species	Dilution	Supplier
Vimentin	chicken	1:200	Abcam (AB5733)
Nestin	Mouse	1:200	Abcam (AB18102)
CD44	Rabbit	1:200	Abcam (AB157107)
S100β	Rabbit	1:200	Abcam (AB868)
PAX6	Rabbit	1:1000	Abcam (AB5790)
GFAP	Rabbit	1:200	Dako (Z0334)
NDGR2	Mouse	1:200	Santacruz (sc-376202)
ALDH1L1	Rabbit	1:1000	Abcam (AB87117)
Secondary Antibodies			
Alexia 488	Rabbit	1:1000	Invitrogen
Alexia 488	Mouse	1:1000	Invitrogen
Alexia 488	Chicken	1:1000	Invitrogen
Alexia 568	Rabbit	1:1000	Invitrogen
Alexia 568	Mouse	1:1000	Invitrogen

Table 2.7| Galactose Media

Media Constituent	Concentration/Volume	Supplier
Dulbecco's Modified Eagle's Medium with L-Glutamine and without Glucose	500mls	Corning, USA
Fetal Bovine Serum	50mls	Biosera
Penicillin	100IU/ml	Sigma Aldrich
Streptomycin	100IU/ml	Sigma Aldrich
Sodium Pyruvate	5mls of 1M stock	Sigma life sciences
Non-essential Amino Acids	5mls of 0.1mM stock	Lonza
Multi-vitamins	5mls	Lonza
Uridine	50ug/ml	Sigma
Galactose	522mg added to 10mls PBS (5.68mM final concentration)	Sigma Aldrich

Table 2.8| Seahorse XF media

Media Constituent	Concentration	Supplier
Mitochondrial Stress Test		
XF Assay media	50mls	Aligent
Glucose	50µls (Final concentration 1mM)	Sigma life sciences
Sodium Pyruvate	500µls (Final concentration 10µM)	Sigma life sciences
L-Glutamine	500µls (Final concentration 2mM)	Lonza
Glycolysis Stress Test		
XF Assay media	50mls	Aligent
Sodium Pyruvate	500µls (Final concentration 10µM)	Sigma life sciences
L-Glutamine	500µls (Final concentration 2mM)	Lonza

Table 2.9| Seahorse experiments drug locations

Drug	Final Concentrations	Port	Supplier
Mitochondrial Stress Test			
Oligomycin	0.5µM	A	Sigma life sciences
FCCP	0.5µM	B	Sigma life sciences
Rotenone	0.5µM	C	Sigma life sciences
Glycolysis Stress Test			
Glucose	10mM	A	Sigma life sciences
Oligomycin	1µM	B	Sigma life sciences
2-Deoxy Glucose	50mM	C	Sigma life sciences

Table 2.10 | ATP Substrate Assay Buffer

Buffer Constituent	Concentration/Volume	Supplier
Potassium Chloride	150mM	SigmaAldrich
Trisaminomethane Hydrochloride	25mM	SigmaAldrich
Ethylenediaminetetraacetic acid	2mM	SigmaAldrich
Bovine Serum Albumen (add daily)	0.1%	Sigma life sciences
Potassium Phosphate,	10mM	SigmaAldrich
Magnesium Chloride	0.1mM	SigmaAldrich

Table 2.11 | ATP Substrate Assay complex substrates

Complex	Media Constituent	Stock Concentration/Volume per well	Supplier
Complex I Substrates			
	PAPP	6mM/5ul	SigmaAldrich
	Malate	80mM/2.5µl	Sigma
	Glutamate	80mM/2.5µl	Sigma
Complex II Substrates			
	PAPP	6mM/5µl	SigmaAldrich
	Succinate	80mM/5µl	Sigma
	Rotenone	400µg/ml (10µl)	SigmaAldrich
Inhibitor (added to the constituents of either complex I or II)			
	Oligomycin	0.2mg/ml (2µl)	SigmaAldrich

Table 2.12 | qPCR forward and reverse primers

Gene	Forward	Reverse	Supplier	Cells tested
Drp1	ATTATGCCAGCCAGTCCACAA	CGCTGTCCCCGAGCAGATA	Sigma-Aldrich	Fibroblast
MFN1	CACTCCAGCAACGCCAGATA	CGGACGCCAATCCTGTTACT	Sigma-Aldrich	Fibroblast
MFN2	GTCTGACCTGGACCACCAAG	TGCAGTTGGAGCCAGTGTAG	Sigma-Aldrich	Fibroblast
OPA1	AGCCAGTCCAAGCAGGATTC	TGCTTTTCAGAGCTGTTCCCT	Sigma-Aldrich	Fibroblast
LAMA	CAATACCAAGAAGGAGGGTGAC	AGATCATGCAGCTCGCCC	Sigma-Aldrich	Astrocyte
RanBP17	CACTTCGATGCAGAGAGGCTA	CACTGGTCCGACAGTCTTC	Sigma-Aldrich	Astrocyte
TERF2	TTATTCGAGAAAAGAACTTGGCCC	TGAGGAGGTAGGGCTCGG	Sigma-Aldrich	Astrocyte

Table 2.13 | Glutamate Detection Reagent

Constituent	Volume per well	Supplier
Luciferin Detection Solution	50µl	Promega
Reductase	0.25µl	Promega
Reductase Substrate	0.25µl	Promega
Glutamate Dehydrogenase (GDH)	1.0µl of 1000 U/mL stock	Promega
Nicotinamide Adenine Dinucleotide (NAD)	1.0µl of 40mM stock	Promega

Table 2.14 | Krebs-Ringer-Phosphate-Hepes (KRPH) buffer (pH 7.4)

Constituent	Concentrations	Supplier
HEPES (4-(2-hydroxyethyl)-1-piperazineethanesulfonic acid)	20mM	Thermofischer
Monopotassium phosphate	5 mM	SigmaAldrich
Magnesium Sulphate	1mM	SigmaAldrich
Calcium Chloride	1mM	SigmaAldrich
Sodium Chloride	136mM	SigmaAldrich
Potassium Chloride	4.7mM	SigmaAldrich

Table 2.15 | Drugs used in drug treatment assays

Drug	Concentrations	Supplier
Pentoxifylline	1,10,100µM	Sigma
Probenecid	1,10,100µM	Sigma
Carbachol	1,10,100µM	Sigma
Colchicine	1,10,100µM	Sigma
Rolipram	1,10,100µM	Sigma
Andrographolide	1,10,100µM	Sigma
Thiosalicylic Acid	1,10,100µM	Sigma
Ursodeoxycholic Acid	1,10,100µM	Sigma

Chapter 3: Ursodeoxycholic Acid improves mitochondrial function and redistributes Drp1 in fibroblasts from patients with either sporadic or familial Alzheimer's disease

3.1 Introduction

In this chapter mitochondrial function and morphology are assessed in sporadic and familial AD patient fibroblasts. An alteration in the mitochondrial morphology is identified in both sporadic and familial AD fibroblasts. Mitochondrial functional changes are also identified which suggest a deficit in MMP in both sporadic and familial AD fibroblasts and a reduced efficiency by which the mitochondria consume oxygen as part of OxPHOS. These functional changes, and some of the morphological changes can be altered by the application of Ursodeoxycholic Acid (UDCA). The effect of UDCA appears to be mediated via an alteration in the proteins that control mitochondrial fission and fusion. This is the broad conclusion of the published paper that forms part of this chapter. Work on mitochondrial fission and fusion protein expression was performed by another co-author Katy Barnes.

In extra data sections of this chapter how mitochondrial morphology and function is affected by ApoE genotype in AD, the total cellular ATP levels in AD fibroblasts, and how the application of UDCA corrects ATP deficits will be presented. In this chapter introduction, mitochondrial fission and fusion will be discussed in more detail, as well as the effect the ApoE gene has on metabolic function in AD.

3.1.2 Mitochondrial Fission and Fusion

As discussed in chapter 1 mitochondrial fission and fusion are controlled by four main proteins. Mitochondrial fission is initiated by Drp1, whereas mitochondrial fusion is activated by the outer mitochondrial membrane proteins MFN1 & MFN2 and the inner mitochondrial membrane protein OPA1 [414].

For fission to occur Drp1 has to move from the cytoplasm to the mitochondria. It is recruited to the mitochondria by one of 4 different mitochondrial proteins collectively referred to as the DRP1 binding proteins. They are Mitochondrial fission 1 protein (Fis1), Mitochondrial fission factor (Mff), Mitochondrial dynamics protein 49 (MiD49) and Mitochondrial dynamics protein 51 (MiD51), [415]. Once Drp1 has bound the mitochondria, it forms a ring like structure around the mitochondrion. The identified mitochondrial can then be removed from the mitochondrial network and either transported to another part of the cell, or broken down if identified as damaged. Mitochondrial fission has multiple roles within a cell including quality control of the mitochondrial network, and allowing the redistribution of mitochondria throughout a cell [132]. Mitochondrial distribution is

particularly important in a cell type like the neuron, due to the size of the cell, and the fact that synapses require high densities of mitochondria that function appropriately [416].

Mitochondrial fusion also has a role in maintenance of the cell mitochondrial network.

Mitochondrial fusion allows different mitochondria to exchange mitochondrial DNA and ETC proteins. This means that these mitochondrial resources can be used most efficiently [417].

Changes in mitochondrial dynamics have been reported both in nervous system cells and peripheral cells in people with AD. Both increased fusion [418], and increased fission [204] of the fibroblast mitochondrial network has been observed in AD, which may reflect the dynamic nature of this organelle. Mitochondrial dynamics in neurons from patients or models of AD tend to report that the network is fragmented, and that all main fission and fusion proteins are down regulated [167, 419]. The CNS changes in mitochondrial fission and fusion may represent the end stage of the disease, or be a consequence of the over expression of amyloid in animal models. It has been shown that increased A β production increases nitric oxide expression. The nitric oxide can increase the activity of Drp1 through S-nitrosylation which can lead to increased mitochondrial network fragmentation [420]. It is not known if neurons from people with AD start with a fused mitochondrial network, like that seen in some fibroblast studies, and then develop the more fragmented network as a result of the presence of A β . The differences in mitochondrial network structure seen between the periphery and CNS may represent different responses by cells to energetic demands, cellular stress, or metabolite availability.

3.1.3 Apo ϵ gene and its effect on metabolism in AD

Apo ϵ gene encodes a 34 kDa protein involved in the metabolism and distribution of lipids. The protein has 3 isoforms (ϵ 2 ϵ 3, ϵ 4), with the presence of the ApoE ϵ 4 allele conferring an increased risk of sporadic AD development 12 times the general population risk [421]. Within the nervous system the protein is mainly distributed in astrocytes and has a central role in the passage of lipids and cholesterol to neurons [422]. ApoE ϵ 4 containing astrocytes have a reduced ability to uptake amyloid when compared to ApoE ϵ 3 astrocytes [423]. This potentially explains why the presence of the ApoE ϵ 4 allele causes early deposition of amyloid within the brain as well as impaired A β clearance [424].

The ApoE protein has been shown to effect both synaptic strength and integrity and can affect brain glucose metabolism and insulin signalling [422]. The exact mechanism by which the ApoE protein affects both synaptic integrity and glucose metabolism is not known, but the effects on glucose metabolism are believed to be mediated through the action on the Peroxisome Proliferator

activated receptor γ (PPAR γ) [425]. PPAR γ pathway becomes inactive in the ApoE ϵ 4 brain which leads to a reduction in glucose transporters and HK activity.

Potentially the ApoE ϵ 4 allele also has an effect on mitochondrial dynamics with reductions in DRP1 and increases in MFN1 seen in the hippocampi of mice expressing 2 ϵ 4 alleles leading to a fused mitochondrial network [426]. The fused mitochondrial network seen in this model has a reduced membrane potential and increased mitochondrial Parkin recruitment which may affect the ability of the mitochondria to produce ATP. It is not addressed in this paper though if the changes in mitochondrial function and dynamics are separate to, or a consequence of, the potential alteration that ApoE ϵ 4 can cause to the delivery and metabolism of glucose. This is an important point to understand as the mitochondrial structural changes could be a result of reduced metabolite availability as opposed to a direct effect of ApoE genotype.

3.1.4 Assessment of oxidative phosphorylation using the Seahorse XF analyser

This chapter describes different components of oxidative phosphorylation in detail. The main experiment used to assess fibroblast oxidative phosphorylation was the Agilent sea horse XF analyser. A mitochondrial stress test was used for this. In this experiment oxygen consumption is measured after the application of different mitochondrial inhibitors. Oxygen is consumed by oxidative phosphorylation at complex IV. Twelve separate readings of the media oxygen concentration are made during the experiment. 3 are taken firstly to measure the basal level of mitochondrial oxygen consumption. This is the amount of oxygen that is consumed by the fibroblasts when oxidative phosphorylation is working at its basal rate. The next 3 measurements are taken after the addition of oligomycin to the cell media. Oligomycin is an inhibitor of the ATP synthase enzyme. This decreases the oxygen consumption and allows for the calculation of the amount of oxygen consumed by the cells to generate ATP. This is referred to as the ATP linked respiration. The next 3 measurements are made after the addition of FCCP. This drug increases the permeability of the inner mitochondrial membrane, which allows protons to move from the inter-membrane space to the matrix. The movement of protons dissipates the MMP, which forces complexes I, III, IV of the ETC to work at their maximum rate. This allows for the measurement of the maximum rate of oxidative phosphorylation that the cells under assessment can achieve (Maximum mitochondrial respiration), but also the mitochondrial spare respiratory capacity (MSRC) which is the difference between basal mitochondrial oxygen consumption rates and maximum mitochondrial oxygen consumption rates. It is a measure of how much oxidative phosphorylation can be increased if the ATP demands of the cell increase. The final 3 measurement are taken after the addition of

rotenone which is an inhibitor of complex I of the ETC. This ceases all oxygen consumption related to oxidative phosphorylation, and allows for the calculation of the none oxidative phosphorylation sources of oxygen consumption. By subtracting the ATP linked respiration figure from this figure the proton leak across the inner mitochondrial membrane can also be calculated. From the different parameters gleaned from this data set two ratios can also be calculated. The first is referred to as the coupling efficiency or ATP Coupling. This refers to the amount of oxygen that is consumed to produce ATP as a proportion of the basal mitochondrial oxygen consumption. The second is the respiratory control ratio which is a measure of what the maximum oxidative phosphorylation rate is that can be achieved at a certain level of proton leak. This is calculated by dividing the maximum mitochondrial respiration by the proton leak. Figure 3.1 highlights the different measurement of oxidative phosphorylation that have been made.

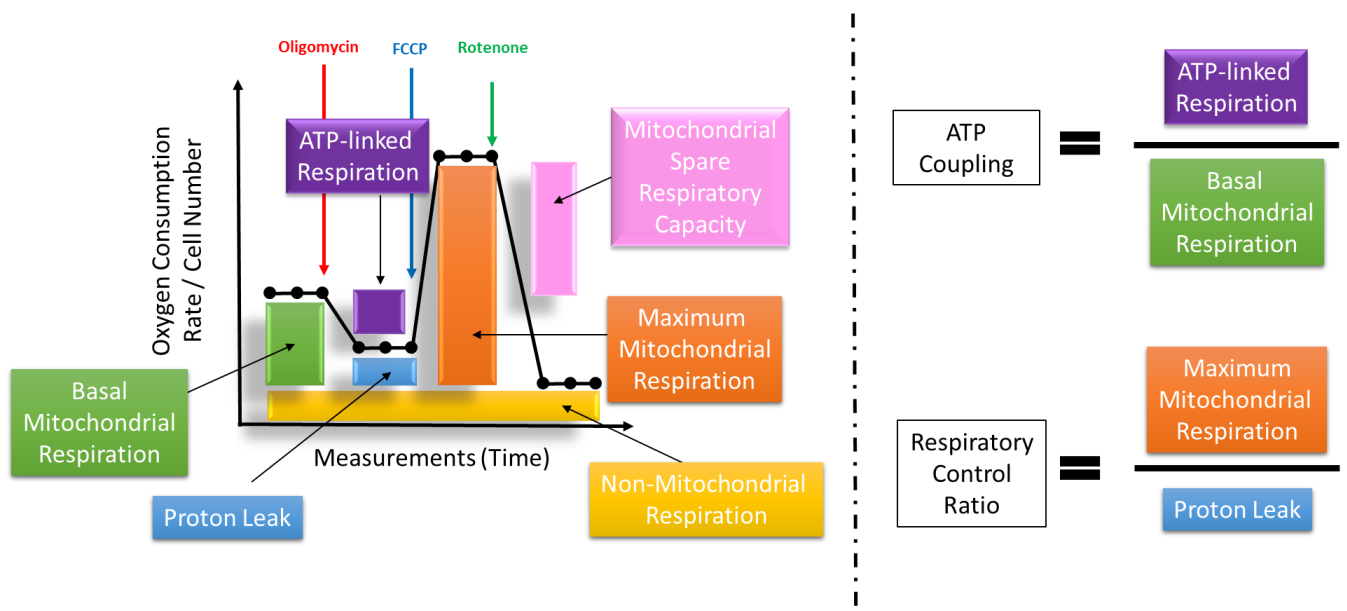


Figure 3.1 | Mitochondrial Stress Test Seahorse Trace graph: This figure highlights the different elements of oxidative phosphorylation that are assessed using the mitochondrial stress test. Each coloured box represents a particular measure with the height of the box indicating the value. The graph also displays the points at which each of the separate mitochondrial inhibitors are added; Oligomycin in red, FCCP in blue and Rotenone in green. To the right hand side of the figure are the two ratios that are calculated using the information gleaned from the stress test trace.

3.1.5 Reason for presenting additional results

The additional results added to this chapter include data on mitochondrial fusion proteins, gained from mRNA qPCR data, and fibroblast total cellular ATP data that was not included in the chapter

publication. The sporadic AD fibroblast metabolic parameters that are presented in the chapter publication are separated based on ApoE genotype in the extra results section. These results have been added as in sporadic AD the presence of the ApoE ϵ 4 alone has a huge effect on a person's risk of developing AD, therefore as the allele has been shown to affect metabolism, it is important to understand how the changes in mitochondrial function and ApoE ϵ 4 genotype interact.

Included in the extra results section in this thesis chapter are a further 6 sporadic AD lines that were not included in the chapter paper. They have been added to the ApoE ϵ 4 analysis at this stage to help develop the understanding of how ApoE and metabolism interact. These lines were not included in the original paper as they were collected after the time of publication.

Data on how total cellular ATP is affected by UDCA is also added to this section as these results were not included in the original paper.

3.1.6 Published Paper contributions by PhD Candidate

My contributions to this paper included:

- Gaining ethical approval for all Sheffield biopsies to be performed.
- Taking all biopsies for Sheffield cohorts.
- Performing ATP assays on 1 familial line and 4 sporadic AD lines and associated controls discussed in the paper, and the extra 6 Sheffield sporadic AD and control fibroblast lines discussed in the additional results.
- Performing mitochondrial morphology assays on 1 familial line and 4 sporadic AD lines and associated controls discussed in the paper, and the extra 6 Sheffield sporadic AD and control fibroblast lines discussed in the additional results.
- Performing all seahorse mitochondrial stress test assays.
- Performing all Quantitative Polymerase Chain Reaction (qPCR) experiments.
- Performing all UDCA treatment MMP/ATP assays for 1 familial line and 4 sporadic AD lines and associated controls, and performed all UDCA treatment seahorse-based assays for all fibroblast lines.
- Culturing and performing assays for Drp1 knock down experiment, but I did not perform westerns or perform data analysis for this section.
- Contributed to writing the manuscript and data analysis.

3.2 Published Paper

This Paper was published in the Journal of Molecular Biology The citation is

**Bell, S. M., K. Barnes, H. Clemmens, A. R. Al-Rafiah, E. A. Al-Ofi, V. Leech, O. Bandmann, P. J. Shaw,
D. J. Blackburn, L. Ferraiuolo and H. Mortiboys (2018). "Ursodeoxycholic Acid Improves
Mitochondrial Function and Redistributes Drp1 in Fibroblasts from Patients with Either Sporadic or
Familial Alzheimer's Disease." J Mol Biol 430(21): 3942-3953.**



Ursodeoxycholic Acid Improves Mitochondrial Function and Redistributes Drp1 in Fibroblasts from Patients with Either Sporadic or Familial Alzheimer's Disease

Simon M. Bell, Katy Barnes, Hannah Clemmens[†], Aziza R. Al-Rafiah[‡], Ebtisam A. Al-ofi[§], Vicki Leech, Oliver Bandmann, Pamela J. Shaw, Daniel J. Blackburn, Laura Ferraiuolo and Heather Mortiboys

Sheffield Institute for Translational Neuroscience (SITraN), University of Sheffield, 385a Glossop Road, Sheffield, S10 2HQ, UK

Correspondence to Heather Mortiboys: H.Mortiboys@sheffield.ac.uk

<https://doi.org/10.1016/j.jmb.2018.08.019>

Edited by Edward Chouchani

Abstract

Alzheimer's disease (AD) is the leading cause of dementia worldwide. Mitochondrial abnormalities have been identified in many cell types in AD, with deficits preceding the development of the classical pathological aggregations. Ursodeoxycholic acid (UDCA), a treatment for primary biliary cirrhosis, improves mitochondrial function in fibroblasts derived from Parkinson's disease patients as well as several animal models of AD and Parkinson's disease. In this paper, we investigated both mitochondrial function and morphology in fibroblasts from patients with both sporadic and familial AD. We show that both sporadic AD (sAD) and PSEN1 fibroblasts share the same impairment of mitochondrial membrane potential and alterations in mitochondrial morphology. Mitochondrial respiration, however, was decreased in sAD fibroblasts and increased in PSEN1 fibroblasts. Morphological changes seen in AD fibroblasts include reduced mitochondrial number and increased mitochondrial clustering around the cell nucleus as well as an increased number of long mitochondria. We show here for the first time in AD patient tissue that treatment with UDCA increases mitochondrial membrane potential and respiration as well as reducing the amount of long mitochondria in AD fibroblasts. In addition, we show reductions in dynamin-related protein 1 (Drp1) level, particularly the amount localized to mitochondria in both sAD and familial patient fibroblasts. Drp1 protein amount and localization were increased after UDCA treatment. The restorative effects of UDCA are abolished when Drp1 is knocked down. This paper highlights the potential use of UDCA as a treatment for neurodegenerative disease.

© 2018 The Authors. Published by Elsevier Ltd. This is an open access article under the CC BY license (<http://creativecommons.org/licenses/by/4.0/>).

Introduction

Alzheimer's disease (AD) is the leading cause of dementia worldwide and is characterized by the build-up of amyloid plaques and neurofibrillary tangles with a loss of neurons later in the disease course [1]. Mounting evidence indicates that amyloid plaques and neurofibrillary tangles do not correlate well with disease severity [2].

Mitochondrial dysfunction is a well-established mechanism in familial and sporadic forms of AD (sAD), with evidence from both post-mortem and peripheral patient tissue as well as animal models. Fluorodeoxyglucose positron emission tomography imaging in living patients has identified hypometabolism in parietal and temporal brain regions, even in early disease. Alterations in glucose metabolism and cellular respiration have also been found in AD patient fibroblasts [3–7]. Post-mortem data from AD patients show reduced activity of tricarboxylic acid enzymes and reduced complex IV activity, with complex IV activity decreasing during disease progression [8,9]. Mitochondrial enzymatic failure, reduced glucose metabolism and increased reactive oxygen species production have all been shown to occur before amyloid pathology [10]. Expression of mitochondrial subunits from all respiratory chain complexes is reduced in the entorhinal cortex (which is an area of early pathological change in AD) of AD patients at post-mortem [11]. In addition, similar

bolism in parietal and temporal brain regions, even in early disease. Alterations in glucose metabolism and cellular respiration have also been found in AD patient fibroblasts [3–7]. Post-mortem data from AD patients show reduced activity of tricarboxylic acid enzymes and reduced complex IV activity, with complex IV activity decreasing during disease progression [8,9]. Mitochondrial enzymatic failure, reduced glucose metabolism and increased reactive oxygen species production have all been shown to occur before amyloid pathology [10]. Expression of mitochondrial subunits from all respiratory chain complexes is reduced in the entorhinal cortex (which is an area of early pathological change in AD) of AD patients at post-mortem [11]. In addition, similar

changes in expression of mitochondrial genes have been shown early in disease progression in whole blood samples of AD patients [12]. It is not only mitochondrial function that is altered in AD; of particular importance in neurons is mitochondrial dynamics. Mitochondria are in a constant state of flux undergoing fission and fusion events allowing them to adapt and meet local energy requirements. Evidence from both neurons and patient fibroblasts shows that mitochondria are more elongated and have altered distribution throughout the cell [6]. In particular mitochondria are localized around the perinuclear region in sAD fibroblasts suggesting a collapse of the mitochondrial network [13]. Mitochondrial dysfunction is a shared mechanism between sAD and familial forms of AD. Transgenic models of familial AD that incorporate amyloid precursor protein (APP) show impaired mitochondrial function and changes in mitochondrial morphology, specifically reduced mitochondrial membrane potential and tricarboxylic acid enzyme activities as well as reduced ATP levels [14,15]. In addition, genetic risk factors for AD alter mitochondrial function. Possession of the *APOE4* allele is the largest genetic risk factor for sAD, and possession of this allele is associated with reduced expression of respiratory chain complex proteins and activity of complex IV [16,17]. Much work has been done trying to elucidate

the mechanisms which cause AD with a view to finding therapeutic targets to slow or stop the progression of AD. To date, however, these interventions have not succeeded in modifying clinical outcome. The search for therapeutic targets has focused mostly around the amyloid cascade.

Mitochondrial abnormalities are also found in fibroblasts of patients with other neurodegenerative diseases. We and others have extensively characterized these changes in Parkinson's disease (PD) genetic subtypes [18–23] and MND sporadic and genetic subtypes [24,25]. We were the first to use the mitochondrial functional deficits as a primary screen in a drug screening cascade for PD [20]. We identified ursodeoxycholic acid (UDCA) in a drug screen of fibroblasts from *parkin* mutant PD patients, which we have subsequently validated in other forms of PD and other model systems [21]. UDCA is a promising compound as it is already in clinical use for the treatment of primary biliary cirrhosis.

We therefore hypothesized that mitochondrial abnormalities are detectable in fibroblasts from sAD and familial presenilin 1 (PSEN1) patients, and that these abnormalities could be improved with UDCA treatment. Here we describe our findings of mitochondrial membrane potential, mitochondrial morphology and localization, metabolic activity and

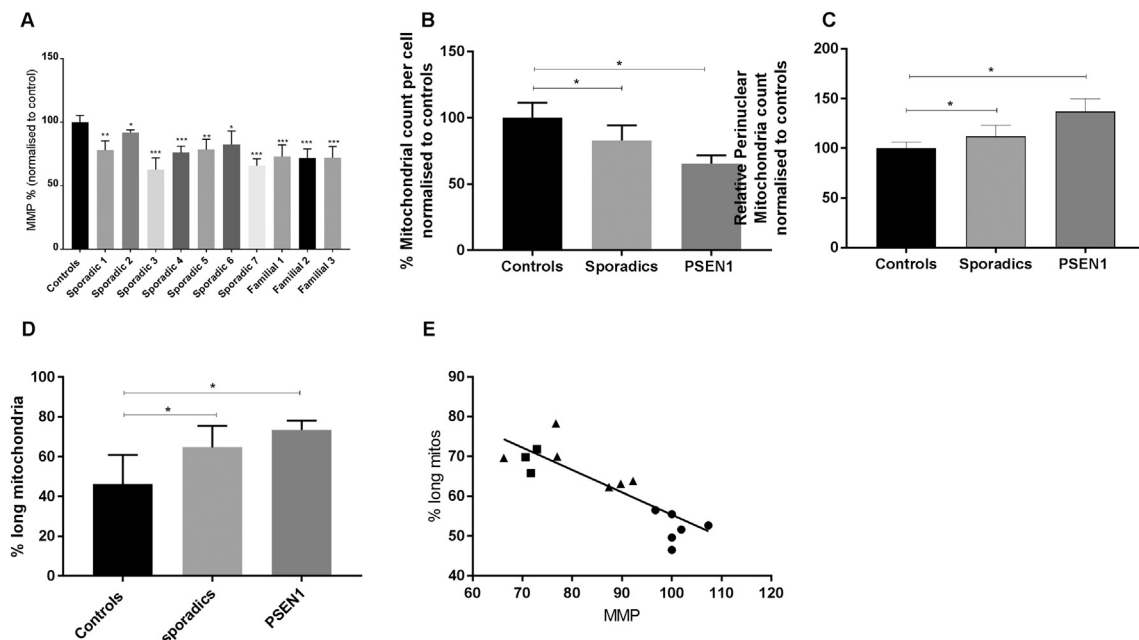


Fig. 1. (A) Mitochondrial membrane potential in each of the seven sporadic and three familial AD lines. When compared to controls ($n = 7$), all sporadic lines and all familial lines showed a significant reduction in mitochondrial membrane potential ($*p < 0.05$, $**p < 0.01$, $***p < 0.005$). (B) The total mitochondrial count was significantly reduced in both sporadic ($*p < 0.05$) and familial groups ($*p < 0.05$). (C) Perinuclear mitochondrial count was significantly increased in both sporadic ($*p < 0.05$) and familial ($***p < 0.005$) groups. (D) The percentage of cell area occupied by long mitochondria is increased in both sAD and PSEN1 patient fibroblasts ($*p < 0.05$). (E) Correlation of mitochondrial membrane potential and % long mitochondria shows negative correlation ($p = 0.0002$, $R^2 = 0.7$). The circles represent controls; triangles, sAD; and squares, PSEN1. All measurements were carried out on three separate passages of each fibroblast line.

mitochondrial fission/fusion machinery expression in sAD and PSEN1 fibroblasts. In addition, we describe a new mode of action of UDCA on mitochondrial respiration which is abolished when dynamin-related protein 1 (Drp1) is knocked down, indicating that Drp1 is involved in the recovery mechanism in AD.

Results

Mitochondrial function and morphology are altered in both sAD and PSEN1 patient fibroblasts

We initially investigated global mitochondrial function and morphology to address if there is a general mitochondrial phenotype present in AD. We assessed these mitochondrial parameters in two separate cohorts of fibroblasts from sAD patients, one collected locally (Sheffield cohort, $n = 4$) and one sourced from the Coriell cell repository ($n = 3$) in addition to a cohort of PSEN1 patient lines ($n = 3$ also sourced from Coriell cell repository and compared to controls ($n = 4$ from Sheffield and $n = 3$ from Coriell)). We found reduced mitochondrial membrane potential in all sAD fibroblasts (controls 100 ± 5.3 , sAD 83 ± 9 ; $p < 0.05$) and PSEN1 fibroblasts (controls 100 ± 5.3 , PSEN1 71 ± 1.1 ; $p < 0.01$; Fig. 1A). Every AD fibroblast line had a significant reduction in mitochondrial membrane potential, ranging from a 35% to an 8% reduction.

In these same lines (both sAD cohorts and the PSEN1 fibroblasts), we also identified significant alterations in mitochondrial morphology and subcellular localization (Fig. 1B and C). We analyzed the mitochondria as three different entities: long mitochondria defined as mitochondria with form factor > 0.48 , short mitochondria defined as mitochondria with form factor < 0.48 and all mitochondria. When considering total mitochondria, mitochondrial count per cell was reduced in the sporadic group (controls 100 ± 11.3 , sAD 82.3 ± 11.5 ; $p < 0.05$; Fig. 1B) and in the PSEN1 group (controls 100 ± 11.3 , PSEN1 55.8 ± 18.3 ; $p < 0.05$; Fig. 1B). In both the sporadic and PSEN1 groups, the localization of mitochondria was focused more around the cell nucleus when compared to controls. Specifically, there was an increase in perinuclear mitochondria (controls 100 ± 6.2 , sAD 112 ± 11.1 , PSEN1 136.9 ± 12.9 ; $p < 0.05$ and $p < 0.005$ respectively; Fig. 1C). Both sAD and PSEN1 fibroblasts had a higher proportion of long mitochondria (% long mitochondria of total mitochondria controls 46 ± 14 , sAD 65 ± 11 , PSEN1 73 ± 11 ; Fig. 1D) indicating a more fused mitochondrial network. Conversely, the % of the cell area occupied by small mitochondria was decreased. The form factor of the overall mitochondria network was altered, which upon further investigation was due to the "small" mitochondrial components having higher form factor than in controls (data normalized

to controls: controls $100\% \pm 3\%$, sAD $106\% \pm 2.5\%$, PSEN1 $111\% \pm 3\%$). We also found a correlation between the functional abnormalities and morphological changes; mitochondrial membrane potential and % long mitochondria showed a negative correlation ($p = 0.0002$, $R^2 = 0.7$; Fig. 1E).

Next we investigated mitochondrial respiration in both sAD fibroblasts and PSEN1 mutant fibroblasts using the "mito stress test" on the Seahorse Analyser. This assay was undertaken on a limited number of sAD fibroblast lines ($n = 5$) and PSEN1 fibroblast lines ($n = 2$) due to poor growth of the other fibroblast lines. The Seahorse trace shows a reduction in oxygen consumption in each sAD fibroblast line measured compared to controls, whereas there is an increase in each PSEN1 patient fibroblast line (Fig. 2A–E). Specifically, we found a significant reduction in spare capacity in sAD fibroblasts of 34% when compared to controls ($p < 0.05$); this varied between a 15% reduction and a 35% reduction in the sAD fibroblasts; the variability is shown in Fig. 2A–E. The PSEN1 patient fibroblasts showed significant increases in mitochondrial respiration (increased by 52%, $p < 0.01$), ATP-coupled respiration (increased by 48%, $p < 0.01$) and spare capacity (increased 58%, $p < 0.05$; Fig. 2F). The reductions in spare mitochondrial capacity show correlation with mitochondrial membrane potential deficits ($p = 0.003$, $R^2 = 0.65$; Fig. 2G); this is with the exclusion of the PSEN1 sample as this has reduced mitochondrial membrane potential, yet increased spare capacity. The Seahorse Analyser also simultaneously measures extracellular acidification rate (ECAR); we, however, did not find any significant alterations in basal or stimulated ECAR rates in the sAD or PSEN1 patient fibroblasts (data not shown).

UDCA improves mitochondrial phenotype in sAD and PSEN1 fibroblasts

After identifying mitochondrial abnormalities in both sAD and PSEN1 patient fibroblasts, we next investigated if these mitochondrial parameters could be improved by treatment with UDCA. Treatment with 100 nM UDCA increased mitochondrial respiration and ATP-coupled respiration in both sAD and PSEN1 patient fibroblasts by 32% and 51%, respectively (Fig. 2F, $*p < 0.05$). There was no effect of UDCA on maximal capacity or uncoupled respiration. Treatment with UDCA also increased MMP (controls 2.1 ± 1.6 , sAD 11.2 ± 2 , PSEN1 24.7 ± 1.5 ; $p < 0.05$; Fig. 3A). This increase varied across AD fibroblast lines with an increase in mitochondrial membrane potential of between 12% and 28% (Fig. 3A). Furthermore, although the total mitochondrial morphology parameters were not significantly altered by UDCA treatment, the % long mitochondria was significantly reduced (controls $+5 \pm 2.8$, sAD -24.5 ± 10.7 , PSEN1 -40.2 ± 2.1 ; $p < 0.05$; Fig. 3B).

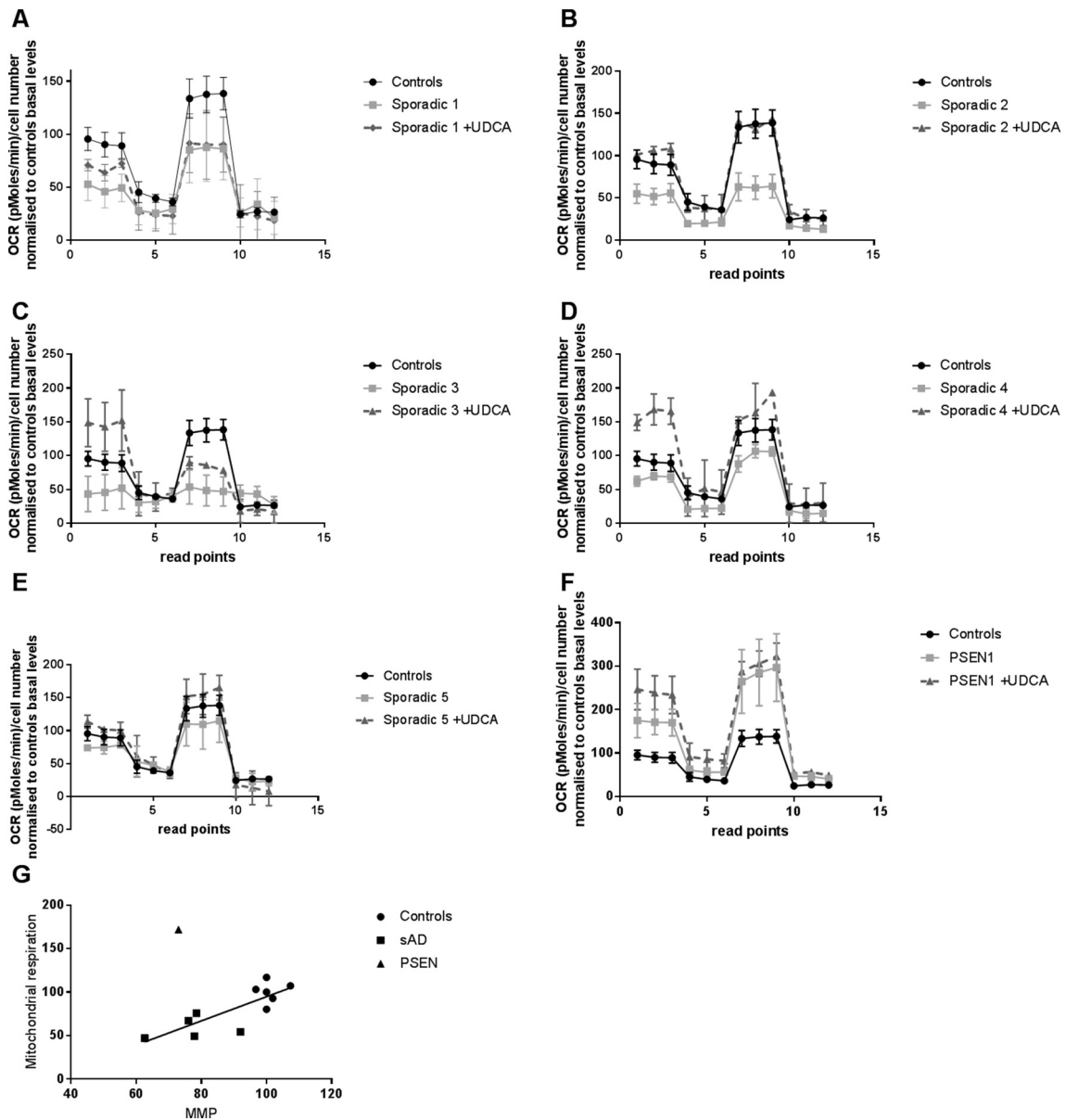


Fig. 2. OCRs. Panels A–F show an OCR trace for controls (black circle solid line, $n = 6$), sporadic [gray squares and solid line, sAD1 (A), sAD2 (B), sAD3 (C), sAD4 (D), sAD5 (E)] and PSEN1 [gray squares and solid line, PSEN1 (F)] cell lines in the untreated condition. Sporadic patient fibroblasts have a reduction in OCR compared to controls at baseline and when measuring maximal capacity, but PSEN1 cell lines have an increase at both points. Panels A–F show the reduction seen in spare capacity in sporadic cell lines ($*p < 0.05$) and the increase seen in PSEN1 cell lines compared to controls ($*p < 0.05$). Fibroblasts after treatment with 100 nM UDCA for 24 h show increased mitochondrial respiration in both sAD ($*p < 0.05$) and PSEN1 ($*p < 0.05$) fibroblasts (A–F). Each measurement was repeated on three separate passages of each cell line. (G) Mitochondrial membrane potential shows correlation with spare respiratory capacity ($p = 0.003$, $R^2 = 0.65$). The circles represent controls; squares, sAD; and triangles, PSEN1. The PSEN1 fibroblasts were excluded from linear regression calculations.

Mitochondrial morphology proteins are changed in AD patient fibroblasts; UDCA modulates mitochondrial fission proteins

We investigated both mRNA and protein expression of the mitochondrial fission and fusion modulators Drp1, mitofusin 1 (Mfn1), Mfn2 and optic atrophy 1

(Opa1). We found no significant alterations in mRNA expression of any mitochondrial fission/fusion modulators in the sAD or PSEN1 patient fibroblasts (Supplementary Fig. 1A–D). Furthermore, we assessed the protein expression of the same mitochondrial modulators and found a reduction in the total cellular protein expression of Drp1 in both sAD and PSEN1

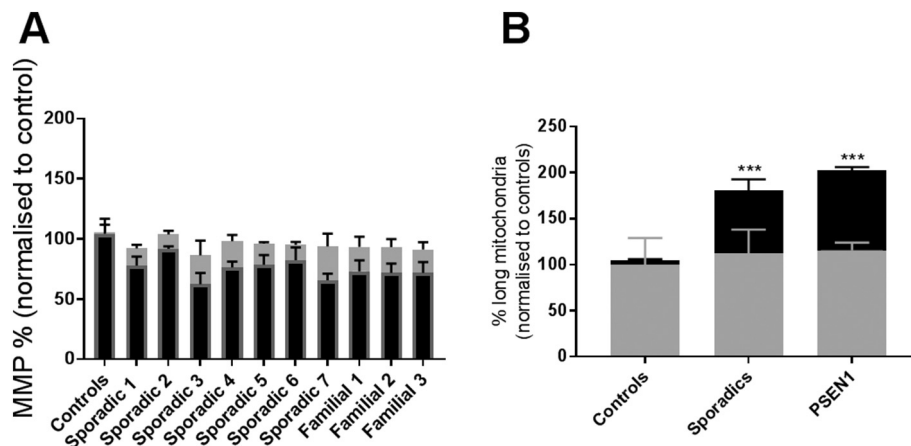


Fig. 3. Recovery with UDCA treatment. (A) Fibroblasts are treated for 24 h with 100 nM UDCA. UDCA treatment, however, increases mitochondrial membrane potential. The increase from the untreated state for controls, sporadics and familial cell lines varies between 0 and 5% for controls, 12% and 28% for sAD and 19% and 21% for PSEN1 ($*p < 0.05$). (B) The increase in mitochondrial membrane potential when fibroblasts are treated with 100 nM of UDCA. The relative increase from the untreated state for controls, sporadics and familial cell lines is 0%, 11% and 25%, respectively ($*p < 0.05$). Each measurement was repeated on three separate passages of each cell line.

cohorts (controls 100 ± 12.2 , sAD 37.8 ± 19.7 , PSEN1 64.5 ± 22.5 ; $p < 0.05$; Fig. 4A). Example Western blots from each fibroblast line are given in Fig. 4A(ii) and Supplementary Fig. 1E. Total levels of Drp1 expression were increased after treatment with UDCA in sAD [sAD dimethyl sulfoxide (DMSO) treated 37.4 ± 11.5 , sAD UDCA treated 74.5 ± 31.6 ; $p < 0.05$; Fig. 4A]. Levels of the other mitochondrial modulators were unaltered at protein level (Supplementary Fig. 1G). We next assessed the subcellular distribution of Drp1 using immunofluorescence staining. Drp1 is normally cytosolic and is recruited to the outer mitochondrial membrane at points of fission by receptors on the outer mitochondrial membrane such as mitochondrial fission 1 protein (Fis1), MFF, Mid49 and Mid51. Drp1 then acts in a pincer-like fashion to surround the outer mitochondrial membrane and pinch it together forming two daughter mitochondria. The quantification of our Drp1 staining showed that the AD patient fibroblasts (both sAD and PSEN1) have less Drp1 specifically at their mitochondria (controls 100 ± 11.13 , sAD 32.77 ± 11.63 , PSEN1 36.58 ± 9.35 ; $p < 0.01$; Fig. 4B). This indicates that Drp1 is not being recruited successfully to mitochondria. UDCA treatment increased the amount of Drp1 localized at the mitochondria membrane in both the sAD and PSEN1 patient fibroblasts (sAD DMSO treated 43.66 ± 4.62 , sAD UDCA treated 74.88 ± 6.67 , PSEN1 DMSO treated 33.86 ± 1.83 , PSEN1 UDCA treated 74.5 ± 8.2 ; $p < 0.05$; Fig. 4B).

Drp1 knockdown abolishes UDCA protective effect in sAD and PSEN1 fibroblasts

To elucidate if the protective effect of UDCA was mediated by Drp1, we undertook knockdown experiments of Drp1 in control and AD patient fibroblasts. We

achieved a knockdown of Drp1 protein levels at 48 h post-transfection of 40% compared to scramble siRNA negative control for each fibroblast line (Fig. 5A). This meant that the Drp1 level in the AD fibroblasts after knockdown was 25% of control levels as Drp1 levels are already lower in AD fibroblasts. Drp1 knockdown in control fibroblasts did not result in reductions in mitochondrial membrane potential; however, mitochondrial morphology was altered. Mitochondria were more elongated [form factor (normalized to controls as %) controls 100 ± 5 , controls with Drp1 k/d 113 ± 3.3 ; $p < 0.05$, Fig. 5B] with an increased amount of the cell area occupied by long mitochondria (controls scramble 46 ± 2.3 , controls Drp1 k/d 59 ± 3.4 ; $p < 0.05$). Similar changes were observed in AD fibroblasts after Drp1 knockdown with no effect on mitochondrial membrane potential but increased further % of cell area occupied by long mitochondria (sAD scramble 65 ± 3.4 , sAD Drp1 k/d 74.4 ± 4.5 ; PSEN1 scramble 72.7 ± 5.3 , PSEN1 Drp1 k/d 81.2 ± 5.2). However, the increase in mitochondrial membrane potential observed in AD fibroblasts after UDCA treatment was not seen in the Drp1 knockdown condition (Fig. 5D). Similarly, the “corrections” in mitochondrial morphology seen after UDCA treatment were not seen in the Drp1 knockdown condition (Fig. 5B). We investigated Drp1 cellular localization under conditions of Drp1 knockdown. We observed, as expected, less Drp1 colocalizing with mitochondria in all cells with Drp1 knockdown; UDCA treatment was not able to change this (Fig. 5C).

Discussion

Here we show that detectable alterations in both mitochondrial function and morphology are found in

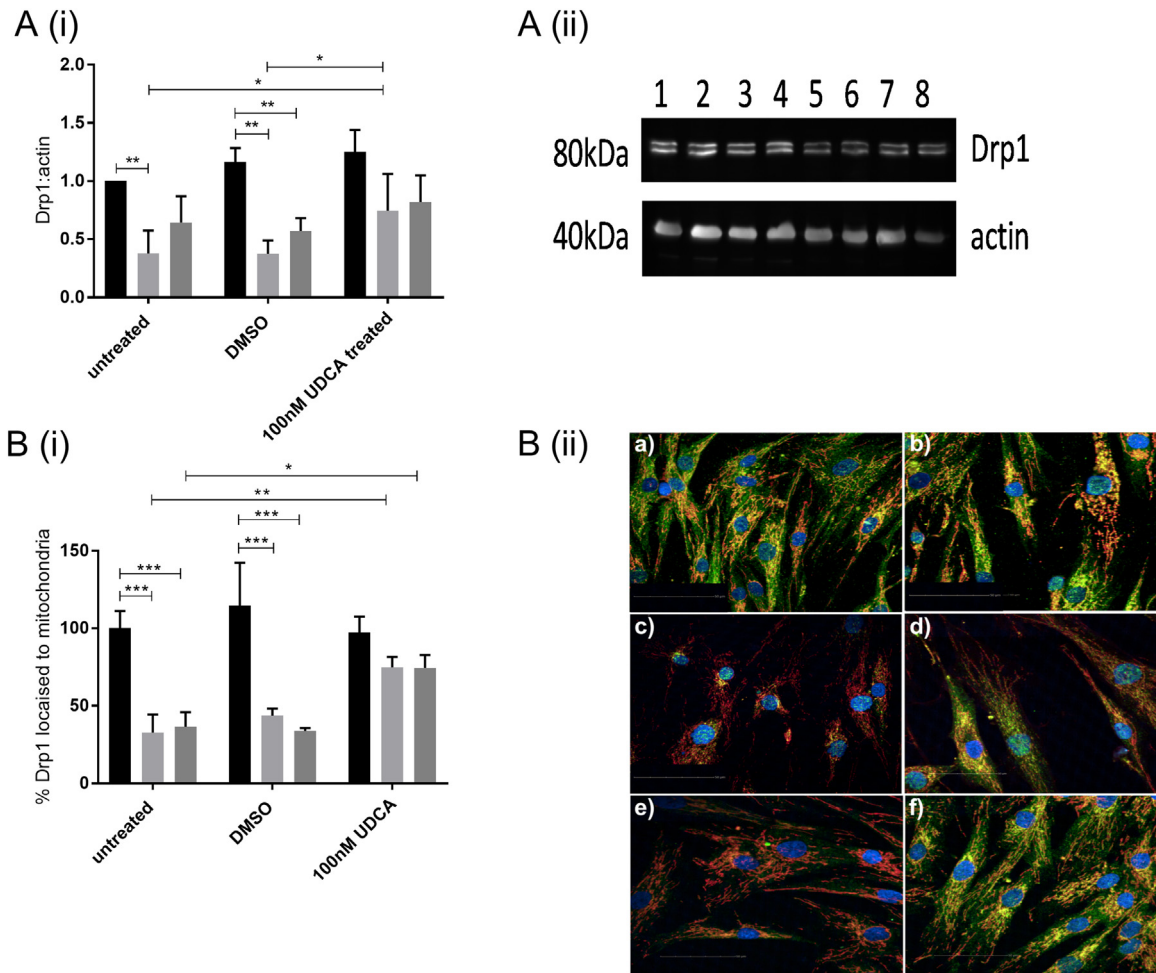


Fig. 4. Drp1 protein expression. (A) Total Drp1 protein expression levels are reduced in both sAD (light gray bars) and PSEN1 (dark gray bars) fibroblasts (** $p < 0.01$). After treatment with 100 nM UDCA, total Drp1 levels are increased in the sAD fibroblasts (* $p < 0.05$). A(ii) Representative western blot showing control untreated (lane 1), control DMSO treated (lane 2), control 100 nM UDCA (lane 3), control 10 μM UDCA (lane 4), sAD untreated (lane 5), sAD DMSO treated (lane 6), sAD 100 nM UDCA treated (lane 7) and sAD 10 μM UDCA treated (lane 8) for Drp1 and loading control actin. (B) Drp1 cellular localization is altered in sAD and PSEN1 fibroblasts. Significantly less Drp1 colocalizes with the mitochondrial marker (TOMM20) in the sAD (light gray bars) and PSEN1 (dark gray bars) fibroblasts (** $p < 0.005$); however, after treatment with 100 nM UDCA for 24 h, the amount of Drp1 which colocalizes with the mitochondria is increased (* $p < 0.05$; ** $p < 0.01$). B(ii) Representative images of control fibroblasts vehicle treated (a) and treated with UDCA (b) and sAD fibroblasts vehicle treated (c) and treated with UDCA (d) and PSEN1 vehicle treated (e) and treated with UDCA (f). Blue staining is Hoechst for the nucleus, green staining is Drp1 and red staining is TOMM20 for the mitochondria. Each measurement was repeated on three separate passages of each cell line; for immunocytochemistry measurements, at least 150 cells were imaged per fibroblast line per experiment.

peripheral fibroblasts from two separate cohorts of sAD patients and a group of PSEN1 familial AD patients. Mitochondrial membrane potential is reduced in all seven sAD fibroblast lines tested and the three PSEN1 fibroblast lines. It is noteworthy that we did not stress the cells at any point in order to reveal these mitochondrial abnormalities; they were identifiable under “normal glucose” culture conditions. Mitochondrial membrane potential was more variable in the AD patient fibroblasts than the control fibroblasts. We postulate that this is a feature of investigating sAD

patients; the underlying cause of sporadic disease and disease stage at which each biopsy was collected is not known for every patient. These factors are likely to increase variability in these mitochondrial measures more than in controls without a neurodegenerative condition.

Abnormalities in the mitochondria of patients have been shown before [4,6,26], and it has also been shown that the amyloid protein itself can affect the function of mitochondria [27]. This is one of the first studies to directly compare sAD and familial AD

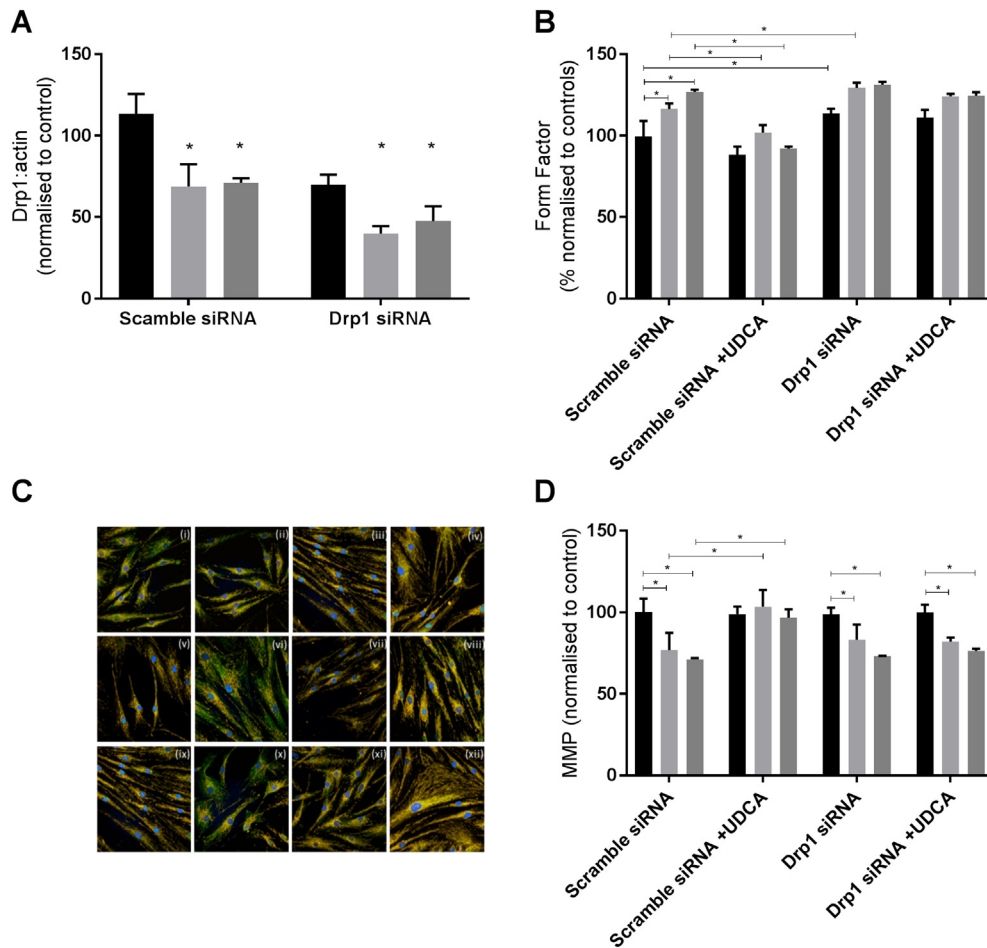


Fig. 5. Drp1 knockdown data. (A) Drp1 protein expression knockdown of 48% from scramble siRNA levels ($*p < 0.05$). (B) Mitochondrial form factor is increased in sAD and PSEN1 fibroblasts in the scramble siRNA condition, which is reduced again after UDCA treatment. Drp1 knockdown increases form factor in all fibroblasts. UDCA does not have an effect on mitochondrial form factor in the Drp1 knockdown condition. (C) Image showing Drp1 staining in green, mitochondria in red and nuclei in blue. A representative image is shown for each condition. Control scramble siRNA (i), control scramble siRNA + UDCA (ii), control Drp1 siRNA (iii), control Drp1 siRNA + UDCA (iv); sAD scramble siRNA (v), sAD scramble siRNA + UDCA (vi), sAD Drp1 siRNA (vii), sAD Drp1 siRNA + UDCA (viii); PSEN1 scramble siRNA (ix), PSEN1 scramble siRNA + UDCA (x), PSEN1 Drp1 siRNA (xi), PSEN1 Drp1 siRNA + UDCA (xii). (D) Mitochondrial membrane potential is reduced in sAD and PSEN1 fibroblasts in the scramble siRNA condition, which is increased with UDCA treatment. In the Drp1 siRNA condition, there is no further decrease in mitochondrial membrane potential; however, UDCA treatment does not increase mitochondrial membrane potential.

patient derived fibroblasts at the same time. Although both sAD and PSEN1 patient fibroblasts have mitochondrial abnormalities, the level of defect varies between sAD and PSEN1 fibroblasts. Particularly striking is the increase in mitochondrial respiration in the PSEN1 mutant fibroblasts, whereas the spare respiratory capacity was reduced in the sAD fibroblast cohort. These biochemical data are difficult to interpret; the opposite effects found when investigating respiration and mitochondrial membrane potential in PSEN1 patient fibroblasts may suggest that the mitochondria are uncoupled. Some evidence for this can be gained from the Seahorses traces as the coupling efficiency is reduced in PSEN1 fibroblasts

even if respiration is increased. Alternatively, as fibroblasts do not rely heavily on oxidative phosphorylation in order to maintain energy state, particularly in glucose media, this could suggest that PSEN1 mutants rely heavily on alternative energy pathways. This would best be investigated in additional cell types which rely to varying degrees on glycolysis versus oxidative phosphorylation. The recent study by Sonntag *et al.* [7] investigated mitochondrial respiration in a cohort of late-onset AD patient fibroblasts and found the mitochondrial respiration rates to be higher than controls, similar to the PSEN1 fibroblast lines we tested here. The apparent discrepancy between our sAD and the study by Sonntag *et al.* could in part be

due to differences in the age of the patients, the cell culture conditions and passage of the cells at measurement. The sAD patients included in this study, particularly those from the Sheffield cohort, were young due to the patients being recruited at the Sheffield young-onset clinic, whereas those sAD patients biopsied in the study by Sonntag *et al.* were late-onset sAD patients. The age of the donors is also likely to explain the differences seen between our sAD cohort and that of Sonntag *et al.* with regard to cellular ATP levels. The global reductions in MMP we describe here largely concur with the previously published literature from AD patient fibroblasts (both familial and sporadic) [4,6,26,28,29]. The literature is clear that mitochondrial abnormalities are present and detectable in peripheral fibroblasts from AD patients.

The reasons for these abnormalities, however, are still being investigated. We show alterations in the protein expression and subcellular localization of Drp1. Drp1 levels have been implicated as a cause of mitochondrial abnormalities in sAD before, with reductions in Drp1 protein levels found in sAD fibroblasts [13,29], which could be rescued by Drp1 over expression [13]. PSEN1 fibroblasts appear to be less affected than sAD fibroblasts. PSEN1 has been shown to increase activity at the mitochondrial associated membrane [30]; therefore, it may be having a direct role in controlling mitochondrial morphology, which is not present in sAD patients. The sAD cohort used in our study may have mitochondrial impairment as a more central pathological mechanism, and therefore, abnormalities are more pronounced when measured in particular in young onset sAD patients, as these patients mitochondria seem to have aged more rapidly than that of late-onset sAD patients and controls. The recycling of dysfunctional mitochondria is a process that Drp1 is also intimately involved with and has been shown by others to be defective in at least PSEN1 patient fibroblasts [29]. We did not investigate mitophagy in this report; however, this is a potential mechanism that could be investigated further.

Previous work by Manczak and colleagues [31] has shown an interaction between Drp1 and the amyloid protein in the brain of an APP mouse model. In this paper, partial reduction of Drp1 protein expression reduces the production of amyloid-beta and improves the mitochondrial dysfunction seen in an APP mouse model of AD. This same group has also shown that a reduction in Drp1 leads to a reduction in phosphorylated tau in the mouse brain [32]. It is plausible that the mis-localization of Drp1 that we have shown in our study is exacerbated in the brain by interaction with amyloid-beta as described in the above mouse models of AD. Our work further highlights the need to investigate Drp1 manipulation in other cell types such as neurons.

UDCA has been used in the treatment of primary biliary sclerosis for over 30 years. It has a limited

side effect profile and is a relatively safe drug [33]. Furthermore, UDCA has been tested in several cell and animal models of AD and showed a putative protective effect [34–37]. Here we show that UDCA restores mitochondrial membrane potential in both sAD and PSEN1 mutant fibroblasts; it, however, has no significant effect on mitochondrial morphology. However, we did find significant changes in the amount of Drp1 localizing to the mitochondria which increased in both sAD and PSEN1 fibroblasts, close to control levels. To verify if UDCA is acting via a pathway involving Drp1 in AD fibroblasts, we examined the protective effect of UDCA under a Drp1 knockdown condition; we found that knockdown of Drp1 levels abolished the protective effect of UDCA on mitochondrial membrane potential and mitochondrial morphology. This knockdown was transient as it was employed in the primary fibroblasts as a further validation sAD fibroblasts could be immortalized with subsequent Drp1 knockdown; further validation using single siRNA's would also strengthen this mechanistic link. As Drp1 knockdown in control cells did not result in significant reduction of mitochondrial membrane potential, it is plausible that UDCA modulation of Drp1 is part of a wider pathway altered by UDCA treatment without UDCA interacting directly with Drp1 itself. Drp1 is known to undergo a complex array of post-translational modifications including nitrosylation, ubiquitinylation, sumoylation and phosphorylation. In particular several phosphorylation sites have been identified; some promote mitochondrial fragmentation (via cyclin B) and others promote elongation via phosphorylation by protein kinase A. This phosphorylation site has been shown to inhibit disassembly of the Drp1 catalytic cycle, therefore accumulating large Drp1 oligomers on the outer mitochondrial membrane [38]. In this study, we did not investigate any of the post-translational modifications of Drp1 or any of the other known pathways that can affect Drp1 localization or phosphorylation state (including AMPK, protein kinase A and ERK); therefore, this should be investigated further to fully elucidate the mechanism of action of UDCA in AD. Furthermore, Drp1 has been implicated in the ER–mitochondrial contact sites (or mitochondrial associated membranes) where PSEN1 is known to increase activity in AD. The investigation of ER–mitochondrial contact sites is beyond the scope of this study; however, it would be important to investigate this pathway to assess the target by which UDCA is acting. Identifying the exact subcellular target by which UDCA is acting in AD is important for future therapeutic applications of UDCA and other potential neuroprotective compounds. Altering mitochondrial fission modulators has not been proposed before as a mechanism for UDCA and therefore warrants further investigation in other patient derived models and other animal models that have previously showed protection of UDCA.

In conclusion, our study has shown for the first time that reduced mitochondrial membrane potential in AD patient fibroblasts can be corrected with the treatment of UDCA via a pathway, which includes Drp1. Our study has identified a potential novel pathway by which UDCA has mitochondrial protective effects and further builds the case for the use of UDCA as a potential neuroprotective therapy for neurodegenerative disease.

Methods and Materials

Patient details

Fibroblasts from patients with sporadic and PSEN1 mutations were obtained from the NIGMS Human Genetic Cell Repository at the Coriell Institute for Medical Research: GM08243, GM07375, and GM07376 (all male, mean age 67.6 years, SD 6.65) and ND41001, ND34733, and ND34730 (2 male, 1 female, mean age 48.33 years, SD 11.06). These fibroblasts were compared with control fibroblasts (mean age 59.3 years, SD 6.35) from the same repository [GM07924, GM02189, GM23967 (all male)].

A second cohort of sporadic patient fibroblasts (2 male, 2 female, mean age 59.25 years, SD 5.37) and two aged matched controls (3 male, 1 female, mean age 60.66 years, SD 2.08) were also sampled from a local population of patients involved in the MODEL-AD research study (Research and Ethics Committee number: 16/YH/0155). The McKhann *et al.* [39] criteria were used to diagnose AD, and participants took part in the European wide Virtual Physiological Human: Dementia Research Enabled by IT (VPH-DARE@IT).

Cell culture

Primary fibroblast cells were cultured continuously using methods performed essentially as described by Mortiboys *et al.* [24]. Cells were grown in EMEM (4500 g/L glucose), supplemented with 10% FBS, 100 UI/ml penicillin, 100 µg/ml streptomycin, 50 µg/ml uridine and 1 mM sodium pyruvate, 0.1 mM amino acids, and 0.1 × MEM vitamins. For mitochondrial membrane potential, morphology cells were plated at a density of 2500 cells per well in a black 96-well plate. UDCA (Sigma-Aldrich Ltd) was added to culture media (10 mM and 100 nM) 24 h prior to assay. DMSO was used as vehicle control.

Mitochondrial morphology

Mitochondrial membrane potential and mitochondrial morphological parameters were measured using tetramethylrhodamine staining of live fibroblasts. Briefly, 24 h after drug treatment, cells were incubated

with 80 nM tetramethylrhodamine and 10 µM Hoescht in phenol red-free media for 1 h. Cells were washed and imaged using the InCell Analyzer 2000 high-content imager (GE Healthcare). Raw images were processed and parameters obtained using a custom protocol in InCell Developer software (GE Healthcare) allowing for segmentation of mitochondria, nuclei and cell boundaries.

Western blots

Cell pellets from patient and control fibroblasts were lysed using RIPA buffer and Protein Inhibitor Cocktail on ice, and protein levels were measured using a Bradford Assay. Twenty micrograms of protein was run on a 12% SDS-PAGE gel and transferred to a polyvinylidene fluoride membrane. Membranes were incubated overnight at 4 °C, with mouse anti-Drp1 (Abcam; 1:1000), mouse anti-OPA1 (BD Biosciences; 1:1000), mouse anti-Mfn1 (Abcam; 1:1000) or rabbit anti-Mfn2 (St Johns Laboratory; 1:500). Membranes were also probed for β actin as a loading control (St Johns Laboratory; 1:1000). Membranes were then incubated with goat anti-mouse HRP (Abcam; 1:10,000) or goat anti-rabbit HRP (Dako; 1:5000), as appropriate. Membranes were imaged using the G box chemi system using GeneSnap software (Syngene). Densitometry was analyzed using GeneTools software (Syngene).

RNA extraction and qPCR

Fibroblasts were treated with UDCA 10µM and 100 nM 24 h prior to harvesting. Approximately 750,000 cells were harvested for each RNA extraction. RNA extraction was performed using an RNAeasy Plus Mini Kit (Qiagen) and by following Quick-start supplied protocol. RNA was converted into complementary DNA using the QuantiTect Reverse Transcription Kit (Qiagen), standard Quick-Start supplied protocols were followed. qPCR was performed on a Stratgene PCR machine. Samples were loaded at 12.5 ng/µl per well. Sybr Green was used as the detection dye for the chain reaction, and a standard two-step program with 40 amplification cycles was used during the PCR. Primer sequences were as follows: Drp1: forward ATTATGCCAGCCAGTCCACAA, reverse CGCTGTTCCCGAGCAGATA; Mfn1: forward CACTCCAGCAACGCCAGATA, reverse CGGACGC CAATCCTGTTACT; Mfn2: forward GTCTGACCTGG ACCACCAAG, reverse TGCAGTTGGAGCCAGTGT AG; and Opa1: forward AGCCAGTCCAAGCAGG ATTC, reverse TGCTTTCAGAGCTGTTCCCT.

Metabolic flux assay

Oxygen consumption rate (OCR) and ECAR were measured using a 24-well Agilent Seahorse XF analyzer machine (Agilent). Human fibroblasts were

plated at a density of 60,000 cells per well. Cells were treated with UDCA 100 nM for 24 h prior to measurement. Three measurements of OCR and ECAR were taken in each state: basal state, after the addition of oligomycin (0.5 μ M), FCCP (0.5 μ M) and rotenone (1 μ M). A cell count was then done on a fixed assay plate using a Hoechst dye (1 μ M). Data presented in this paper are normalized to cell number.

Immunocytochemistry

Cells were fixed in 4% paraformaldehyde and then permeabilized with 0.1% Triton. After blocking, cells were incubated with anti-mouse Drp1 (BD Biosciences; 1:1000) and anti-rabbit TOM20 (Santa Cruz Biotechnology; 1:1000). Cells were then incubated with Alexa Fluor anti-rabbit 568 and Alexa Fluor anti-mouse 488 and 1 μ M Hoechst. Cells were imaged using the Opera Phenix high-content imager (PerkinElmer). z Stacks were collected and analyzed using Harmony software (PerkinElmer).

Drp 1 knockdown experiments

Cells were plated as above for the mitochondrial membrane potential and morphology assays. Cells were treated with either 100 nM Drp1 siRNA SMART pool Accell probes (Horizon Discovery) or 100 nM scramble siRNA-negative Accell probes in Accell delivery media. After 24 h, 100 nM UDCA was added to the treatment conditions, and 24 h later, the assays carried out.

Statistical tests

Data are presented as normalized mean \pm SD unless otherwise stated. For UDCA-treated parameters (ATP and MMP), data are presented as percentage increase from untreated basal levels. Data were analyzed using GraphPad Prism Software (V7.02): one-way ANOVA with Tukey's multiple comparisons posttest or, for UDCA-treated data, two-way ANOVA with Tukey's multiple comparisons posttest. In addition, *t* test was used to compare each individual AD fibroblast line to the control group for MMP.

Supplementary data to this article can be found online at <https://doi.org/10.1016/j.jmb.2018.08.019>.

Acknowledgments

We would like to thank all research participants for their help with this study. Grant support from Parkinson's UK (Grant No. F1301), Alzheimer Research UK (Grant No. ARUK-PCRF2016A-1), Alzheimer research UK Yorkshire network and the National Institute for Health Research Sheffield Biomedical

Research Centre (Translational Neuroscience) is gratefully acknowledged.

Received 12 January 2018;

Received in revised form 8 August 2018;

Accepted 14 August 2018

Available online 29 August 2018

Keywords:

UDCA;
presenilin;
treatment;
neurodegeneration;
mitochondrial morphology

†Academic Unit of Oral and Maxillofacial Pathology, School of Clinical Dentistry, University of Sheffield, 19 Claremont Crescent, Sheffield, S10 2TA.

‡Department of Laboratory Technology, Faculty of Applied Medical Sciences, King Abdulaziz University Jeddah 201,589, Kingdom of Saudi Arabia.

§Department of Physiology, Faculty of Medicine, King Abdulaziz University Jeddah 201,589, Kingdom of Saudi Arabia.

Abbreviations used:

Drp1, dynamin-related protein; PSEN1, presenilin 1; Mfn1, mitofusin 1; Mfn2, mitofusin 2; Opa1, optic atrophy 1.

References

- [1] D.P. Perl, Neuropathology of Alzheimer's disease, *Mt Sinai J. Med.* 77 (2010) 32–42, <https://doi.org/10.1002/msj.20157>. *Neuropathology*.
- [2] G. Forster, B. Sc, F.E. Matthews, D. Ph, C. Brayne, *Age, Neuropathology, and Dementia*, 2009.
- [3] A. Leuzy, E. Rodriguez-Vieitez, L. Saint-Aubert, K. Chiotis, O. Almkvist, I. Savitcheva, M. Jonasson, M. Lubberink, A. Wall, G. Antoni, A. Nordberg, Longitudinal uncoupling of cerebral perfusion, glucose metabolism, and tau deposition in Alzheimer's disease, *Alzheimers Dement.* (2017) 1–12, <https://doi.org/10.1016/j.jalz.2017.11.008>.
- [4] M.J. Pérez, D.P. Ponce, C. Osorio-Fuentealba, M.I. Behrens, R.A. Quintanilla, Mitochondrial bioenergetics is altered in fibroblasts from patients with sporadic Alzheimer's disease, *Front. Neurosci.* 11 (2017) <https://doi.org/10.3389/fnins.2017.00553>.
- [5] C. Cadonic, M.G. Sabbir, B.C. Albeni, Mechanisms of mitochondrial dysfunction in Alzheimer's disease, *Mol. Neurobiol.* 53 (2016) 6078–6090, <https://doi.org/10.1007/s12035-015-9515-5>.
- [6] N.E. Gray, J.F. Quinn, Alterations in mitochondrial number and function in Alzheimer's disease fibroblasts, *Metab. Brain Dis.* 30 (2015) 1275–1278, <https://doi.org/10.1007/s11011-015-9667-z>.
- [7] K.C. Sonntag, W.I. Ryu, K.M. Amirault, R.A. Healy, A.J. Siegel, D.L. McPhie, B. Forester, B.M. Cohen, Late-onset

- Alzheimer's disease is associated with inherent changes in bioenergetics profiles, *Sci. Rep.* 7 (2017) 1–13, <https://doi.org/10.1038/s41598-017-14420-x>.
- [8] S.J. Kish, C. Bergeron, A. Rajput, S. Dozic, F. Mastrogiacomo, L.-J. Chang, J.M. Wilson, L.M. Distefano, J.N. Nobrega, Brain cytochrome oxidase in Alzheimer's disease, *J. Neurochem.* 59 (1992) 776–779, <https://doi.org/10.1111/j.1471-4159.1992.tb09439.x>.
- [9] E.M. Mutisya, A.C. Bowling, M.F. Beal, Cortical cytochrome oxidase activity is reduced in Alzheimer's disease, *J. Neurochem.* 63 (1994) 2179–2184, <https://doi.org/10.1046/j.1471-4159.1994.63062179.x>.
- [10] L.A. Demetrius, J. Driver, Alzheimer's as a metabolic disease, *Biogerontology* 14 (2013) 641–649, <https://doi.org/10.1007/s10522-013-9479-7>.
- [11] F.I. M. Armand-Ugon, B. Ansoleaga, S. Berjaoui, Reduced mitochondrial activity is early and steady in the entorhinal cortex but it is mainly unmodified in the frontal cortex in Alzheimer's disease, *Curr. Alzheimer Res.* 14 (12) (2017) 1327–1334.
- [12] K. Lunnon, A. Keohane, R. Pidsley, S. Newhouse, J. Riddoch-Contreras, E.B. Thubron, M. Devall, H. Soininen, I. Kloszewska, P. Mecocci, M. Tsolaki, B. Vellas, L. Schalkwyk, R. Dobson, A.N. Malik, J. Powell, S. Lovestone, A. Hodges, Mitochondrial genes are altered in blood early in Alzheimer's disease, *Neurobiol. Aging* 53 (2017) 36–47, <https://doi.org/10.1016/j.neurobiolaging.2016.12.029>.
- [13] X. Wang, B. Su, H. Fujioka, X. Zhu, Dynamin-like protein 1 reduction underlies mitochondrial morphology and distribution abnormalities in fibroblasts from sporadic Alzheimer's disease patients, *Am. J. Pathol.* 173 (2008) 470–482, <https://doi.org/10.2353/ajpath.2008.071208>.
- [14] S. Hauptmann, I. Scherping, S. Dröse, U. Brandt, K.L. Schulz, M. Jendrach, K. Leuner, A. Eckert, W.E. Müller, Mitochondrial dysfunction: an early event in Alzheimer pathology accumulates with age in AD transgenic mice, *Neurobiol. Aging* 30 (2009) 1574–1586, <https://doi.org/10.1016/j.neurobiolaging.2007.12.005>.
- [15] U. Keil, A. Bonert, C.A. Marques, I. Scherping, J. Weyermann, J.B. Strosznajder, F. Müller-Spahn, C. Haass, C. Czech, L. Pradier, W.E. Müller, A. Eckert, Amyloid β -induced changes in nitric oxide production and mitochondrial activity lead to apoptosis, *J. Biol. Chem.* 279 (2004) 50310–50320, <https://doi.org/10.1074/jbc.M405600200>.
- [16] H.K. Chen, Z.S. Ji, S.E. Dodson, R.D. Miranda, C.I. Rosenblum, I.J. Reynolds, S.B. Freedman, K.H. Weisgraber, Y. Huang, R.W. Mahley, Apolipoprotein E4 domain interaction mediates detrimental effects on mitochondria and is a potential therapeutic target for Alzheimer disease, *J. Biol. Chem.* 286 (2011) 5215–5221, <https://doi.org/10.1074/jbc.M110.151084>.
- [17] H.M. Wilkins, J.D. Mahnken, P. Welch, R. Bothwell, S. Koppel, R.L. Jackson, J.M. Burns, R.H. Swerdlow, A mitochondrial biomarker-based study of S-equol in Alzheimer's disease subjects: results of a single-arm, pilot trial, *J. Alzheimers Dis.* 59 (2017) 291–300, <https://doi.org/10.3233/JAD-170077>.
- [18] W. Haylett, C. Swart, F. Van Der Westhuizen, H. Van Dyk, L. Van Der Merwe, C. Van Der Merwe, B. Loos, J. Carr, C. Kinneer, S. Bardien, Altered mitochondrial respiration and other features of mitochondrial function in parkin-mutant fibroblasts from Parkinson's disease patients, *Parkinsons Dis.* 2016 (2016) <https://doi.org/10.1155/2016/1819209>.
- [19] T.D. Papkovskaia, K.-Y. Chau, F. Inesta-Vaquera, D.B. Papkovsky, D.G. Healy, K. Nishio, J. Staddon, M.R. Duchon, J. Hardy, A.H.V. Schapira, J.M. Cooper, G2019S leucine-rich repeat kinase 2 causes uncoupling protein-mediated mitochondrial depolarization, *Hum. Mol. Genet.* 21 (2012) 4201–4213, <https://doi.org/10.1093/hmg/dds244>.
- [20] H. Mortiboys, J. Aasly, O. Bandmann, Ursocholan acid rescues mitochondrial function in common forms of familial Parkinson's disease, *Brain* 136 (2013) 3038–3050, <https://doi.org/10.1093/brain/awt224>.
- [21] H. Mortiboys, R. Furrmston, G. Bronstad, J. Aasly, C. Elliott, O. Bandmann, UDCA exerts beneficial effect on mitochondrial dysfunction in LRRK2(G2019S) carriers and in vivo, *Neurology* 85 (2015) 846–852, <https://doi.org/10.1212/WNL.0000000000001905>.
- [22] H. Mortiboys, K.K. Johansen, J.O. Aasly, O. Bandmann, Mitochondrial impairment in patients with Parkinson disease with the G2019S mutation in LRRK2, *Neurology* 75 (2010) 2017–2020, <https://doi.org/10.1212/WNL.0b013e3181ff9685>.
- [23] H. Mortiboys, K.J. Thomas, W.J.H. Koopman, P. Abou-Sleiman, S. Olpin, N.W. Wood, P.H.G.M. Willems, J.A.M. Smeitink, M.R. Cookson, NIH Public Access, 64, 2009 555–565, <https://doi.org/10.1002/ana.21492.Mitochondrial>.
- [24] S.P. Allen, S. Rajan, L. Duffy, H. Mortiboys, A. Higginbottom, A.J. Grierson, P.J. Shaw, Superoxide dismutase 1 mutation in a cellular model of amyotrophic lateral sclerosis shifts energy generation from oxidative phosphorylation to glycolysis, *Neurobiol. Aging* 35 (2014) 1499–1509, <https://doi.org/10.1016/j.neurobiolaging.2013.11.025>.
- [25] E. Onesto, C. Colombrita, V. Gumina, M.O. Borghi, S. Dusi, A. Doretti, G. Fagioli, F. Invernizzi, M. Moggio, V. Tiranti, V. Silani, A. Ratti, Gene-specific mitochondria dysfunctions in human TARDBP and C9ORF72 fibroblasts, *Acta Neuropathol. Commun.* 4 (2016), 47. <https://doi.org/10.1186/s40478-016-0316-5>.
- [26] H.M. Huang, C. Fowler, H. Xu, H. Zhang, G.E. Gibson, Mitochondrial function in fibroblasts with aging in culture and/or Alzheimer's disease, *Neurobiol. Aging* 26 (2005) 839–848, <https://doi.org/10.1016/j.neurobiolaging.2004.07.012>.
- [27] C.S. Casley, L. Canevari, J.M. Land, J.B. Clark, M.A. Sharpe, Beta-amyloid inhibits integrated mitochondrial respiration and key enzyme activities, *J. Neurochem.* 80 (2002) 91–100, <https://doi.org/10.1046/j.0022-3042.2001.00681.x>.
- [28] P. Martín-Maestro, R. Gargini, G. Perry, J. Avila, V. García-Escudero, PARK2 enhancement is able to compensate mitophagy alterations found in sporadic Alzheimer's disease, *Hum. Mol. Genet.* 25 (2016) 792–806, <https://doi.org/10.1093/hmg/ddv616>.
- [29] P. Martín-Maestro, R. Gargini, E. García, G. Perry, J. Avila, V. García-Escudero, Slower dynamics and aged mitochondria in sporadic Alzheimer's disease, *Oxidative Med. Cell. Longev.* 2017 (2017), 9302761. <https://doi.org/10.1155/2017/9302761>.
- [30] E. Area-Gomez, M. Carmen, L. Castillo, M.D. Tambini, C. Guardia-Laguarta, A.J.C. De Groof, M. Madra, J. Ikenouchi, M. Umeda, T.D. Bird, S.L. Sturley, E.A. Schon, Upregulated function of mitochondria-associated ER membranes in Alzheimer disease, *EMBO J.* 31 (2012) 4106–4123, <https://doi.org/10.1038/emboj.2012.202>.
- [31] M. Manczak, R. Kandimalla, D. Fry, H. Sesaki, P. Hemachandra Reddy, Protective effects of reduced dynamin-related protein 1 against amyloid beta-induced mitochondrial dysfunction and synaptic damage in Alzheimer's disease, *Hum. Mol. Genet.* 25 (2016) 5148–5166, <https://doi.org/10.1093/hmg/ddw330>.
- [32] R. Kandimalla, M. Manczak, D. Fry, Y. Suneetha, H. Sesaki, P.H. Reddy, Reduced dynamin-related protein 1 protects against phosphorylated Tau-induced mitochondrial

- dysfunction and synaptic damage in Alzheimer's disease, *Hum. Mol. Genet.* 25 (2016) 4881–4897, <https://doi.org/10.1093/hmg/ddw312>.
- [33] G. Paumgartner, U. Beuers, Ursodeoxycholic acid in cholestatic liver disease: mechanisms of action and therapeutic use revisited, *Hepatology* 36 (2002) 525–531, <https://doi.org/10.1053/jhep.2002.36088>.
- [34] R.M. Ramalho, P.M. Borralho, R.E. Castro, S. Solá, C.J. Steer, C.M.P. Rodrigues, Tauroursodeoxycholic acid modulates p53-mediated apoptosis in Alzheimer's disease mutant neuroblastoma cells, *J. Neurochem.* 98 (2006) 1610–1618, <https://doi.org/10.1111/j.1471-4159.2006.04007.x>.
- [35] A.C. Lo, Z. Callaerts-Vegh, A.F. Nunes, C.M.P. Rodrigues, R. D'Hooge, Tauroursodeoxycholic acid (TUDCA) supplementation prevents cognitive impairment and amyloid deposition in APP/PS1 mice, *Neurobiol. Dis.* 50 (2013) 21–29, <https://doi.org/10.1016/j.nbd.2012.09.003>.
- [36] P.A. Dionísio, J.D. Amaral, M.F. Ribeiro, A.C. Lo, R. D'Hooge, C. M.P. Rodrigues, Amyloid- β pathology is attenuated by tauroursodeoxycholic acid treatment in APP/PS1 mice after disease onset, *Neurobiol. Aging* 36 (2015) 228–240, <https://doi.org/10.1016/j.neurobiolaging.2014.08.034>.
- [37] R.J.S. Viana, a F. Nunes, R.E. Castro, R.M. Ramalho, J. Meyerson, S. Fossati, J. Ghiso, A. Rostagno, C.M.P. Rodrigues, Tauroursodeoxycholic acid prevents E22Q Alzheimer's ab toxicity in human cerebral endothelial cells, *Cell. Mol. Life Sci.* 66 (2009) 1094–1104, <https://doi.org/10.1007/s00018-009-8746-x>.
- [38] R.A. Merrill, R.K. Dagda, A.S. Dickey, J.T. Cribbs, S.H. Green, Y.M. Usachev, S. Strack, Mechanism of neuroprotective mitochondrial remodeling by pka/akap1, *PLoS Biol.* 9 (2011) <https://doi.org/10.1371/journal.pbio.1000612>.
- [39] G. McKhann, D.S. Knopman, H. Chertkow, B. Hymann, C.R. Jack, C. Kawas, W. Klunk, W. Koroshetz, J. Manly, R. Mayeux, R. Mohs, J. Morris, M. Rossor, P. Scheltens, M. Carrillo, S. Weintraub, C. Phelps, The diagnosis of dementia due to Alzheimer's disease: recommendations from the National Institute on Aging–Alzheimer's Association workgroups on diagnostic guidelines for Alzheimer's disease, *Alzheimers Dement.* 7 (2011) 263–269, <https://doi.org/10.1016/j.jalz.2011.03.005.The>.

3.3 Additional results

Table 3.1 highlights cell lines used in this chapter and donor demographic information.

Fibroblast Line	Cohort	Apoε genotype	Mutation	Age	Sex	Used in Chapter Paper
Control 1	Sheffield	3/3	NA	53	Male	No
Control 2	Sheffield	3/4	NA	54	Male	Yes
Control 3	Sheffield	2/3	NA	61	Female	Yes
Control 4	Sheffield	3/3	NA	66	Male	Yes
Control 5	Sheffield	3/4	NA	100	Female	No
Control 6	Sheffield	3/4	NA	54	Female	No
Control 7	Sheffield	2/3	NA	56	Male	Yes
Control 8	Sheffield	3/3	NA	73	Female	No
Control 9	Sheffield	2/3	NA	75	Male	No
Control 10	Sheffield	3/3	NA	75	Female	No
Control 11	Coriell (GM07924)	Unknown	NA	63	Male	Yes
Control 12	Coriell (GM02189)	Unknown	NA	63	Male	Yes
Control 13	Coriell (GM23967)	Unknown	NA	52	Male	Yes
Sporadic 1	Sheffield	2/3	NA	53	Male	No
Sporadic 2	Sheffield	3/3	NA	60	Male	No
Sporadic 3	Sheffield	3/3	NA	57	Male	No
Sporadic 4	Sheffield	4/4	NA	63	Male	Yes
Sporadic 5	Sheffield	2/3	NA	59	Female	Yes
Sporadic 6	Sheffield	Unknown	NA	63	Female	Yes
Sporadic 7	Sheffield	4/4	NA	60	Male	Yes
Sporadic 8	Sheffield	3/3	NA	60	Male	No
Sporadic 9	Sheffield	3/4	NA	79	Female	No
Sporadic 10	Sheffield	3/3	NA	61	Female	No
Sporadic 11	Coriell (GM08243)	4/4	NA	72	Male	Yes
Sporadic 12	Coriell (GM07375)	4/4	NA	71	Male	Yes
Sporadic 13	Coriell (GM07376)	4/4	NA	60	Male	Yes
Familial 1	Coriell (ND41001)	Unknown	14q24.3 Intron 4, G deletion	47	Female	Yes
Familial 2	Coriell (ND34733)	Unknown	P264L	60	Male	Yes
Familial 3	Coriell (ND34730)	Unknown	E184D	38	Male	Yes

Table 3.1| Fibroblast line demographics This table displays the different fibroblast lines used in this thesis chapter. Cell lines taken from the Coriell institute are labelled with the Coriell cell line identification. Apoε genotype is displayed for sporadic AD fibroblast lines. The specific mutations for the 3 PSEN1 fibroblast lines is displayed. Age, sex and whether the line has been used in the published chapter paper is highlighted.

3.3.1 Mitochondrial fusion mRNA is not changed in sporadic or familial AD fibroblasts

qPCR was performed on 6 sporadic AD fibroblasts lines and 2 PSEN1 mutation familial AD fibroblasts lines and matched controls by the PhD candidate. No difference in the expression of MFN1&MFN2 or OPA1 mRNA was seen (see figure 3.1).

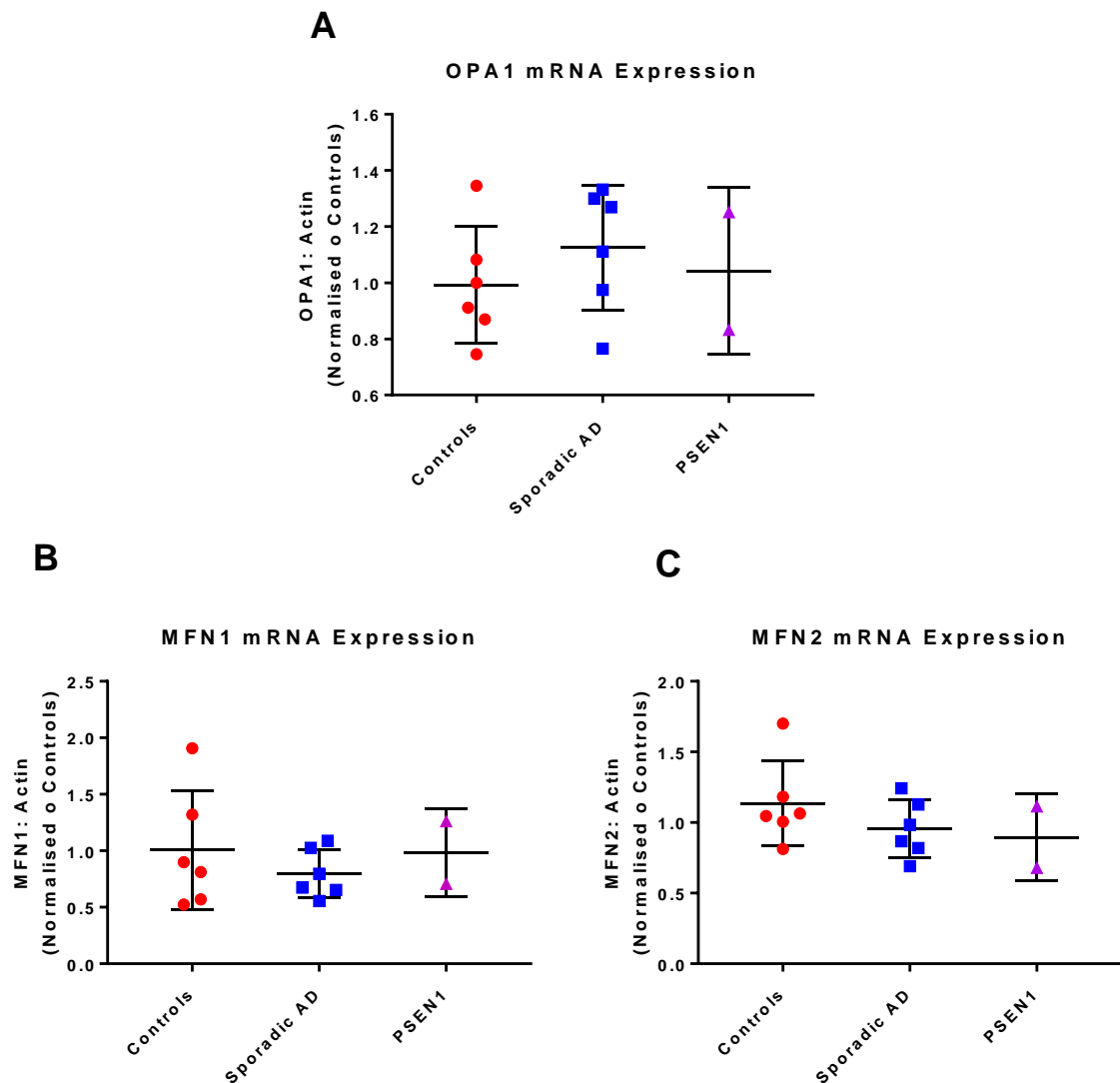


Figure 3.2| Mitochondrial Fusion protein RNA qPCR results No significant difference was seen in the expression of RNA for OPA1 (Figure 3.1A), MFN1 (Figure 3.1B), or MFN2 (Figure 3.1C). Data displayed is for control fibroblasts (red bars, n=6), sporadic fibroblasts (blue bars, n=6) and familial fibroblasts (PSEN1, purple bars, n=2). T-tests were performed for statistical comparisons, error bars indicate standard deviation. In each sample 3 technical repeats were performed.

3.3.2 Fibroblasts with the ApoE ϵ 4/4 genotype have a more severe mitochondrial morphology disease phenotype

Mitochondrial morphology was reviewed for the larger cohort of sporadic AD lines (n=13) which included the fibroblast lines presented in the chapter paper (n=7). On a group level there was still a statistically significant increase in mitochondrial length (9% increase, p=0.031) in sporadic AD fibroblasts (Figure 3.2A). A significant reduction was also seen in MMP in sporadic AD fibroblasts (16% reduction, p= 0.002) in the extended cohort (Figure 3.2B). Form factor, or how interconnected the mitochondrial network is, was decreased in both the larger cohort of sporadic fibroblast lines (3.7% reduction, p= 0.004) (Figure 3.2 C) and the smaller cohort presented in the chapter paper. The equation used to calculate the form factor is inverted, therefore a lower value for a group suggests greater interconnectedness. In the small cohort of sporadic AD fibroblasts lines presented in the chapter paper, a significant reduction in mitochondrial count was seen, as was a significant increase in the percentage of mitochondria found in close proximity to the nucleus. In this larger cohort of sporadic AD fibroblast lines, the same trends were seen as in the smaller group, but the changes to mitochondrial count (p=0.189) and percentage of mitochondria in close proximity to the nucleus (p=0.323) were not significant (Figures 3.2D&E).

The larger cohort of sporadic AD fibroblasts, lines were split based on ApoE genotype. This showed that having an ApoE ϵ 4/4 genotype in the fibroblasts exacerbates the pathological morphological changes seen in AD mitochondria. AD fibroblasts with ApoE ϵ 4/4 genotype had a significantly higher percentage of long mitochondria (16% increase, p=0.013) (Figure 3.2F), and a significantly reduced MMP (26% reduction, p=0.0001) when compared to controls (Figure 3.2G). A trend towards a lower form factor (Figure 3.2H), lower mitochondria number (Figure 3.2G) and greater percentage of mitochondria in the perinuclear region (Figure 3.2H) when compared to controls was also seen in the ApoE ϵ 4/4 genotype, but these changes were not significant. A significant reduction (27% reduction, p=0.0009) in MMP was also seen in ApoE ϵ 2/3 AD fibroblasts when compared to controls (Figure 3.2F). A trend to an increased percentage of long mitochondria (Figure 3.2E), and reduced form factor was also seen in the sporadic AD fibroblast ApoE ϵ 2/3 genotype (Figure 3.2H). For sporadic fibroblasts with the ApoE ϵ 3/3 or 3/4 genotypes, the percentage of long mitochondria was only slightly increased when compared to controls and MMP showed no difference when compared to controls. Trends toward a reduced form factor was seen in both ApoE ϵ 3/4 and 3/3 genotypes, with no real change in perinuclear mitochondria or mitochondrial count seen in either genotype.

For each morphological parameter the sporadic AD fibroblast groups were compared based on ApoE genotype using one-way Analysis of variance (ANOVA). No significant differences were seen between sporadic AD fibroblast ApoE genotypes except for the in the MMP parameter. Both ApoE

$\epsilon 4/4$ ($p=0.007$) and ApoE $\epsilon 2/3$ ($p=0.022$) groups has significant reductions in MMP when compared to the sporadic AD fibroblasts with the ApoE $\epsilon 3/3$ genotype (Figure 3.2G).

For the above analysis control fibroblast lines were presented as one group not split according to ApoE genotype. For each of the above described mitochondrial morphological parameters the effect of ApoE genotype was assessed for differences in the control group prior to comparing to the sAD fibroblast group. Using an ordinary ANOVA no statistical difference in any of the five morphological parameters investigated was seen when ApoE genotype groups were compared in the control cohort. Therefore, to increase statistical power when comparing controls with sporadic AD fibroblasts, the control cohort were assessed with all ApoE groups combined. Figures 3.3A-E display the control group split by ApoE status for each of the five mitochondrial morphological parameters. Only 10 fibroblast lines are presented as the ApoE genotypes for the Coriell control fibroblasts was not known.

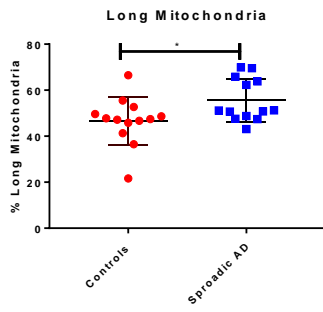
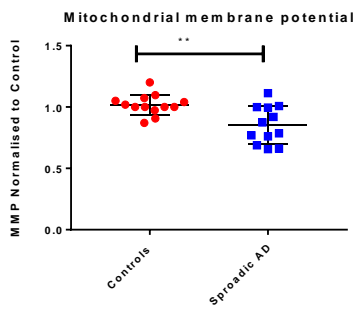
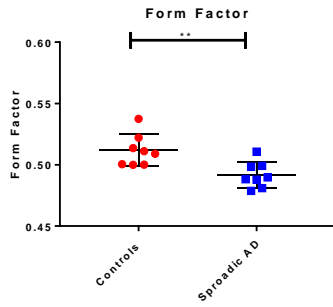
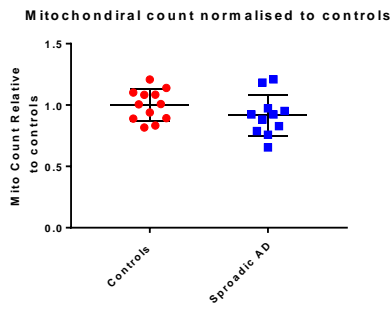
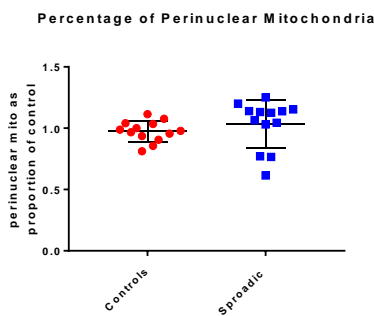
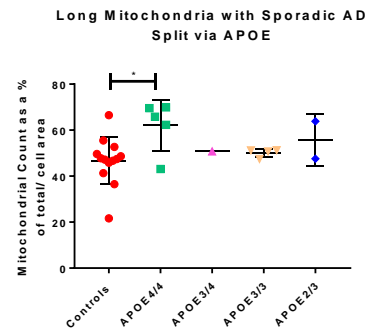
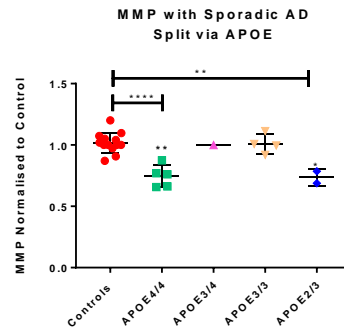
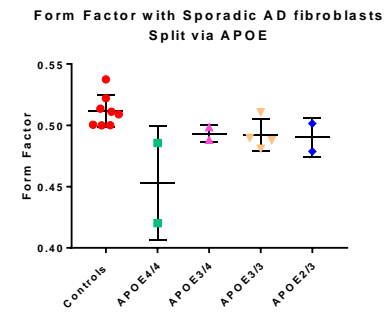
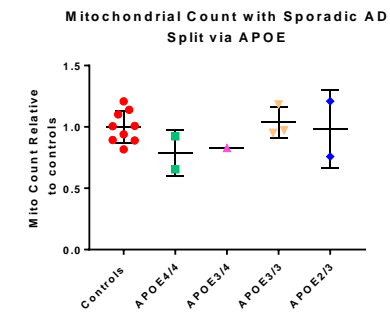
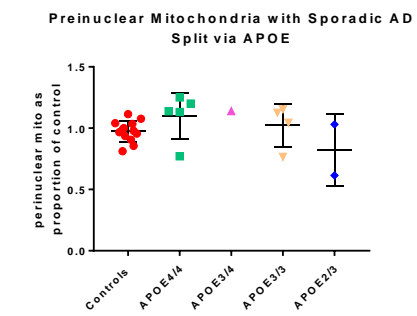
A**B****C****D****E****F****G****H****I****J**

Figure 3.3| Mitochondrial morphology results split by sporadic AD fibroblast ApoE

genotype Figure displays the morphological changes seen in AD fibroblasts, and how ApoE genotype effected this change. On a group level a significant increase in the percentage of long mitochondria was seen in sporadic AD fibroblasts (Figure 3.2A). A significant reduction in mitochondrial membrane potential (Figure 3.2 B) and form factor (Figure 3.2C) was seen in the sporadic AD fibroblasts. On a group level no significant difference was seen in mitochondrial count (Figure 3.2D) and the percentage of mitochondria in close proximity to the nucleus (Figure 3.2E) when compare control and sporadic AD fibroblasts. When sporadic AD fibroblasts were separated based on ApoE genotype significant increase in the percentage of long mitochondria was seen sporadic AD fibroblasts with an ApoE ϵ 4/4 genotype (Figure 3.2F). Mitochondrial membrane potential was significantly reduced in the ApoE ϵ 4/4 and 2/3 genotype sporadic AD fibroblasts when compared to controls, and when ApoE ϵ 4/4 (indicated by significance stars and bar) and 2/3 genotypes were compared to the ApoE ϵ 3/3 genotype sporadic AD fibroblasts (Indicated by significance stars alone) (Figure 3.2G). No significant difference in form factor (Figure 3.2H), mitochondrial count (Figure 3.2I) and mitochondria in close proximity to the nucleus (Figure 3.2J) was seen when sporadic AD fibroblasts were split based on ApoE genotype and compared to controls. Red dots represent control fibroblasts (n=13), blue dots represent all sporadic AD fibroblasts (n=13). Green dots represent sporadic AD fibroblasts with an ApoE ϵ 4/4 genotype(n=2), pink dots represent sporadic AD fibroblasts with a 4/3 genotype (n=1), orange dots sporadic AD fibroblasts with a ApoE ϵ 3/3 genotype (n=3) and blue dots represent sporadic AD fibroblasts with a ApoE ϵ 2/3 genotype (n=2). *= $p < 0.05$, **= $p < 0.01$ ***= $p < 0.001$ ****= $p < 0.0001$. T-tests were performed for statistical comparisons.

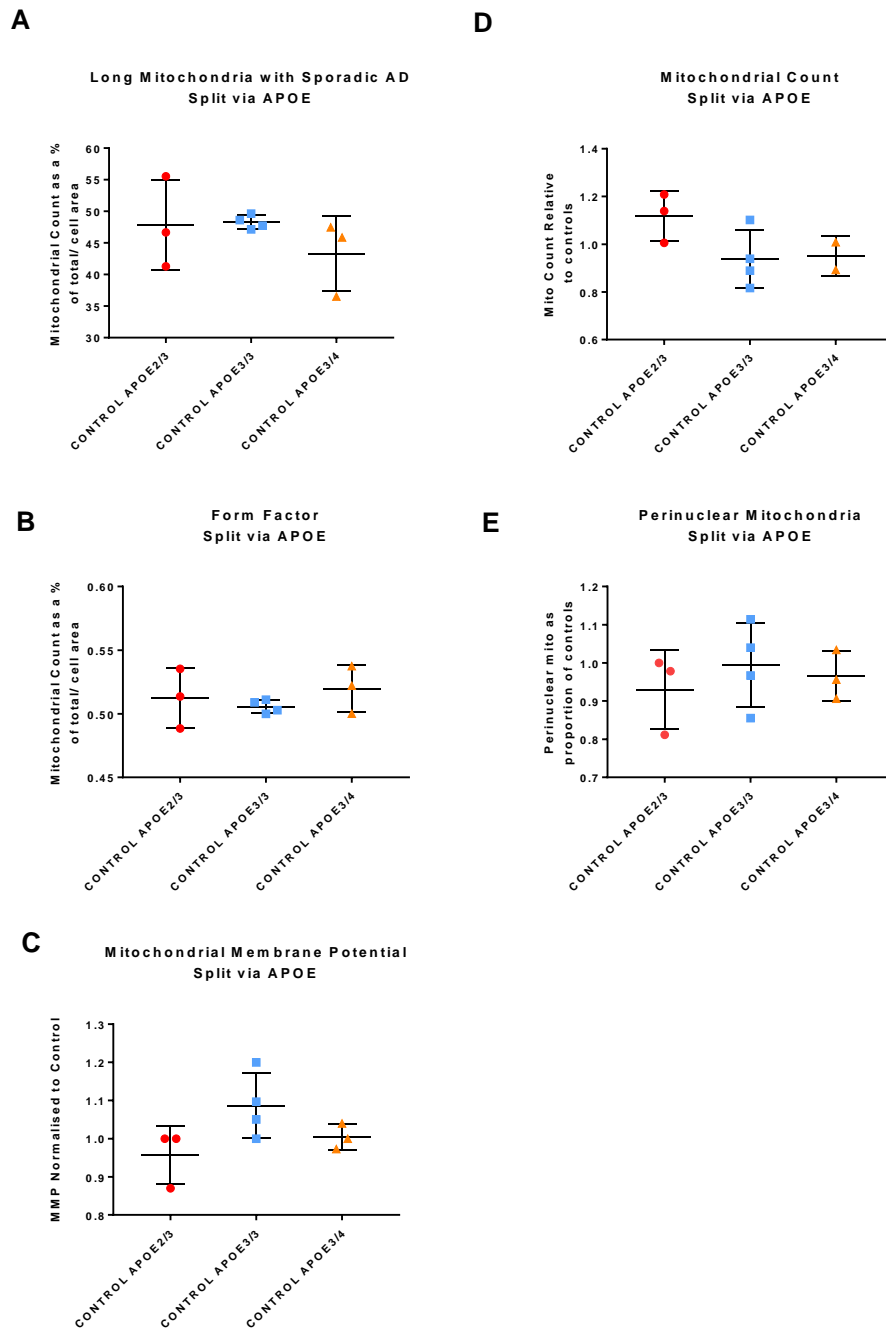


Figure 3.4| Variance in mitochondrial morphology parameters of control fibroblast based on ApoE genotype This figure displays the variance in each of the five mitochondrial morphological parameters assessed. For all five parameters no significant difference was seen between the control fibroblast cohort when it was separated based on ApoE genotype (Figures 3.3A-E). In each graph ApoE ϵ 2/3 control fibroblasts are represented by red dots (n=3), ApoE ϵ 3/3 controls represented by blue dots, (n=4) and ApoE ϵ 3/4 controls represented by orange dots (n=3). A one-way ANOVA was performed to assess statistical significance for each morphological parameter.

3.3.3 Fibroblasts with the ApoE ϵ 4/4 have reduced levels of ATP which can be corrected with the application of UDCA

The ability of the AD fibroblasts to maintain a control level of total cellular ATP was assessed. A reduction in total cellular ATP was seen in both sporadic (18% reduction, $p=0.009$) and PSEN1 familial AD fibroblasts (22% reduction) when compared to controls, although the reduction in familial AD fibroblast total cellular ATP was not significant ($p=0.07$) (Figure 3.4A). On closer inspection of the familial fibroblast AD lines revealed that 2 fibroblasts lines had a significant reduction in total ATP, whereas one line had a higher level of total cellular ATP when compared to controls. When the sporadic lines were split based on apoE genotype, only sporadic AD fibroblasts that had a 4/4 genotype had a significant reduction in total cellular ATP (36% reduction, $p<0.0001$) (Figure 3.4B). The data presented for the total cellular ATP includes all sporadic AD lines for which apoE genotype was available for (Sporadic $n=12$).

Next, whether treatment with 100 μ M of UDCA could correct the deficits seen in sporadic and familial AD fibroblasts total cellular ATP levels was assessed. Application of UDCA increased total cellular ATP in all AD fibroblasts lines (Figure 3.4C). A significant increase in total cellular ATP was seen in the sporadic AD fibroblasts treated with UDCA when compared to sporadic AD fibroblasts treated with the drug vehicle only, Dimethyl sulfoxide (DMSO) (65% increase, $p=0.012$). Familial AD fibroblasts show a non-significant increase in total cellular ATP when compared to DMSO (45% increase, $p=0.166$), and controls also showed a non-significant increase when compared to DMSO (5% increase, $p=0.963$). The data presented here for total cellular ATP levels after UDCA treatment represents the fibroblast lines used in the chapter paper (sporadic $n=7$, familial $n=3$). The sporadic fibroblast lines used in this part of the study were a mixture of ApoE ϵ 4 positive and negative lines, see table 3.1.

3.3.4 All sporadic AD fibroblasts independent of ApoE genotype have a deficit in mitochondrial spare respiratory capacity

Mitochondrial spare respiratory capacity (MSRC) was assessed again with the increased number of cell lines. For these experiments the whole Sheffield cohort of sporadic AD lines was used as well as 1 Coriell sporadic fibroblast line. ($n=11$). The other 2 Coriell sporadic lines were not used due to poor growth. The familial cell line reported in the chapter paper was included in this analysis. In this extended sporadic AD fibroblast cohort, we saw a significant reduction in MSRC (33.7% reduction, $p=0.002$) this was similar to that reported in the smaller chapter paper cohort (Figure 3.4D).

MSRC in the sporadic AD fibroblasts was investigated with cell lines split based on ApoE genotype. A trend towards a reduction was seen in all ApoE genotypes when comparing MRSC to controls,

suggesting that apoε genotype does not have a specific affect MRSC in AD. (Figure 3.4E). A significant difference was only seen between controls and sporadic fibroblasts with an ApoE ε3/3 (34% reduction, p=0.03) genotype, both ApoE ε4/4 (30% reduction, p=0.15) and ApoE ε2/3 (37.9% reduction, p=0.07) were not significant.

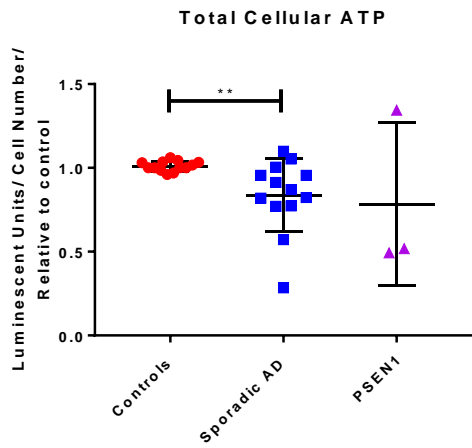
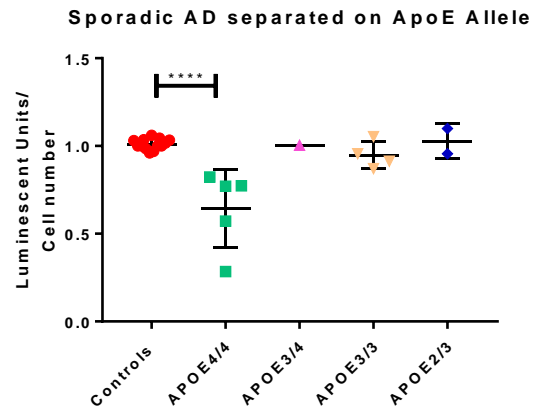
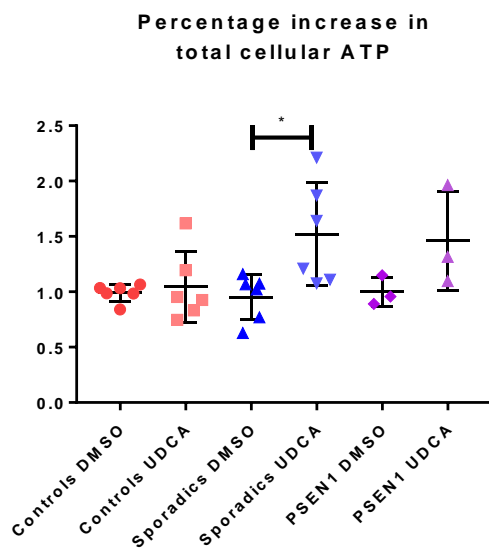
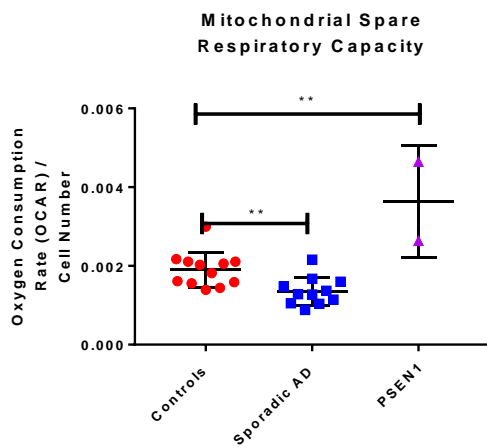
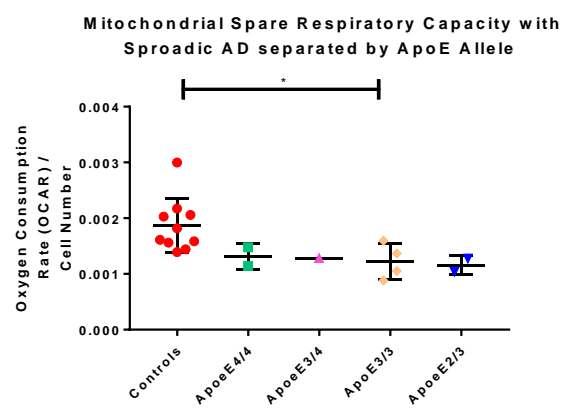
A**B****C****D****E**

Figure 3.5| Total cellular ATP and Mitochondrial Spare Respiratory Capacity split by AD fibroblast ApoE genotype

This figure displays the total cellular ATP and MSRC changes seen in AD fibroblasts, and how ApoE genotype affected this change. A reduction in total cellular ATP was seen in both sporadic AD fibroblasts and familial AD fibroblasts when compared to controls, but the reduction in the sporadic AD fibroblasts total cellular ATP was significant ([Figure 3.4A](#)). When sporadic AD fibroblasts were split based on ApoE genotype only sporadic AD fibroblasts with a 4/4 genotype had a reduction in total cellular ATP when compared to controls ([Figure 3.4B](#)). When fibroblasts were treated with UDCA an increase in total cellular ATP was seen in all cell lines when compared to fibroblasts treated with the drug vehicle dimethyl sulphoxide (DMSO) alone. Only sporadic AD fibroblasts saw a significant increase in total cellular ATP ([Figure 3.4C](#)). A significant decrease in mitochondrial spare respiratory capacity (MSRC) was seen in sporadic AD fibroblasts and a significant increase in MSRC in familial AD fibroblasts was seen when compared to controls ([Figure 3.4D](#)). All sporadic AD fibroblasts irrespective of ApoE genotype had a reduction in MSRC ([Figure 3.4E](#)). Red dots represent control fibroblasts (n=12, and n=7 in figure 3.4C), blue dots represent all sporadic AD fibroblasts (n=11, and n=7 in figure 3.4C) purple dots represent familial (PSEN1) AD fibroblasts (n=3, or n=2 in figure 3.4D). Green dots represent sporadic AD fibroblasts with an ApoE ε4/4 genotype (n=2), pink dots represent sporadic AD fibroblasts with a 4/3 genotype (n=1), orange dots sporadic AD fibroblasts with a ApoE ε3/3 genotype (n=3) and blue dots represent sporadic AD fibroblasts with a ApoE ε2/3 genotype (n=2). * =p<0.05, **=p<0.01, ****=p<0.0001. T-tests were performed for statistical comparisons.

3.3.5 Mitochondrial Spare Respiratory Capacity was the only element of the Mito Stress test to show differences between AD and control fibroblasts

As with the smaller AD fibroblasts groups described in the chapter paper, no significant difference was seen in basal mitochondrial respiration, ATP linked respiration, proton leak, non-mitochondrial oxygen consumption, respiratory control ratio and ATP coupling efficiency when control groups were compared with sporadic AD and PSEN1 fibroblast groups. Figure 3.2 displays this data

Parameter	Control Value Mean	Sporadic AD Mean	P-value	PSEN1 Mean	P-value
MSRC	0.00186	0.001327	0.011	0.00364	0.005
Basal Mitochondrial Respiration	0.00191	0.00178	0.604	0.00426	0.082
ATP Linked Respiration	0.00159	0.00164	0.843	0.00422	0.100
Proton Leak	0.000349	0.000476	0.0663	0.00045	0.903
Non-OXPHOS respiration	0.0003866	0.0003012	0.329	0.00039	0.885
Respiratory Control Ratio	12.15	10.3	0.1299	13.24	0.101
ATP Coupling Efficiency	0.852	0.830	0.3578	0.896	0.468

Table 3.2| Mitochondrial Stress Test parameters Table 3.1 displays the parameters assessed as part of the “mito stress test” only mitochondrial spare respiratory capacity showed a significant difference when AD fibroblasts were compared to controls. Apart from respiratory control ratio and coupling efficiency, all other parameters are expressed as oxygen consumption rate/cell number. Respiratory control ratio and coupling efficiency are ratios. For the control group 12 fibroblast lines were assayed, for the sporadic group 11 fibroblast lines were assayed and for the PSEN1 group 2 fibroblast lines were assayed. The full cohort of lines was not assessed in this experiment due to either limited growth of some of the Coriell fibroblasts lines or limited availability of samples.

3.4 Discussion

The results in this chapter reveal that mitochondrial function and morphology are altered in both sporadic and familial AD fibroblast lines. These functional and morphological alterations can be corrected with the application of UDCA. The mechanism by which UDCA ameliorates the mitochondrial functional abnormalities appears to be Drp1 dependent. The mechanism of action of UDCA was identified through work performed by myself, and paper co-author Katy Barnes. As well as the mentioned discussion points in the chapter paper the following discussion points are presented from the additional data in this section.

3.4.1 Mitochondrial morphology is altered in AD

In this chapter it has been shown that the mitochondrial network in both sporadic and PSEN1 AD fibroblasts is more fused when compared to controls. It has been suggested that a more fused mitochondrial network can occur in a cell to improve the efficiency of ATP production [417], and also work as a defensive mechanism employed against oxidative damage [427]. Increased levels of ROS are reported in AD fibroblasts in the studies by Wang et al and Perez et al which show altered mitochondrial dynamics [204, 418]. The level of increased ROS is very different in both studies, which could suggest that the differences reported in mitochondrial dynamic change in the above studies are a result of studying different time points in the course of the fibroblast's response to ROS. ROS were not measured as a part of the results presented in this chapter. Combining the results of this chapter with that of the cited papers highlights the importance of measuring mitochondrial stress parameters when investigating mitochondrial dynamics, as the level of metabolic stress a fibroblast is exposed is likely to affect its mitochondrial dynamics. Further experiments investigating mitochondrial dynamics in AD fibroblasts or other cell types should control for disease length, age of fibroblast donor, level of oxidative stress and metabolic stress as all these factors may confound results, and may also explain the heterogeneity reported in the literature so far.

Both sporadic and familial AD fibroblasts showed no reduction in the amount of Drp1 mRNA identified by myself and a reduction in Drp1 protein identified by chapter paper co-author Katy Barnes, but no change was seen in the mitochondrial fusion proteins/mRNA of MFN1&2 and OPA1. This finding has been reported by other groups [418]. This result though is not consistently reported across the AD fibroblast literature with some groups suggesting that MFN1 is increased, OPA1 is decreased, and Drp1 levels remain unchanged in AD fibroblasts [204]. As described above amyloid can affect the function of mitochondrial fission proteins, and it is known that fibroblasts can produce A β . Fibroblast A β levels were not measured in these studies, but potentially differences reported

with regard to mitochondrial fission and fusion proteins, may be dependent on the expression level of A β within the fibroblast [414].

3.4.2 Fibroblasts with ApoE ϵ 4/4 genotype produce less ATP and have altered mitochondrial morphology

Deficits in total cellular ATP and changes to the mitochondrial morphology were seen in both sporadic and familial AD fibroblasts, although these changes were not uniform across both groups. An ATP deficit was only seen in sporadic AD fibroblasts that had an ApoE ϵ 4/4 genotype. The mitochondrial morphological changes seen in sporadic AD fibroblasts, including an increased percentage of long mitochondria, more mitochondria focused around the cell nucleus, decreased MMP, decreased form factor and decreased mitochondrial count, were more pronounced in the ApoE ϵ 4/4 genotype AD fibroblasts. The separate ApoE genotype group sizes were very small in this study, and when interpreting these results this must be considered. It is well known that the ApoE ϵ 4/4 genotype increases the likelihood of developing sporadic AD and also reduces the age of onset, so the finding that ApoE ϵ 4/4 genotype AD fibroblasts have a more affected mitochondrial phenotype than other ApoE genotypes is consistent with current literature describing the effect of ApoE in AD.

It is unclear as to how the ApoE ϵ 4/4 genotype may affect mitochondrial morphology and total cellular ATP levels. The pattern of mitochondrial morphological changes and deficit in total cellular ATP seen in the AD fibroblasts suggests a stressed mitochondrial network not meeting the energy demands of the cell. Studies looking at brain glucose metabolism of people with ApoE ϵ 4/4 genotype have shown a reduced ability to uptake glucose [428]. Mice with the ApoE ϵ 4/4 genotype have also been shown to have increased expression of complex III of the ETC, and decreased MMP. It could be postulated that fibroblasts with the ApoE ϵ 4/4 have a reduced ability to use glucose, which means that glycolysis is impaired and therefore other substrates for metabolism and other ATP generating pathways such as OxPHOS have increased activity to meet cellular energy demands. This would increase the metabolic stress placed on OxPHOS which eventually may affect the shape and function of the mitochondrial network as the disease progresses. The more exacerbated mitochondrial morphology changes seen in ApoE ϵ 4/4 genotype in this chapter may have been precipitated by increased demands on OxPHOS from reduced glycolysis function. The glycolytic function of the fibroblasts is discussed in detail in chapter 4. The ApoE changes seen in this chapter may also be dependent on the length of time the patient has had AD. Fibroblasts from patients with MCI or early AD, and an ApoE ϵ 4/4 genotype, may have a mitochondrial morphology and functional changes that are not as severe as those seen when AD is well established. In this chapter it has been identified that other ApoE genotypes have mitochondrial morphological changes similar to that seen in the

ApoE ϵ 4/4 genotype group. The ApoE ϵ 2/3 genotype also showed changes in mitochondrial morphology. This could be evidence that in AD a background mitochondrial inefficiency may be compounded by the presence of the ApoE ϵ 4/4 genotype, meaning that both factors work synergistically to effect mitochondrial function. ApoE ϵ 4/4 genotype has been associated with increased MAM contacts which may affect the calcium balance within the mitochondria. This may also impact the mitochondria's ability to meet the energetic requirements of the cell [429].

It is an interesting finding that ApoE genotype may affect mitochondrial function, but further work is needed in studies with much larger sample sizes to fully understand the effect ApoE has on cellular energetic properties. Experiments in which the ApoE ϵ 4/4 genotype is changed using CRISPR would also develop the understanding of the interaction between mitochondrial function and ApoE.

Only 2 of the 3 PSEN1 familial AD fibroblasts lines tested had a deficit in total cellular ATP. The 2 cell lines that had deficits in total cellular ATP were both male patients, whereas the PSEN1 fibroblasts without a deficit came from a female donor. Several mutations have been identified within the PSEN1 gene which cause AD [88, 89, 430, 431], all of which may have a different effect on total cellular ATP. Each PSEN1 fibroblast line in this study has a different PSEN1 mutation, this may explain the variability in results. There was a uniform change in mitochondrial morphology markers in PSEN1 fibroblasts, which may suggest that mitochondrial morphology is effected by all PSEN1 gene mutations that cause AD, but only certain mutations cause these changes in morphology to affect total cellular ATP. It is also important to mention that the PSEN1 fibroblast group is small (n=3) so study in a larger patient group is warranted to confirm the hypotheses for the discrepancies seen in the 3 PSEN1 fibroblast lines.

3.4.3 All Fibroblasts independent of ApoE genotype have a decreased mitochondrial spare respiratory capacity

MSRC was found to be low in all sporadic AD fibroblasts, and this appears to be independent of ApoE genotype. This is an interesting finding, as it suggests that in sporadic AD mitochondrial changes may be independent of one of the main genetic risk factors that determines the disease presentation.

MRSC is a measure of the capacity of a mitochondrial network to increase OxPHOS above the rate needed for unstressed ATP production. In non-disease states it is very unlikely that MRSC is reached by a cell, therefore total cellular ATP demands can be met by the metabolic pathways within the cell. In a disease state several factors probably combine to increase the ATP demand on a cell, such as ROS damage and calcium homeostasis failure and this is likely to be when MSRC plays an important part in maintaining cellular ATP demands. The sporadic fibroblasts studied in this chapter without an ApoE ϵ 4/4 genotype could match total cellular ATP production of controls. Fibroblasts used in this

study were maintained in an optimum environment, so the presence of metabolic or oxidative stress would be unlikely. ATP deficits may be seen in AD fibroblasts without the ApoE ϵ 4/4 genotype if grown in a media, or environment that exposes them to metabolic stress, as their MSRC is lower than controls.

Further work is needed to understand what the cause of the reduced MSRC seen in sporadic AD fibroblasts is. Interestingly, Familial AD fibroblasts studied in this chapter had an increased MSRC, which could suggest that the MSRC deficits are independent of amyloid production. Evidence from studying cardiac myocytes and SOD2 deficient mice has suggested the MSRC is dependent on the activity of complex II of the ETC [432, 433], therefore investigating the activity of the ETC complexes individually in AD would be logical next step to identify the mechanism behind low and high MSRC seen in the AD fibroblasts.

3.4.4 Study limitations

The data presented in this chapter has several limitations, the analysis based on ApoE is based on very small numbers of patient's fibroblasts, with the ApoE ϵ 3/3 genotype limited to only one cell line. This means that the statistical analysis is very likely to be underpowered due to the small sample sizes. This needs to be considered when interpreting the results with regard to mitochondrial morphology and total cellular ATP. The low numbers of separate ApoE genotypes may also explain why the results seem to suggest that having ApoE ϵ 2/3 genotype has similar pathological properties to having the ApoE ϵ 4/4 genotype. Based on previous literature it would be expected that the ApoE ϵ 2/3 genotype may have a positive effect on the morphological and functional mitochondrial parameters, as this genotype protects a person from developing AD. It is also important to mention that the expression of Apo ϵ within fibroblasts is debated, with sources claiming that fibroblasts express the protein [434] but others claiming they do not [435]. Lack of expression of Apo ϵ within fibroblasts would mean that differences seen in metabolism are likely not caused by this protein. Future work investigating differences in metabolic function in fibroblasts separated by Apo ϵ genotype should immunoblot samples first to identify if fibroblasts used do express the protein.

Within the published paper the presentation of control and disease group data is different in figures 1A and 3A. It was requested that control data was presented as a group mean whereas data was given separately for each disease line under assessment. This means that error bars in the control group represent the standard deviation of the whole cohort but error bars for disease represent the standard deviation of the technical repeats. Although this presentation of the data is misleading, it was requested by the reviewers of the article. Ideally data should have been presented as grouped means and standard deviations for each cohort. Furthermore, it was requested in figure 4B by the

reviewer that UDCA treatment statistics were compared to the untreated condition and not DMSO. The more experimentally appropriate comparison would be DMSO alone (the drug vehicle that UDCA was dissolved in) to the UDCA treated condition. When comparing the effect of DMSO alone and UDCA on Drp1 protein location, there was a statistically significant increase in Drp1 localised to the mitochondria in the UDCA treatment group suggesting that the effect of Drp1 localisation is mediated through the actions of UDCA and not through the drug vehicle DMSO.

Results on mitochondrial dynamics are based on one particular time point, which is the nature of the experimental paradigm used for investigation here. The dynamic nature of the fibroblast mitochondrial network would benefit from being studied over many time points in both an untreated and UDCA treated situation. This would help to understand the natural cycle of mitochondrial fusion and fission dynamics in AD and if this is affected by the application of UDCA. Evidence from APP over expression animal models in which mitochondrial dynamics are assessed at several time points would suggest that abnormalities in the rate of mitochondrial fusion are present [418]. This is likely to have a significant effect on the function of the mitochondrial network.

3.5 Chapter Conclusions

1. Sporadic AD fibroblasts have morphological changes suggestive of a stressed mitochondrial network. This includes elongated mitochondria, decreased MMP and a trend towards decreased mitochondrial count and a perinuclear focusing of the mitochondrial network.
2. The mitochondrial morphology changes may be exacerbated by the ApoE ϵ 4/4 genotype.
3. Sporadic AD fibroblasts have a reduced MSCR which appears to be independent of ApoE genotype.
4. Familial PSEN1 AD fibroblasts have similar changes to their mitochondrial morphology when compared with sporadic AD fibroblasts but have an increased MSRC which may be the result of uncoupling of their mitochondria.
5. Reductions in total cellular ATP are seen in AD fibroblasts with the ApoE ϵ 4/4 genotype but not in other ApoE genotypes.
6. UDCA can correct the deficits in ATP production, MMP and mitochondrial elongation when applied to both sporadic and familial fibroblasts for 24 hours at a concentration of 100 μ M.
7. UDCA can correct the deficit in MRSC in sporadic AD fibroblasts.

Chapter 4: Deficits in Mitochondrial Spare Respiratory Capacity Contribute to the Neuropsychological Changes of Alzheimer's Disease

4.1 Introduction

In chapter 3 it was identified that mitochondria have morphological and functional deficits in sporadic and familial AD fibroblasts. In sporadic fibroblasts, deficits in Mitochondrial Spare Respiratory Capacity (MSRC) and Mitochondrial Membrane Potential (MMP) were common to all cell lines. As sporadic AD fibroblasts have mitochondrial deficits that may predispose them to metabolic failure when challenged by multiple stressors, this may lead to the fibroblasts having to rely on other metabolic pathways for ATP generation. For this reason, in this chapter the glycolytic ability of sporadic AD fibroblasts has been assessed.

As well as further characterising the glycolysis pathway within the sporadic AD fibroblasts, this chapter also investigates if the mitochondrial and glycolytic abnormalities seen in sporadic AD fibroblasts correlate with neuropsychological and neuroimaging changes seen early in the course of AD. Ideally this chapter would also include the PSEN1 familial AD fibroblast lines, but due to the lack of clinical phenotypic data available these lines were excluded. The Coriell sporadic AD lines were also excluded for the same reasons.

The following introductory sections will discuss the early changes seen in neuroimaging and neuropsychological testing in AD.

4.1.1 Structural Neuroimaging changes in AD

Structural brain imaging was one of the first brain imaging modalities used to aid in the diagnosis of AD. Computed Tomography (CT) and Magnetic Resonance imaging (MRI) are both used depending on clinical setting and resource availability [436]. The main brain structural imaging change used to identify AD is selective cortical atrophy. Cortical atrophy develops in a characteristic pattern in AD that starts in the medial temporal lobe, specifically the entorhinal cortex, and then moves through the brain in a pattern that corresponds with the deposition of NFT [437]. Temporal lobe atrophy progression follows the clinical progression of the disease, and is good marker for differentiating AD from normal ageing related cognitive changes [438]. The pattern of cortical atrophy in AD can resemble that seen in other forms of dementia, such as vascular dementia, and there are certain AD presentations that do not have a classical pattern of cortical atrophy [94], which impedes using cortical atrophy alone as a biomarker for AD.

Cortical atrophy represents a pathological loss of neurons, and therefore suggests an already established pathological process. This is exemplified by studies showing 20-30% of entorhinal

cortical atrophy in AD patients when only mild deficits on neuropsychological testing are present [439]. It is also important to consider that cortical atrophy is a pathological demonstration of neuronal loss, but as to what is causing the neuronal loss is difficult to ascertain. Amyloid and tau accumulation clearly play a role in neuronal loss, but metabolic failure is also likely to be implicated as a cause of atrophy and subsequently cell death [440]. Chronic hypoperfusion of the brain in AD likely contributes to the development of atrophy as well [441]. Hypoperfusion may cause atrophy by accelerating metabolic deficits, or exacerbating amyloid and tau pathology [442].

4.1.2 Neuropsychological changes in early AD

Neuropsychological assessment has been used as a tool to diagnose AD for at least the last 30 years. Neuropsychological assessment involves examining different cognitive functions that relate to neuroanatomical brain regions to develop a profile of cognitive impairment. Classical patterns of cognitive impairment are seen at the start of many dementias, allowing for the differentiation between different subtypes. In AD the earliest neuropsychological abnormalities are typically seen in episodic memory and semantic memory [73]. Episodic and semantic memory are both types of declarative or explicit memory which concerns the retaining of facts and information. Semantic memory refers to memory associated with encyclopaedic or conceptual knowledge, such as names of animals and types of fruit, whereas episodic memory refers to the remembering of certain autobiographical events, such as birthdays [443]. Episodic and semantic memory are encoded in the medial temporal lobe. Episodic memory does decline with age naturally, but semantic memory has been shown to improve with normal ageing [444]. The rate of decline of episodic memory has been associated with a high degree of accuracy in diagnosing AD with studies performing delayed recall memory tests (i.e. recalling of information given 10 minutes prior) having a 90% accuracy in differentiating normal ageing from dementia [445]. It is thought that in AD the organization of semantic memory within the brain is lost, which causes the memory retrieval deficits [446]. Phonemic fluency is a type of executive functioning that describes the ability to list words without semantic context (letter fluency). Phonemic fluency is characteristically affected later in the course of AD [447]. As AD progresses and the traditional pathological aggregates spread to the rest of the brain, impairments in executive function and working memory become apparent. These memory functions are sustained by the prefrontal cortex and which is the main reason they are affected later in the disease course.

Semantic memory is a good example of a memory function that has representation in multiple brain regions. As well as the medial temporal lobe, the temporal neocortex is important in the storage of semantic information, suggesting a network of brain regions that work together to sustain semantic memory functions [448]. Neuropsychology has advanced as a field to correlate cognitive functioning

with brain networks. This includes neuroanatomical and functional neural networks and is often exploited while investigating how disease affects different aspects of cognition. Several brain functional networks exist including the salience network, thought to be involved with integrating emotional and sensory stimuli [449], and the visual network involved with the processing of visual information [450]. Switching between different functional networks has metabolic complications, and is therefore affected by the metabolic functions of brain cells. One functional network that has been studied extensively in AD is the default mode network (DMN) [451-453]

4.1.3 The Default Mode Network

The DMN refers to a network of functionally connected brain areas that have been shown to have increased blood flow, and glucose metabolism when a person is involved in quiet introspective thought [454]. Examples of the cognitive processes being performed when the DMN is most active would be autobiographical memory retrieval, envisaging the future, or considering the perspective of others [410]. The anatomical regions that are part of the DMN network include [410]:

- The ventral medial prefrontal cortex
- Posterior cingulate and retrosplenial cortex
- Inferior Parietal lobule
- Lateral Temporal cortex
- Dorsal medial prefrontal cortex
- Hippocampal formation

The DMN should be thought of as a group level pattern of statistical regularities identified after functional brain image processing. This means that the DMN is difficult to interpret as a phenomenon when thinking about a single person, with most techniques used to create a DMN map based on comparisons between a cohort of disease individuals and controls, or a single cohort of participants. The pattern of the DMN will change based on sample size, and group under investigation, but multiple studies using different MRI machines and different cohorts of patients have reported a consistent pattern of brain activation that represents the DMN [455]. There is evidence that functional connectivity patterns created using a group level analysis are seen consistently in individual subjects [456], which suggests that viewing the DMN connectivity pattern for a single participant in a study is an appropriate methodology.

The DMN is of interest in the study of AD as changes in the functional connectivity of this network are seen very early in the condition. When considering the brain areas that are part of the DMN it is obvious why this is the case. The functional connections between different areas of the DMN do not necessarily decrease as AD progresses, with some studies showing increased connectivity between

regions of the DMN [451]. There is also evidence that in AD increased DMN connectivity is seen as a maladaptive mechanism to compensate for poor semantic memory performance [457]. The theory for increased connectivity within the DMN in certain disease states is thought to relate to a reduction of efficiency in the functional network, meaning that either new brain regions, or increased activity is needed to maintain the DMN overall function. As neurodegenerative diseases progress it has been shown that the functional connectivity maps for different brain networks start to merge together. The inter-network inhibition that exists in healthy brain networks becomes impaired in neurodegenerative states leading to separate brain networks needing to rely on more brain regions to maintain connectivity [457].

A landmark paper in 2005 showed that the anatomical areas of the DMN are the same areas of the brain that are most affected by amyloid deposition, cortical atrophy and decreased glucose metabolism in AD [452]. This paper also showed that the DMN was active in the acquisition of stored memories, therefore linking amyloid pathology, brain atrophy, abnormal metabolism and memory acquisition together in a specific pattern of areas affected in AD. The observation that DMN is disrupted by amyloid deposition has been confirmed by other groups [458, 459]. The idea that the connected brain regions that form the DMN are specifically targeted in AD has been taken further by groups exploring the deposition of tau throughout the brain showing a pattern of tau deposition that corresponds with DMN brain areas [460]. The areas of the DMN have a disproportionately high glucose and oxygen consumption compared to other brain regions [461-463]. This has led to the hypothesis that due to the continual high metabolic rate of the DMN regions, AD may be initiated by metabolic failure when the capacity of these regions to maintain network homeostasis (forming and switching between different brain networks) starts to fail. [440, 452] For this reason, understanding the relationship between cellular metabolism and DMN changes in AD is of significant interest.

4.1.4 Assessment of glycolysis using the Agilent XF seahorse analyser

In this chapter the assessment of glycolysis is discussed using the glycolysis stress test devised to be performed with an Agilent Seahorse analyser. Assessment is performed in a very similar way to that described in chapter 3 (section 3.1.4) when discussing the mitochondrial stress test. The process of glycolysis releases hydrogen ions via the actions of glyceraldehyde-3-phosphate dehydrogenase this increases the acidity of the media that the cells being assessed are grown in. As a result of this for this experiment extracellular acidification rate is measured instead of oxygen consumption. The cells being assessed are initially cultured in a media that does not contain glucose. After this stage the rate of glycolysis is measured by adding glucose to the cell media. Once the rate of glycolysis has

been measured oligomycin is then added to the cell media to stop ATP production via oxidative phosphorylation. This means that the rate of glycolysis increases to meet the ATP production demands of the cells. This allows for measurement of both the glycolytic capacity of the cell, which is a measure of the maximum rate of glycolysis, and the glycolytic reserve which is a measure of the extra glycolysis above the basal level that can be attained. Finally, 2-deoxyglucose is added to the cell media which is an inhibitor of glycolysis. This stops all hydrogen ion release caused by glycolysis, and also allows for the non-glycolytic acidification of the media to be identified. Figure 4.1 highlights the different parts of the glycolysis stress test.

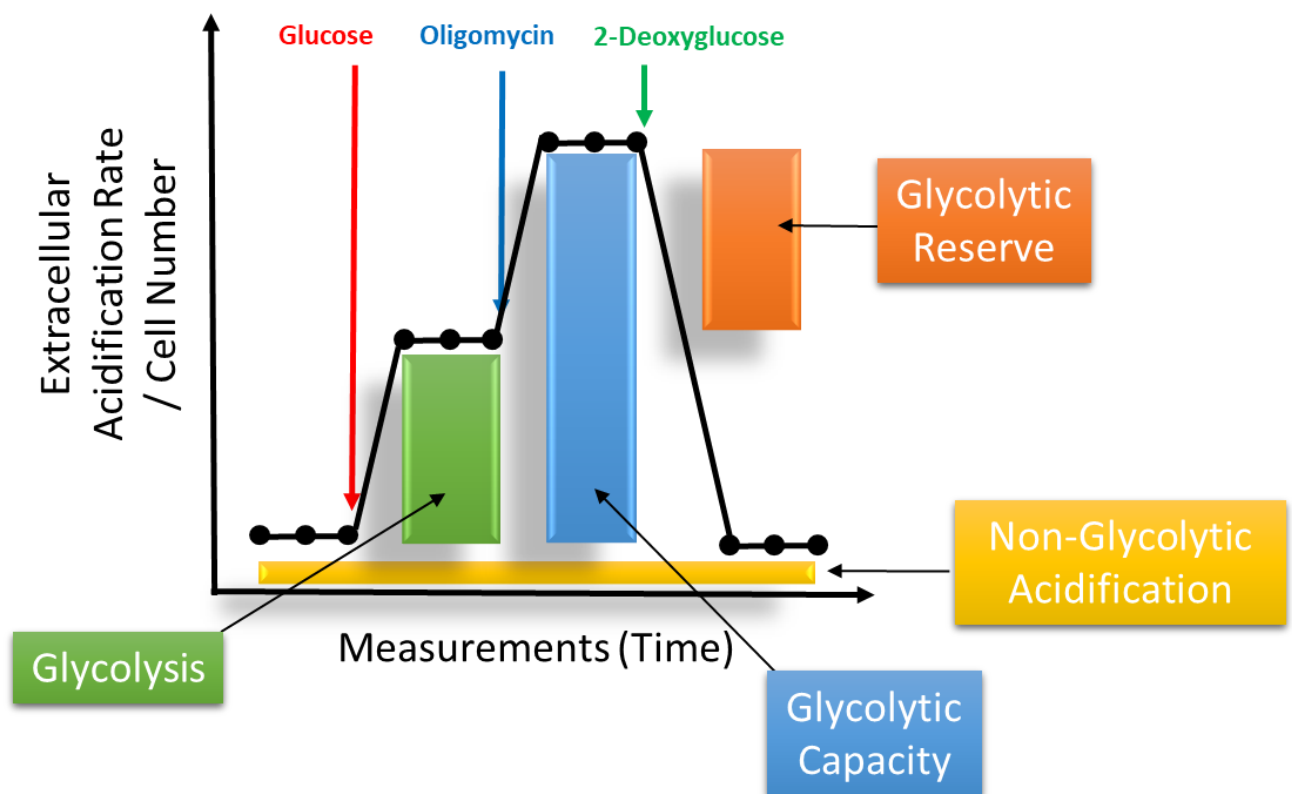


Figure 4.1 | Glycolysis Assessment using the Agilent Glycolysis Stress Test This figure displays the different parameters of glycolysis that are measured using the glycolysis stress test. The height of each coloured bar represents the value for the parameter described. The addition points of glucose (in red), oligomycin (in blue) and 2-deoxyglucose (in green) are highlighted.

4.1.4 Reasoning for additional results

This chapter looks at how metabolic function in fibroblasts specifically, OxPHOS and glycolysis are related to, or may help to develop the understanding of the neuropsychological and neuroimaging changes seen in AD. The chapter paper focuses on how OxPHOS and glycolytic changes may contribute to the neuroimaging and neuropsychological changes seen in AD. The additional results section firstly investigates how ApoE genotype may affect glycolysis in fibroblasts, and then

investigates if OxPHOS markers shown to correlate with neuropsychological changes in AD, correlate with connectivity changes seen in the DMN.

4.1.5 Published Paper contributions by PhD Candidate

- Performed all mitochondrial stress test and glycolysis stress test seahorse assays.
- Performed all extracellular lactate assays.
- Performed MMP assays on 14 of 20 fibroblasts lines used in this paper.
- Performed ATP assays on 14 of 20 fibroblast lines used in this paper.
- Performed all correlations and covariate analyses of data sets.

4.2 Published Paper

This Paper was published in the Journal of Personalised Medicine The citation is

Bell, M. S., M. De Marco, K. Barnes, J. P. Shaw, L. Ferraiuolo, J. D. Blackburn, H. Mortiboys and A. Venneri (2020). "Deficits in Mitochondrial Spare Respiratory Capacity Contribute to the Neuropsychological Changes of Alzheimer's Disease." Journal of Personalized Medicine 10(2).

Article

Deficits in Mitochondrial Spare Respiratory Capacity Contribute to the Neuropsychological Changes of Alzheimer's Disease

Simon M. Bell , Matteo De Marco, Katy Barnes, Pamela J. Shaw, Laura Ferraiuolo, Daniel J. Blackburn , Heather Mortiboys ^{*,†} and Annalena Venneri ^{*,†}

Sheffield Institute for Translational Neuroscience (SITraN), University of Sheffield, 385a Glossop Road, Sheffield S10 2HQ, UK; s.m.bell@sheffield.ac.uk (S.M.B.); m.demarco@sheffield.ac.uk (M.D.M.); kabarnes1@sheffield.ac.uk (K.B.); pamela.shaw@sheffield.ac.uk (P.J.S.); l.ferraiuolo@shef.ac.uk (L.F.); d.blackburn@sheffield.ac.uk (D.J.B.)

* Correspondence: h.mortiboys@sheffield.ac.uk (H.M.); a.venneri@sheffield.ac.uk (A.V.);
Tel.: +44-(0)114-222-2259 (H.M.); +44-(0)114-271-3430 (A.V.)

† These two authors are joint senior authors.

Received: 30 March 2020; Accepted: 24 April 2020; Published: 29 April 2020



Abstract: Alzheimer's disease (AD) is diagnosed using neuropsychological testing, supported by amyloid and tau biomarkers and neuroimaging abnormalities. The cause of neuropsychological changes is not clear since they do not correlate with biomarkers. This study investigated if changes in cellular metabolism in AD correlate with neuropsychological changes. Fibroblasts were taken from 10 AD patients and 10 controls. Metabolic assessment included measuring total cellular ATP, extracellular lactate, mitochondrial membrane potential (MMP), mitochondrial respiration and glycolytic function. All participants were assessed with neuropsychological testing and brain structural MRI. AD patients had significantly lower scores in delayed and immediate recall, semantic memory, phonemic fluency and Mini Mental State Examination (MMSE). AD patients also had significantly smaller left hippocampal, left parietal, right parietal and anterior medial prefrontal cortical grey matter volumes. Fibroblast MMP, mitochondrial spare respiratory capacity (MSRC), glycolytic reserve, and extracellular lactate were found to be lower in AD patients. MSRC/MMP correlated significantly with semantic memory, immediate and delayed episodic recall. Correlations between MSRC and delayed episodic recall remained significant after controlling for age, education and brain reserve. Grey matter volumes did not correlate with MRSC/MMP. AD fibroblast metabolic assessment may represent an emergent disease biomarker of AD.

Keywords: Alzheimer's disease; mitochondrial spare respiratory capacity; mitochondrial; membrane potential; glycolytic reserve; semantic memory; phonemic fluency; episodic memory; neuropsychology; neuroimaging

1. Background

Alzheimer's disease (AD) is the most common cause of dementia worldwide and in 2018 was estimated to cost the global economy 1 trillion US dollars [1]. The clinical symptoms of the disease are the progressive loss of different aspects of cognitive function until a patient becomes completely dependent on the care of family members and healthcare workers [2]. Median survival after diagnosis is 7 to 10 years for people in their 60s to 70s, and 3 years for people in their 90s [3].

The disease is characterized pathologically by the presence of extracellular amyloid plaques comprising mainly of the amyloid beta protein; and intracellular neurofibrillary tangles (NFT) made mainly of the cytoskeletal protein tau [4]. To date the cause of AD still remains poorly understood.

As the buildup of amyloid appears to be a key step in the development of both familial and sporadic forms of the disease, the amyloid cascade hypothesis has become the leading theory for the cause of the condition [5]. In brief, this hypothesis states that the key step in developing AD is the accumulation of amyloid beta through reduced breakdown and clearance, and/or increased production. Strategies aimed at reducing the amyloid load in the brain, however, have failed to control the disease [6] and have resulted in a large number of clinical trials that have failed to achieve primary outcome measures [7]. Even in pre-clinical carriers of dominantly inherited AD mutations, amyloid removal therapies have not slowed disease progression [8]. Furthermore, brain amyloid load does not correlate with clinical symptoms [9]. This has led researchers to investigate alternative pathophysiological mechanisms [10].

AD is clinically defined by distinctive changes in cognitive status identified by neuropsychological assessment. Brain imaging changes and amyloid and tau protein levels in the cerebrospinal fluid are used to confirm the diagnosis in vivo [11]. The changes seen in a patient's ability to perform a cognitive task are often difficult to explain from a cellular perspective. Tau deposition does explain elements of the observed neuropsychological abnormalities [12], but does not fully account for all cognitive changes observed in AD patients [13,14].

Cognitive processing, such as that required while performing memory tasks, puts an increased metabolic demand on the brain [15]. This is evidenced by neuroimaging studies of the brain which use tracers of metabolism such as 2-[18F]fluoro-2-Deoxy-D-glucose (FDG) that have shown poor glucose utilization in patients who perform poorly on memory tasks [16,17]. Positron-emission tomography (PET) imaging studies that use oxygen-15 labelled water also show reduced uptake when AD patients perform cognitive tasks [18]. These imaging studies suggest that any deficit in metabolic function, such as deficits in mitochondrial respiration or glycolysis, are likely to affect an individual's performance on cognitive tasks. It is therefore possible that mitochondrial respiration or glycolytic dysfunction might contribute to cognitive deficits in AD, making these cellular processes suitable pharmacological targets to improve the cognitive symptoms of AD.

Cellular metabolic changes within the brains of patients with AD and in peripheral cell populations are seen very early in the condition, and often precede the development of both amyloid plaques and NFT. Abnormalities have been shown in many metabolic pathways in AD [19]. Mounting evidence suggests that deficits in glycolysis and the function of mitochondria, specifically how they control oxidative phosphorylation, are likely to be key in the development and establishment of AD [20–22].

A mitochondrial cascade hypothesis has been suggested for the aetiology of AD, and states that people who inherit mitochondrial genes that predispose them to lower mitochondrial respiration rates may be more likely to develop the condition [23]. In animal models of AD, changes in mitochondrial function are seen prior to amyloid deposition [20,24], and cell models show changes in mitochondrial function and oxidative stress without the presence of amyloid [25], giving further evidence for the key role of mitochondrial dysfunction in AD.

Impairment of glycolysis is also seen early in patients with AD. A 2-[18F]fluoro-2-Deoxy-D-glucose positron-emission tomography (FDG-PET) imaging of the brain shows a reduction in glucose metabolism [26]. In particular, there is a reduction in aerobic glycolysis in brain areas susceptible to amyloid deposition [27], and in those regions where high levels of tau accumulation are seen [28].

We have previously shown that fibroblasts from sporadic AD (sAD) patients have multiple mitochondrial structural and functional abnormalities, and that these can be ameliorated by treatment with ursodeoxycholic acid (UDCA) [29]. Other studies have shown that glycyl-L-histidyl-L-lysine (GHK-Cu), by increasing gene expression, has an effect on improving mitochondrial activity and influencing cognitive decline [30]. In our previous study we showed sAD fibroblasts to have deficits in mitochondrial membrane potential (MMP) and mitochondrial spare respiratory capacity (MSRC). MSRC refers to the difference in oxidative phosphorylation rates between the basal level of mitochondrial respiration and the maximal level a cell can achieve [31]. In essence, MSRC measures the cellular reserve respiratory capacity. In animal models of AD it has been shown that deficits in MSRC cause cognitive deficits that treatment with the antioxidant pyrroloquinoline quinone can improve [32]. It has

not been previously shown, however, whether changes in MSRC in human cell lines obtained from sAD patients correlate with their performance on neuropsychological tests.

As deficits in both glycolysis and mitochondrial function have been shown in AD patients and models, in this proof of concept study we explored metabolic function in fibroblasts from sporadic AD patients and its role in the cognitive decline experienced by these patients. To this end, we assessed mitochondrial functional changes in a larger cohort of patients compared to the findings described in our previous study [29]. We have then assessed additional metabolic parameters in the sAD fibroblasts including glycolytic function and cellular ATP levels, which have previously not been described. Finally, we investigated whether these metabolic abnormalities detected in sAD fibroblasts correlated with neuropsychological and neuroimaging features typical of the early stages of this disease.

2. Results

2.1. Patient Demographic Details

Skin biopsies were taken from ten sAD patients (mean age 61.3 years, 6 male) and ten controls (mean age 66.7 years, 5 male). Body mass index (BMI) did not differ significantly between the groups (sAD mean 27.8 kg/m² SD 5.37 kg/m² Controls mean 28.2 kg/m² SD 4.00 kg/m² *t*-test *p* = 0.44). Table 1 shows patient and control demographic data.

Table 1. Patient Demographic Information and contemporary treatment status.

Patient Number	Age (Years)	Sex	MMSE	Length of Education (Years)	AD Treatment (in Disease Cohort, at Time of Biopsy)
1	63	Male	20	16	None
2	57	Male	18	15	Donepezil
3	53	Male	14	11	Donepezil
4*	60	Male	18	9	None
5*	59	Female	23	11	Galantamine
6*	63	Female	26	10	Donepezil
7*	60	Male	18	11	Memantine
8	60	Male	18	11	None
9	79	Female	28	15	None
10	61	Female	25	11	Donepezil
Group Mean (Standard Dev)	61.33 (7.19)		20.8 (4.4)	12.0 (2.4)	
Controls					
1	66	Male	29	11	NA
2*	54	Male	27	17	NA
3*	53	Male	29	16	NA
4*	56	Male	24	11	NA
5	61	Female	30	NA	NA
6	54	Female	29	17	NA
7*	100	Female	24 #	14	NA
8	75	Female	28	18	NA
9	73	Female	26	12	NA
10	75	Male	27	10	NA
Group Mean (Standard Dev)	65.77 (14.7)		27.6 (1.8)	14 (3.1)	

For control 7 some items of the Mini Mental State Examination (MMSE) could not be tested due to sensory impairment * indicates fibroblast lines in which Mitochondrial Membrane Potential (MMP) and Mitochondrial Spare Respiratory Capacity (MRSC) values were published in our previous paper [29].

2.2. Neuropsychological Profiles

Neuropsychological profiling of controls and patients used in this study was performed as part of the VPH-DARE research project (<http://www.vph-dare.eu/>), (see Methods section for additional details). For the present study, a subgroup of neuropsychological tests was selected to be correlated with metabolic findings. The tests which can detect the earliest typical cognitive impairments in mild sAD were selected. These included assessment of semantic memory, immediate and delayed episodic recall. Phonemic fluency was also selected as dysfunction on this cognitive test is seen later in AD but not in its earlier stages [33]. All 10 controls and 10 patients with AD were assessed. The Mini-Mental

State Examination (MMSE) [34] was also used, as this test is useful in staging disease severity in sAD [34,35].

Patients with sAD performed at a lower level than controls on all tests (see Figure 1). The most significant differences were seen in the tests of semantic memory (mean score in controls 42.6 points, mean score in sAD 17.5 points, difference between means 25.1 points, SD 4.774 $p < 0.0001$); immediate (mean score in controls 15.8 points, mean score in sAD 6.4 points, difference between means 25.1 points, SD 1.468 $p < 0.0001$); and delayed recall of the Prose Memory test (mean score in controls 18.6 points, mean score in sAD 5.5 points, difference between means 13.4 points, SD 1.488 $p < 0.0001$). The phonemic fluency test performance was also significantly different between the 2 groups (mean score in controls 50.5 points, mean score in sAD 27.4 points, difference between means 23.1 points, SD 6.837 $p = 0.0033$), but to a lesser extent than the other neuropsychological tests. As expected, MMSE scores of sAD patients were significantly lower than those of controls (mean score in controls 27.3 points, mean score in sAD 21.3 points, mean difference 6.0 points, SD 1.54 $p = 0.0011$).

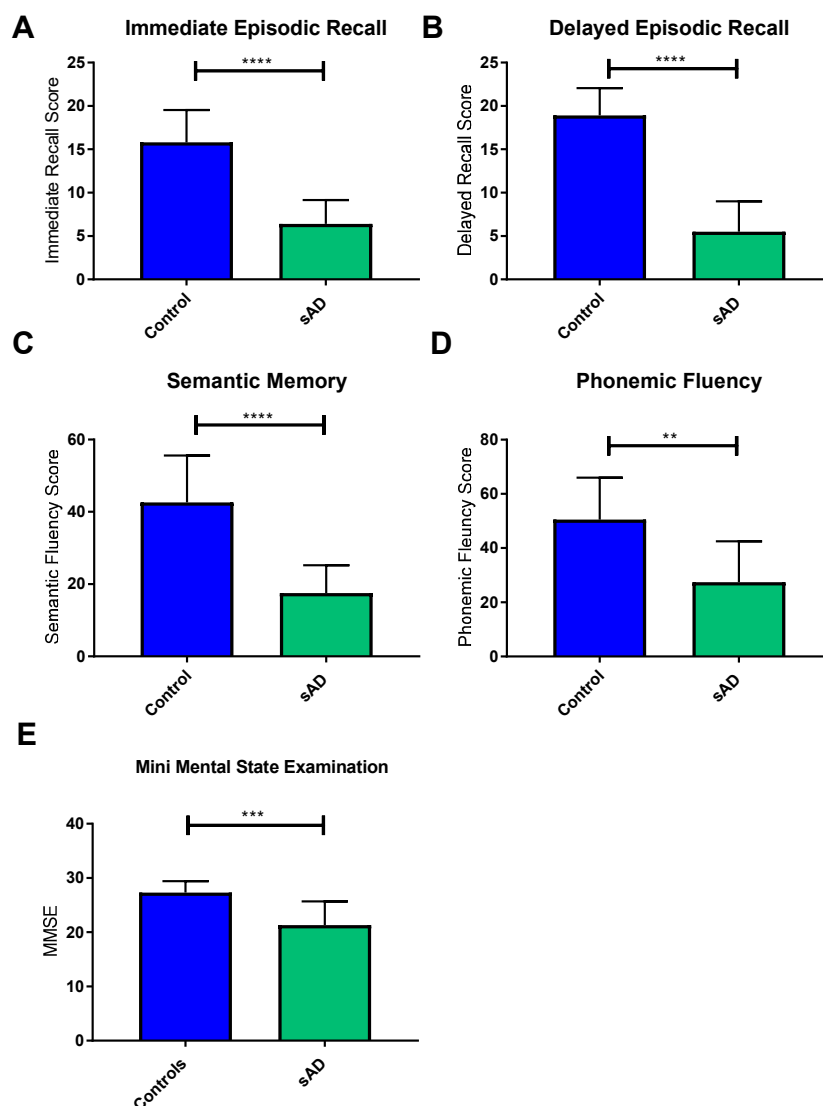


Figure 1. Mean scores of sporadic AD (sAD) patients and controls on cognitive tests included in the neuropsychological assessment. Graphs show mean with error bars indicating standard deviation. **** $p < 0.0001$; *** $p < 0.001$; ** $p < 0.01$. Controls are indicated by blue bars and sAD patients indicated by green bars. Significant reductions were seen in sAD immediate recall (A), delayed recall (B), semantic memory (C), phonemic fluency (D) and Mini Mental State Examination (E) when compared to controls.

2.3. Neuroimaging Profiles

Volumetric structural MRI scans were acquired on 9 controls and 10 patients with sAD. One control did not complete their MRI scan as an incidental finding (of no diagnostic significance for this study) on initial scans meant the participant could no longer take part in the VPH-DARE@IT original study. For the remaining participants, the left and right parietal lobes, anterior medial pre-frontal cortex and posterior cingulate gyrus, and left hippocampal grey matter volumes were extracted as these brain areas are affected early in AD [36].

Comparisons between the 2 groups showed no significant differences between the grey matter volumes of the preselected areas when performing a *t*-test. Brain grey matter volumes can be affected by age, education and brain reserve [37,38]. For these reasons a further analysis of the 2 groups was completed controlling for these covariates. A significant difference emerged in the volume of the left hippocampus, left parietal, right parietal and anterior medial prefrontal cortex in patients with sAD after controlling for confounding variables. Table 2 highlights the F-test and *p*-values for these differences. No significant difference was seen in the posterior cingulate cortex grey matter volume between the 2 groups.

Table 2. Differences in Control and sAD brain volumes. This table shows the significance of the differences in brain volumes between controls and patients with sAD when controlling for age, years of education and brain reserve.

Brain Volume	F-Test	<i>p</i> -Value
Left Hippocampal Volume	9.420	0.001
Left Parietal Volume	7.882	0.002
Right Parietal Volume	10.051	<0.0001
Anterior Medial Prefrontal Cortex	0.056	0.017
Posterior Cingulate Cortex	0.752	0.575

2.4. Fibroblast Metabolic Assessment

Mitochondrial function was investigated in both sAD patients and controls. We measured elements of both mitochondrial function and glycolysis. Five metabolic parameters were chosen that best describe different factors influencing the ability of the fibroblast to meet its energy demands. Mitochondrial parameters included: total cellular ATP, as this is a global marker of the energetic status of the cell; MMP and MSRC. MMP and MSRC were selected as these parameters are important in maintaining the rate of ATP production as cellular energy demand changes. These are also the two parameters which we have previously identified as being relevant to the mitochondrial phenotype in sAD fibroblasts [29]. Measures of glycolysis included glycolytic reserve and extracellular lactate levels. Glycolytic reserve, like MSRC and MMP for mitochondrial function, is a measure of cellular metabolic flexibility and deficits in this parameter are likely to contribute to an inability to maintain cellular energy production. Extracellular lactate is the final breakdown product of glycolysis and contributes information about how well the cell can utilize glucose as a metabolite.

First, we assessed MMP and MRSC as we have done in our previous work [29]. In this cohort, MRSC was significantly reduced (36% reduction $p < 0.0001$) in sAD when compared to controls (Figure 2A). MMP was also significantly reduced in the sAD fibroblast lines (14% reduction $p = 0.011$) (See Figure 2B). Figure 2C shows a representative oxygen consumption trace for the mitochondrial stress test experiment.

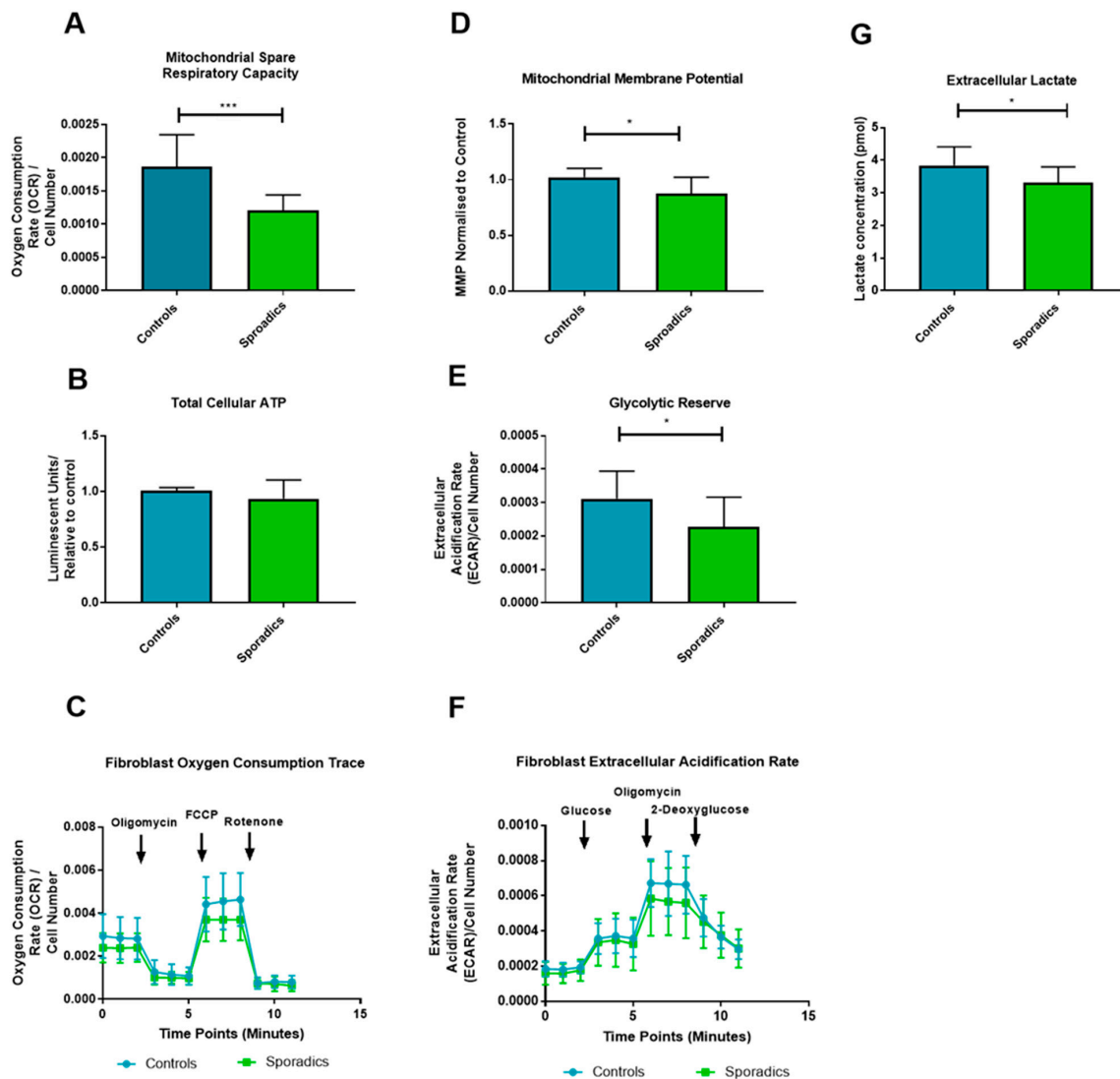


Figure 2. Oxidative phosphorylation and Glycolytic fibroblast Assessment: *** = $p < 0.001$; * = $p < 0.05$. Significant reductions in mitochondrial spare respiratory capacity (A), Mitochondrial Membrane potential (D), Glycolytic Reserve (E) and Extracellular lactate (G) was detected in sAD when compared to controls. No significant difference was seen in total cellular ATP (B). OCR and ECAR traces for mitochondrial stress test and glycolysis stress test are displayed in panels (C) and (F) respectively. For all panels controls are represented in blue and sAD are represented in green. Graphs represent mean with error bars indicating standard deviation.

Next, we assessed total cellular ATP, which showed no significant difference between sAD patient fibroblasts and controls when comparing mean values ($p = 0.165$, Figure 2D). The final metabolic assessment of the fibroblast lines involved assessment of glucose metabolism using the glycolysis stress test programme on the Seahorse analyzer and extracellular lactate measurement. A significantly lower glycolytic reserve was found in sAD fibroblasts when compared to controls (see Figure 1E, 25.8% reduction, $p = 0.031$). No significant differences were seen in maximum glycolytic rate ($p = 0.792$), or basal glycolytic rate ($p = 0.381$). Figure 1F shows the extracellular acidification rate (ECAR) trace for the glycolysis stress test, comparing the group of controls against the sAD fibroblast group. Measurement of extracellular lactate levels revealed significantly lower lactate levels released from sAD fibroblasts (14% reduction, $p = 0.0227$, Figure 2G).

2.5. Neuropsychological/Metabolic Correlations

Next, we sought to correlate the neuropsychological scores of the sAD patients and controls combined with their metabolic parameters measured in fibroblasts. As five neuropsychological measures and five fibroblast metabolic markers had been assessed to identify differences in the control and sAD fibroblast groups, we controlled for the effect of multiple comparisons by adjusting what we deemed to be a significant association to $p \leq 0.01$ (0.05/5). Using this new statistical threshold, only MSRC and MMP metabolic tests and immediate, delayed and semantic memory neuropsychological assessments were identified as significantly different between control and sAD groups. Correlations were, therefore, performed only for these data sets.

MSRC had a significant positive correlation with immediate episodic recall ($r = 0.612, p = 0.004$), delayed episodic recall ($r = 0.669, p = 0.001$) and semantic memory scores ($r = 0.614, p = 0.003$). MMP correlated only with semantic memory scores ($r = 0.565, p = 0.009$). Immediate episodic recall ($r = 0.552, p = 0.0134$) and delayed episodic recall correlated positively with MMP, but at a lower level of significance ($r = 0.540, p = 0.015$). Figure 3 displays these correlations graphically.

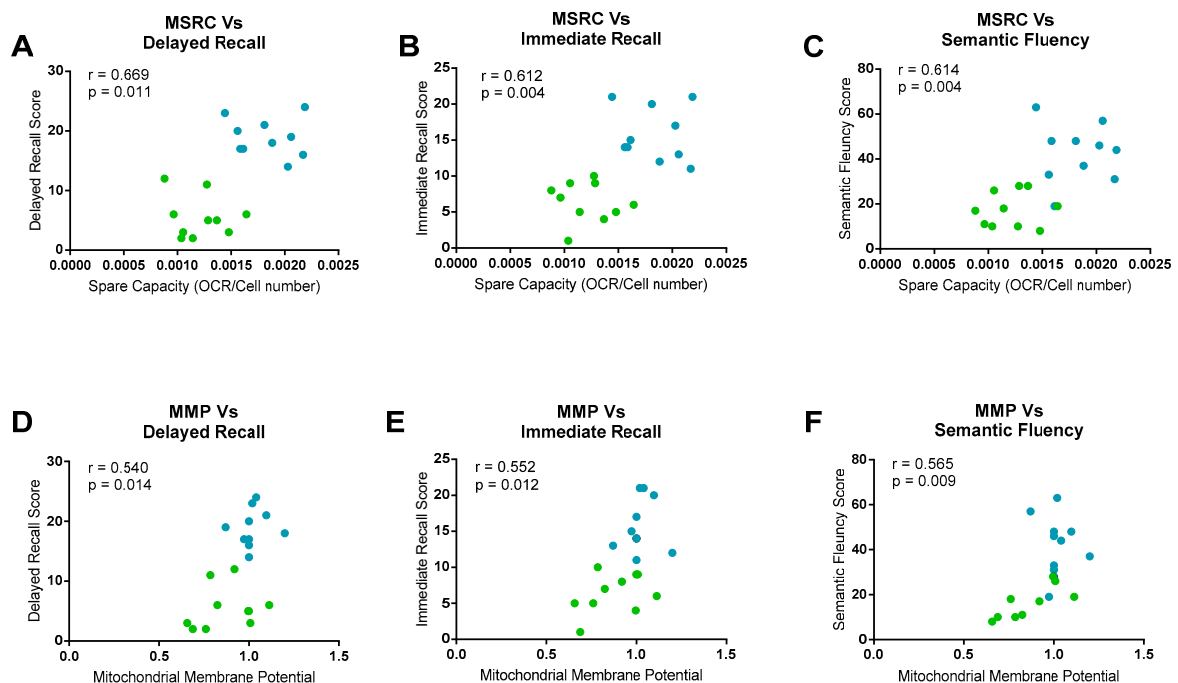


Figure 3. Neuropsychological Fibroblast Metabolism Correlations. Significant correlations were seen between mitochondrial spare respiratory capacity (MSRC) and delayed recall (A), Immediate recall (B) and semantic fluency (C). Mitochondrial membrane potential (MMP) correlated significantly with semantic fluency (F), and with delayed recall (D) and immediate recall (E) but to a lesser extent. For all panels controls are represented in blue and sAD are represented in green. Correlation coefficients and p -values for each correlation are displayed.

Age, years of education and brain reserve can potentially confound the correlations between neuropsychological measurements and the fibroblast metabolic markers, as all three factors have been shown to affect either performance on neuropsychological tests [39,40] or mitochondrial function [41]. To control for the effect of these three covariates, a further analysis was performed taking these parameters into account. This further analysis showed that the correlation between delayed episodic recall and MSRC was still significant at the more conservative significance threshold. Both immediate episodic recall ($p = 0.013$) and semantic memory ($p = 0.012$) correlations with MSRC were no longer significant once covariates were included in the analysis at the new more stringent p -value. All correlations seen between the neuropsychological tests and MMP were no longer significant after controlling for age,

education and brain reserve. Table 3 displays the new correlation coefficients and *p*-values for the neuropsychological data.

Table 3. Neuropsychological fibroblast metabolism correlations corrected for age, years of education and grey matter reserve.

Psychological Test	Fibroblast Marker	R Value	<i>p</i> -Value
Immediate Episodic Recall	MSRC	0.605	0.013
	MMP	0.196	0.466
Delayed Episodic Recall	MSRC	0.695	0.003
	MMP	0.204	0.448
Semantic Memory	MSRC	0.610	0.012
	MMP	0.345	0.191

2.6. Neuroimaging/Metabolic Correlations

Volumetric imaging for areas of the brain known to be affected by AD were correlated with metabolic markers of the disease. Only the grey matter volumes that had shown significant differences between the sAD and control groups (with a *p*-value equal to or less than 0.01) were included. None of the grey matter volumes showed a significant correlation with changes in cellular metabolism. Table 4 shows the results of the correlations.

Table 4. Grey Matter Volume Fibroblast metabolic correlations: No significant correlations were seen between MMP nor MSRC and any grey matter volume when controlling for age, length of disease or brain reserve.

Grey Matter Volume	Fibroblast Marker	R Value	<i>p</i> -Value
Left Hippocampal Volume	MSRC	0.371	0.157
	MMP	0.041	0.881
Left Parietal Volume	MSRC	0.341	0.196
	MMP	−0.047	0.862
Right Parietal Volume	MSRC	0.418	0.107
	MMP	−0.043	0.875

3. Discussion

This proof of concept study shows that fibroblast MSRC correlates with established neuropsychological abnormalities that are affected early in AD. This is one of the first studies to show a functional biomarker of AD correlating with a marker of fibroblast mitochondrial function. MSRC is a measure of the ability of mitochondria within cells to increase the production of ATP in response to an increased energy demand. The correlation of MSRC with neuropsychological scores potentially helps to describe the cellular pathology underlying these neuropsychological changes seen in AD. This is the first study in humans to show that peripheral cell MSRC correlates with neuropsychological profiles. Correcting the abnormality in MSRC could be a future therapeutic approach in AD. The fact that this abnormality in mitochondrial function correlates with a clinical biomarker of AD also opens the avenue for monitoring drug response in future clinical trials.

MSRC has been shown to be abnormal in multiple diseases including acute myeloid leukaemia (AML) [42], Parkinson’s disease [43,44] and motor neuron disease (MND) [45]. MSRC deficits may not be disease specific, but the combination of cellular metabolic changes seen here may represent

a cellular metabolic profile specific to sAD. This metabolic phenotype could potentially represent a biomarker that can stratify and define a specific subset of sAD patients that might then respond to a personalised therapeutic approach. Previous research has shown that the metabolic profile identified in fibroblasts from sporadic Parkinson's disease patients differs from that identified here in fibroblasts from sAD [46,47].

Reductions in MSRC and MMP were seen in all sAD fibroblast lines when compared to controls at a group level. These data reinforce and extend the findings reported in our previous paper [29], and show that the finding of reduced MSRC and MMP is reproducible and more robust in sporadic AD fibroblasts when sample size is increased. Extracellular lactate levels and cellular glycolytic reserves, both markers of glycolytic function, were significantly reduced in all sAD fibroblasts. These measures, however, did not meet the statistical significance for correlation with neuropsychological markers of the disease. The deficits in markers of mitochondrial function and glycolysis in the fibroblasts reflect a lack of flexibility of metabolic pathways in sAD. This lack of flexibility is likely to be very important when performing cognitive tasks that depend on the coordination of multiple brain regions. Taken together, these results suggest that sAD fibroblasts may have limited ability to respond to increased cellular energy demand.

MMP did correlate with neuropsychological markers, but correlations did not survive the correction for confounding factors unlike MSRC, for which correlation with delayed episodic recall (a core feature in the clinical diagnostic criteria for sAD) remained significant. Semantic memory and immediate episodic memory did not significantly correlate with MSRC at the more conservative significance threshold after confounder consideration, but *p*-values for both of these correlations were less than 0.02. Potentially, these correlations would reach significance level with an increased sample size. The difference in MMP between control and sAD groups was much smaller than the difference seen in MSRC. MMP has a key role in maintaining many pathways in the mitochondria outside that of ATP generation, such as apoptosis fates [48]. It is likely that several mechanisms not affected by sAD in the fibroblast cell help to maintain MMP levels, which may explain the reduced variability seen in this parameter in sAD and the lack of a significant correlation with neuropsychological scores.

Baseline ATP levels were not significantly different between the two groups. These results suggest that, in a controlled environment when cells are not stressed, they can maintain ATP levels similar to that of controls. Interestingly though, the functional capacity of mitochondria is impaired, as described above, suggesting a potential inability to respond appropriately to increased ATP demand. The measurements of ATP we performed in this study only gives information about the total cellular ATP level. We did not investigate the rate of ATP breakdown nor how ATP levels change when the cell is under stressed conditions or the ratio of ATP/ADP in the cell. This may explain why no significant correlations were seen with ATP measurements, but were seen with the other markers of mitochondrial respiration.

It is interesting that the correlation between scores on phonemic fluency, a neuropsychological test not affected early in sAD, and cell metabolism markers did not reach significance threshold. It. The medial temporal lobe is important in semantic memory processing [49], an area of cognition that is impaired very early in sAD [50]. This is not the case for phonemic fluency which is supported by processes associated with frontal executive regions [51]. It could be that the correlations we see between neuropsychological tests and cellular metabolic function may reflect which areas of the brain are more susceptible to metabolic failure. It has been previously shown that areas of the brain that are affected early in sAD express lower levels of electron transport chain (ETC) genes when compared to controls [52], suggesting that this might be the case. Data from FDG-PET studies also support the concept of focal brain hypometabolism in sAD, with areas such as the medial temporal lobes, precuneus and lateral parietal lobes all preferentially affected [53].

We did not see a significant correlation between mitochondrial function or glycolysis and brain structural imaging markers of sAD. This may be explained by the fact that multiple factors can affect grey matter volume such as age, levels of education and brain reserve. It has been previously shown

that smaller grey matter volumes in the frontal lobes associated with ageing are associated with worse performance on frontal lobe cognitive tests [54]. The neuropsychological assessment performed in this study mainly focused on temporal lobe cognitive functioning and not frontal lobe function. Potentially, the effect of brain ageing on grey matter volumes may mask any effect metabolic function may have.

The limitations of our study include a small sample size, and the fact that we have used fibroblasts to measure metabolic function. It could also be argued that a correlation between metabolic function of central nervous system cells and neuropsychological parameters would be more meaningful. This is not the first study, however, to show that the metabolism of peripheral cells outside the nervous system is affected in sAD. White blood cells [55], platelets [56] and fibroblasts have been shown to have metabolic abnormalities in multiple studies [46,47,57,58]. Identifying that fibroblast mitochondrial abnormalities correlate with neuropsychological markers of AD opens up avenues to use fibroblast metabolic parameters as biomarkers of sAD, and also as a high throughput drug screening model, as well as potential outcome measures of therapeutic efficacy. Replication of the findings of this study in larger cohorts and by other groups is needed, however, to consolidate the evidence that fibroblast metabolic function is a reliable biomarker of sAD.

Our patient cohort were selected at an early stage of sAD to try and reduce group variability. To understand the use of fibroblast metabolic abnormalities as a biomarker, further work investigating cohorts of patients with amnesic mild cognitive impairment (MCI), the prodromal stage of sAD, would be advantageous as well as investigating these parameters in more advanced sAD patients.

Future work could extend the findings of metabolic-neuropsychological correlations by creating neuronal lineage cells via cellular reprogramming methods such as that described by Takahashi et al. [59]. This type of model would allow for direct comparison between human nervous system cells and human nervous system function in a context where reprogrammed cells would maintain their ageing phenotype [60].

4. Methods

4.1. Patient Details

Skin biopsies and fibroblast metabolic assessments were performed as part of the MODEL-AD research study (Yorkshire and Humber Research and Ethics Committee number: 16/YH/0155). Due to the initial success of fibroblast metabolic assessment, the initial cohort of four controls and four patients (previously reported in [29]) with sAD was expanded to ten healthy controls (mean age: 65.77 years, SD 14.70 years) and 10 patients with sAD (mean age: 61.33 years, SD 7.19 years). All patients had been involved in the EU-funded Framework Programme 7 Virtual Physiological Human: Dementia Research Enabled by IT (VPH-DARE@IT) initiative (<http://www.vph-dare.eu/>). A diagnosis of sAD was made based on clinical criteria [11]. Ethical approval for the neuropsychological and neuroimaging measures collected was gained from Yorkshire and Humber Regional Ethics Committee, Reference number: 12/YH/0474. Informed written consent was obtained from each participant. Investigations were carried out following the rules of the Declaration of Helsinki of 1975 (<https://www.wma.net/what-we-do/medical-ethics/declaration-of-helsinki/>), revised in 2013.

4.2. Neuropsychological Testing

A battery of tests was devised to detect impaired performance in the cognitive domains most susceptible to sAD neurodegeneration. This included tests of short- and long-term memory, attention and executive functioning, language and semantics, and visuoconstructive skills. A detailed description of each task is provided elsewhere [61]. Most tests were exclusively used as part of the clinical assessment of patients and controls. Three tests were also included as part of the experimental protocol. Immediate and delayed recall on the Logical Memory test were used as measures of episodic memory, the cognitive domain centrally defined by diagnostic criteria for a diagnosis of sAD. The performance on the Category Fluency test was used as an index of semantic memory, the cognitive domain affected by

the accumulation of neurofibrillary pathology in the transentorhinal cortex [50]. Finally, the Letter Fluency test (phonemic fluency) was used as a methodological control, since performance on this task is often within normal age limits in patients with mild sAD [33,62].

4.3. MRI Acquisition and Processing

An MRI protocol of anatomical scans was acquired on a Philips Ingenia 3 T scanner. Several acquisitions (including T1-weighted, T2-weighted, FLAIR and diffusion-weighted sequences) were used for diagnostic purposes. Three-dimensional T1-weighted images (voxel size: 0.94 mm × 0.94 mm × 1.00 mm; repetition time: 8.2 s; echo delay time: 3.8 s; field of view: 256 mm; matrix size: 256 × 256 × 170) were also used for the calculation of hippocampal volumes. These were processed with the Similarity and Truth Estimation for Propagated Segmentations routine [63]. This procedure, available at niftyweb.cs.ucl.ac.uk, allows automated segmentation of the left and right hippocampus in the brain's native space using multiple reference templates. Hippocampal volumes were then quantified using Matlab (version R2014a) and the "get totals" script (http://www0.cs.ucl.ac.uk/staff/G.Ridgway/vbm/get_totals.m). Fractional measures were also obtained dividing hippocampal volumes by the volume of the total intracranial space. The left hippocampal volume and left hippocampal ratio were chosen as structural markers of AD as evidence suggests the left hippocampus is affected early in the progression of the disease [64]. Native space maps created to extract hippocampal volume from MRI images are shown in Supplementary Figure S1. Additional regions of interest (listed in Table 2) were then defined as binary image masks. Segmented grey matter maps were registered to the Montreal Neurological Institute space, and mask-constrained volumes were extracted.

4.4. Tissue Culture

Fibroblasts were cultured as described previously [29]. In brief, all 10 control and all 10 sAD lines were cultured in EMEM-based media (Corning) incubated at 37 °C in a 5% carbon dioxide atmosphere. Sodium pyruvate (1%) (Sigma Aldrich), non-essential amino acids (1%) (Lonza), penicillin and streptomycin (1%) (Sigma Aldrich), multi-vitamins (1%) (Lonza), Fetal Bovine Serum (10%) (Biosera) and 50 µg/mL uridine (Sigma Aldrich) were added to the media. All experiments described were performed on all 20 cell lines. Fibroblasts were plated at a density of 5000 cells per well in a white 96 well plate for ATP assays. For MMP assays fibroblasts were plated at a density of 2500 cells per well in a black 96 well plate. Each assay was performed on three separate passages of fibroblasts; cells between passages 5–10 were used. All experiments were performed on passage-matched cells.

4.5. Intracellular ATP levels

Cellular adenosine triphosphate (ATP) levels were measured using the ATPlite kit (Perkin Elmer) as described previously [65]. ATP levels were corrected for cell number by using CyQuant (ThermoFisher) measurements, as previously described [29]. These values were then normalised to control levels.

4.6. Mitochondrial Membrane Potential

MMP was measured using tetramethylrhodamine (TMRM) staining of live fibroblasts, as previously described [29]. Cells were plated in a black 96 well plate, incubated at 37 °C for 48 h. TMRM dye was added one hour prior to imaging on an InCell Analyzer 2000 high-content imager (GE Healthcare).

4.7. Extracellular Lactate Measurement

Extracellular lactate was measured from confluent flasks of fibroblasts using an L-Lactate assay kit (Abcam ab65331). The assay was performed according to the manufacturer's instructions.

4.8. Metabolic Flux Assay

4.8.1. Mito Stress Test

Oxygen consumption rates (OCR) were measured using a 24-well Agilent Seahorse XF analyzer as described previously [29]. In brief, cells were plated at a density of 65,000 cells per well 48 h prior to measurement. Three measurements were taken at the basal point: after the addition of oligomycin (0.5 μ M), after the addition of carbonyl cyanide-4-(trifluoromethoxy)phenylhydrazone (FCCP) (0.5 μ M) and after the addition of rotenone (1 μ M). OCR measurements were normalised to cell count as described in [29]. Measurements of basal mitochondrial respiration, maximal mitochondrial respiration and MSRC were also calculated.

4.8.2. Glycolysis Stress Test

Cells were plated in a Seahorse XF24 Cell Culture Microplate (Agilent) at a density of 65,000 cells per well 48 h prior to measurement. The glycolysis stress test standard protocol was used [66]. This is a completely separate assay to the mitochondrial stress test, and allows for the thorough interrogation of glycolysis via the addition of supplements and inhibitors of the glycolytic pathway. Three measurements were taken at the basal point: after the addition of glucose (10 μ M), after the addition of oligomycin (1.0 μ M) and after the addition of 2-deoxyglucose (50 μ M). The glycolysis stress test can measure several aspects of cellular glycolysis. These include the basal glycolytic rate of the cell, the maximum level of glycolysis the cell can achieve and the glycolytic reserve which refers to the difference between maximum level of glycolysis and the basal level of glycolysis. The different aspects of glycolysis are calculated by measuring the extracellular acidification rate (ECAR). ECAR rates were normalised to cell count as described above.

4.9. Statistical Analysis

For comparing each neuropsychological, neuroimaging and metabolic functional markers, a Student's *t*-test was used, comparing the means of the control group for each parameter to the disease group. Statistics were calculated using GraphPad Prism Software (V7.02). Analyses of covariance were also used for group comparisons including confounding variables. For covariate analysis when comparing control and disease group grey matter volumes, or when correlating neuropsychological and neuroimaging sAD markers with fibroblast functional markers, the IBM SPSS Statistics suite (Version 26; <https://www.ibm.com/uk-en/products/spss-statistics>) was used as this function was not available in the GraphPad Prism Software. Significance levels were adjusted to account for multiple comparisons.

5. Conclusions

These data highlight how in-depth analysis of mitochondrial and glycolytic function in sAD fibroblasts identifies metabolic abnormalities that parallel changes seen in neuropsychological features distinctive of the early stages of sporadic Alzheimer's disease. This model system could be used to develop biomarkers useful in early detection as well as in the development of novel therapeutic approaches for sAD.

Supplementary Materials: The following are available online at <http://www.mdpi.com/2075-4426/10/2/32/s1>, Figure S1: Quantification of hippocampal volumes from T1-weighted MRI scans.

Author Contributions: Conceptualization, S.M.B., D.J.B., H.M., L.F., A.V., M.D.M. and P.J.S.; Methodology, S.M.B., M.D.M., K.B., H.M. and A.V.; Software, S.M.B., and M.D.M.; Validation, S.M.B., D.J.B., K.B., H.M., L.F., A.V., M.D.M. and P.J.S.; Formal Analysis, S.M.B., D.J.B., K.B., H.M., L.F., A.V., M.D.M. and P.J.S.; Investigation, S.M.B., M.D.M., and K.B.; Resources, S.M.B., D.J.B., K.B., H.M., L.F., A.V., M.D.M. and P.J.S.; Data Curation, S.M.B., D.J.B., K.B., H.M., L.F., A.V., M.D.M. and P.J.S.; Writing—Original Draft Preparation, S.M.B.; Writing—Review and Editing, S.M.B., D.J.B., K.B., H.M., L.F., A.V., M.D.M. and P.J.S.; Visualization, S.M.B., D.J.B., K.B., H.M., L.F., A.V., M.D.M. and P.J.S.; Supervision, H.M., P.J.S., A.V., L.F. and D.J.B.; Project Administration, S.M.B.; Funding Acquisition, S.M.B., D.J.B., K.B., H.M., L.F., A.V. and P.J.S. All authors have read and agreed to the published version of the manuscript.

Funding: This research was funded by Wellcome 4ward north (216340/Z/19/Z), ARUK Yorkshire Network Centre Small Grant Scheme (Ref: ARUK-PCRF2016A-1), Parkinson’s UK (F1301), European Union Seventh Framework Programme (FP7/2007 – 2013) under grant agreement no. 601055, NIHR Sheffield Biomedical Research Centre award.

Acknowledgments: We would like to thank all research participants involved in this study. This research was supported by the Wellcome 4ward North Academy and ARUK Yorkshire Network Centre Small Grant Scheme (to SMB), Parkinson’s UK (to HM, F1301) and the NIHR Sheffield Biomedical Research Centre. This is a summary of independent research carried out at the NIHR Sheffield Biomedical Research Centre (Translational Neuroscience). The views expressed are those of the author(s) and not necessarily those of the NHS, the NIHR or the Department of Health and Social Care (DHSC). Support of the European Union Seventh Framework Programme (FP7/2007–2013) under grant agreement no. 601055, VPH-DARE@IT to AV is acknowledged. PJS is supported by an NIHR Senior Investigator award. The support of the NIHR Clinical Research Facility—Sheffield Teaching Hospital is also acknowledged.

Conflicts of Interest: The authors have no financial or personal relationships with other people/organizations that could inappropriately influence (bias) their work.

References

1. Wimo, A.; Guerchet, M.; Ali, G.-C.; Wu, Y.-T.; Prina, A.M.; Winblad, B.; Jönsson, L.; Liu, Z.; Prince, M. The worldwide costs of dementia 2015 and comparisons with 2010. *Alzheimer’s Dement.* **2017**, *13*, 1–7. [[CrossRef](#)]
2. Scheltens, P.; Blennow, K.; Breteler, M.M.B.; de Strooper, B.; Frisoni, G.B.; Salloway, S.; Van der Flier, W.M. Alzheimer’s disease. *Lancet* **2016**, *388*, 505–517. [[CrossRef](#)]
3. Brookmeyer, R.; Corrada, M.M.; Curriero, F.C.; Kawas, C. Survival following a diagnosis of Alzheimer disease. *Arch. Neurol.* **2002**, *59*, 1764–1767. [[CrossRef](#)]
4. Perl, D.P. Neuropathology of Alzheimer’s Disease. *Mt. Sinai J. Med.* **2010**, *77*, 32–42. [[CrossRef](#)] [[PubMed](#)]
5. Hardy, J.; Selkoe, D.J. The Amyloid Hypothesis of Alzheimer’s Disease: Progress and Problems on the Road to Therapeutics. *Science* **2002**, *297*, 353. [[CrossRef](#)] [[PubMed](#)]
6. Honig, L.S.; Vellas, B.; Woodward, M.; Boada, M.; Bullock, R.; Borrie, M.; Hager, K.; Andreasen, N.; Scarpini, E.; Liu-Seifert, H.; et al. Trial of Solanezumab for Mild Dementia Due to Alzheimer’s Disease. *N. Engl. J. Med.* **2018**, *378*, 321–330. [[CrossRef](#)] [[PubMed](#)]
7. Cummings, J.L.; Morstorf, T.; Zhong, K. Alzheimer’s disease drug-development pipeline: Few candidates, frequent failures. *Alzheimers Res. Ther.* **2014**, *6*, 37. [[CrossRef](#)]
8. ALZFORUM. Topline Result for First DIAN-TU Clinical Trial: Negative on Primary. Available online: <https://www.alzforum.org/news/research-news/topline-result-first-dian-tu-clinical-trial-negative-primary> (accessed on 29 March 2020).
9. Savva, G.M.; Wharton, S.B.; Ince, P.G.; Forster, G.; Matthews, F.E.; Brayne, C. Age, neuropathology, and dementia. *N. Engl. J. Med.* **2009**, *360*, 2302–2309. [[CrossRef](#)]
10. Le Couteur, D.G.; Hunter, S.; Brayne, C. Solanezumab and the amyloid hypothesis for Alzheimer’s disease. *BMJ* **2016**, *355*, i6771. [[CrossRef](#)]
11. McKhann, G.M.; Knopman, D.S.; Chertkow, H.; Hyman, B.T.; Jack, C.R., Jr.; Kawas, C.H.; Klunk, W.E.; Koroshetz, W.J.; Manly, J.J.; Mayeux, R.; et al. The diagnosis of dementia due to Alzheimer’s disease: Recommendations from the National Institute on Aging-Alzheimer’s Association workgroups on diagnostic guidelines for Alzheimer’s disease. *Alzheimers Dement. J. Alzheimers Assoc.* **2011**, *7*, 263–269. [[CrossRef](#)]
12. Braak, H.; Braak, E. Neuropathological staging of Alzheimer-related changes. *Acta Neuropathol.* **1991**, *82*, 239–259. [[CrossRef](#)] [[PubMed](#)]
13. Haroutunian, V.; Schnaider-Beeri, M.; Schmeidler, J.; Wysocki, M.; Purohit, D.P.; Perl, D.P.; Libow, L.S.; Lesser, G.T.; Maroukian, M.; Grossman, H.T. Role of the neuropathology of Alzheimer disease in dementia in the oldest-old. *Arch. Neurol.* **2008**, *65*, 1211–1217. [[CrossRef](#)] [[PubMed](#)]
14. Weintraub, S.; Wicklund, A.H.; Salmon, D.P. The neuropsychological profile of Alzheimer disease. *Cold Spring Harb. Perspect. Med.* **2012**, *2*, a006171. [[CrossRef](#)] [[PubMed](#)]
15. Magistretti, P.J.; Allaman, I. A Cellular Perspective on Brain Energy Metabolism and Functional Imaging. *Neuron* **2015**, *86*, 883–901. [[CrossRef](#)]

16. Ewers, M.; Brendel, M.; Rizk-Jackson, A.; Rominger, A.; Bartenstein, P.; Schuff, N.; Weiner, M.W. Alzheimer's Disease Neuroimaging I Reduced FDG-PET brain metabolism and executive function predict clinical progression in elderly healthy subjects. *NeuroImage. Clin.* **2013**, *4*, 45–52. [[CrossRef](#)]
17. Kalpouzos, G.; Eustache, F.; de la Sayette, V.; Viader, F.; Chételat, G.; Desgranges, B. Working memory and FDG–PET dissociate early and late onset Alzheimer disease patients. *J. Neurol.* **2005**, *252*, 548–558. [[CrossRef](#)]
18. Ishii, K.; Sasaki, M.; Yamaji, S.; Sakamoto, S.; Kitagaki, H.; Mori, E. Demonstration of decreased posterior cingulate perfusion in mild Alzheimer's disease by means of H215O positron emission tomography. *Eur. J. Nucl. Med.* **1997**, *24*, 670–673.
19. Morgen, K.; Frolich, L. The metabolism hypothesis of Alzheimer's disease: From the concept of central insulin resistance and associated consequences to insulin therapy. *J. Neural Transm.* **2015**, *122*, 499–504. [[CrossRef](#)]
20. Yao, J.; Irwin, R.W.; Zhao, L.; Nilsen, J.; Hamilton, R.T.; Brinton, R.D. Mitochondrial bioenergetic deficit precedes Alzheimer's pathology in female mouse model of Alzheimer's disease. *Proc. Natl. Acad. Sci. USA* **2009**, *106*, 14670. [[CrossRef](#)]
21. Blass, J.P.; Sheu, R.K.; Gibson, G.E. Inherent abnormalities in energy metabolism in Alzheimer disease. Interaction with cerebrovascular compromise. *Ann. N. Y. Acad. Sci.* **2000**, *903*, 204–221. [[CrossRef](#)]
22. Baik, S.H.; Kang, S.; Lee, W.; Choi, H.; Chung, S.; Kim, J.I.; Mook-Jung, I. A Breakdown in Metabolic Reprogramming Causes Microglia Dysfunction in Alzheimer's Disease. *Cell Metab.* **2019**, *30*, 493–507. [[CrossRef](#)] [[PubMed](#)]
23. Swerdlow, R.H.; Khan, S.M. A “mitochondrial cascade hypothesis” for sporadic Alzheimer's disease. *Med. Hypotheses* **2004**, *63*, 8–20. [[CrossRef](#)]
24. Hartl, D.; Schuldt, V.; Forler, S.; Zabel, C.; Klose, J.; Rohe, M. Presymptomatic Alterations in Energy Metabolism and Oxidative Stress in the APP23 Mouse Model of Alzheimer Disease. *J. Proteome Res.* **2012**, *11*, 3295–3304. [[CrossRef](#)]
25. Gan, X.Q.; Huang, S.B.; Wu, L.; Wang, Y.F.; Hu, G.; Li, G.Y.; Zhang, H.J.; Yu, H.Y.; Swerdlow, R.H.; Chen, J.X.; et al. Inhibition of ERK-DLP1 signaling and mitochondrial division alleviates mitochondrial dysfunction in Alzheimer's disease cybrid cell. *Biochim. Biophys. Acta Mol. Basis Dis.* **2014**, *1842*, 220–231. [[CrossRef](#)] [[PubMed](#)]
26. Mosconi, L.; Tsui, W.H.; De Santi, S.; Li, J.; Rusinek, H.; Convit, A.; Li, Y.; Boppana, M.; de Leon, M.J. Reduced hippocampal metabolism in MCI and AD: Automated FDG-PET image analysis. *Neurology* **2005**, *64*, 1860–1867. [[CrossRef](#)] [[PubMed](#)]
27. Vlassenko, A.G.; Vaishnavi, S.N.; Couture, L.; Sacco, D.; Shannon, B.J.; Mach, R.H.; Morris, J.C.; Raichle, M.E.; Mintun, M.A. Spatial correlation between brain aerobic glycolysis and amyloid-beta (Aβ) deposition. *Proc. Natl. Acad. Sci. USA* **2010**, *107*, 17763–17767. [[CrossRef](#)]
28. Vlassenko, A.G.; Gordon, B.A.; Goyal, M.S.; Su, Y.; Blazey, T.M.; Durbin, T.J.; Couture, L.E.; Christensen, J.J.; Jafri, H.; Morris, J.C.; et al. Aerobic glycolysis and tau deposition in preclinical Alzheimer's disease. *Neurobiol. Aging* **2018**, *67*, 95–98. [[CrossRef](#)]
29. Bell, S.M.; Barnes, K.; Clemmens, H.; Al-Rafiah, A.R.; Al-Ofi, E.A.; Leech, V.; Bandmann, O.; Shaw, P.J.; Blackburn, D.J.; Ferraiuolo, L.; et al. Ursodeoxycholic Acid Improves Mitochondrial Function and Redistributes Drp1 in Fibroblasts from Patients with Either Sporadic or Familial Alzheimer's Disease. *J. Mol. Biol.* **2018**, *430*, 3942–3953. [[CrossRef](#)]
30. Pickart, L.; Vasquez-Soltero, J.M.; Margolina, A. The Effect of the Human Peptide GHK on Gene Expression Relevant to Nervous System Function and Cognitive Decline. *Brain Sci.* **2017**, *7*, 20. [[CrossRef](#)]
31. Desler, C.; Hansen, T.L.; Frederiksen, J.B.; Marcker, M.L.; Singh, K.K.; Juel Rasmussen, L. Is There a Link between Mitochondrial Reserve Respiratory Capacity and Aging? *J. Aging Res.* **2012**, *2012*, 192503. [[CrossRef](#)]
32. Martino Adami, P.V.; Quijano, C.; Magnani, N.; Galeano, P.; Evelson, P.; Cassina, A.; Do Carmo, S.; Leal, M.C.; Castaño, E.M.; Cuello, A.C.; et al. Synaptosomal bioenergetic defects are associated with cognitive impairment in a transgenic rat model of early Alzheimer's disease. *Off. J. Int. Soc. Cereb. Blood Flow Metab.* **2017**, *37*, 69–84. [[CrossRef](#)] [[PubMed](#)]
33. Capitani, E.; Rosci, C.; Saetti, M.C.; Laiacona, M. Mirror asymmetry of Category and Letter fluency in traumatic brain injury and Alzheimer's patients. *Neuropsychologia* **2009**, *47*, 423–429. [[CrossRef](#)] [[PubMed](#)]
34. Folstein, M.F.; Folstein, S.E.; McHugh, P.R. “Mini-mental state”. A practical method for grading the cognitive state of patients for the clinician. *J. Psychiatr. Res.* **1975**, *12*, 189–198. [[CrossRef](#)]

35. Doody, R.S.; Massman, P.; Dunn, J.K. A method for estimating progression rates in Alzheimer disease. *Arch. Neurol.* **2001**, *58*, 449–454. [[CrossRef](#)] [[PubMed](#)]
36. Scahill, R.I.; Schott, J.M.; Stevens, J.M.; Rossor, M.N.; Fox, N.C. Mapping the evolution of regional atrophy in Alzheimer's disease: Unbiased analysis of fluid-registered serial MRI. *Proc. Natl. Acad. Sci. USA* **2002**, *99*, 4703–4707. [[CrossRef](#)] [[PubMed](#)]
37. Boller, B.; Mellah, S.; Ducharme-Laliberte, G.; Belleville, S. Relationships between years of education, regional grey matter volumes, and working memory-related brain activity in healthy older adults. *Brain Imaging Behav.* **2017**, *11*, 304–317. [[CrossRef](#)]
38. Rzezak, P.; Squarzoni, P.; Duran, F.L.; de Toledo Ferraz Alves, T.; Tamashiro-Duran, J.; Bottino, C.M.; Ribeiz, S.; Lotufo, P.A.; Menezes, P.R.; Scazufca, M.; et al. Relationship between Brain Age-Related Reduction in Gray Matter and Educational Attainment. *PLoS ONE* **2015**, *10*, e0140945. [[CrossRef](#)]
39. Harada, C.N.; Natelson Love, M.C.; Triebel, K.L. Normal cognitive aging. *Clin. Geriatr. Med.* **2013**, *29*, 737–752. [[CrossRef](#)]
40. Stern, Y. Cognitive reserve: Implications for assessment and intervention. *Folia Phoniatri. Logop. Off. Organ. Int. Assoc. Logop. Phoniatri. IALP* **2013**, *65*, 49–54. [[CrossRef](#)]
41. Schniertshauer, D.; Gebhard, D.; Bergemann, J. Age-Dependent Loss of Mitochondrial Function in Epithelial Tissue Can Be Reversed by Coenzyme Q10. *J. Aging Res.* **2018**, *2018*, 6354680. [[CrossRef](#)] [[PubMed](#)]
42. Srisanthadevan, S.; Jeyaraju, D.V.; Chung, T.E.; Prabha, S.; Xu, W.; Skrtic, M.; Jhas, B.; Hurren, R.; Gronda, M.; Wang, X.; et al. AML cells have low spare reserve capacity in their respiratory chain that renders them susceptible to oxidative metabolic stress. *Blood* **2015**, *125*, 2120–2130. [[CrossRef](#)] [[PubMed](#)]
43. Yadava, N.; Nicholls, D.G. Spare Respiratory Capacity Rather Than Oxidative Stress Regulates Glutamate Excitotoxicity after Partial Respiratory Inhibition of Mitochondrial Complex I with Rotenone. *J. Neurosci.* **2007**, *27*, 7310–7317. [[CrossRef](#)] [[PubMed](#)]
44. Mortiboys, H.; Johansen, K.K.; Aasly, J.O.; Bandmann, O. Mitochondrial impairment in patients with Parkinson disease with the G2019S mutation in LRRK2. *Neurology* **2010**, *75*, 2017–2020. [[CrossRef](#)] [[PubMed](#)]
45. Tan, W.; Pasinelli, P.; Trotti, D. Role of mitochondria in mutant SOD1 linked amyotrophic lateral sclerosis. *Biochim. Biophys. Acta* **2014**, *1842*, 1295–1301. [[CrossRef](#)]
46. Carling, P.J.; Mortiboys, H.; Green, C.; Mihaylov, S.; Sandor, C.; Schwartzenruber, A.; Taylor, R.; Wei, W.; Hastings, C.; Wong, S.; et al. Deep phenotyping of peripheral tissue facilitates mechanistic disease stratification in sporadic Parkinson's disease. *Prog. Neurobiol.* **2020**, *187*, 101772. [[CrossRef](#)]
47. Milanese, C.; Payán-Gómez, C.; Galvani, M.; Molano González, N.; Tresini, M.; Nait Abdellah, S.; van Roon-Mom, W.M.; Figini, S.; Marinus, J.; van Hilten, J.J.; et al. Peripheral mitochondrial function correlates with clinical severity in idiopathic Parkinson's disease. *Mov. Disord.* **2019**, *34*, 1192–1202. [[CrossRef](#)] [[PubMed](#)]
48. Gottlieb, E.; Armour, S.M.; Harris, M.H.; Thompson, C.B. Mitochondrial membrane potential regulates matrix configuration and cytochrome c release during apoptosis. *Cell Death Differ.* **2003**, *10*, 709–717. [[CrossRef](#)]
49. Grogan, A.; Green, D.W.; Ali, N.; Crinion, J.T.; Price, C.J. Structural correlates of semantic and phonemic fluency ability in first and second languages. *Cereb. Cortex* **2009**, *19*, 2690–2698. [[CrossRef](#)]
50. Venneri, A.; Jahn-Carta, C.; De Marco, M.; Quaranta, D.; Marra, C. Diagnostic and prognostic role of semantic processing in preclinical Alzheimer's disease. *Biomark. Med.* **2018**, *12*, 637–651. [[CrossRef](#)]
51. Baldo, J.V.; Schwartz, S.; Wilkins, D.; Dronkers, N.F. Role of frontal versus temporal cortex in verbal fluency as revealed by voxel-based lesion symptom mapping. *J. Int. Neuropsychol. Soc.* **2006**, *12*, 896–900. [[CrossRef](#)]
52. Liang, W.S.; Reiman, E.M.; Valla, J.; Dunckley, T.; Beach, T.G.; Grover, A.; Niedzielko, T.L.; Schneider, L.E.; Mastroeni, D.; Caselli, R.; et al. Alzheimer's disease is associated with reduced expression of energy metabolism genes in posterior cingulate neurons. *Proc. Natl. Acad. Sci. USA* **2008**, *105*, 4441–4446. [[CrossRef](#)] [[PubMed](#)]
53. Mosconi, L. Brain glucose metabolism in the early and specific diagnosis of Alzheimer's disease. FDG-PET studies in MCI and AD. *Eur. J. Nucl. Med. Mol. Imaging* **2005**, *32*, 486–510. [[CrossRef](#)] [[PubMed](#)]
54. Ramanoël, S.; Hoyau, E.; Kauffmann, L.; Renard, F.; Pichat, C.; Boudiaf, N.; Krainik, A.; Jaillard, A.; Baciù, M. Gray Matter Volume and Cognitive Performance During Normal Aging. A Voxel-Based Morphometry Study. *Front. Aging Neurosci.* **2018**, *10*, 235. [[CrossRef](#)] [[PubMed](#)]

55. Maynard, S.; Hejl, A.M.; Dinh, T.S.T.; Keijzers, G.; Hansen, Å.M.; Desler, C.; Moreno-Villanueva, M.; Bürkle, A.; Rasmussen, L.J.; Waldemar, G.; et al. Defective mitochondrial respiration, altered dNTP pools and reduced AP endonuclease 1 activity in peripheral blood mononuclear cells of Alzheimer's disease patients. *Aging* **2015**, *7*, 793. [[CrossRef](#)]
56. Fisar, Z.; Hroudová, J.; Hansíková, H.; Lelková, P.; Wenchich, L.; Jiráček, R.; Zeman, J.; Martásek, P.; Raboch, J. Mitochondrial Respiration in the Platelets of Patients with Alzheimer's Disease. *Curr. Alzheimer Res.* **2016**, *13*, 930–941. [[CrossRef](#)]
57. Martin-Maestro, P.; Gargini, R.; Garcia, E.; Perry, G.; Avila, J. Slower Dynamics and Aged Mitochondria in Sporadic Alzheimer's Disease. *Oxid. Med. Cell. Longev.* **2017**, *2017*, 9302761. [[CrossRef](#)]
58. Sonntag, K.C.; Ryu, W.I.; Amirault, K.M.; Healy, R.A.; Siegel, A.J.; McPhie, D.L.; Forester, B.; Cohen, B.M. Late-onset Alzheimer's disease is associated with inherent changes in bioenergetics profiles. *Sci. Rep.* **2017**, *7*, 14038. [[CrossRef](#)]
59. Takahashi, K.; Yamanaka, S. Induction of pluripotent stem cells from mouse embryonic and adult fibroblast cultures by defined factors. *Cell* **2006**, *126*, 663–676. [[CrossRef](#)]
60. Mertens, J.; Paquola, A.C.; Ku, M.; Hatch, E.; Böhnke, L.; Ladjevardi, S.; McGrath, S.; Campbell, B.; Lee, H.; Herdy, J.R.; et al. Directly Reprogrammed Human Neurons Retain Aging-Associated Transcriptomic Signatures and Reveal Age-Related Nucleocytoplasmic Defects. *Cell Stem Cell* **2015**, *17*, 705–718. [[CrossRef](#)]
61. Wakefield, S.J.; McGeown, W.J.; Shanks, M.F.; Venneri, A. Differentiating normal from pathological brain ageing using standard neuropsychological tests. *Curr. Alzheimer Res.* **2014**, *11*, 765–772. [[CrossRef](#)]
62. De Marco, M.; Duzzi, D.; Meneghello, F.; Venneri, A. Cognitive Efficiency in Alzheimer's Disease is Associated with Increased Occipital Connectivity. *J. Alzheimers Dis.* **2017**, *57*, 541–556. [[CrossRef](#)] [[PubMed](#)]
63. Cardoso, M.J.; Leung, K.; Modat, M.; Keihaninejad, S.; Cash, D.; Barnes, J.; Fox, N.C.; Ourselin, S. STEPS: Similarity and Truth Estimation for Propagated Segmentations and its application to hippocampal segmentation and brain parcellation. *Med. Image Anal.* **2013**, *17*, 671–684. [[CrossRef](#)] [[PubMed](#)]
64. Vijayakumar, A.; Vijayakumar, A. Comparison of hippocampal volume in dementia subtypes. *ISRN Radiol.* **2013**, *2013*, 174524. [[CrossRef](#)] [[PubMed](#)]
65. Mortiboys, H.; Thomas, K.J.; Koopman, W.J.; Klaffke, S.; Abou-Sleiman, P.; Olpin, S.; Wood, N.W.; Willems, P.H.; Smeitink, J.A.; Cookson, M.R. Mitochondrial function and morphology are impaired in parkin-mutant fibroblasts. *Ann. Neurol.* **2008**, *64*, 555–565. [[CrossRef](#)] [[PubMed](#)]
66. Agilent Technologies, Agilent Seahorse XF Glycolysis Stress Test Kit. Available online: https://www.agilent.com/cs/library/usermanuals/public/XF_Glycolysis_Stress_Test_Kit_User_Guide.pdf (accessed on 29 March 2020).



© 2020 by the authors. Licensee MDPI, Basel, Switzerland. This article is an open access article distributed under the terms and conditions of the Creative Commons Attribution (CC BY) license (<http://creativecommons.org/licenses/by/4.0/>).

4.3 Additional results

Table 4.1. Highlights the fibroblast cell lines used in the additional experiments in this chapter

Fibroblast Line	Cohort	Apoε genotype	Age	Sex	Used in Chapter Paper
Control 1	Sheffield	3/3	53	Male	Yes
Control 2	Sheffield	3/4	54	Male	Yes
Control 3	Sheffield	2/3	61	Female	Yes
Control 4	Sheffield	3/3	66	Male	Yes
Control 5	Sheffield	3/4	100	Female	Yes
Control 6	Sheffield	3/4	54	Female	Yes
Control 7	Sheffield	2/3	56	Male	Yes
Control 8	Sheffield	3/3	73	Female	Yes
Control 9	Sheffield	2/3	75	Male	Yes
Control 10	Sheffield	3/3	75	Female	Yes
Sporadic 1	Sheffield	2/3	53	Male	Yes
Sporadic 2	Sheffield	3/3	60	Male	Yes
Sporadic 3	Sheffield	3/3	57	Male	Yes
Sporadic 4	Sheffield	4/4	63	Male	Yes
Sporadic 5	Sheffield	2/3	59	Female	Yes
Sporadic 6	Sheffield	Unknown	63	Female	Yes
Sporadic 7	Sheffield	4/4	60	Male	Yes
Sporadic 8	Sheffield	3/3	60	Male	Yes
Sporadic 9	Sheffield	3/4	79	Female	Yes
Sporadic 10	Sheffield	3/3	61	Female	Yes

Table 4.1| Fibroblast line demographics: Data for Apoε genotype, age, sex and whether the line was used in the chapter paper is listed.

4.3.1 No significant difference was seen in glycolytic parameters based on fibroblast ApoE genotype

No significant difference was seen in the rate of glycolysis and the glycolytic capacity of sporadic AD fibroblasts (Figures 4.1A&C). A trend towards a reduced rate of glycolysis was seen in the sporadic AD fibroblasts. When sporadic AD fibroblasts were divided based on ApoE genotype no significant change was seen in either glycolysis rate or glycolytic capacity when comparing the genotypes (Figure 4.1 B&D). Glycolytic capacity in sporadic AD fibroblasts with an ApoE ϵ 2/3 genotype had a trend towards a glycolytic capacity greater than that of the control cohort, but this was not statistically significant. Glycolytic rate in ApoE sporadic fibroblasts with an ϵ 4 allele had a trend towards a higher glycolysis rate, but this was not significant.

Glycolytic reserve was significantly reduced in sporadic AD fibroblasts (Figure 4.1E), but no significant difference in reduction in glycolytic reserve was seen between ApoE genotypes (Figure 4.1F). A trend for a higher glycolytic reserve was seen in sporadic AD fibroblasts with an ApoE ϵ 2/3 genotype when compared to controls, with all other sporadic AD ApoE genotypes trending towards a lower glycolytic reserve when compared to controls.

4.3.2 Sporadic AD fibroblasts use OxPHOS more than glycolysis in a glucose starved state

To assess the ratio by which fibroblasts use OxPHOS and glycolysis respectively, the OCAR/ECAR ratio was measured in a starved condition (media without glucose), and in a normal media condition. In the starved condition sporadic AD fibroblasts had a higher OCAR/ECAR ratio than controls, suggesting that glycolysis contributes a lower percentage of cellular metabolism in sporadic AD fibroblasts than controls ($p=0.035$) (Figure 4.1G). When glucose was added to the fibroblast media this OCAR/ECAR ratio decreased significantly in both sporadic and control fibroblasts ($p<0.0001$), and no difference was seen in the OCAR/ECAR rates between control and sporadic AD groups.

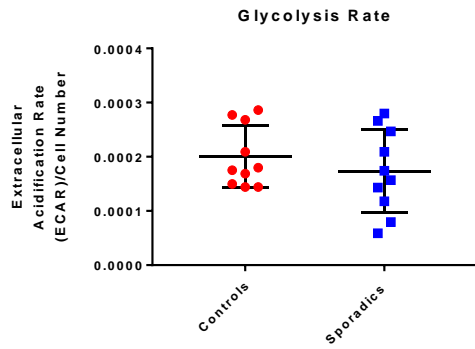
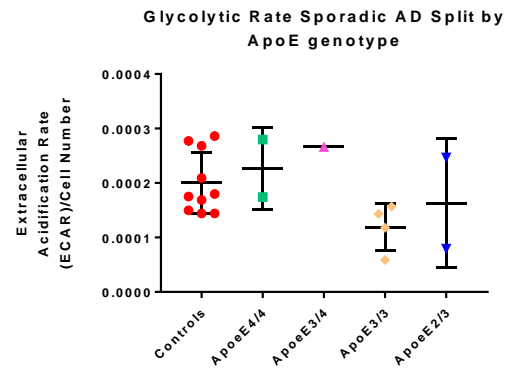
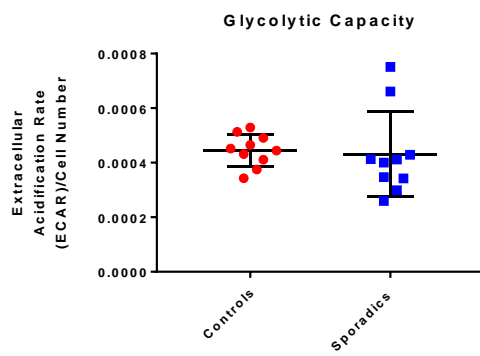
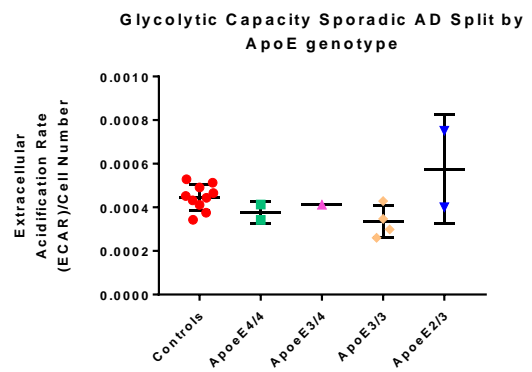
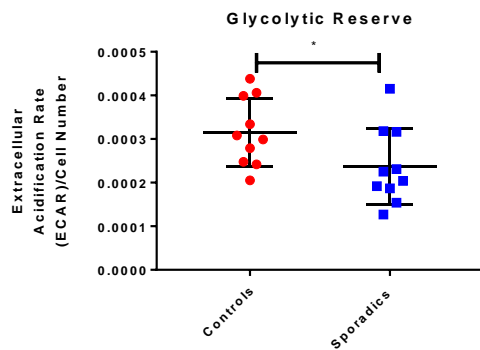
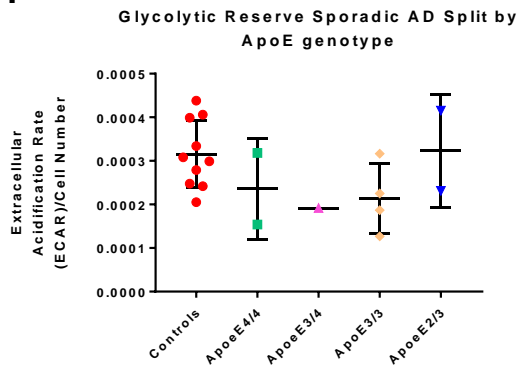
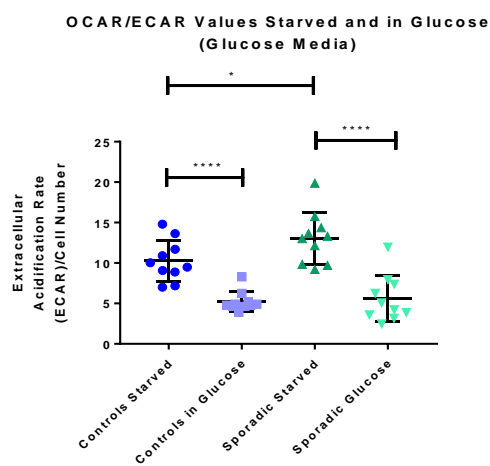
A**B****C****D****E****F****G**

Figure 4.2| Fibroblast glycolytic function split based on ApoE genotype and OCAR/ECAR ratios No significant difference was seen between ApoE and glycolytic parameters (Figures 4.1 A-F). OCAR/ECAR ratios were significantly higher in sporadic AD fibroblasts (Figure 4.1G) In figure 4G (glucose media) in the title refers to the media type the fibroblasts were originally grown in. *= $p < 0.05$, ****= $p < 0.0001$. T-tests were performed for statistical comparisons. Red dots represent control fibroblasts (n=10), blue dots represent all sporadic AD fibroblasts (n=10). Green dots represent sporadic AD fibroblasts with an ApoE $\epsilon 4/4$ genotype(n=2), pink dots represent sporadic AD fibroblasts with a $4/3$ genotype (n=1), orange dots sporadic AD fibroblasts with a ApoE $\epsilon 3/3$ genotype (n=3) and blue dots represent sporadic AD fibroblasts with a ApoE $\epsilon 2/3$ genotype (n=2).

As previously done in chapter 3, when describing the ApoE results for the mitochondrial morphology data, prior to assessing differences between control and sporadic AD fibroblast glycolytic parameters control fibroblasts were assessed using an ordinary ANOVA to ensure no significant differences were seen between control groups with different ApoE genotypes. No significant difference based on control ApoE genotype was seen in the 3 glycolytic parameters measured. Figure 4.2 displays the fibroblast control cohort data split based on ApoE genotype.

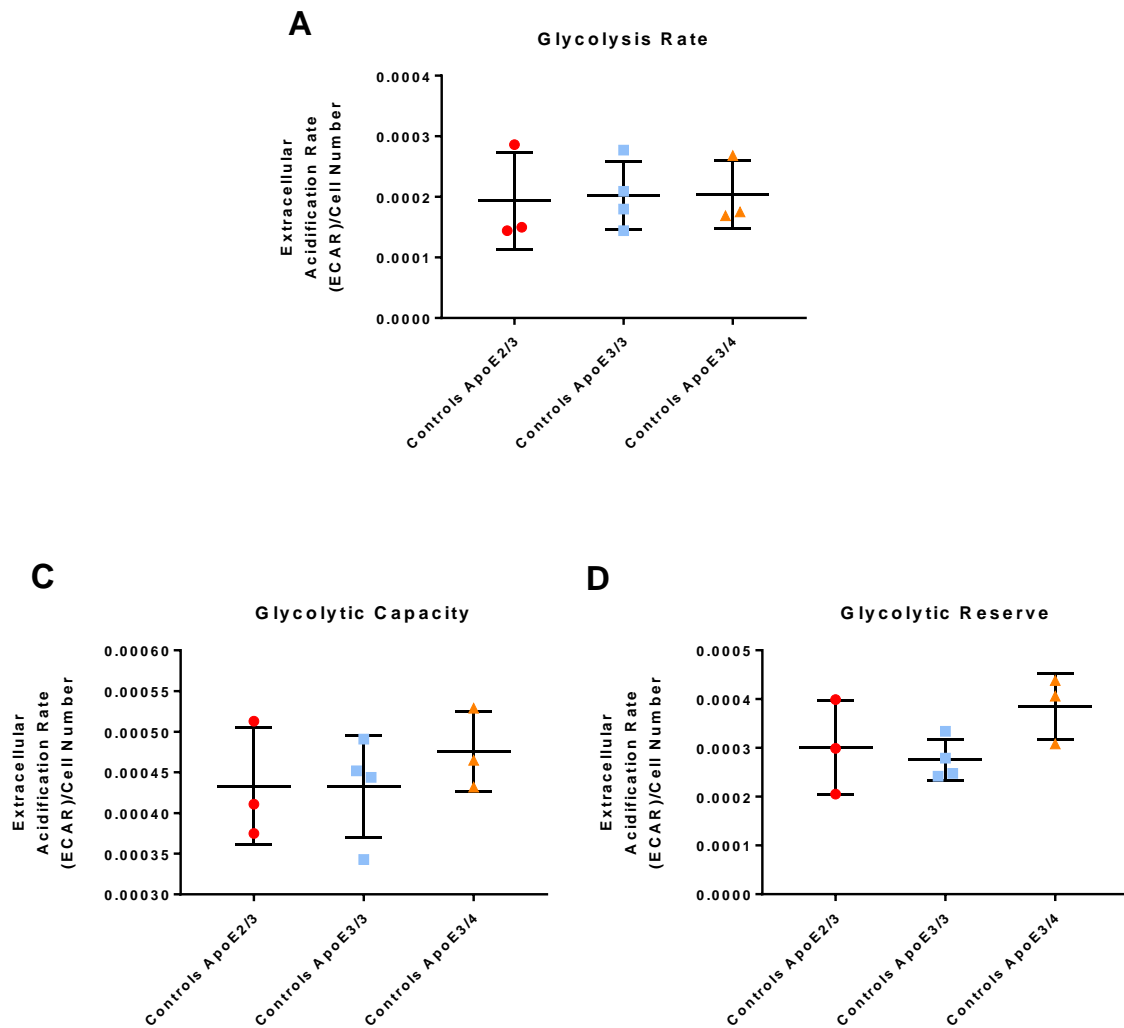


Figure 4.3| Glycolytic parameters for sporadic fibroblast controls split based on ApoE genotype No difference was seen between control fibroblast ApoE genotype groups for the 3 glycolytic parameters assessed (Figures 4.2A-C). In each graph ApoE ϵ 2/3 control fibroblasts are represented by red dots (n=3), ApoE ϵ 3/3 controls represented by blue dots, (n=4) and ApoE ϵ 3/4 controls represented by orange dots (n=3). A one-way ANOVA was performed to assess statistical significance for each morphological parameter.

4.3.3 Extracellular Lactate levels are not different in sporadic AD fibroblasts based on ApoE genotype

Extracellular lactate levels, as discussed in the paper were significantly lower on a group level in AD when compared to controls (Figure 4.3A). When sporadic fibroblasts were separated based on ApoE genotype, no significant difference between sporadic AD genotypes was seen with regard to extracellular lactate levels (Figure 4.3B). No significant differences were seen in control group extracellular lactate levels when different ApoE genotypes were compared. When sporadic fibroblast extracellular lactate levels were compared to each other with respect to ApoE genotype, no significant difference was seen between the groups.

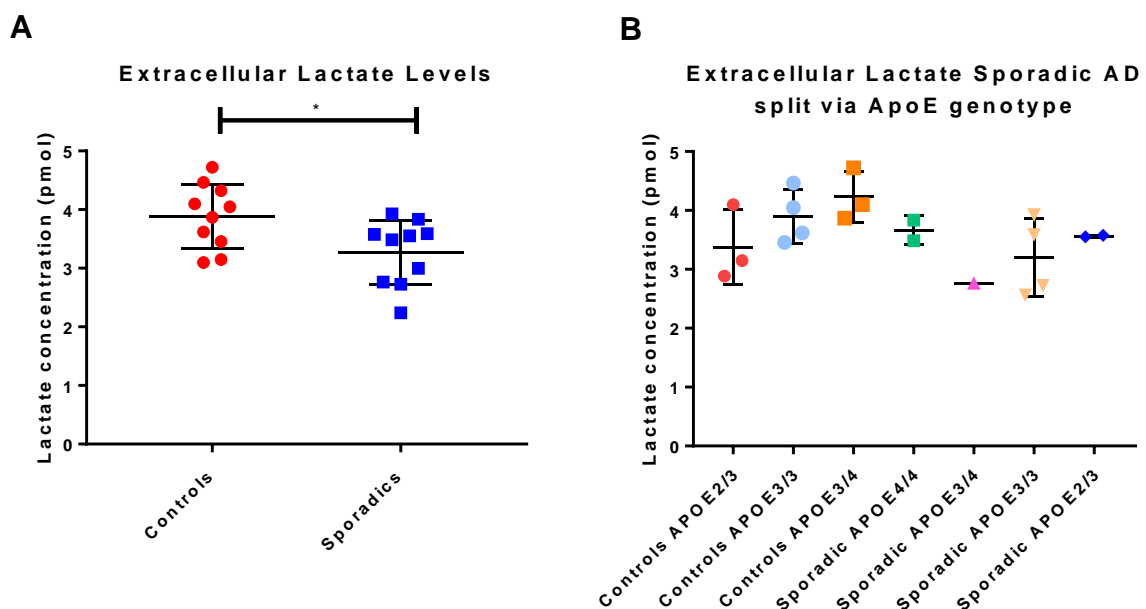


Figure 4.4| Fibroblast extracellular lactate split on ApoE genotype Extracellular lactate levels were significantly reduced in sporadic fibroblasts when compared to controls (Figure 4.3B) No significant difference was seen between ApoE genotypes in controls or sporadic groups and extracellular lactate levels (Figure 4.3B). *= $p < 0.05$. T-tests were performed for statistical comparisons. Red dots represent all control fibroblasts ($n=10$), blue dots represent all sporadic AD fibroblasts ($n=10$). Red dots ($n=3$), ApoE $\epsilon 3/3$ controls represented by blue dots, ($n=4$) and ApoE $\epsilon 3/4$ controls represented by orange dots ($n=3$). Green dots represent sporadic AD fibroblasts with an ApoE $\epsilon 4/4$ genotype($n=2$), pink dots represent sporadic AD fibroblasts with a $4/3$ genotype ($n=1$), orange dots sporadic AD fibroblasts with a ApoE $\epsilon 3/3$ genotype ($n=3$) and blue dots represent sporadic AD fibroblasts with a ApoE $\epsilon 2/3$ genotype ($n=2$).

4.3.4 The connectivity of the default mode network is altered in sporadic AD

As discussed in the introduction the DMN is the outcome of a group level analysis of functionally connected brain areas. To perform a correlation with MRSC and MMP readings as done with neuropsychological and neuroimaging parameters discussed in the paper chapter, a method needed to be devised to express the connectivity of the DMN in the form of a global index (rather than a map) per single participant in the study. In this study DMN was identified using blood oxygenation level dependent (BOLD) imaging.

The images were initially preprocessed one by one following a standardized procedure which included five basic sequential processing steps: slice timing, realignment, normalization, filtering and smoothing. Matlab (Mathworks Inc., UK) and Statistical Parametric Mapping 12 2 (Wellcome Centre for Human Neuroimaging, 166 London, UK) were used for this purpose, this process is the same as described in the chapter paper. An independent component analysis was then run on the entire set of preprocessed images [464] using the GIFT toolbox (<http://mialab.mrn.org/software/gift/>). This served to calculate group-level component maps, which were visualized and interpreted according to their topography. The DMN was identified based on its typical posteromedial-biparietal pattern. To obtain subject-specific regional estimates of DMN strength we focused on its computational cores namely the posterior cingulate cortex, the left and right inferior parietal lobule and the anteromedial prefrontal cortex. The Automated Atlas Labelling atlas [465] was used to draw these regions in the MNI space. Three DMN subregions were thus defined: an anterior section comprising the anteromedial prefrontal cortex bilaterally and three posterior sections, i.e., a left one (left posterior cingulate and left inferior parietal lobule), a right one (right posterior cingulate and right inferior parietal lobule) and a central one (bilateral posterior cingulate). Network strength within each subregion was quantified averaging the voxel-related DMN beta scores for all voxels within each submap. The creation of the DMN subregion maps and fMRI analysis described here was not done by the candidate but performed by Dr Matteo DeMarco, Non-Clinical Lecturer in the Neuroscience of dementia at the University of Sheffield.

Analysis of the connectivity of the separate parts of the DMN showed that connectivity between the bilateral medial prefrontal cortex was significantly higher in sporadic AD patients ($p=0.015$) compared to controls (Figure 4.4A). No significant difference was seen in the connectivity between the bilateral posterior cingulate areas (Figure 4.4B), Left inferior parietal lobule connectivity (Figure 4.4C) and right inferior parietal lobule connectivity (Figure 4.4D). The overall network connectivity of the DMN was higher in sporadic AD participants ($p=0.048$) compared to controls (Figure 4.4E).

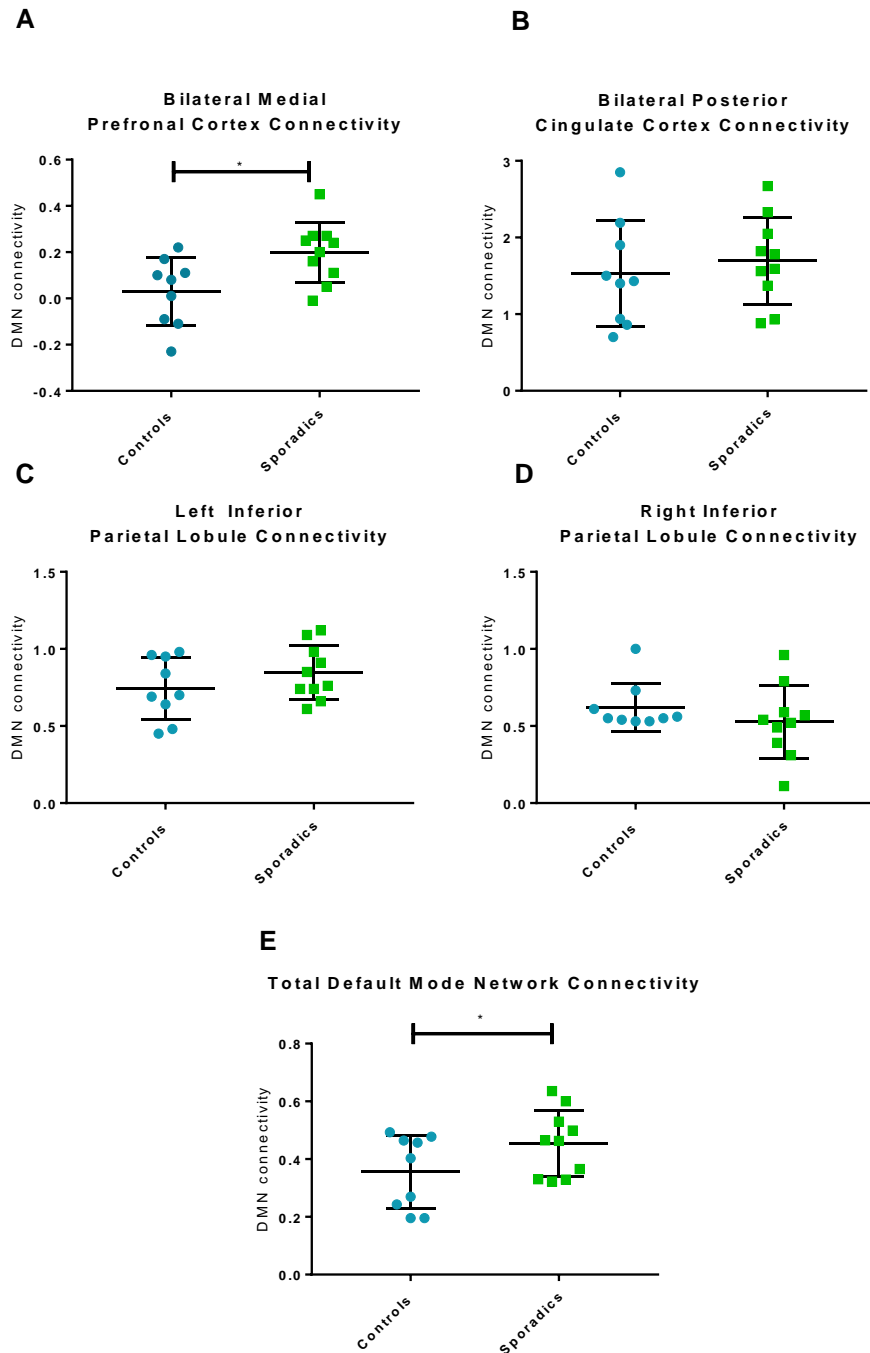


Figure 4.5/ DMN connectivity after network compartmentalization Figure 4.3A

Prefrontal cortex connectivity A significant increase in connectivity was seen in the bilateral medial prefrontal cortex Figures 4.3B Bilateral posterior cingulate cortex Figure 4.3C Left Inferior Parietal Lobule Figure 4.4D Right Inferior Parietal Lobule all showed no difference in connectivity between sporadic AD and controls. Figure 4.3E Total network connectivity An increase in connectivity was seen when sporadic AD patients were compared to controls. *= $p < 0.05$. T-tests were performed for statistical comparisons. Blue dots represent controls, green dots represent disease lines in each graph.

4.3.5 Fibroblast spare capacity correlates with Bilateral pre-frontal cortex connectivity

Correlations were performed between each of the separate DMN connectivity areas defined above and MSRC and MMP. MRSC and MMP were picked to perform correlations for the same reasons stated in the chapter paper. A significant negative correlation was seen between MSRC and the connectivity of the bilateral medial prefrontal cortex (Figure 4.5A). No significant correlations were seen between MSRC and any other element of the DMN (Figure 4.5B-E).

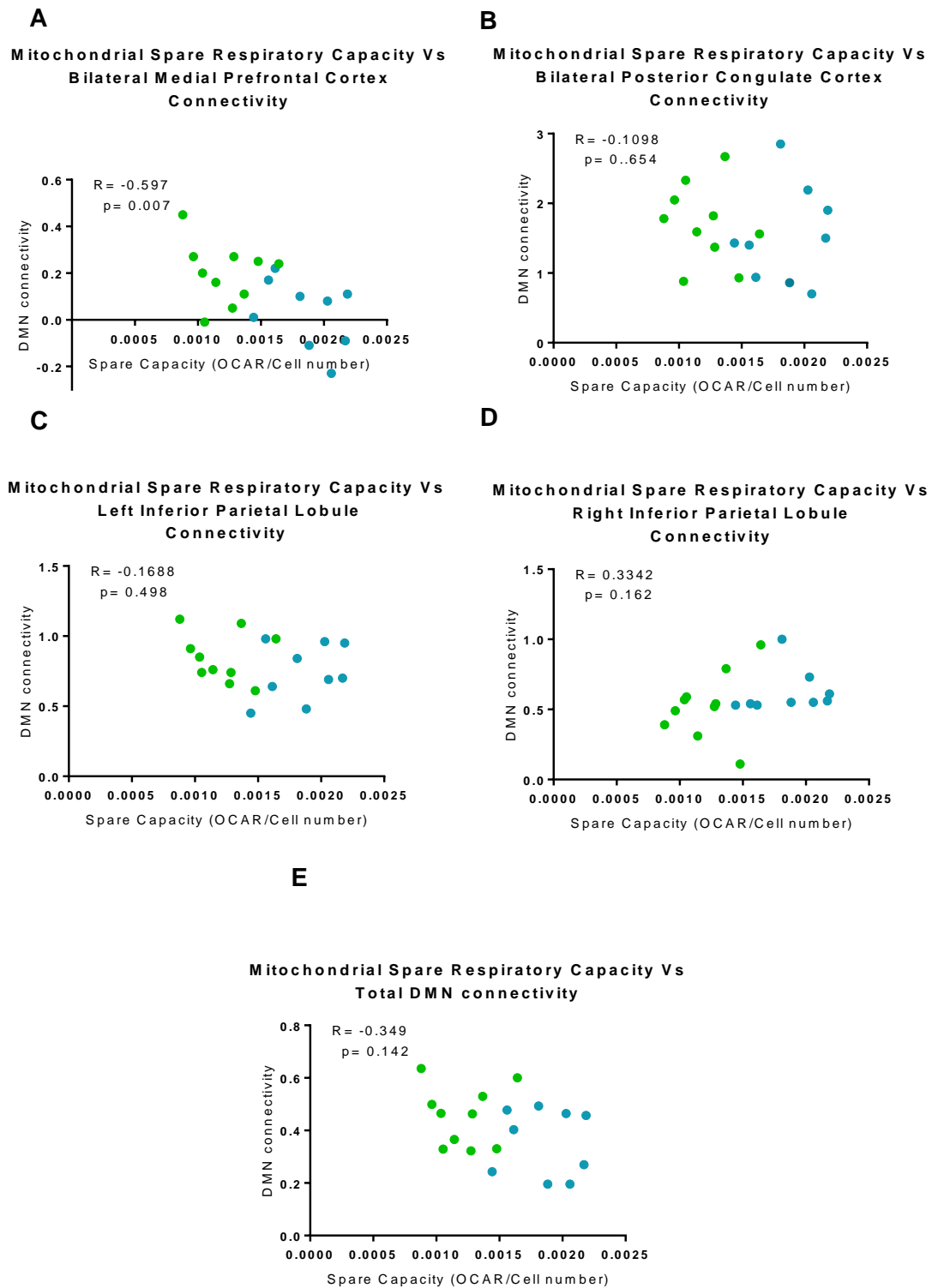


Figure 4.6| DMN connectivity correlations with MSRC A significant negative correlation was seen between MSRC and Bilateral Medial prefrontal cortex connectivity (Figure 4.4A). No other significant correlations were seen (Figures 4.4 B-E). Blue dots represent controls, green dots represent disease lines in each graph. A Pearson's correlation coefficient was used in each panel figure.

4.3.6 Fibroblast MMP correlates with Bilateral Posterior Cortex Connectivity

For the separate parts of the DMN connectivity maps no significant correlation was seen between MMP and bilateral medial prefrontal cortex (Figure 4.6A), bilateral posterior cingulate cortex (Figure 4.6B), and left posterior DMN connectivity (Figure 4.6C). A significant positive correlation was seen between right posterior DMN connectivity and MMP (figure 4.6D). No significant correlation was seen between whole DMN connectivity and MMP (Figure 4.6E).

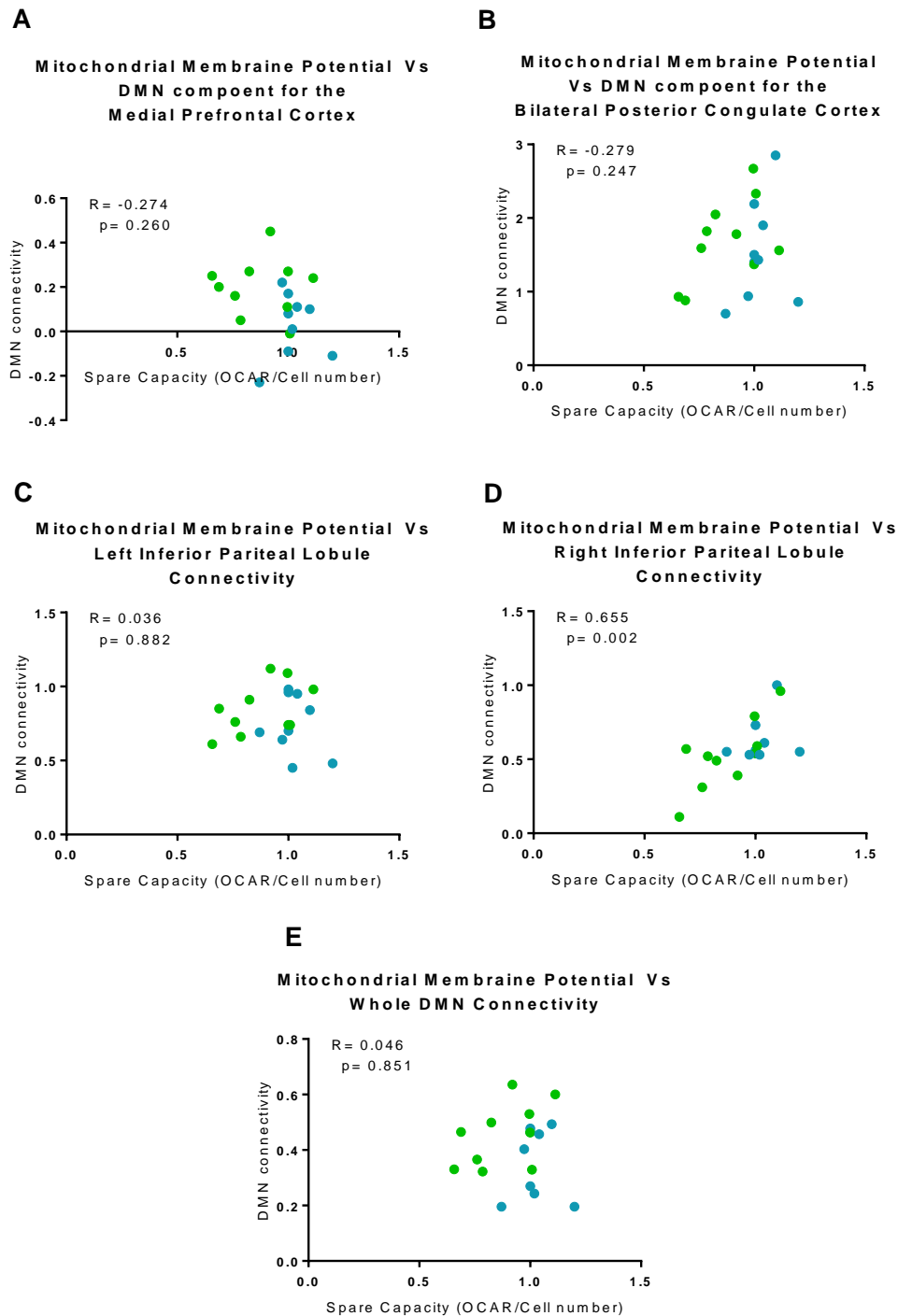


Figure 4.7/ DMN connectivity correlations with MMP No significant correlations were seen with MMP and Medial prefrontal cortex connectivity, Bilateral posterior cingulate cortex connectivity or left inferior parietal lobule connectivity (Figures 4.5 A-C). A significant positive correlation was seen between MMP and the right inferior parietal lobule (Figure 4.5D). No significant correlation was seen between MMP and whole DMN connectivity (Figure 4.5E). Blue dots represent controls, green dots represent disease lines in each graph. A Pearson's correlation coefficient was used in each panel figure.

4.4 Discussion

In this chapter it has been identified that fibroblasts from sporadic AD patients have a reduction in their glycolytic reserve when compared to controls. Sporadic AD fibroblasts also have a reduction in extracellular lactate compared to controls. Both these measures suggest that glycolysis is impaired in fibroblasts of patients with sporadic AD. These markers were not assessed for correlations with neuroimaging and neuropsychological markers of AD because they did not meet the significance threshold of $p < 0.01$ that was set as the level of significance for correlations to safeguard for false positive results, given the multiple models of correlation assessed in this study. The assessment of glycolytic function performed in the glycolysis stress test used in the study depends on stressing the cell line under investigation by either starvation or the addition of inhibitors. As fibroblasts are not very metabolically active when compared to other cell types such as astrocytes and neurons, the experimental paradigm used in this study may have not comprised fibroblast glycolysis enough to show the full extent of the glycolytic changes seen in AD. Future experiments would benefit from increased inhibitor concentrations or prolonged glucose starvation regimes.

The chapter paper also highlights how MSRC and MMP both correlate with neuropsychological changes seen in AD, and the correlation between MSRC and delayed episodic recall remains even after controlling for age, level of education and cognitive brain reserve. This is the first time that MSRC has been correlated with neuropsychological scores and found to correlate with a functional marker of the disease. In the chapter paper due to sample size sporadic AD and control groups were grouped together. Further work investigating correlations between mitochondrial functional parameters and neuropsychology test changes in AD would benefit from having a larger cohort of solely AD patients.

4.4.1 Fibroblasts from sporadic AD patients have reductions in glycolytic capacity and extracellular lactate independent of Apo ϵ genotype.

In the extra results section, it is highlighted that both extracellular lactate levels and glycolytic function, as assessed via the Seahorse glycolysis stress test, do not show a significant difference between sporadic AD fibroblast lines when they are separated based on ApoE genotype. It is again worth highlighting that the separate ApoE groups have a very small sample size. As with investigating the relationship between ApoE and mitochondrial function, as done in chapter 3, these results should be interpreted with caution.

Previously it has been identified that glucose metabolism within the brain is altered by the presence of the different ApoE genotypes, with the ApoE $\epsilon 4/4$ associated with reduced Hexokinase (HK) activity and decreased GLUT4 expression [425, 466]. It is interesting that our results did not show a

difference in glycolysis based on ApoE genotype. Sample size and fibroblast metabolic activity may account for this apparent discrepancy in brain metabolism findings seen between fibroblast glycolytic function and the existing literature. Of note both glycolytic capacity and glycolytic reserve show a trend towards a higher than control level in the ApoE ϵ 2/3 fibroblasts. This would be consistent with the results on how ApoE genotype effects glucose metabolism in the brain [425]. Further work could focus on looking at the expression of the GLUT4 receptor and HK activity in fibroblasts to see if ApoE genotype affects their expression.

An alternative explanation for the group level reduction in extracellular lactate and glycolytic reserve seen in this study could be that an ApoE genotype independent mechanism exists that is contributing to altered glycolysis in sporadic AD fibroblasts. Altered glycolysis in sporadic AD fibroblasts has been reported previously but thought secondary to dysfunction of the ETC [207]. Sonntag et al (2017) [207] report an increase in glycolytic capacity in AD fibroblasts but do not measure glycolytic reserve. These findings are opposite to what is described in this chapter. The Sonntag study does not split sporadic AD fibroblasts based on ApoE genotype, making comparisons with the work presented in this chapter and other papers more difficult. The study does report an effect of age on the rate of glycolysis in fibroblasts, which is seen to increase in both AD and control lines as they age, which maybe an example of the Warburg effect. The mean age of the AD fibroblasts (70.1 years) used in Sonntag et al 2017 is approximately ten years older than the AD fibroblast cell lines used in this chapter (61.5 years). Experimental paradigms were different between Sonntag et al and this chapter, which may also explain the difference in results. Alternatively the divergence in results on glycolytic performance between those presented in this chapter and those presented by Sonntag et al (2017) [207] may reflect the heterogeneous pathology that can cause sporadic AD, and are an example of the need for large scale studies on fibroblast metabolism with appropriate sample size that can give adequate statistical power. Future work should also focus on identifying the mechanism for the change in glycolysis rates identified in these studies, and if this is affected by ApoE status.

4.4.2 Connectivity of the DMN is altered in sporadic AD

In this new method proposed in this chapter to investigate the DMN, an increased connectivity of the DMN as a whole was seen in AD as was an increased connectivity in the bilateral prefrontal cortex areas. Increased connectivity in the DMN can be a sign of disease, as stated within the chapter introduction [451, 457]. This is the first study to offer this particular method for analysis of the DMN, so is difficult to compare with other techniques. A previous study has investigated whether age and ApoE genotype affect the connectivity within the DMN, by breaking the DMN down into separate nodes [467]. In this study the authors showed a decrease in connectivity when viewing

the whole DMN in older participants with an ApoE $\epsilon 4/4$ genotype, with lower scores on neurocognitive testing. In the results of the present chapter, an increased connectivity is seen, which is the opposite result to that in the published paper. The subjects in the published study did not have a diagnosis of AD, but share neurocognitive deficits. Experimental structural differences may explain the difference between the chapter results and this published study with change in connectivity likely to be very dependent on the study sample. A joint conclusion that can be made from both studies is that abnormalities in cognitive function modulate brain connectivity of the DMN in an attempt, of the affected system, to support performance. This has been previously suggested by the study of cognitive efficiency in early sporadic AD patients by De Marco et al (2017) [468]. Further work is needed to investigate if this method of analysing DMN has any clinical significance.

4.4.3 Fibroblast spare capacity and MMP correlates with elements of DMN connectivity

MSRC and MMP each correlated with levels of connectivity in separate regions of the DMN. MSRC correlated negatively with the bilateral medial prefrontal cortex. This particular area of the DMN showed an increased connectivity in the AD group compared to the controls. It could be hypothesized that the increased connectivity seen in this particular region of the DMN in sporadic AD is a result of the reduced mitochondrial capacity, evidenced by the low MSRC. If the reduced mitochondrial capacity seen in fibroblasts is also seen in the cells of this particular brain region, upregulation of regional connectivity levels may be needed to maintain function in this network.

MMP correlated positively with the connectivity of the right inferior parietal lobule. Potentially MMP level is what determines the integrity of the network connections. It could be postulated that if the level of MMP in the neurons of a particular brain region starts to drop this leads to reduced connections between this region and other brain regions, as the metabolic change that comes with a drop in MMP cannot meet local network metabolic demands.

It must be stated that MSRC and MMP correlated significantly with the connectivity of only one area of the DMN, and there were no significant correlations detected with other DMN regions. This could suggest that the statistically significant correlations might be artefactual, but they could also reflect metabolic diversity within different brain regions. Several studies have shown that mitochondrial ETC gene and protein expression is not homogenous across the brain [168-170, 174], the same can also be said for glycolysis enzyme activity [277, 278]. The correlations between DMN connectivity and mitochondrial function seen in this chapter may reflect how changes in brain cell metabolism in AD lead to the changes in DMN connectivity. It would be interesting to perform correlations in a larger group of participants without AD to investigate if the connectivity changes are secondary to the AD process or are directly linked to metabolic function.

4.4.4 Chapter Limitations

The neuropsychological MRSC and MMP correlations described in this chapter are interesting but performing the same correlations in cells from the central nervous system would advance the understanding of how mitochondrial function may impact cognitive function. That being said the accessibility of fibroblasts allows for larger cohorts of patients to be studied, which would be an appropriate model if the correlations seen in this study are retained when central nervous system tissue is examined. The metabolic correlation results would benefit from comparison with a familial AD group, as this may also help to understand the relationship the correlations highlighted in this chapter have with amyloid, although this was not possible in this study. The correlations described in this chapter should be thought of as a proof of principle study rather than a fully explained cellular metabolic reasoning behind neuropsychological changes seen in AD. The sample used for the correlation element of this paper included both sporadic AD patients and controls. The correlations would be further improved if examined in a cohort of only sporadic AD patients. This was not done in this thesis as the sample size was thought too small to make reasonable conclusions. It should also be considered that the correlations may only be present because we have identified two variables that are altered in AD, as opposed to the notion that cellular metabolism alterations lead to neuropsychological change. Repeating these experiments in a much larger sample, and possibly in mouse models of AD in which metabolic abnormalities have been corrected genetically would help strengthen the argument for a metabolic basis to neuropsychological change in AD.

Performance on the neuropsychological tests used in this chapter is affected early in AD, and the chapter results suggest that there are potential correlations with mitochondrial function. Performing a wider battery of neuropsychological tests might be helpful in determining if the identified metabolic abnormalities correlate with different neuropsychological tests in different dementia subtypes.

Although these correlations between neuropsychological tests and metabolic markers are interesting, a causal link cannot be determined using this experimental system. Further work using animal models with deficits in MSRC or glycolytic reserve that can be corrected could be neuropsychological assessed. If deficits in neuropsychological performance can be corrected by correcting metabolic deficits this may show a causal link between metabolism change and neuropsychology performance.

4.5 Chapter Conclusions

1. Fibroblasts from patients with sporadic AD have a reduction in glycolytic reserve when compared to controls

2. Sporadic AD fibroblasts have a reduction in extracellular lactate when compared to controls.
3. Both MMP and MSRC are reduced in sporadic AD fibroblasts when compared to controls.
4. MSRC correlates with Semantic memory, Immediate recall and delayed recall. These correlations remain between MSRC and delayed recall after controlling for age, level of education, and cognitive reserve.
5. Changes in sporadic AD glycolysis in AD fibroblasts appear to be independent of ApoE genotype.
6. Reductions in sporadic AD fibroblast extracellular lactate levels appear to be independent of ApoE genotype
7. When the DMN is separated into different connectivity nodes, increased connectivity is seen in the bilateral medial prefrontal cortex connectivity and in the total DMN connectivity.
8. MSRC correlates negatively with bilateral medial prefrontal cortex connectivity, and MMP correlates positively with right inferior parietal lobule connectivity.
9. These correlations may suggest that the altered connectivity seen within the DMN is a result of changes in mitochondrial function, or that DMN connectivity may be affected by changes in cell metabolism.

Chapter 5 Astrocytes derived from human fibroblasts show deficits in both mitochondrial function and glucose metabolism in sporadic and familial Alzheimer's disease

5.1 Introduction

In this chapter the mitochondrial and glycolytic functional abnormalities identified in fibroblasts from patients with sporadic and familial AD are investigated in astrocytes derived from the same group of patients. The astrocyte was chosen for metabolic functional interrogation, due to the prominent role it has in maintaining the tripartite synapse, cerebral blood flow and neuron metabolism as discussed in the introduction [304, 307].

Assessment of astrocyte metabolic function has been difficult in the past due to limitations of model systems. PM sample assessment can assess enzyme function but differentiating between different cell types in PM specimens can be difficult [469, 470]. Animal models can offer astrocytes to investigate, but as highlighted previously, AD patients appear to have inherent metabolic abnormalities, which are difficult to study without access to human cells. Mouse astrocytes have been shown to have very different gene expression profiles to human astrocytes, which will affect how metabolic changes seen in this type of model system are interpreted [471]. iPSC technology does offer human astrocytes for study, however to develop truly aged astrocytes for investigation in neurodegenerative disease requires long differentiation protocols, which can be costly [388].

In this chapter astrocytes have been differentiated using a direct reprogramming method that allows for the aged phenotype of the donor cell, in this case a fibroblast, to be expressed in the differentiated astrocyte. After identifying metabolic deficits in the differentiated astrocytes, they were treated with compounds previously identified to boost cellular ATP levels. In this chapter introduction iNPC generation is again briefly summarized, and reasoning behind drug compound selection is discussed.

5.1.2 Induced neuronal progenitor cell (iNPC) reprogramming

The iNPC direct reprogramming method used in this study produces neuronal progenitors faster than iPSC methods, has a high reprogramming efficiency, and produces iNPCs that are not clonal copies of each other. The polyclonal nature of iNPCs means multiple experiments on different cell colonies derived from the initial neural progenitors are not needed. In brief, the reprogramming method includes transducing fibroblasts with viruses containing the vectors OCT3/4, Sox2, Lin28 and KLF4 for 12 hours (modified from [350]). 48 hours after transduction, the cells are treated with

neuronal precursor cell inducing factors FGF-b, and EGF. iNPCs are generated in approximately 6 weeks post transduction, with astrocyte differentiation taking 7 days after iNPCs are created (see figure 5.1A chapter 5 paper). Neurons do not need to be differentiated prior to astrocyte differentiation. This makes this particular method of cell reprogramming cheaper than most iPSC methods.

The main benefit of direct reprogramming, such as described here, is the ability for differentiated cells that maintain the aged phenotype of the donor cell. This has been previously shown by Mertens et al 2015, who report that RAN binding protein 17 (RanBP17) and laminin subunit alpha 3A (LAMA3A) are expressed in directly reprogrammed neurons, but not in iPSC derived cells [393]. These proteins, along with telomeric repeat-binding factor 2 (TERF2) have been shown to have decreased expression in several tissue types as the body ages [393, 472, 473]. As ageing plays an important role in the development of most neurodegenerative conditions, having cells that express an aged phenotype allows for a more physiological model system in which to study disease.

The direct reprogramming used in this study was developed approximately 6 years ago initially to study the astrocyte motor neuron interaction in MND [350]. Study of metabolism in astrocytes derived from patients with familial MND and sporadic MND and PD has shown deficits in astrocyte metabolic flexibility and loss of the enzyme glycogen phosphatase, an enzyme used in the breakdown of glycogen [395, 396]. The interaction between neurons and astrocytes in MND has also been investigated, highlighting changes in vesicular cargoes given to neurons via astrocytes, which may mediate astrocyte induced toxicity [400]. iNPC derived neuronal models have also identified deficits in lactate transport to neurons in MND [397], and impairment of neuronal mitophagy in familial forms of MND and PD [401, 474]. This is the first study in which this particular differentiation protocol has been used to derive astrocytes from sporadic and familial AD patients.

5.1.3 Selection of drugs assessed in chapter paper

In the chapter paper the results of 8 compounds selected as they are known to improve metabolic function are discussed with regards to their ability to improve total cellular ATP levels in AD astrocytes. All 8 compounds are drug repurposing candidates, as they are already in clinical use for other conditions. The mechanism of improving cellular ATP is not already known, but was identified during a drug repurposing screen undertaken in the candidate's supervisor's lab.

Development of a completely new therapeutic is expensive, with some estimates suggesting costs close to \$2 billion dollars [475]. Drug repurposing is more cost effective way to search for therapeutics for neurodegenerative conditions, with the potential to speed up the process of medication development [476]. Drug repurposing though does have unique challenges when

developing drugs for central nervous system use. Passage through the blood brain barrier for a systemically administered therapeutic can often be difficult, and off target systemic effects need to be considered. Repurposing of drugs though, does allow for identification of these issues relatively early in the drug development process. The drug re-purposing screen undertaken in the supervisor's lab, first in silico ranked the compounds on their ability to cross the BBB; and only the compounds that ranked highly in this metric were screened in the laboratory. This strategy allows only compounds with either high known BBB permeability or a high chance of BBB permeability to be screened and progressed along the drug discovery pipeline. If a positive effect of a particular drug is seen during drug repurposing, the mechanism of action and chemical structure of the drug can be investigated, which may lead to development of compounds with reduced off target effects, or high brain penetrance. As there are currently no disease modifying drugs available to treat AD, repurposing of old therapeutics is an important way to increase the speed at which the first of this type of therapy can be developed. The 8 drugs selected for use in this thesis were the ones shown to have the greatest effect on mitochondrial function in the initial drug repurposing screen.

5.1.4 Reasoning for additional results

In the extra results section differences in mitochondrial function and glycolysis in sporadic AD astrocytes separated based on ApoE genotype are reported. Correlations of astrocyte metabolic function with DMN connectivity, first discussed in chapter 4 in regard to fibroblast metabolic function, are also presented due to the potential importance the DMN areas of the brain have in the initiation of the pathology of AD. As displaying an aged phenotype is a key feature of this model system, qPCR results are shown for RanBP, LAMA3 and TERF2 genes for astrocytes derived from young (≤ 3 years old) and old (greater than 40 years old) donors, to highlight the maintenance of the aged phenotype in iNPC derived astrocytes.

5.1.5 Candidates paper contributions

- Reprogrammed all sporadic AD, Sporadic Controls and PSEN1 iNPC lines
- Differentiated all astrocytes for experiments
- Performed all mitochondrial morphology and ATP assays on astrocyte lines
- Performed all seahorse assays on astrocyte lines
- Performed all glucose uptake, and ETC substrate experiments
- Performed neuropsychological metabolic data correlations
- Performed all astrocyte drugging experiments
- Performed all qPCR experiments.
- Wrote paper manuscript, created all figures.

5.2 Paper in preparation for submission

This paper is currently intended to be submitted to Alzheimer's Disease and Dementia

Astrocytes derived from human fibroblasts show deficits in both mitochondrial function and glucose metabolism in sporadic and familial Alzheimer's disease

5.2.1 Abstract

INTRODUCTION; Metabolic abnormalities have been shown in imaging and postmortem studies of Alzheimer's disease (AD) patients. Understanding the contribution of different brain cell types to these abnormalities has been difficult due to model limitations. This study uses human derived neuronal progenitor cells to metabolically profile astrocytes in AD.

METHODS; Fibroblasts from controls (n=10), Sporadic AD (n=7) and familial AD patients (Presenilin 1 mutation, n=3) were reprogrammed in to neuronal progenitor cells and differentiated into astrocytes. Mitochondrial and glycolytic functional assessment was performed.

RESULTS; Deficits in total cellular ATP, Mitochondrial morphology, spare respiratory capacity, glycolytic reserve, and extracellular lactate were seen in both sporadic and familial astrocytes. Changes correlated with neuropsychological scores and could be corrected with metabolism enhancing drugs.

DISCUSSION; Astrocytes derived from both familial and sporadic AD patients have multiple metabolic deficits which may both contribute to the disease and offer a new avenue for therapeutic investigation.

Key words: Sporadic, Presenilin 1, Astrocyte, Mitochondria, Glycolysis, Mitochondrial Spare Respiratory Capacity, Glycolytic Capacity, induced Neuronal Progenitor Cells, Human, Alzheimer's

5.2.2 Highlights

- AD Astrocytes have reductions in mitochondrial spare respiratory capacity.
- AD Astrocytes have reductions in extracellular lactate and glycolytic reserve.
- These changes correlate with neuropsychological scores effected early in AD.
- Deficits in ATP can be corrected we drugs known to enhance metabolism.

5.2.3 Research In Context

- **Literature Review:** The authors performed a literature review of metabolic abnormalities in Alzheimer's disease, focusing on the role the astrocyte plays in the metabolic disruption seen in AD. PubMed, Google Scholar, and research gate were all used as sources of literature. We identified that metabolic abnormalities had been shown in PM studies in astrocytes, but functional assessment had proved difficult due to limitations with previous model systems. We decided to differentiate astrocytes from human fibroblasts of patients who had sporadic and familial AD to try and identify functional metabolic deficits.

- **Interpretation:** We have shown abnormalities in both mitochondrial function and glucose metabolism in AD astrocytes from both sporadic and familial patients. These deficits may help to explain the functional imaging changes seen in patients with AD, but also help to understand *post-mortem* study findings.
- **Future Directions:** Further work is needed to identify the mechanistic cause of the astrocyte metabolic abnormalities, and to develop therapeutics that could potentially correct them.

5.2.4 Background

Alzheimer's disease (AD) is the most common cause of dementia worldwide [1]. It is estimated that over 44 million people have the condition across the globe, with numbers of patients with the condition expected to triple by 2050 [4]. The sporadic form of AD accounts for the majority of cases of the disease, with familial disease accounting for roughly 5% of cases [81]. All familial forms of AD lead to an increase in the production and deposition of amyloid beta ($A\beta$) within the brain [82-86, 89]. As amyloid deposition within the brain is also seen in sporadic forms of AD, this led to the development of the amyloid hypothesis for the initiation of the pathogenesis of AD [12-15]. Research has focused on familial models for AD, which have allowed for a deep exploration of the role that tau and amyloid play in AD.

Amyloid and tau aggregates within the brain are clearly an important part of the pathology of AD however therapeutics designed to remove amyloid from the brain have unfortunately not led to improvements in clinical outcomes for people with AD [20-22]. Aducanumab an amyloid clearance monoclonal antibody developed by Biogen has shown some initial success in improving cognitive performance in patients with AD, but failed to meet primary end points in randomised control trials [104]. This has led to the suggestion that other pathophysiological processes maybe important in the establishment of the clinical phenotype of AD [22].

Metabolic changes are seen early within the brain of people with AD, and brain areas of high glucose metabolism have been shown to be the same areas of brain which are effected by $A\beta$ aggregates, tau accumulation, and cortical atrophy first in the disease [452, 460]. This has led to the suggestion that metabolic failure, or reductions in metabolic efficiencies of brain cells may be a key step in the development of AD [208].

We and other groups have shown that the nervous system is not the only site of both mitochondrial dysfunction and glycolytic change in AD, with fibroblasts [205, 207, 418, 477-479], platelets[184] and white blood cells [238] all showing metabolic abnormalities. We have also shown that the

parameters of mitochondrial function; mitochondrial spare respiratory capacity (MRSC) and mitochondrial membrane potential (MMP) in fibroblasts correlate with neuropsychological changes seen in AD [478]. This suggests that both central and peripheral metabolism changes have an important role in AD.

In our previous work we have shown that the capacity for both OxPHOS and glycolysis is impaired in the fibroblasts of patients with sporadic and familial AD [477, 478]. The changes we report are associated with a reduction in MMP, which may lead to ATP reduction in times of stress. If the metabolic capacity of CNS cells becomes impaired in the same way then this could lead to the development of metabolic failure of the brain in times of increased energy expenditure. Imaging studies undertaken in people with AD suggest that metabolic failure occurs early in AD, as the brain is less able to uptake glucose as the disease progresses [276, 480-483].

The two main cell types which account for the vast majority of brain metabolism are the neuron and the astrocyte. These two cell types form a metabolic relationship, which sees the astrocyte play a pivotal role in maintaining many cellular functions within the neuron [302, 304, 305, 484]. Astrocytes provide neurons with metabolic substrates such as lactate, maintain the concentration of ion gradients and neurotransmitters at neuronal synapses, and can divert blood flow to brain areas with high metabolic activity allowing increased oxygen and glucose uptake [319, 485, 486]. Astrocyte glucose metabolism has been shown to have a key role in learning and memory with astrocytic glycogen shown to be a key metabolic substrate of memory encoding [311, 312, 340]. This dependent relationship that the neuron has on the astrocyte puts specific metabolic demands on this cell type meaning that any abnormalities in the function of mitochondria, or the ability to metabolise glucose will affect both that astrocyte and neuron function.

Multiple studies have shown that pathological changes occur in astrocytes in AD. Altered insulin signalling has been identified [487], as have changes in calcium homeostasis [488, 489], and the ability of astrocytes to metabolise amyloid [490]. As astrocytes have a key role in neuronal support, memory acquisition, and the AD pathological process, a thorough understanding of their metabolic properties may highlight new AD therapeutic targets or biomarkers. Metabolic change in astrocytes has been difficult to study in human AD astrocytes until recently due the lack of living human metabolically active astrocytes available for experimentation.

Over the last 10 years induced pluripotent stem cell (iPSC) technology has revolutionized neuroscience research, as it allows the creation of multiple nervous system cell lineages from patients who have the condition under investigation [349, 491-493]. This technology reprograms terminally differentiated human cells, usually fibroblasts, into stem cells, which can then be differentiated into

many different cell types. An initial criticism of this technique when applied to neuroscience research was that neuronal lineage cells created shared gene expression profiles, and functions more similar to foetal cells than adult ones [494, 495]. Recent advances in iPSC technology have meant that direct reprogramming of terminally differentiated cells can now be performed without returning cells to a true stem cell phase [350, 393]. This reprogramming method has been shown to allow cells to maintain the aged phenotype of their parent cell. This is obviously a big advantage to studying AD, as increasing age is the greatest risk factor for developing the disease.

In this paper we use induced neuronal progenitor cell technology [397, 400, 401] to derive astrocytes from patients with sporadic and familial (Presenilin 1 mutations) AD. We investigated glycolysis and mitochondrial function, and how this correlates with neuropsychological changes seen early in AD. Finally, we treated the astrocytes with compounds known to improve cellular ATP levels and mitochondrial function to investigate if the metabolic changes seen in AD astrocytes can be targeted as a future therapeutic site.

5.2.5 Methods

Patient Details

Sporadic AD (sAD) Patients and matched controls were recruited as part of the MODEL-AD study (Yorkshire and Humber Research and Ethics Committee number: 16/YH/0155) for fibroblast biopsy. All sporadic patients and matched controls who were selected for biopsy had previously participated in the European EU-funded Framework Programme 7 Virtual Physiological Human: Dementia Research Enabled by IT (VPH-DARE@IT) initiative (<http://www.vph-dare.eu/>). A diagnosis of Alzheimer's disease was made in sAD patients based on clinical guidelines [71]. Table 5.2 shows the demographic details of the sporadic patients.

Presenilin 1 AD patient fibroblasts (fAD) and matched controls were acquired from the NIGMS Human Genetic Cell Repository at the Coriell Institute for Medical Research: (ND41001, ND34733, AGO6848, GMO2189), and a cohort from a Sheffield based MND study (155 and 161). All Presenilin 1 AD patients had a confirmed pathological mutation in the presenilin 1 gene (See Table 5.3)

Tissue Culture

Fibroblasts were cultured in a DMEM based media (Corning) incubated at 37°C in a 5% carbon dioxide atmosphere. Sodium pyruvate (1%) [Sigma Aldrich], penicillin & streptomycin (1%) [Sigma Aldrich], and Fetal Bovine Serum (10%) [Biosera] was added to the media. Cells were cultured in T75cm² (Greiner bio-one) culture flask until they reached confluency. Fibroblasts were split twice

before plating for reprogramming. Splitting was performed using 5mls of 1X Trypsin-Versene (Lonza) which was placed on the cells for 5 minutes.

Fibroblast Reprogramming

Fibroblast reprogramming into iNPCs and astrocyte differentiation has been previously described, [350]. In brief, fibroblasts were plated at a density of 250,000 cells per well. 24 hours after plating fibroblasts were transduced with adenoviral non-integrating vectors (OCT3, Sox2, KLF4, Lin28 and Nonog). 48 hours after transduction, cells were treated with neuronal progenitor cell (NPC) inducing factors (FGF-b, and EGF). Once iNPCs lines were established expression of the neuronal progenitor markers PAX-6 and Nestin was confirmed through immunohistochemistry. Induced Neuronal Progenitor Cells (iNPCs) were maintained for ~30 passages.

After iNPCs were established, to differentiate them into astrocytes, iNPCs were seeded on a 10cm dish coated with fibronectin (5 µg/ml, Millipore) in DMEM media (Lonza) containing 10% FBS (Biosera), and 0.3% N2 (Gibco) and differentiated for 7 days. After differentiation expression of several astrocyte cell markers was confirmed using immunohistochemistry (details described in section below). This included GFAP, Vimentin, CD44, ALDH1 and NDGR2. A key functional ability of astrocytes is the ability to uptake glutamate. This was confirmed in our astrocyte cell populations through performing a glutamate uptake assay (see below). We have also previously published evidence highlighting that astrocytes differentiated in this way maintain an aged cell phenotype, which is essential for studying diseases such as AD[496].

Immunohistochemistry

For immunohistochemistry astrocytes or iNPCs were plated on a black 96-well plate (Greiner bio-one) at a density of 2500 cells/well. After 24 hours cells were fixed with 4% paraformaldehyde (PFA) for 10 minutes. Cells were permeabilised in a solution of 0.1% triton, PBS and TWEEN 20 (1:1000) (PBST) for 30 minutes. Following this, cells were washed with PBST twice. Cells were then blocked in PBST and horse serum (5%) for 60 minutes. Fixed cells were incubated with primary antibodies overnight (see table 5.2). Secondary antibodies were added at a concentration of 1:1000 for 1 hour, then Hoechst dye (Life Technologies) at a concentration of 1:8000 for 10minutes. Staining was visualised using an OPERA high content imager (Perkin Elmer).

Antibody	Species	Dilution	Supplier
Vimentin	chicken	1:200	Abcam (AB5733)
Nestin	Mouse	1:200	Abcam (AB18102)
CD44	Rabbit	1:200	Abcam (AB157107)
S100 β	Rabbit	1:200	Abcam (AB868)
PAX6	Rabbit	1:1000	Abcam (AB5790)
GFAP	Rabbit	1:200	Dako (Z0334)
NDGR2	Mouse	1:200	Santacruz (sc-376202)
ALDH1L1	Rabbit	1:1000	Abcam (AB87117)
Secondary Antibodies			
Alexia 488	Rabbit	1:1000	Invitrogen
Alexia 488	Mouse	1:1000	Invitrogen
Alexia 488	Chicken	1:1000	Invitrogen
Alexia 568	Rabbit	1:1000	Invitrogen
Alexia 568	Mouse	1:1000	Invitrogen

Table 5.2| Antibodies used for Immunocytochemistry In this table details of antibodies used to characterise both iNPCs and astrocytes are displayed with supplier and dilution that they were applied to the cells.

Glutamate Uptake Assay

An Abcam colorimetric Glutamate Assay kit (ab83389) was used to measure astrocyte glutamate uptake. Assay was performed as per manufacturers guidance. In brief, astrocytes were plated on a black 96 well plate at a density of 10,000 cells/well at day 5 of differentiation. On day 7 of differentiation the astrocyte media was changed to Hank's Balanced Salt Solution (HBSS) (Gibco), without calcium or magnesium for 30 minutes. This media was then changed to HBSS containing magnesium and calcium for 3 hours which also contained 100 μ l of glutamate at a concentration of 1:1000. Samples were then collected as described by manufacturer and snap frozen in liquid nitrogen. Glutamate measurement was performed from this point onwards as per kit protocol. Percentage glutamate uptake was then calculated based on the known concentration of glutamate added to the astrocytes.

Total Cellular ATP levels & ATP Inhibitor Assay

Cellular Adenosine Triphosphate (ATP) levels were measured with the ATPlite kit (Perkin Elmer). Astrocytes were plated at a density of 5000 cells per well in a white Greiner 96 well plate on day 5 of differentiation. ATP levels were corrected for cell number using CyQuant (ThermoFisher) kit, as previously described [478], and then disease lines were normalized to controls. The same assay was performed using the inhibitors of glycolysis (2-deoxyglucose 50mM, [Sigma]) and OxPHOS (Oligomycin 1 μ M, [Sigma]) to assess the reliance on each metabolic pathway for total cellular ATP. A glycolysis and OxPHOS inhibitor assay was performed. Oligomycin (OxPHOS inhibitor) or 2-

deoxyglucose (glycolysis inhibitor), or both inhibitors were added to the cells for 30 minutes and incubated at 37°C during this time. The ATP assay was then performed as described above.

Mitochondrial Membrane Potential

Astrocytes were plated at a density of 2500 cells per well in a black griener 96-well plate at day five after the start of differentiation. On day 7 of differentiation cells were incubated with tetramethylrhodamine (TMRM) for 1 hour (concentration 80nM) and hoescht (concentration 10nM) (Sigma Aldrich). Cells were incubated at 37°C during this time. TMRM was then removed and astrocytes were maintained in MEM media whilst imaging using an InCell Analyzer 2000 high-content imager (GE Healthcare). 25 fields with an average number of 500 cells per well at an emission/excitation spectra of 543/604m was imaged. Mitochondrial morphological parameters and cell area were quantified using an INCELL developer protocol[407].

Extracellular Lactate Measurement

Extracellular lactate was measured using an L-Lactate assay kit (Abcam ab65331). At day 7 of differentiation 1µl of media was removed from a 10cm dish containing confluent astrocytes and used in the assay as per the manufacturer's instructions. Briefly, 1µl of media was added to 49µl of lactate assay buffer, to this 50µl reaction mix was then added and the samples are then incubated at room temperature for 30minutes. Lactate measurements are then made on a PHERAstar Plate reader absorbance filter at 570nm. To calculate the lactate concentration a standard curve was created (2-10nmol range of lactate concentrations), and background lactate measurements were made. Measurements were normalized to controls on each separate day of experimentation.

ATP Substrate Assay

The ATP substrate assay was used to investigate mitochondrial ATP production in the presence of complex I and II substrates. 500,000 cells are collected at day 7 of astrocyte differentiation. Methods have been previously described by Manfredi et al 2002, [409]. In brief, cells are suspended in 250µl of buffer A (KCL 150mM, Tris HCL 25mM, EDTA 2mM, BSA 0.1%, K₃PO₄ 10mM, and MgCL 0.1mM, pH 7.4). Cells were then permeabilised with histone 2ug/ml for 5 minutes. After permeabilization 5 volumes of buffer A (1250mls) was added to the cell suspension. The suspension was then centrifuged for 5 minutes at 10,000rpm. Cells were then resuspended in 150µl of Buffer A. 550µl of buffer A was added to the remaining 100µl of suspension for use in the substrate assay. The assessment of total cellular ATP at this stage must be performed with 15minutes of adding the 550µl of buffer A to samples.

A PHERAstar plate reader (BMG Labtech) in luminescence mode was used to read complex activity. A background luminescence reading is made of each well on the assay plate containing 160µl of cell suspension then one of either the complex I substrates (malate 1.25mM and galactose 1.25mM), or complex II substrates (succinate 1.25mM, rotenone 1µM added as complex I inhibitor) is added. After baseline kinetics were measured the machine was paused and 5µls of Adenosine diphosphate (ADP, 4µM) and 10µl of the ATP substrate solution, described above in the ATP assay section were added to each well. The kinetics assay is then resumed and measurements of substrate use are made for approximately the next 30 minutes. The gradient of the kinetics curve is then calculated and normalised to protein content using a Bradford assay. Disease samples are normalised to controls of the day.

Metabolic flux assay

Mitochondrial Stress Test

Astrocyte OxPHOS was assessed by measuring oxygen consumption rates (OCR) using a 24-well Agilent Seahorse XF analyzer. Astrocytes were plated at a density of 10,000 cells per well at day 5 of differentiation. At day 6 of differentiation cells were either switched to a galactose containing media or continued to be maintained in glucose. At day 7 of differentiation astrocytes were switched to XF media (Aligent) and then assessed using the previously described *Mitochondrial Stress Test Protocol* [477]. During this protocol measurements were taken at the basal point: after the addition of oligomycin (0.5µM), after the addition of carbonyl cyanide-4-(trifluoromethoxy)phenylhydrazone (FCCP) (0.5µM) and after the addition of rotenone (1µM). OCR measurements were normalized to cell count, as previously described [477]. ATP linked respiration, Mitochondrial respiration, Mitochondrial Spare Respiratory Capacity, Respiratory control ratio and ATP couple respiration are all calculated from this experiment.

Glycolysis Stress Test

Astrocyte glycolysis was measured using the glycolysis stress test protocol on a 24-well Agilent Seahorse XF analyzer. Astrocytes were plated at a density of 10,000 cell per well at day 5 of differentiation. At day 7 of differentiation as with the mitochondrial stress test astrocytes were transferred to XFmedia (Aligent) and glycolysis was assessed. The glycolysis stress test was used to assess glycolysis, this has been described previously, [478]. In brief, three measurements were taken at the basal point: after the addition of glucose (10µM), after the addition of oligomycin (1.0µM) and after the addition of 2-deoxyglucose (50µM). Basal rate of glycolysis, Glycolytic capacity, Glycolytic

reserve and non-glycolytic acidosis are all measured during the glycolysis stress test. Measurements were normalized to cell count, as previously described [477]

Glucose Uptake

Glucose uptake of astrocytes was measured using the Glucose Uptake Assay Kit (Fluorometric) (Abcam, ab136956). Astrocytes were plated at a density of 2500 cells per well in a 96 well black griener plate on day 5 of differentiation. On day 7 of differentiation the astrocytes were incubated for 40 minutes in a 100µl of Krebs-Ringer-Phosphate-Hepes (KRPH) buffer with 2% bovine serum albumen added pH 7.4. Astrocytes were then treated with 2-deoxyglucose at a concentration of 50mM for 20minutes suspended in KRPH (volume 100µl per well). Cells were then treated with 90µl of Extraction buffer (Abcam), snap frozen in liquid nitrogen, and then thawed on ice. 25µl of sample was then placed in a black 96-well plate, with the volume made up to 50µl with glucose uptake assay buffer (Abcam). The assay from this point onwards was performed according to the manufacturer's instructions. Briefly, Using the 2-deoxyglucose standard a standard curve was created with concentrations between 0µM-20µM of 2-Deoxyglucose. 50µl of each standard was plated on the black 96-well plate. 50µl of reaction mix (47µl Glucose uptake assay buffer, 2µl of enzyme mix and 1µl of PicoProbe, all supplied by Abcam) was added to each sample and standard well. Samples were then incubated for 40 minutes at 37°C. Measurements of Fluorescence at Ex/Em=535/587nm were then taken using PHERAstar plate reader (BMG Labtech).

Glutamine/Glutamate assessment

A Glutamine/Glutamate-Glo™ Assay (Promega) was used to measure intracellular concentrations of glutamine and glutamate. A 10cm dish of Astrocytes (≈ 2,000,000 cells) was immersed in Inactivation solution (2mls of HCL 0.3N and 1ml PBS) for 5 minutes on day 7 of differentiation. After this the dish was scraped and 1ml of Tris solution (2-Amino-2-(hydroxymethyl)-1,3-propanediol, 450mM at pH 8.0) was added to the cells. 200µl of this solution was then added to 200µls of PBS. 25µl of this dilution is then placed in a well of a white 96-well greiner plate. After sample preparation the assay was performed as per the protocol provided by Promega.

Drug treatment assay

Astrocytes were treated with 8 different compounds known to improve mitochondrial function. Doses of 1,10,100µM were assessed after 24 hours of treatment. Astrocytes were plated at a density of 1000 cell per well for ATP assays, and 500 cells per well MMP assays on day 5 of differentiation. Drugs were dispensed onto astrocytes using an ECHO 550 Liquid Handler (Labcyte) machine. ATP and MMP assays were performed as described above on day 7 of differentiation.

Metabolic neuropsychological correlations

Correlations between metabolic parameters and neuropsychological tests were performed as described previously [478].

Statistical Analysis

Statistical analysis for this data set is the same as detailed in [478]. In brief metabolic comparisons between AD group and control groups are compared using t-tests. A pearson correlation was performed for metabolic neuropsychological correlations. Statistics were calculated using the GraphPad v8 software and IBM SPSS statistics version 25.

5.2.6 Results

Patient Demographic Details

sAD astrocytes had a mean age of 63.14 years (4 Female) sAD controls had a mean age of 66.6 years (5 female). Table 5.3 details the Age, MMSE and length of education for both sAD and control astrocytes. For the fAD group the mean age was 48.33 years (1 female). The controls for this group had a mean age of 44.66 years (3 Male). Table 5.3 details the age, sex, and PSEN1 mutations of PSEN1 and associated control lines.

Patient Line	Age (Years)	Sex	MMSE	Length of Education (Years)	AD Treatment (at biopsy)
1	60	Male	18	9	None
2	59	Female	23	11	Galantamine
3	63	Female	26	10	Donepezil
4	60	Male	18	11	Memantine
5	60	Male	18	11	None
6	79	Female	28	15	None
7	61	Female	25	11	Donepezil
Group Mean (Standard Dev)	63.14 (7.10)		22.2 (4.27)	11 (1.86)	
Control lines					
1	54	Male	27	17	NA
2	56	Male	24	11	NA
3	61	Female	30	NA	NA
4	54	Female	29	17	NA
5	100	Female	24#	14	NA
6	75	Female	28	18	NA
7	73	Female	26	12	NA
Group Mean (Standard Dev)	66.6 (18.15)		27 (2.53)	15.4 (2.88)	

Table 5.3| Patient Demographic Information and contemporary treatment status #For control 7 some items of the MMSE could not be tested due to sensory impairment

Control Line	Age (Years)	Sex	Presenilin 1 Mutation
Sheffield 161	31	Male	NA
Sheffield 155	40	Male	NA
Coriell (GM02189)	63	Male	NA
Group Mean (Standard Dev)	44.66 (16.5)		
Familial Line	Age (Years)	Sex	Presenilin 1 Mutation
Coriell (ND41001)	47	Female	14q24.3 Intron 4, G deletion
Coriell (ND34733)	60	Male	P264L
Coriell (ND34730)	38	Male	E184D
Group Mean (Standard Dev)	48.33 (11.06)		

Table 5.4| Patient demographics for Familial AD presenilin 1 lines and associated controls

iNPC derived sporadic and familial AD astrocytes display astrocyte markers and functional properties

This is the first study to reprogram sporadic and familial AD patient fibroblasts to iNPCs and to derive astrocytes from them using the method described previously [350, 397]. Figure 5.1A highlights the major steps of the reprogramming procedure used in this study. As this is the first study to use this type of reprogramming to derive AD astrocytes, we assessed the derived cells for expression of known astrocytic/iNPC markers and functional properties. iNPCs from control, sporadic and familial AD patients all expressed the neuronal precursor markers Nestin and PAX6 (See figure 5.1B). Astrocytes were assessed for a combination of markers that have been previously shown to be expressed by astrocytes, [395, 396, 400]. These markers included CD44, GFAP, Vimentin, NDGR2, and ALD1L1 with all astrocyte lines showing expression of these markers (Figure 5.1C). Astrocyte cell area was assessed, showing that both sporadic (mean area $1848\mu\text{m}^2$ SD \pm 355.5, $p=0.0316$) and familial (mean area $1319\mu\text{m}^2$ SD \pm 36.04, $p=0.0424$) AD astrocytes had a smaller cell area than control astrocytes (Sporadic controls mean area $2953\mu\text{m}^2$ SD \pm 263.7, familial controls mean area $2206\mu\text{m}^2$ SD \pm 299.7) (Figure 5.1D).

To assess if the derived astrocytes have key functional properties seen in *in vivo* astrocytes, the ability to uptake glutamate, and the concentrations of intracellular glutamate and glutamine in the astrocyte was assessed. Glutamate uptake from the synaptic cleft is a key functional property of *in vivo* astrocytes [497], and is a key measure in showing *in vitro* astrocytes are functionally active [498, 499]. Glutamate uptake in sAD astrocytes was similar to that seen in controls (Figure 5.1E). fAD astrocyte glutamate uptake was not assessed due to limited resources. Control, sporadic and familial AD astrocytes all had similar intracellular proportions of glutamine and glutamate (Figure 5.1F). No significant differences were seen between controls and AD astrocytes with regard to intracellular glutamate and glutamine amounts.

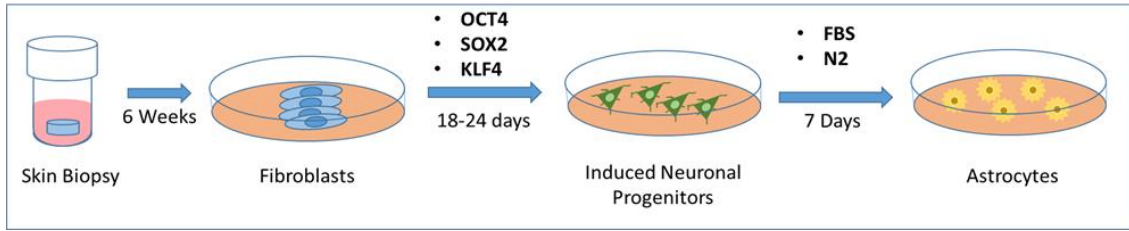
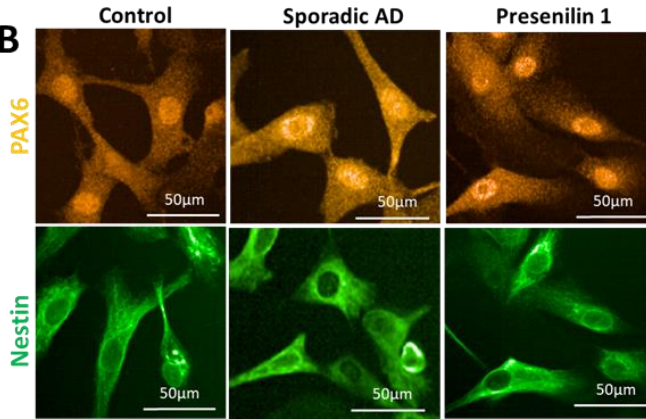
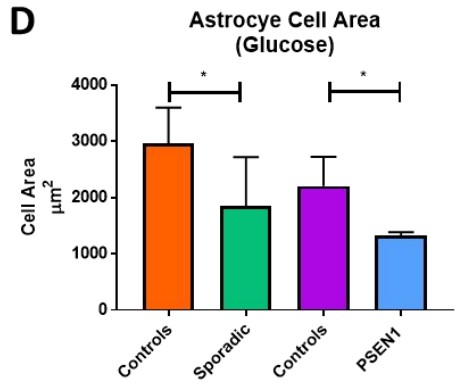
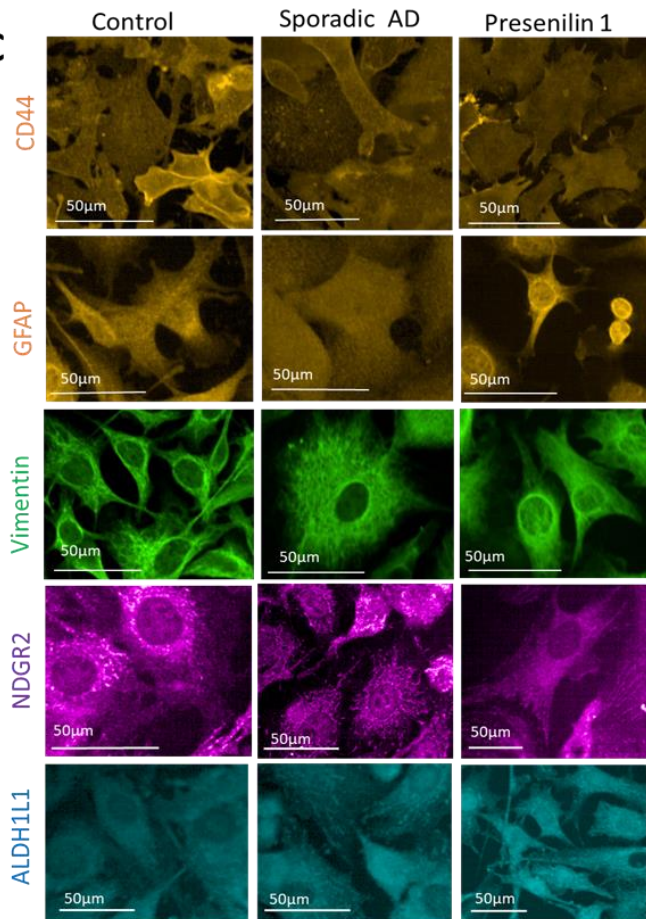
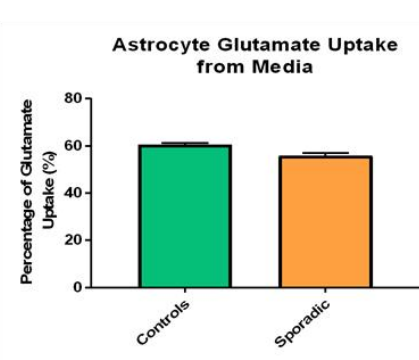
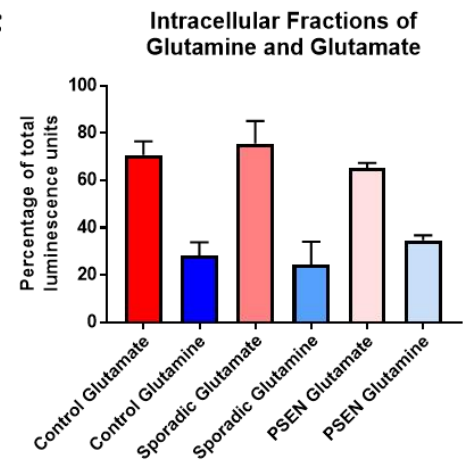
A**B****D****C****E****F**

Figure 5.1 | Astrocyte characterization *Figure 1A Astrocyte differentiation:* this panel shows the process of creating the derived astrocytes. *Figure 1B iNPC staining:* Control, sporadic and familial AD astrocytes all display the neuronal progenitor cell markers PAX-6 and Nestin. *Figure 1C astrocyte staining* Control, sporadic and familial AD astrocytes display staining for CD44 (orange), GFAP (orange), Vimentin (green), NDGR2 (purple), and ALDH1L1 (blue). *Figure 1D Astrocyte cell size* Both sporadic and familial AD astrocytes had a significantly smaller cell area than control astrocytes. *Figure 1E Glutamate uptake* Control and sporadic AD astrocytes both uptake glutamate. *Figure 1F Intracellular Glutamine and Glutamate concentrations* Controls, Sporadic and Familial AD astrocytes all contained similar levels of intracellular glutamate and glutamine $*=p<0.05$.

Astrocytes rely more on glycolysis than OxPHOS to produce ATP and have reduced total cellular ATP levels in AD.

Total cellular ATP content was assessed in both iNPCs and astrocytes. No significant difference was seen in total cellular ATP when sporadic and familial AD iNPCs were compared to controls (Figure 5.2A). A significant reduction in total cellular ATP was seen in both sporadic (18% reduction, $p=0.0323$) and familial (42% reduction, $p=0.0014$) AD astrocytes when compared to controls (Figure 5.2B).

The reliance on either glycolysis or OxPHOS for total cellular ATP was assessed in iNPC's and astrocytes. In both iNPCs and astrocytes a greater proportion of total cellular ATP was produced via glycolysis when compared to OxPHOS in all astrocyte types (Figures 5.2C&D). A reduction of 56% in control, 77% in sporadic and 50% in familial iNPC's total cellular ATP was seen when the cells were incubated with 2-deoxyglucose (glycolysis inhibitor). When cells were incubated with oligomycin (an OxPHOS inhibitor), control iNPCs showed an 8% reduction, sporadics a 27% reduction, and familial a 37% reduction in total cellular ATP was seen.

Astrocyte total cellular ATP had a mean reduction of 71.6% across all three astrocyte groups (Control 76%, Sporadic 76% and familial 63% reduction), whereas a mean reduction of 27.3% in total cellular ATP was seen when oligomycin was added (Controls 23%, Sporadic 29% and familial 30% reduction). These findings reflect the known metabolic dependency of iNPC's and astrocytes on glycolysis for ATP production and provides further characterization of this model. For astrocytes total cellular ATP was assessed in both glucose and galactose based media, with similar results in total cellular ATP and proportion of total cellular ATP dependent on glycolysis and OxPHOS seen (supplementary figure 1).

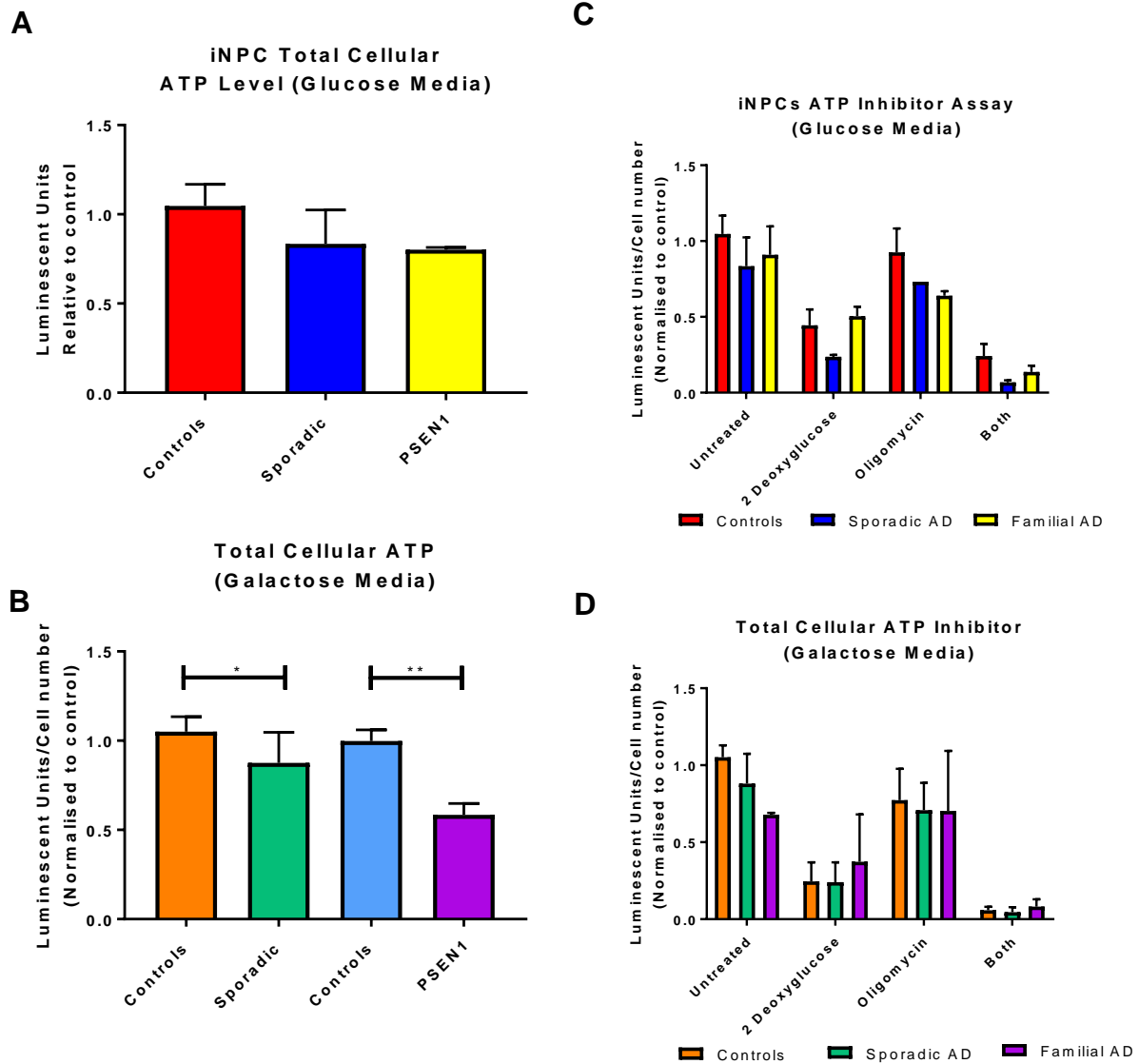


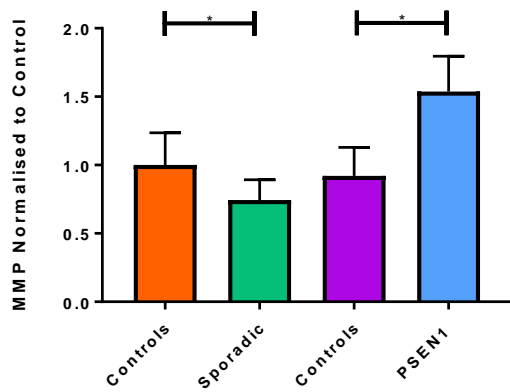
Figure 5.2 | Astrocyte and iNPC total cellular ATP *Figure 2A Inpc total cellular ATP* a trend towards a reduction in total cellular ATP was seen in both sporadic (blue bars) and familial (yellow bars) AD iNPC's when compared to controls (red bars). *Figure 2 B Astrocyte Total Cellular ATP* Both sporadic (green bars) and familial (purple bars) AD astrocytes have a significant reduction in total cellular ATP when compared to controls (orange bars). *Figure 2C iNPC ATP Inhibitor Assay* Control (Red bars), Sporadic (Blue bars) and Familial AD astrocytes (Yellow bars) all show a greater reduction in total cellular ATP when 2-deoxyglucose (glycolysis inhibitor) is added to the cells than when oligomycin (OxPHOS inhibitor) is added. Little total cellular ATP signal remains after addition of both compounds. *Figure 2D Astrocyte ATP inhibitor assay* Control (Orange bars), Sporadic (Green bars) and Familial (Purple bars) AD astrocytes show a greater reduction in total cellular ATP when 2-deoxyglucose (glycolysis inhibitor) is added to the cells than when oligomycin (OxPHOS inhibitor) is added.

AD astrocytes have an altered mitochondrial morphology and MMP.

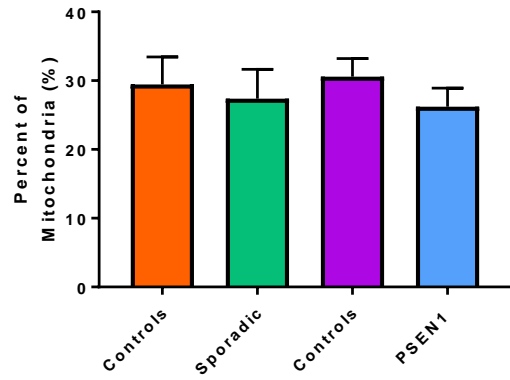
After characterising the AD astrocytes and determining ATP levels, we next assessed mitochondrial morphology and function. Sporadic AD astrocytes had a significant reduction in their MMP when compared to controls (26% reduction, $p=0.048$), whereas familial AD astrocytes had a higher MMP than controls (52% increase, $p=0.032$) (Figure 5.3A). Mitochondrial morphology was also altered in AD, with both sporadic and familial AD astrocytes showing an increased number of elongated mitochondria (Sporadic Astrocytes 4.9% increase, $p=0.032$, familial astrocytes 7.2% increase, $p=0.030$), and a significantly reduced form factor (Sporadic astrocytes 5.01% reduction, $p=0.031$, familial astrocytes 7.2% reduction, $p=0.039$) (Figures 5.3B&C). Form factor in this situation refers to how interconnected the mitochondrial network is, with a lower number suggesting a more interconnected network.

The percentage of small mitochondria in the mitochondrial network showed a trend towards a reduction in both sporadic ($p=0.409$) and familial ($p=0.114$) AD astrocytes when compared to controls, but this was not significant (Figure 5.3D). A trend towards an increase in the percentage of perinuclear mitochondria was seen in both sporadic and familial AD astrocytes when compared to controls (Figure 5.3E), but no change in mitochondrial number was seen in AD astrocytes when compared to controls (Figure 5.3F). The same changes in mitochondrial function and morphology were seen when experiments were performed in glucose based media (Supplementary figure 2).

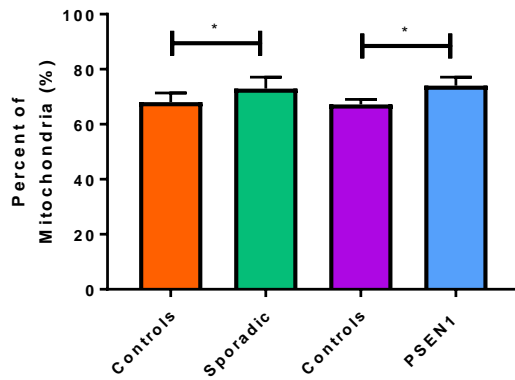
A Mitochondrial Membrane Potential (Galactose Media)



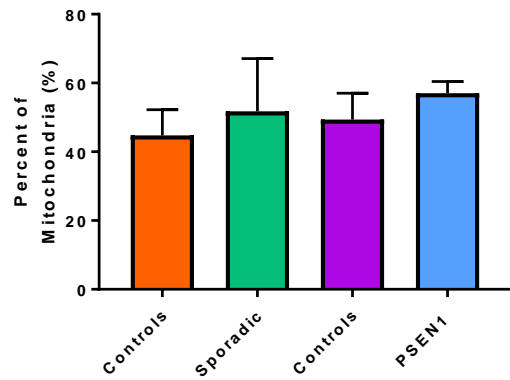
D Percentage of Short Mitochondria (Galactose Media)



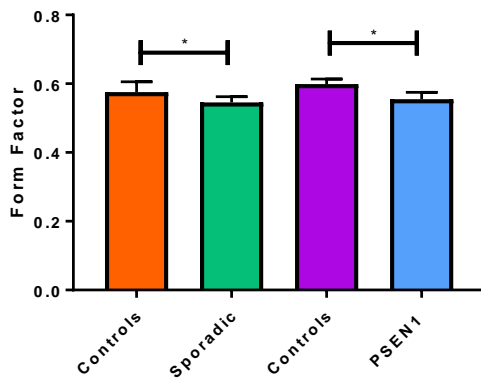
B Percentage of Long Mitochondria (Galactose Media)



E Percentage of Perinuclear Mitochondria (Galactose Media)



C Form Factor (Galactose Media)



F Mitochondrial Count (Controlled for Cell Area)

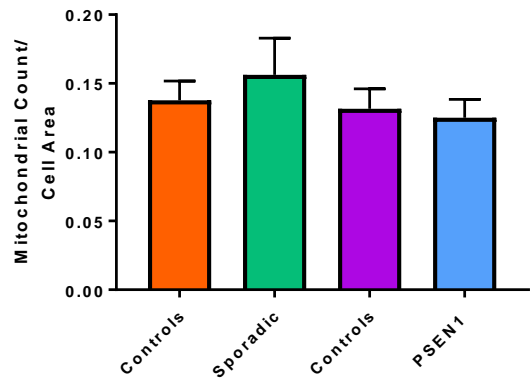


Figure 5.3 | Astrocyte Mitochondrial Function and Morphology *Figure 3A Mitochondrial Membrane Potential* a significant decrease was seen in sporadic AD astrocyte MMP and a significant increase was seen in familial astrocyte MMP. *Figure 3B Percentage of Long Mitochondria* A significant increase in long mitochondria was seen in both sporadic and familial AD astrocytes. *Figure 3C Form Factor* A significant reduction in form factor was seen in both sporadic and familial AD astrocytes when compared to controls. *Figure 3D Percentage of short mitochondria, Figure 3E Perinuclear Mitochondria Figure 3F Mitochondrial Count* all three of these measures were not significantly different between control and disease astrocytes $*=p<0.05$. In all panels sporadic controls are represented in orange, sporadic AD lines in green, Familial controls in purple and familial AD astrocyte lines in blue.

OxPHOS is altered in AD astrocytes

After showing that AD astrocytes had mitochondrial morphological changes and lower total cellular ATP levels, we next wanted to assess if OxPHOS was also impaired in AD astrocytes. OxPHOS was assessed in both a glucose and galactose based media. The results described below represent the galactose based media data, as galactose media forces the astrocytes to utilize OxPHOS rather than glycolysis. Figures 5.4A&B show Oxygen consumption rates (OCR) for sporadic and familial AD astrocytes respectively in galactose media.

Basal mitochondrial respiration (59% reduction, $p=0.0075$) and ATP linked respiration (61% reduction, $p=0.006$) were both significantly lower in fAD astrocytes when compared to their controls (Figures 5.4C&D). A trend to a reduction in basal mitochondrial respiration (reduction 12.5%, $p=0.3943$) and ATP linked respiration (reduction 18.9%, $p=0.315$) was seen with sAD astrocytes, but this was not significant. MSRC was shown to be significantly reduced in both sporadic (44% reduction, $p=0.0416$) and familial AD astrocytes (80% reduction, $p=0.0269$) when compared to controls (Figure 4E). fAD astrocytes showed a significant reduction in proton leak when compared to controls, (69.5% reduction, $p=0.0154$), whereas sAD astrocytes only showed a trend towards a reduction (Figure 5.4F). No significant difference was seen in coupled respiration or respiratory control ratio in sporadic or familial AD astrocytes when compared to controls (Figures 5.4G&H). These data together suggest that fAD astrocytes have a greater compromise of OxPHOS than sAD astrocytes, although both sporadic and familial AD astrocytes have a significant reduction in MSRC.

To assess further the reliance of astrocytes on a particular metabolic pathway the OCR/ECAR ratios were investigated using the mito stress test seahorse program under basal conditions, before mitochondrial inhibitors were added. In both sporadic and familial astrocytes a reduction in the OCR/ECAR ratio was seen (sporadic reduction 32%, $p=0.0193$, familial 31.5% reduction, $p=0.0119$). This suggests that both sporadic and familial AD astrocytes have an altered ratio by which they used glycolysis or OxPHOS. This may be a reflection of the fact that both types of AD astrocytes appear to have a deficit in OxPHOS, but could also suggest a glycolysis deficit. (Figure 5.4I).

Similar results to those described above were seen when astrocytes were assessed in a glucose based media, but non-significant decreases in fAD astrocyte proton leak, and reduction in both sporadic and familial astrocyte OCR/ECAR ratios was seen (Supplementary figure 3).

Sporadic and Familial AD mitochondria produce less ATP when supplied with complex I substrates.

As both sporadic and familial astrocytes have a deficit in OxPHOS the activity of the ETC was assessed at the mitochondrial level. Both sporadic and familial astrocytes showed a significant

reduction in mitochondrial ATP production when supplied with complex I substrates (sAD: 34% reduction, $p=0.0468$, familial AD: 56% reduction, $p=0.0485$) (Figure 4J). No differences in mitochondrial ATP production were seen when complex II substrates were supplied to the permeabilised cells, suggesting no deficit in complex II activity (Figure 5.4K). These data suggest a specific deficit in complex I activity, rather than global respiratory chain dysfunction.

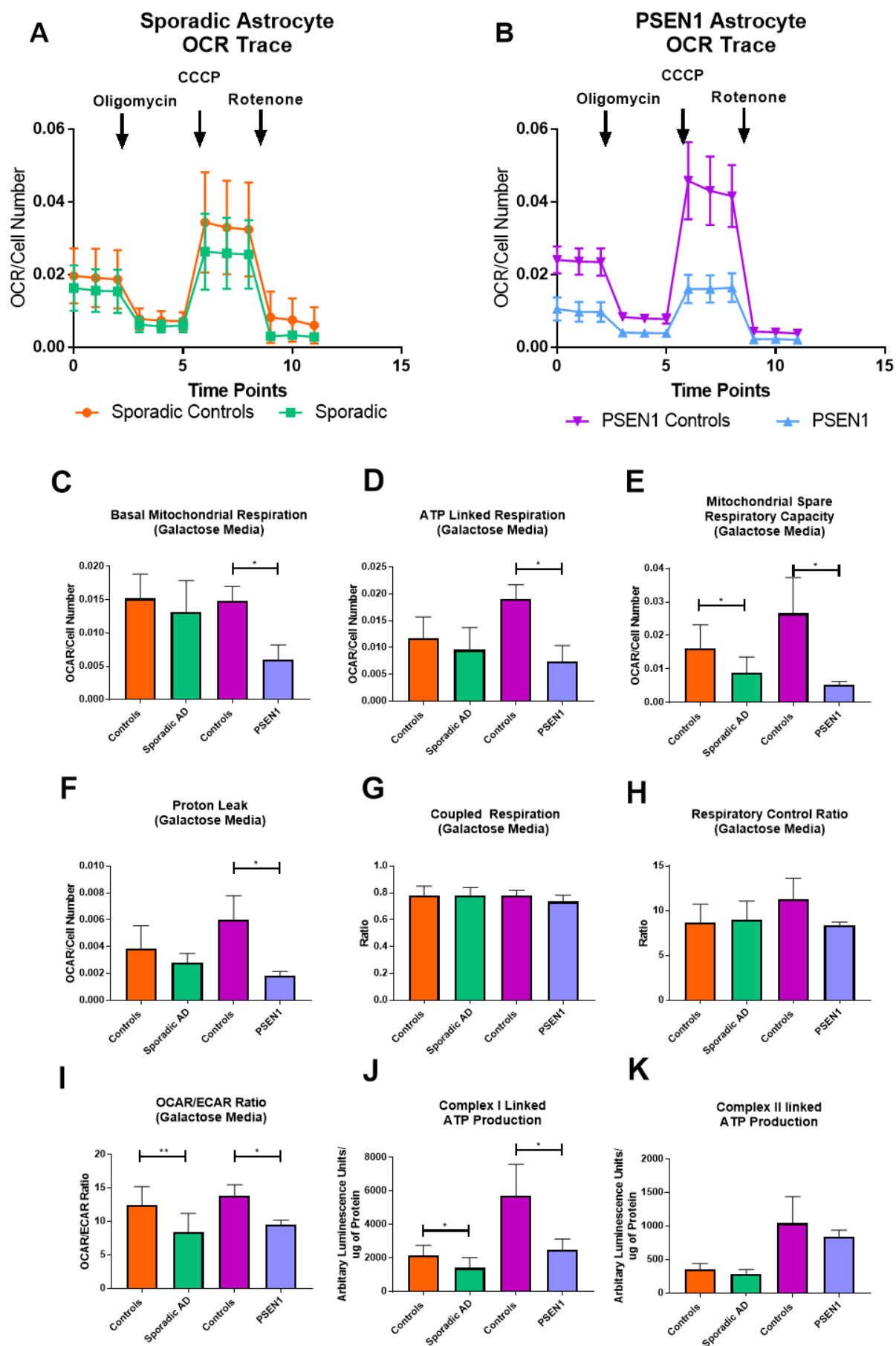


Figure 5.4 | Astrocyte Oxidative Phosphorylation Assessment *Figure 4A Sporadic AD Astrocyte OCR trace, Figure 4B Familial AD astrocyte OCR trace Figure 4C Basal Mitochondrial Respiration* Basal respiration was reduced in both sporadic and familial AD astrocytes *Figure 4D ATP Linked Respiration* A reduction in sporadic and familial AD astrocyte ATP linked respiration was seen *Figure 4E MSRC* MSRC was significantly reduced in both sporadic and familial AD astrocytes *Figure 4F Proton leak* a significant reduction was seen in familial astrocytes, but not sporadic *Figure 4G Coupled Respiration & Figure 4H Respiratory Control ratio* Both parameters were unchanged in sporadic and familial astrocytes. *Figure 4I OCR/ECAR Ratio* Significant reductions were seen in both sporadic and familial astrocytes when compared to controls. *Figure 4J Complex I Substrates* Significant reduction in both sporadic and familial AD mitochondria has deficits in ATP production in the presence of complex I substrates. *Figure 4K Complex II Substrates* No significant difference in ATP production was seen when sporadic and familial AD astrocytes in the presence of complex II substrates. *= $p < 0.05$ **= $p < 0.01$. In all panels sporadic controls are represented in orange, sporadic AD lines in green, Familial controls in purple and familial AD astrocyte lines in blue.

Astrocyte glycolytic function is impaired in AD astrocytes

As reported in the results sections earlier, glycolysis is the main metabolic pathway used by astrocytes to maintain total cellular ATP levels. Therefore glucose metabolism was assessed in the AD astrocytes. Figures 5.5A&B show the glycolysis stress test trace performed in sporadic and familial AD astrocyte lines, and how they compare to controls (Figure 5.5A&B). As with OxPHOS assessment, astrocytes were cultured in a glucose and galactose based media. The results presented below represent the data for the galactose based media, to be consistent with the mitochondrial stress test discussed above. A significant reduction in glycolysis rate were seen in sporadic astrocytes (29.7% reduction, $p= 0.0451$), but only a trend towards a reduction was seen in familial astrocytes (36% reduction, $p= 0.333$) when compared to controls (Figure 5.5C). Glycolytic reserve was significantly reduced in both sporadic (34% reduction, $p= 0.031$) and familial (40% reduction, $p=0.045$) AD astrocytes when compared to controls (Figure 5.5D). A trend towards a reduction in glycolytic capacity was seen in the sporadic AD astrocytes, and a significant decrease (52% decrease, $p=0.0172$) was seen in familial AD astrocytes (Figure 5.5E). No significant difference in non-glycolytic acidosis was seen in both familial and sporadic AD astrocytes when compared to controls (Figure 5.5F). Glycolysis assessment performed in a glucose based media, showed the same trends as that in galactose, but only the reduction in glycolytic capacity was significant in this media (Supplementary figure 4). Together this data suggest that both sporadic and familial AD astrocytes have impairments in their ability to metabolise glucose when compared to controls.

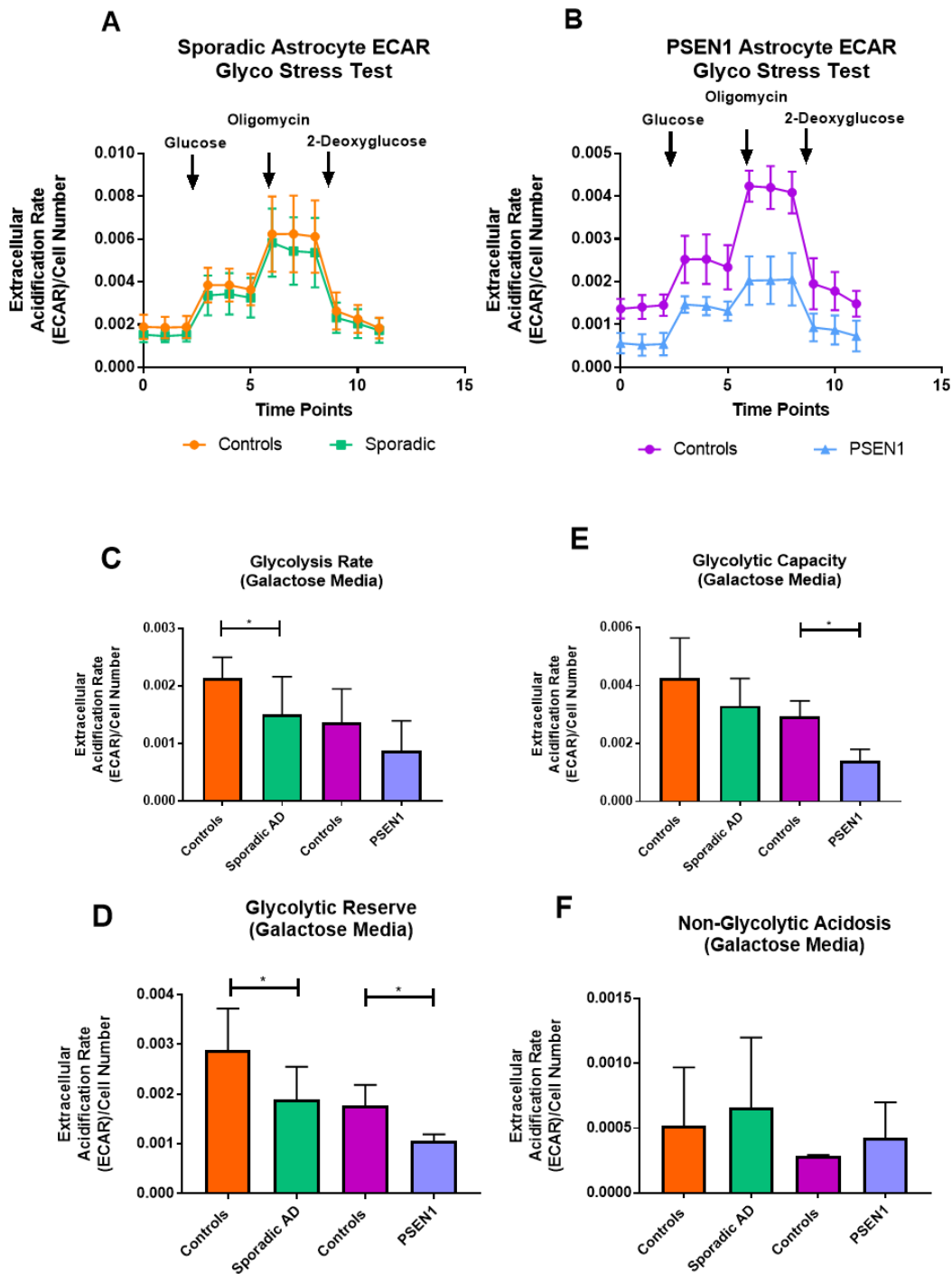


Figure 5.5 | Astrocyte glycolysis assessment *Figure 5A ECAR trace Sporadic astrocytes* *Figure 5B ECAR Trace Familial Astrocytes* *Figure 5C Glycolysis rate* Reductions in glycolysis rates were seen in both sporadic and familial AD astrocytes *Figure 5D Glycolytic Capacity* Reduction in glycolytic capacity was seen in familial AD astrocytes. *Figure 5E Glycolytic Reserve* Significant reductions in both sporadic and familial AD astrocytes were seen *Figure 5F Non-glycolytic acidosis* No significant changes were seen. In all panels sporadic controls are represented in orange, sporadic AD lines in green, Familial controls in purple and familial AD astrocyte lines in blue.

Sporadic and Familial AD astrocyte release less lactate than controls

After highlighting that glycolysis is impaired in AD astrocytes, we next investigated if this affected the astrocytes ability to release lactate, a key metabolite shared between neurons and astrocytes. Extracellular lactate levels were reduced in both sporadic (43% reduction, $p=0.0062$) and familial AD astrocytes (59% reduction, $p=0.0187$) when compared to controls in a glucose based media (Figure 5.6A). To assess if impairments in glycolysis in astrocytes were due to their ability to uptake glucose this was also measured using 2-deoxyglucose. Due to time restrictions assessment of the full cohort of cells lines was not performed with regards to the glucose uptake assay. 7 control lines, 4 sporadic and 3 familial AD astrocyte lines were assessed. A trend to a reduction in 2-deoxyglucose uptake was seen, but this was not significant (Figure 5.6B). These results suggest that glucose uptake may be affected in sporadic and familial AD astrocytes, and that this combined with deficits in glycolysis impairs lactate release into the extracellular media.

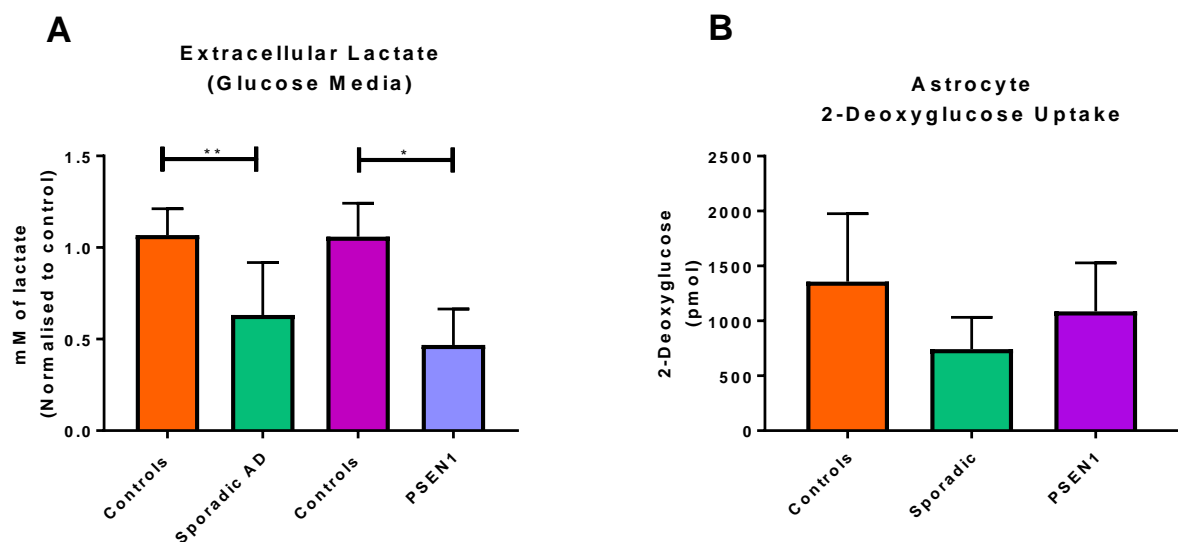


Figure 5.6| Astrocyte Lactate excretion and Glucose uptake *Figure 6A Astrocyte extracellular lactate* A significant decrease in extracellular lactate was seen in both sporadic and familial AD astrocytes when compared to controls. *Figure 6B Astrocyte 2-deoxyglucose uptake* Trends to a reduction in 2-deoxyglucose uptake were seen in both sporadic and familial AD astrocytes *= $p<0.05$, **= $p<0.01$. In all panels sporadic controls are represented in orange, sporadic AD lines in green, Familial controls in purple and familial AD astrocyte lines in blue.

Mitochondrial Spare Respiratory Capacity and Glycolytic markers Correlate with neuropsychological markers of AD

In our previous paper we investigated if MSRC and MMP measured in sAD fibroblasts correlated with neuropsychological markers of AD [500]. As we have now identified a distinct metabolic phenotype in sporadic AD astrocytes to that which we previously identified in the fibroblasts from which the astrocytes are derived, we decided to investigate if the same correlations were present. Although similarities are seen in the mitochondrial and glycolytic deficits in both sAD fibroblasts and astrocytes, sAD fibroblasts have more pronounced structural change to their mitochondrial network when compared to sAD astrocytes. This includes an increase in perinuclear mitochondria, and a reduced mitochondrial number that is not seen in astrocytes when both cell types are compared to controls. Astrocytes have a more profound metabolic deficit signified by reductions in total cellular ATP and glycolytic rate, which is not seen in sAD fibroblasts. Astrocytic glycolytic function is more significantly impaired than in fibroblasts for sAD patient derived cells [500], therefore we also investigated if glycolytic reserve and extracellular lactate correlated with neuropsychological markers of AD. Neuropsychological data was only available for sporadic AD astrocytes and their control lines, therefore familial AD astrocytes could not be assessed. Semantic fluency, immediate and delayed recall were assessed as these were the neuropsychological markers previously investigated, and are known to be affected in the early stages of AD.

A significant positive correlation was seen with immediate recall and MSRC ($R=0.669$, $p=0.005$), (Figure 5.7B). A positive correlation, which did not reach significance was seen between MSRC and semantic fluency (Figure 5.7A) and delayed episodic recall (Figure 5.7C). Positive correlations that were not significant were seen between MMP and semantic fluency, (Figure 5.7D), immediate recall, (Figure 5.7E) and delayed episodic recall (Figure 5.7F).

Glycolytic reserve showed a trend towards a positive correlation with semantic memory ($R=0.524$, $p=0.054$), (Figure 5.8A). A significant positive correlation was seen between both glycolytic reserve and immediate recall ($R=0.570$, $p=0.033$) (Figure 5.8B), and glycolytic reserve and delayed recall ($R=0.541$, $p=0.045$) (Figure 5.8C). Extracellular lactate showed significant positive correlations with all three neuropsychological tests, semantic fluency ($R=0.634$, $p=0.014$, Figure 8D), Immediate recall ($R=0.617$, $p=0.018$, Figure 8E), delayed recall ($R=0.578$, $p=0.038$, Figure 8F). After identifying the above correlations, as we had done previously in our paper using fibroblasts from the same participants we assessed the correlations after controlling for brain reserve, length of education and participant age [500]. Only correlations that were statistically significant were assessed. After controlling for the 3 factors, positive correlations remained between immediate recall and glycolytic reserve ($r=0.824$, $p=0.003$), delayed recall and glycolytic reserve ($r=0.658$, $p=0.039$) and semantic

fluency and extracellular lactate levels ($r=0.865$, $p=0.003$). A trend towards significance was seen with the correlation between immediate recall and MSRC ($r=0.586$, $p=0.075$), but the correlations between extracellular lactate and immediate recall ($r=0.552$, $p=0.123$) and delayed recall were no longer significant ($r=0.368$, $p=0.330$). Table 5.5 displays these correlations. In conclusion this data highlights that both mitochondrial and glycolytic astrocytic parameters shown to be abnormal in AD correlate with neuropsychological tests known to be affected early in the course of the condition.

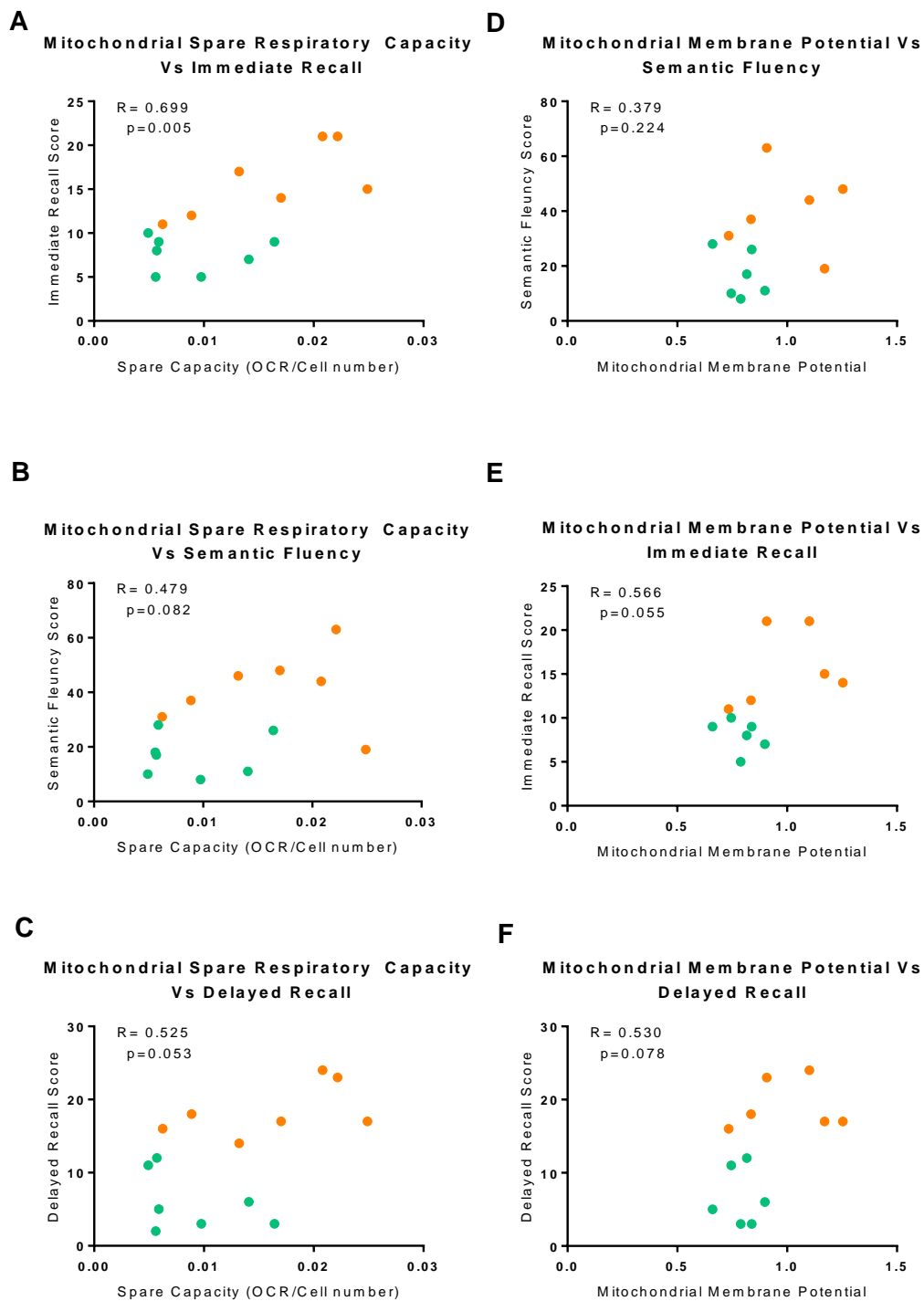


Figure 5.7 | MSRC and MMP correlations with Neuropsychological tests This figure highlights the mitochondrial spare respiratory capacity (MSRC) correlations with immediate recall (Figure 7A) semantic memory (Figure 7B) and delayed recall (Figure 7C). Mitochondrial membrane potential correlations with semantic memory (Figure 7D) immediate recall (Figure 7E) and delayed recall (Figure 7F) are also displayed. Green points represent sporadic AD patients and orange points represent control subjects.

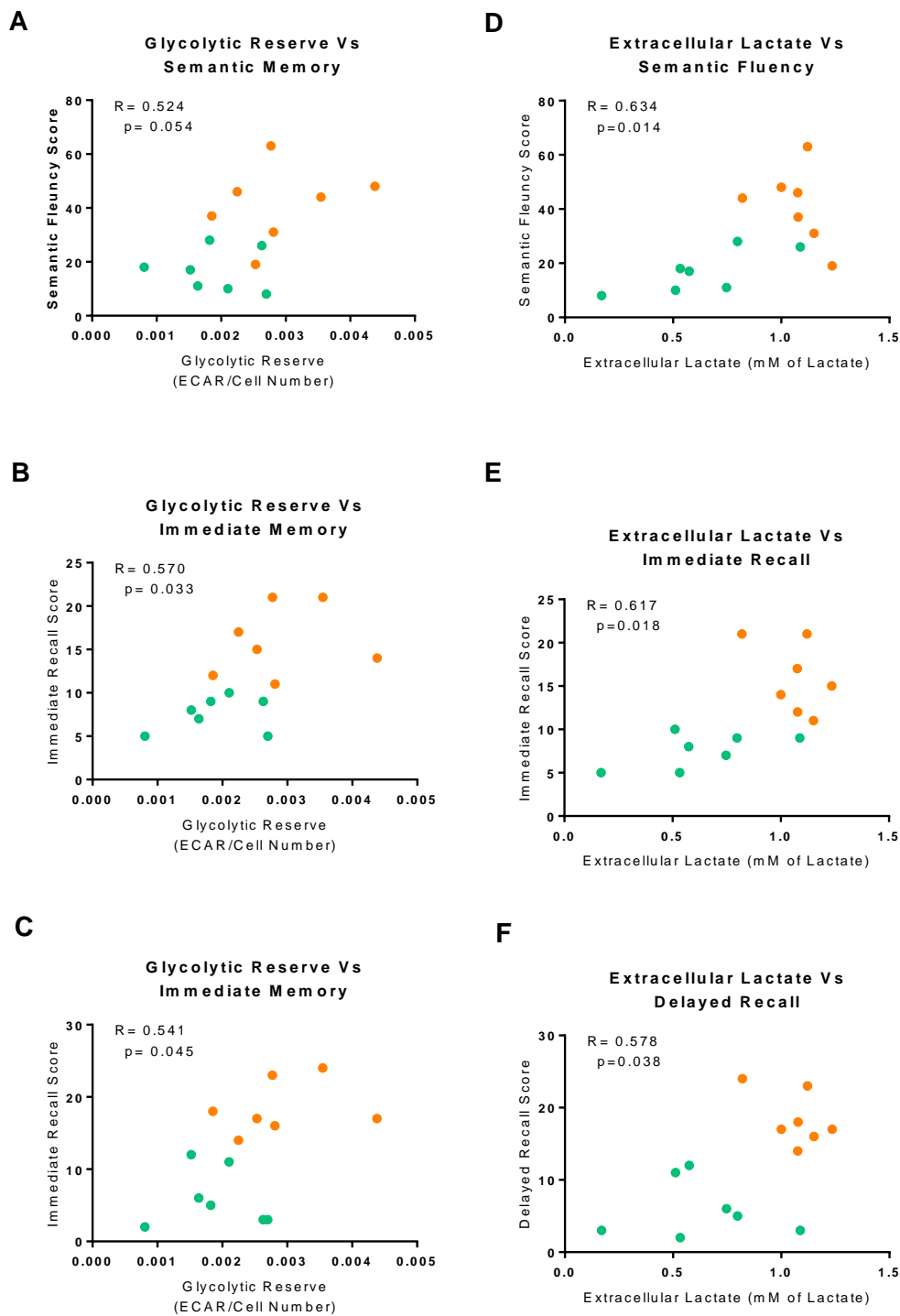


Figure 5.8 | Glycolytic reserve and extracellular lactate correlations with Neuropsychological tests This figure highlights the glycolytic reserve correlations with semantic memory (Figure 8A) immediate recall (Figure 8B) and delayed recall (Figure 8C). Astrocyte extracellular lactate correlations with semantic memory (Figure 8D) immediate recall (Figure 8E) and delayed recall (Figure 8F) are also displayed. Green points represent sporadic AD patients and orange points represent control subjects.

Neuropsychological Tests	Astrocyte Metabolic Marker	R-Value	P-value
Immediate Recall			
	Mitochondrial Spare Respiratory Capacity	0.586	0.075
Immediate Recall			
	Glycolytic Reserve	0.824	0.003
Delayed Recall			
	Glycolytic Reserve	0.658	0.039
Immediate Recall			
	Extracellular Lactate Level	0.552	0.123
Delayed Recall			
	Extracellular Lactate Level	0.368	0.330
Semantic Fluency			
	Extracellular Lactate Level	0.865	0.003

Table 5.5 | Astrocyte neuropsychological metabolic correlations This table displays the correlations between different astrocyte metabolic parameters and neuropsychological testing after controlling for participant age, brain reserve and length of education. For this analysis the controls and sAD astrocytes were considered as one group. Numbers highlighted in bold are statistically significant correlations.

Total cellular ATP and morphology deficits can be corrected with the application of drugs that enhance mitochondrial function.

In order to fully assess if mitochondrial dysfunction is a viable therapeutic target in AD, we wanted to investigate if the mitochondrial phenotype we have characterized in the fAD and sAD astrocytes could be restored using treatment with small molecules. Eight compounds were selected which have previously been shown to restore mitochondrial function and morphology in other neurodegenerative conditions such as PD and MND and in systemic disease. Therefore, total cellular ATP and the mitochondrial morphology parameters that were shown to be significantly different in AD astrocytes in figure 5.3 were assessed after the application of the eight compounds. The mitochondrial morphology parameters assessed were long and short mitochondrial percentage, mitochondrial area and mitochondrial form factor. For each of the eight compounds assessed

astrocytes were treated with concentrations of 1,10 and a 100 μ M for 24 hours. Treatment with all 8 compounds did not affect cell area (data not shown), and a similar effect was seen at each of the three concentrations tested for each compound. As a result of this the data in this paper has been presented for the middle concentration of 10 μ M.

Figures 9-12 display the results for total cellular ATP and mitochondrial morphology parameters after treatment with 10 μ M of each of the eight compounds. Results are shown for both sporadic and familial lines and their controls. Parameters displayed are total cellular ATP (Figures 5.9A-5.12A), percentage long mitochondria (Figures 5.9B-5.12B), percentage short mitochondria (Figures 5.9C-5.12C) and form factor (Figure 5.9D-5.12D). Table 5.6 shows how application of each of the separate drugs affected total cellular ATP and mitochondrial morphology parameters. This table details the percentage change in each parameter when the compounds were added and colours indicate if this was in a direction that brought the morphological parameter in the AD lines closer to or further away the level seen in the controls.

Total cellular ATP was shown to be significantly reduced in sAD astrocytes when compared to controls (Figures 5.9A-5.12A and table 5.4). When sAD astrocytes were treated with the eight compounds total cellular ATP was not significantly different between controls and sAD astrocytes with all drug treatments except for compound F. This shows that the other 7 compounds can correct the ATP deficit seen in sporadic AD astrocytes. A significant difference in long mitochondrial percentage was seen in the sporadic AD astrocytes when compared to controls. Treatment with all eight compounds reduced the percentage of long mitochondria, removing this significant difference. The percentage of short mitochondria in the sporadic AD astrocytes was increased with the application of the eight drugs. After drug application there was no longer a significant difference in short mitochondrial percentage between controls and sporadic AD astrocytes. Compounds A,C,D, and E all increased mitochondrial form factor suggesting that the mitochondrial network was becoming less interconnected in sporadic AD astrocytes. Compound B decreased the form factor of sporadic AD astrocytes, and compounds F,G and H had no effect.

Application of the eight compounds to the PSEN1 AD astrocytes had less of an effect than that seen when the sporadic AD astrocytes were treated. All drugs increased total cellular ATP, but the effect on the other parameters was less consistent. Compounds A, B D, E and F all reduced the long mitochondria percentage, but only probenecid had a positive effect on the short mitochondrial percentage. Compound F was the compound that had the most positive effect on the PSEN1 morphological parameters, but at doses greater than 10 μ M astrocyte cell death was seen (data not shown).

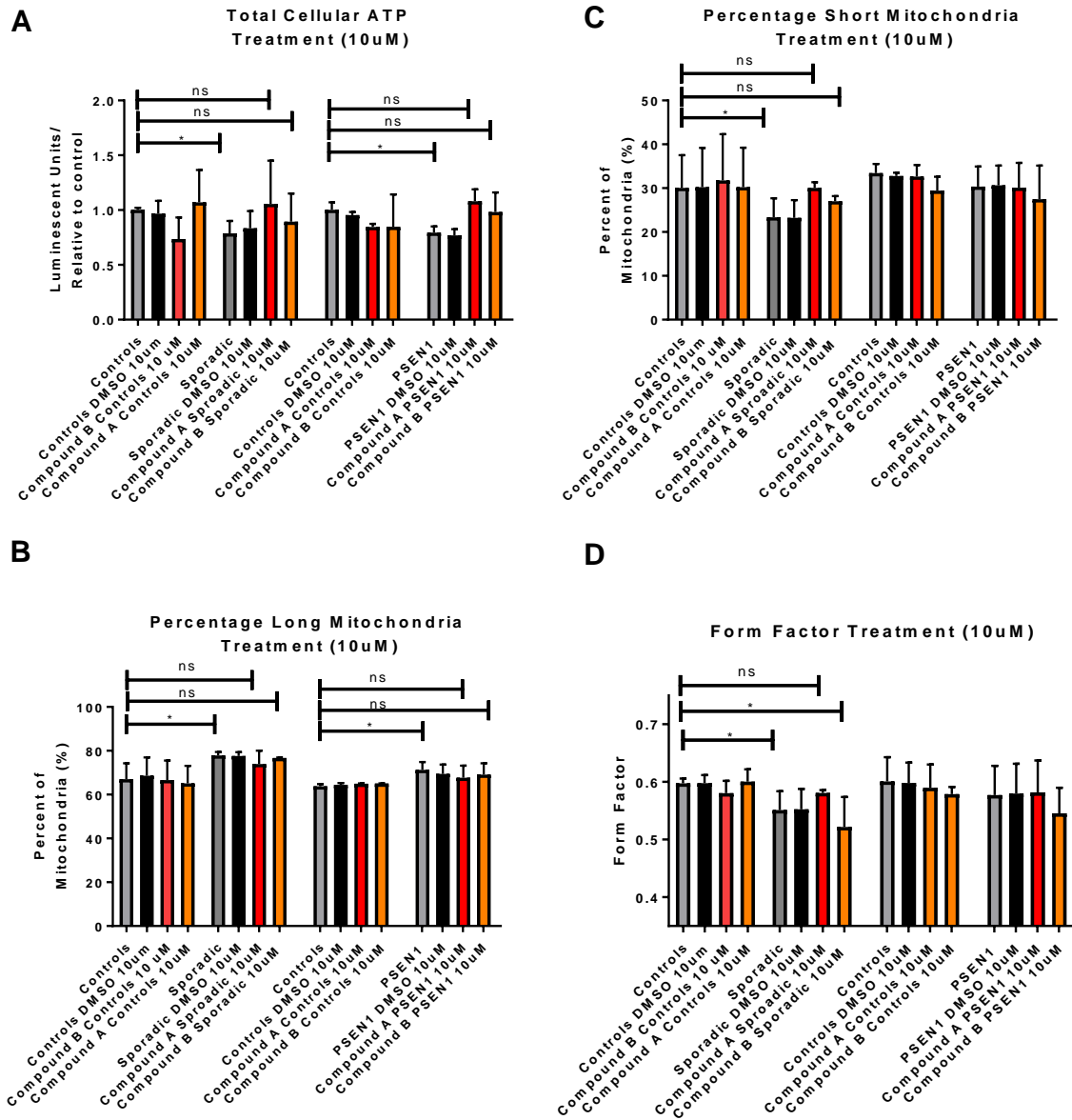


Figure 5.9/ Compounds A&B treatment of control sporadic and familial AD Astrocytes

This figure displays Functional and morphological parameters that treatment of astrocytes with 10µM of compound A or 10µM colchicine effected. Compound A and Compound B increased total cellular ATP in both sporadic and familial AD fibroblasts towards that seen in control astrocytes (Figure 5.9A). Long mitochondrial percentage was reduced in both sporadic and familial AD astrocytes (Figure 5.9B), and short mitochondrial percentage was increased by compound A and reduced by compound B (Figure 5.9C). Form factor increased in both sporadic and familial AD astrocytes, when treated with compound A but a reduction was seen with colchicine (Figure 5.9D). Control bars are in grey, DMSO vehicle in black, compound A treated parameters are in red and compound B treated parameters are in orange

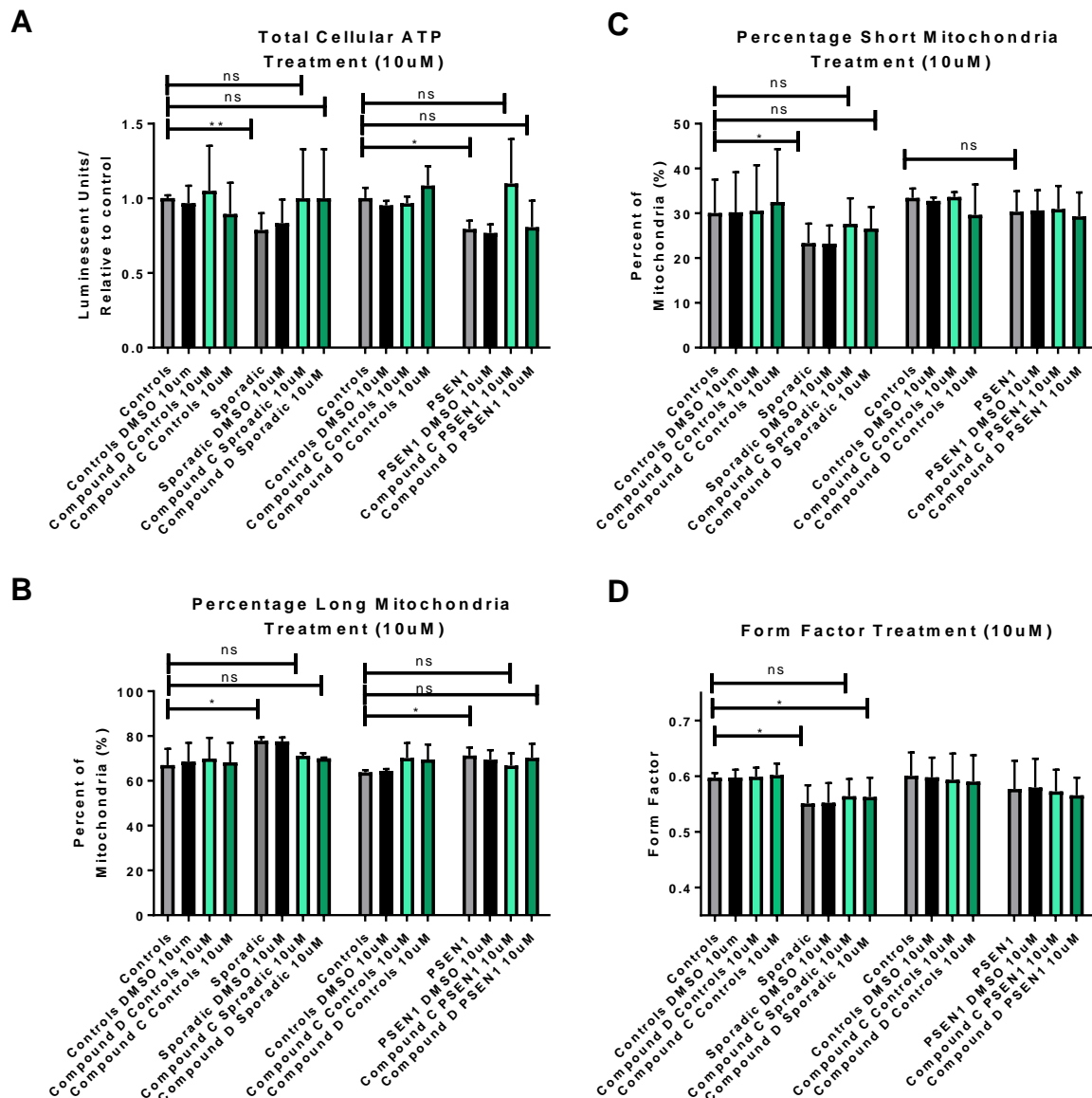


Figure 5.10/ Compounds C&D treatment of control, sporadic and familial AD

Astrocytes This figure displays functional and morphological parameters that treatment of astrocytes with 10µM of compounds C or D effected. Compounds C & D increased total cellular ATP in both sporadic and familial AD fibroblasts towards that seen in control astrocytes (Figure 5.10A). Long mitochondrial percentage was reduced in both sporadic and familial AD astrocytes (Figure 5.10B), and short mitochondrial percentage was increased by compound C and reduced by compound D (Figure 5.10C). Compound C and compound D had no effect on form factor in familial AD but showed an increase in sporadic AD astrocytes (Figure 5.10D). Control bars are in grey, DMSO vehicle in black, compound C treated parameters are in mint and compound D treated parameters are in green.

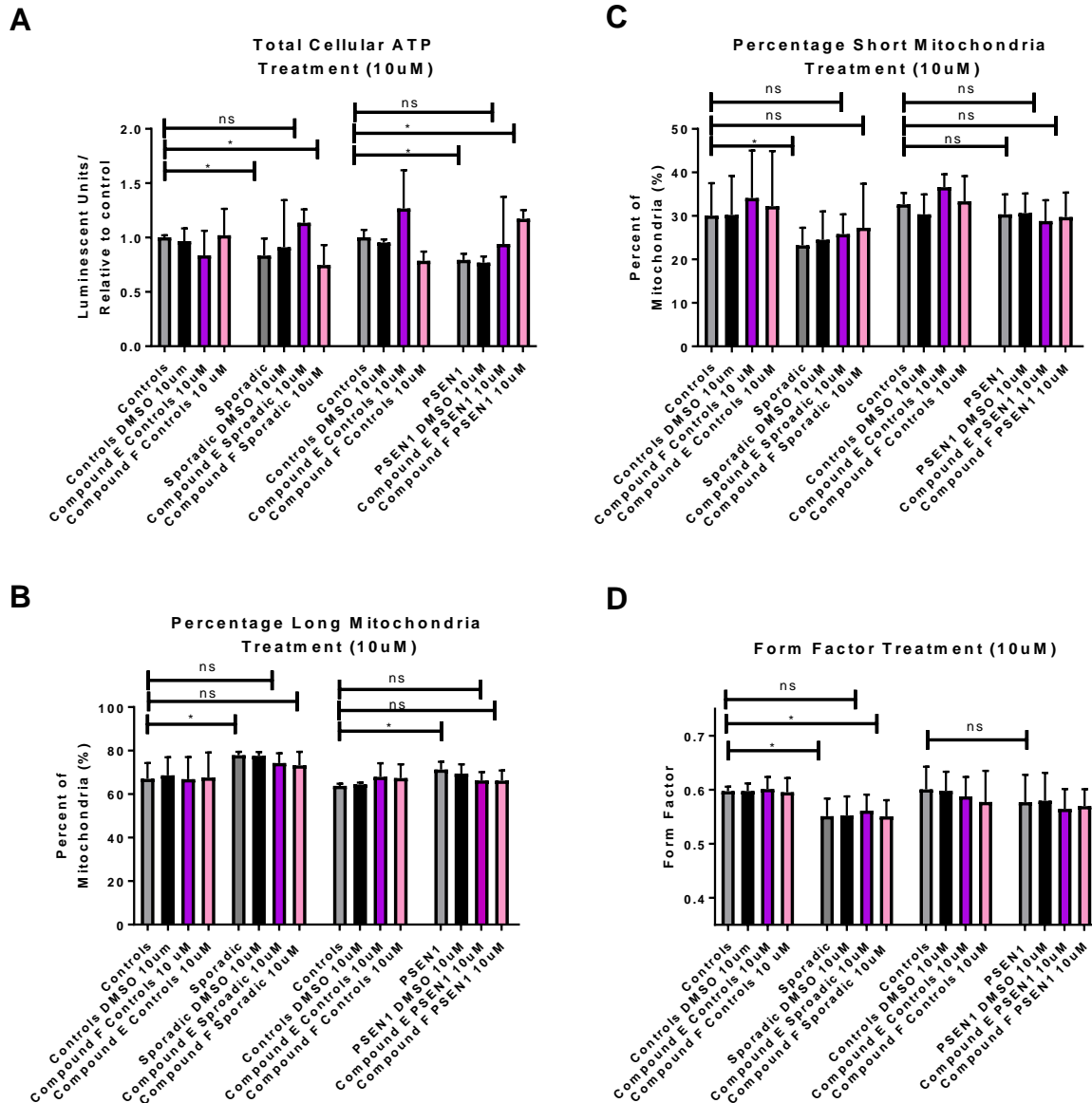


Figure 5.11 /Compounds E&F treatment of control, sporadic and familial AD

Astrocytes This figure displays functional and morphological parameters that treatment of astrocytes with 10µM of Compounds E or F effected. Compounds E and F increased total cellular ATP in both sporadic and familial AD fibroblasts towards that seen in control astrocytes (Figure 5.11A). Long mitochondrial percentage was reduced in both sporadic and familial AD astrocytes (Figure 5.11B), and short mitochondrial percentage was increased by compounds E and F (Figure 5.11C). Compounds E and F had no effect on form factor in familial AD but showed an increase in sporadic AD astrocytes (Figure 5.11D). Control bars are in grey, DMSO vehicle in black, Compounds E treated parameters are in purple and compound F treated parameters are in pink.

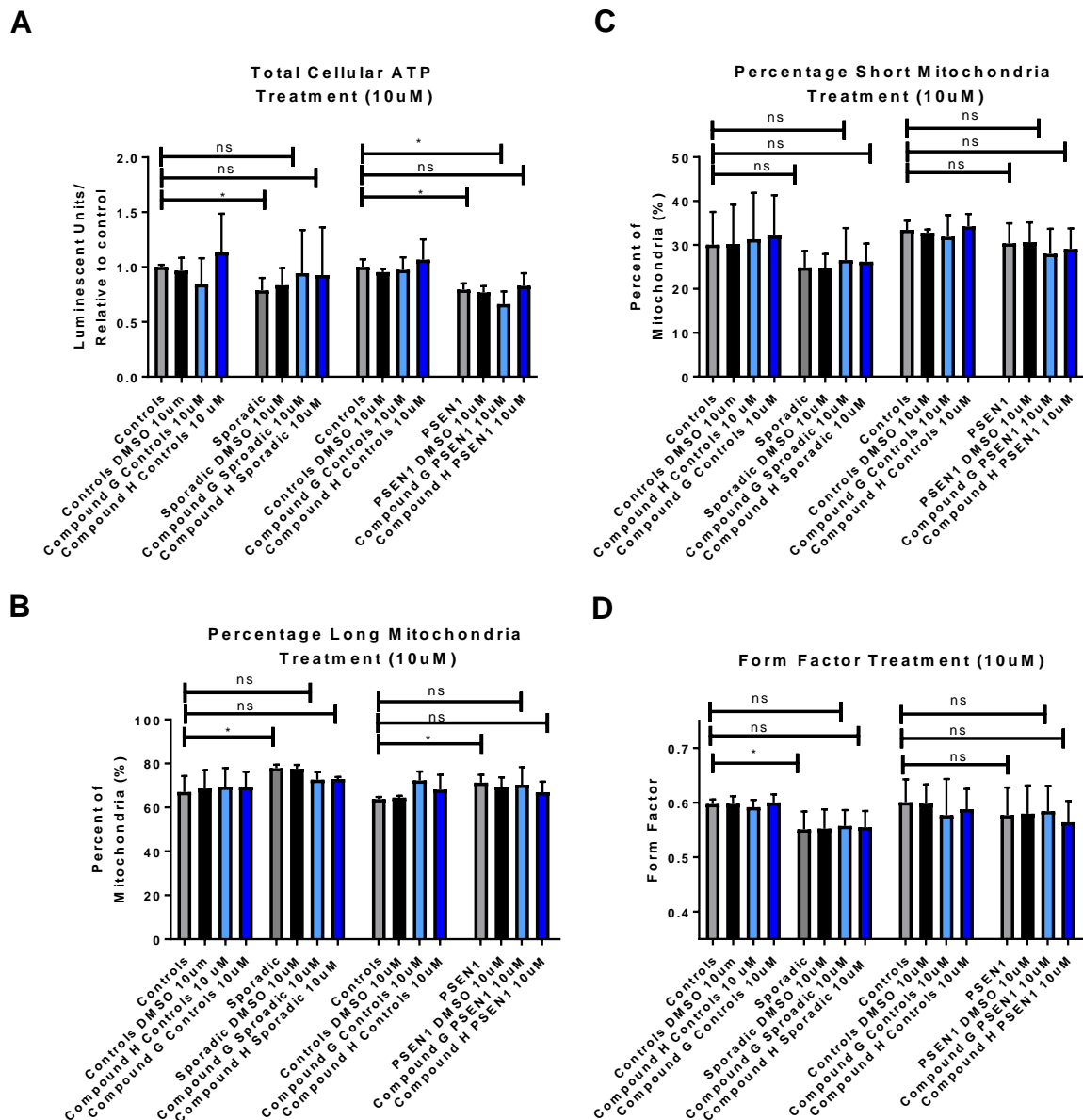


Figure 5.12/ Compound G & H treatment of control, sporadic and familial AD

Astrocytes This figure displays functional and morphological parameters that treatment of astrocytes with 10µM of *Compound G & H* effected. Compound H decreased and compound G increased total cellular ATP in both sporadic and familial AD astrocytes (Figure 5.12A). Long mitochondrial percentage was reduced in both sporadic and familial AD astrocytes (Figure 5.12B). Short mitochondrial percentage was increased by *Compound G & H* (Figure 5.12C). *Compound G & H* had no effect on form factor in familial AD but showed an increase in sporadic AD astrocytes (Figure 5.12D). Control bars are in grey, DMSO vehicle in black, compound H treated parameters are in light blue and compound G treated parameters are in dark blue.

Sporadic Astrocytes				
Drug	ATP	Short Mitochondria	Long Mitochondria	Form Factor
A	27% Increase	17% increase	4% Decrease	5% Increase
B	11% Increase	4% Increase	2% Decrease	2.5% reduction
C	22% Increase	4% Increase	6% Decrease	2.5% Increase
D	22% Increase	3% Increase	7% Decrease	2.5% Increase
E	30% Increase	3% Increase	3% Decrease	2.5% Increase
F	No change	4% Increase	4% Decrease	No change
G	16% Increase	2.5% Increase	5% Decrease	No change
H	£ 14% Increase	2.5% Increase	5% Decrease	No change
Familial Astrocytes				
Drug	ATP	Short Mitochondria	Long Mitochondria	Form Factor
A	29% Increase	No change	4% Decrease	No change
B	19% Increase	3% Decrease	2% Decrease	3% reduction
C	30% increase	No change	5% Decrease	No change
D	3% Increase	No change	No change	1.5% reduction
E	23% Increase	No change	5% Decrease	No change
F	38% Increase	No change	5% Decrease	No change
G	13% reduction	No change	No change	No change
H	£ 3% Increase	No change	No change	1.5% reduction

Table 5.6 | Effects of drug compounds of ATP and mitochondrial morphology Table displays the changes that occurred with addition of the separate drugs at a concentration of a 100nM to each ATP/mitochondrial marker. Were a cell is coloured green this indicates the value returned to control levels. When a cell is coloured red this indicates a value moved further away from controls. When a cell is blue no change in parameter was seen. When a cell is coloured purple an unexpected effect was seen. £ indicates effect was only seen at 100nM concentration

5.2.6 Discussion

In this study we have shown that astrocytes derived from patients with both sporadic and familial AD have deficits in key metabolic pathways, including several mitochondrial abnormalities and glycolytic abnormalities. That some of these abnormalities correlate with neuropsychological abnormalities seen early AD, and that certain small molecule compounds can correct these abnormalities. In the discussion we will discuss the three elements of the paper separately.

5.2.1 The AD astrocyte metabolic phenotype

Our study builds upon limited studies available to date of metabolism in astrocytes derived from AD patients. One of the few published studies utilizing astrocytes derived from AD patients, found decreased rate of glycolysis, decreased glycolytic reserve and lower extracellular lactate levels in astrocytes derived from 3 PSEN1 mutation carriers when compared to controls [389]. Here we confirm the same changes in glycolytic pathways in astrocytes derived via an alternative reprogramming method and different PSEN1 patients; furthermore we add to the literature finding this same glycolytic profile in sporadic AD astrocytes. Other studies that have investigated glycolysis in AD astrocytes have used cells from either PM brain tissue, or animal models of disease, although specific data about astrocyte glycolysis is limited. The activity of Phosphofructokinase (PFK), the enzyme that converts fructose-6-phosphate into fructose-1,6-bisphosphate is thought to have increased activity in the astrocytes of people with AD [278]. There is also evidence that several other enzymes of the glycolytic pathway are upregulated in the PM AD brain including lactate dehydrogenase and pyruvate kinase [277, 279]. In this study we have shown parameters that focus on the overall rate of glycolysis are lower in AD astrocytes, this could be consistent with several enzymes of the pathway having increased activity. Both the results from our study and the evidence of increased enzyme activity could be explained by a reduced glucose uptake by the astrocyte. There is evidence that the glucose transporters GLUT1&3 have reduced expression as AD progresses [280], which could lead a situation in which astrocytes have lower overall rates of glycolysis, but increase enzyme activity to compensate. Human imaging studies also suggest that the brain has a reduced glucose uptake in both ageing and AD [274] this could be explained by a reduced number of glucose receptors in the brain, or a decreased ability to perform glycolysis in astrocytes as seen here.

Studies of enzyme activity in fibroblasts from patients with sporadic AD have shown a reduction in the activity of hexokinase, the first enzyme in the glycolytic pathway, [281]. It has also been shown that fibroblasts from sporadic AD patients rely more on glycolysis than controls, but have a limited ability to increase glucose uptake [282]. These abnormalities in fibroblasts from patients with AD may explain the changes we see here in the glycolytic function of our astrocytes derived from

fibroblasts. It could be argued that the changes in glycolytic function seen in this study are an expression of changes in fibroblast glycolysis and may not be found in true primary astrocytes. The astrocyte cells produced in this study though have a completely different expression profile to that of their parent fibroblasts. The metabolic profile of the astrocytes produced in this project is also different to that of the fibroblasts that they are reprogrammed from. The parent fibroblasts do not have deficits in glycolytic capacity or glycolysis rate and on a group level total cellular ATP is effected much less [477, 478]. Therefore, it is reasonable to assume that the changes seen in this *in vitro* astrocyte model reflect changes that would be present *in vivo*. Further evidence to support that these changes may reflect *in vivo* astrocytes metabolic change in AD comes from data highlighting that the brain becomes less sensitive to glucose uptake through the course of AD, and the fact that the majority glucose metabolism within the brain is thought to be linked to astrocytic maintenance of glutamatergic synapses [306] These are strong indicators that the abnormalities seen in this study, and that by Oksanen [389] are reflective of changes to glycolysis in primary astrocytes and not just tessellations of fibroblast glycolytic function.

It has previously been shown that astrocytes can shuttle lactate to neurons as a fuel source, with neurons having a preference for lactate over glucose in times of increased energy expenditure [308-310]. In this study we have shown that astrocytes from both sporadic and familial AD patients have reduced extracellular lactate levels, which has potential consequences for the neuron astrocyte relationship. Neurons rely mainly on OxPHOS to meet their energy requirements [302], as a result of this they are at high risk of oxidative damage from free radicals produced via the electron transport chain. It has been shown that lactate preference, as an energy source, in neurons allows for the utilization of neuronal glucose to produce antioxidant molecules such as glutathione via the pentose-phosphate shunt (PPS) [308]. If the supply of astrocyte lactate is impaired to neurons, as the results from this study would suggest is the case in AD, then there would be an increase in oxidative damage to neurons in AD, as a result of glucose being diverted away from the PPS. Oxidative damage to neurons has been reported when AD astrocytes are co-cultured with non-AD neurons [389], and in multiple PM studies of the AD brain [337, 501, 502]. This suggests that decreased release of lactate from astrocytes, may have a pivotal role in the pathogenesis of AD, and therefore would make a suitable future therapeutic target.

In this study as well as deficits in astrocyte glycolysis we have also identified changes in mitochondrial function and morphology. Previous work on human derived fAD astrocytes has suggested that the oxygen consumption rate (OCR) is higher than that of matched controls [389]. Trends towards deficits in MSRC have also been identified but have not been shown to be significant [503]. Both these studies focus on the same 3 PSEN1 astrocyte lines. The changes in MSRC are

consistent with what we found in this study, although we found a significant decrease. The basal OCR in our study was significantly lower in AD astrocytes which is the opposite finding seen by Oksanen and colleagues [389]. The difference seen here may be explained by the fact that we have studied point mutations in the PSEN1 gene that cause AD, whereas the Oksanen group have studied astrocytes created from an exon 9 deletion model of AD. In this study we have shown that astrocytes are more dependent on glycolysis than OxPHOS for ATP production. Potentially the exon 9 deletion causes a more severe glycolysis deficit than the point mutations that we have investigated in this study. This would lead to a greater reliance on OxPHOS, and may lead to higher OCR rates.

The morphology of the mitochondrial network is altered in both sporadic and familial AD astrocytes showing longer mitochondria that are more interconnected. Potentially these changes could suggest that the astrocyte is under metabolic stress, and the trend towards an increase in the percentage of perinuclear mitochondria would suggest a collapsing mitochondrial network. As the AD astrocytes have a deficit in glycolysis as well as OxPHOS, it is difficult to know if the mitochondrial changes seen are a consequence of glucose metabolism failure, leading to an increased need for OxPHOS, or if the astrocytes have inherent deficits in mitochondrial function. The fact that MSRC and glycolytic reserve were significantly reduced in both sporadic and familial AD astrocytes, suggests primary deficits in both metabolic pathways, as opposed to the glycolysis defect causing a secondary mitochondrial functional change. The reduction in mitochondrial cellular ATP production when complex I substrates are supplied to astrocytes, is also further evidence of a primary deficit in OxPHOS.

In our previous work in AD fibroblasts using the same sporadic lines we see very similar mitochondrial morphological changes [477]. The changes we see to the astrocyte mitochondrial network in AD in this study are likely to lead to increased production of reactive oxygen species, as they are very suggestive of a stressed mitochondrial network. Astrocytes are exposed to increased amounts of oxidative stress in AD due to the accumulation of amyloid beta within them [370]. Potentially, the changes in mitochondrial structure and changes to OxPHOS and glycolysis reported here would be able to propagate a cycle of increasing oxidative damage and decreased metabolic function in a brain exposed to increased amounts of amyloid beta.

This study offers further characterisation of astrocyte OxPHOS and glycolysis in both sporadic and familial AD. We have highlighted that glycolysis is significantly impaired in AD astrocytes, and that this is likely to affect their ability to support neuronal function. Further work is needed to identify the mechanistic basis of the OxPHOS, and glycolysis deficits identified in the study. This would include examination of glycolytic enzyme function, quantification of GLUT receptors on the

astrocytes, and completion of glucose uptake experiments, which time restrictions did not allow. Mitochondrial ETC complex activity should be further investigated to identify the cause of the reduced MSRC. Co-culture of the astrocytes with neurons would also be essential to identify if the above changes lead to neuronal functional impairment.

5.2.2 Astrocyte metabolism correlations with neuropsychological changes

In our previous paper we have shown that deficits in MSRC and MMP correlate with neuropsychological changes seen early in AD. We repeated this analysis with the patient derived sporadic astrocytes and saw very similar correlations. As well as looking at mitochondrial functional parameters we also investigated if glycolytic reserve, and extracellular lactate correlated with neuropsychological changes. We found in both cases that immediate and delayed recall correlated significantly with extracellular lactate levels and glycolytic reserve. Extracellular lactate also correlated with semantic fluency significantly. When studying fibroblasts, significant correlations were not seen with glycolysis parameters, but have been seen in astrocytes. This could reflect the fact that the astrocyte depends on glycolysis to a higher degree than the fibroblast. It is also interesting that extracellular lactate correlates with neuropsychological measures considering the importance lactate has in neuronal metabolism. The correlations between extracellular lactate and immediate and delayed recall did not survive controlling for factors that can affect scoring on neuropsychological tests such as age, brain reserve and years of education. This may be explained by the small sample size of study. The fact that both MSRC and glycolytic reserve correlate with neuropsychological measures is interesting, as both these tests assess capacity in metabolic systems. We and many other groups have shown that metabolic capacity is affected in AD [165, 184, 207, 477, 478, 504]. How metabolic capacity is implicated at the start of disease would be very interesting area of future research.

This is the first study to show that astrocytic glycolytic reserve, extracellular lactate and MSRC correlates with scoring on neuropsychological tests shown to be affected early in AD. This is an important finding, as there is potential to develop a metabolic biomarker from these functional deficits. The development of clinical studies investigating astrocyte metabolism enhancers in AD could also use these correlations to track compound effect. Caution in interpreting this correlation is needed as this is a small cohort of sporadic patients. Further work on larger cohorts of sporadic AD patients would be needed before these correlations could be developed into a clinically useful tool.

5.2.3 Small molecule compounds correct astrocyte metabolic deficits

After thoroughly characterizing the metabolic phenotype in AD astrocytes, we went on to assess if the mitochondrial abnormalities could be modulated by small molecule treatment; the first step in assessing mitochondrial dysfunction in AD astrocytes for a therapeutic target. The compounds were pre-selected for known restorative mitochondrial effects in cells derived from patients with either PD or ALS and systemic disease. The effect on mitochondrial function and morphology was different when comparing sporadic and familial AD astrocytes. sAD astrocytes had a reduction in mitochondrial length and the mitochondrial network became less interconnected, which may suggest a reduction in metabolic stress. fAD astrocytes showed a reduction in mitochondrial length, but mitochondrial interconnectedness was affected less. This difference may be due to the smaller number of lines used in the familial AD experiments, making morphological changes more difficult to identify. The familial AD astrocytes had greater deficits in OxPHOS than the sporadic AD astrocytes, which may also explain why the familial AD astrocytes saw less improvement in mitochondrial morphology when drug treated.

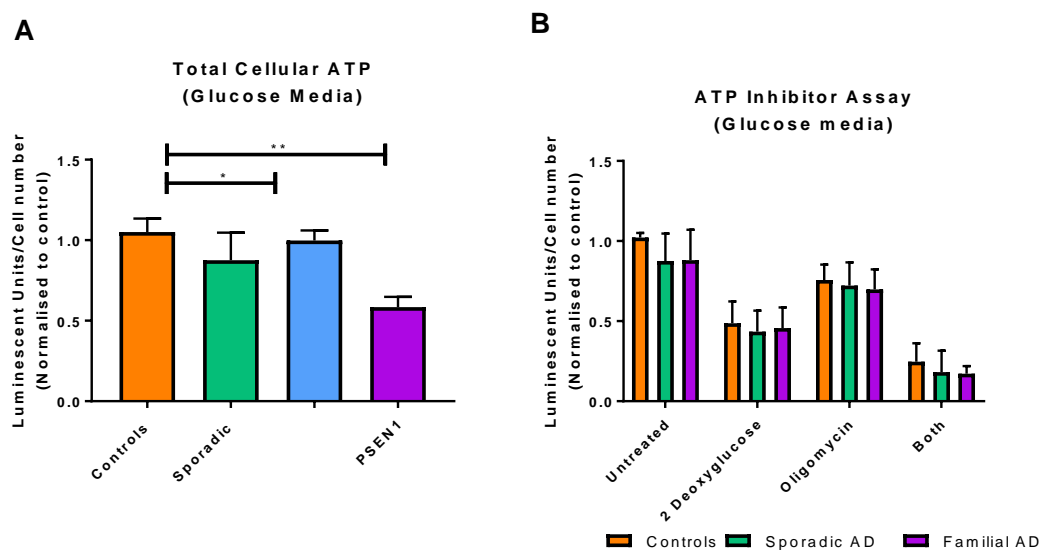
As mitochondrial morphology did not undergo dramatic changes after application of the compounds to the astrocytes, it could be postulated that the method of ATP increase was not generated by improved mitochondrial function. Several of the compounds used in this study are known to increase glycolysis as well as OxPHOS, therefore the effect on ATP production may be caused by improvement in glycolysis. The exact mechanism of action of each compound needs to be thoroughly investigated however our study shows that mitochondrial function can be manipulated by small molecule treatment. This is the first study to show that deficits in ATP production in astrocytes can be corrected with the application of drugs known to improve mitochondrial function.

This study is limited by sample size but is one of the larger studies investigating metabolic abnormalities in astrocytes derived from both sporadic and familial AD patients. As we have identified glycolytic pathways as playing a greater contribution to the metabolic disruption in astrocytes than mitochondrial function further work could focus on characterization of astrocyte glucose receptors, and glycolytic enzyme activity which has not been done as part of this study. Further work is also needed to identify if the compounds used in this study improve glycolytic function, as this may also be contributing to the increased total cellular ATP generated when they are applied to astrocytes. It would be important to also investigate how these metabolic deficits identified in this study affect the ability of astrocytes to support neurons in co-culture, and if each of the 8 compounds tested can correct any deficits in astrocyte neuronal support.

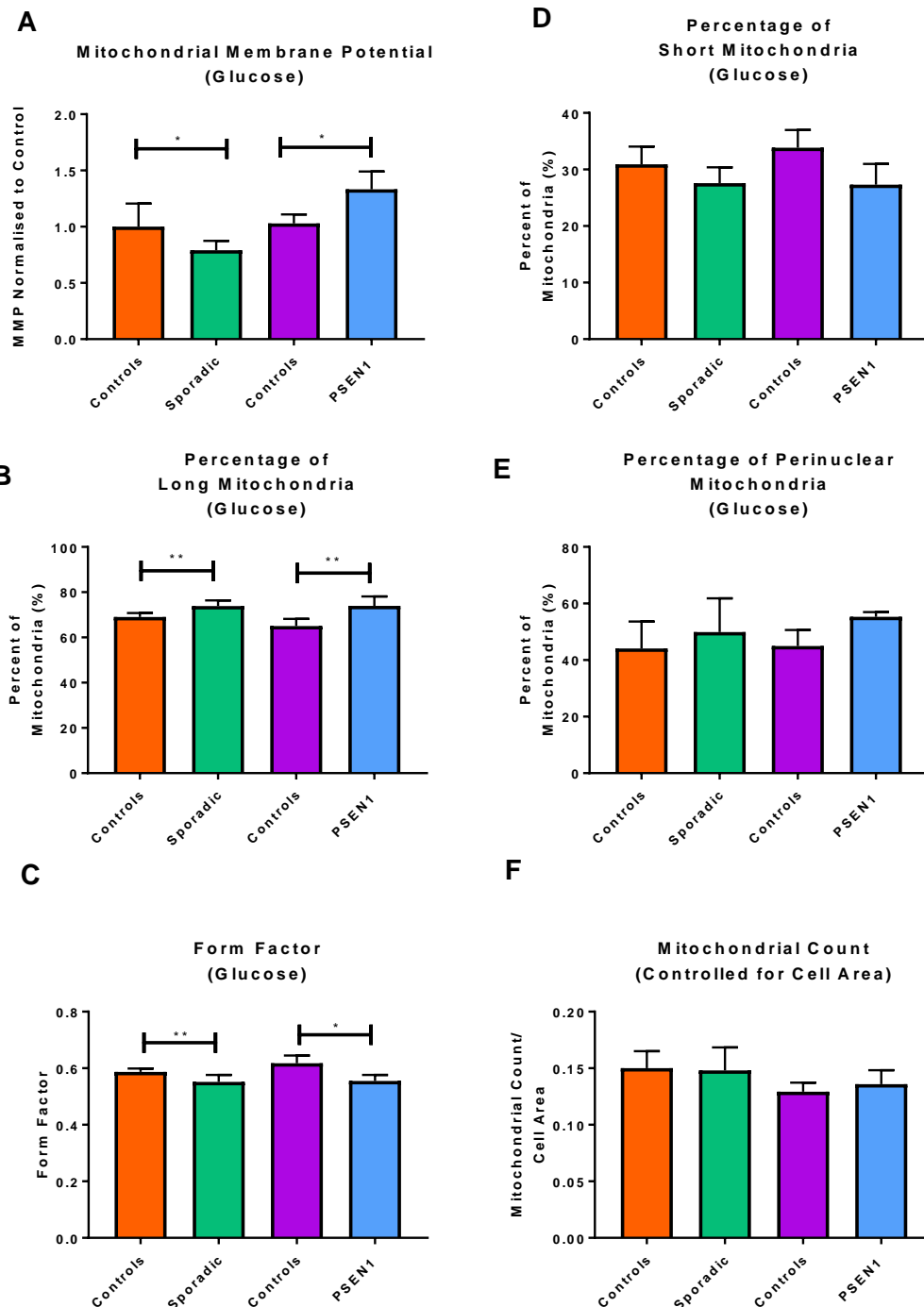
5.2.7 Conclusions

In this study we show that astrocytes derived from patients with sporadic or familial AD have deficits in both mitochondrial function and glycolysis. These deficits correlate with neuropsychological tests which show early change in AD and can be corrected with the application of drugs that alter both mitochondrial function and glycolysis. The metabolic deficits could have a profound effect on the astrocytes ability to support neurons in co-culture, and are a future therapeutic target for both sporadic and familial AD. This is the first study to show that iNPC technology can be used to derive astrocytes from patients with sporadic or familial AD.

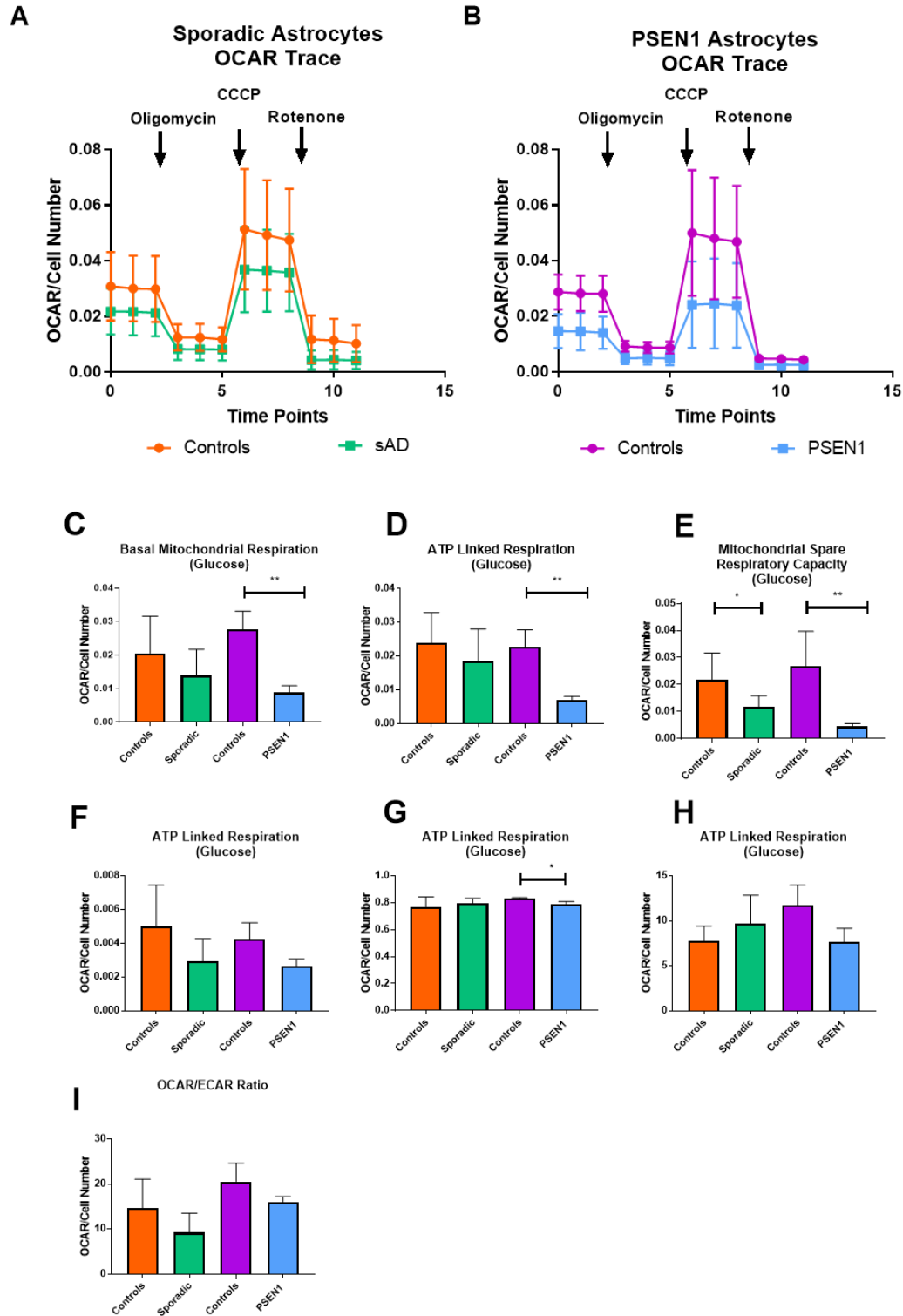
5.2.8 Supplementary figures



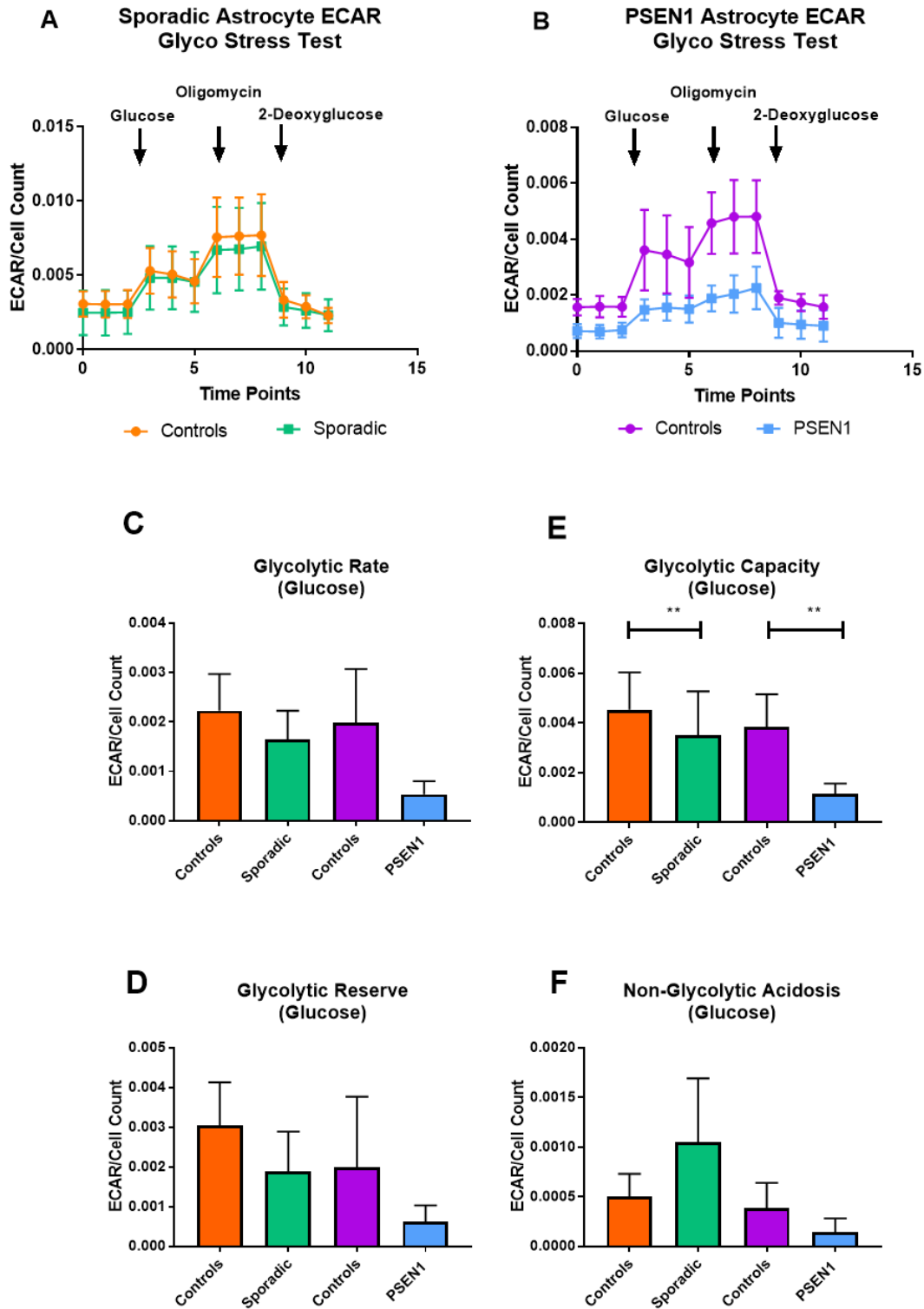
Supplementary Figure 1| Glucose media Total Cellular ATP This figure displays the results for total cellular ATP measurement in astrocytes when grown in a glucose based media. As with the galactose based media the astrocytes from both sporadic and familial AD patients have a significant reduction in total cellular ATP ([Figure S1A](#)), and depend more on glycolysis for total cellular ATP levels ([Figure S1B](#)) In all panels sporadic controls are represented in orange, sporadic AD lines in green, Familial controls in purple and familial AD astrocyte lines in blue.



Supplementary Figure 2 / Mitochondrial Morphology Glucose Media Mitochondrial morphology parameters of mitochondrial membrane potential (Figure S2A), percentage long mitochondria (Figure S2B), mitochondrial form factor (Figure S2C), percentage short mitochondria (Figure S2D), perinuclear mitochondria (Figure S2E) and total mitochondrial count (Figure S2F) are displayed in glucose media, similar trends are seen to that astrocytes grown in galactose based media. In all panels sporadic controls are represented in orange, sporadic AD lines in green, Familial controls in purple and familial AD astrocyte lines in blue.



Supplementary Figure 3 Astrocyte Oxidative Phosphorylation in glucose media This figure highlights the changes seen to oxidative phosphorylation when sporadic and familial AD astrocytes were cultured in glucose based media. In all panels sporadic controls are represented in orange, sporadic AD lines in green, Familial controls in purple and familial AD astrocyte lines in blue.



Supplementary Figure 4 | Astrocyte Glycolysis in glucose media this figure highlights the changes seen in glycolysis when sporadic and familial AD astrocytes were cultured in a glucose based medium. In all panels sporadic controls are represented in orange, sporadic AD lines in green, Familial controls in purple and familial AD astrocyte lines in blue.

END OF CHAPTER PAPER

5.3 Additional results

5.3.1 Total cellular ATP levels are lower in ApoE ϵ 4/4 genotype astrocytes

Astrocyte sporadic lines were divided based on ApoE genotype which showed a significant reduction in total cellular ATP in the ApoE ϵ 4/4 genotype group (36% reduction $p=0.001$) when compared to controls (Figure 5.11A). A non-significant reduction in total cellular ATP was seen in the 3/4 and 2/3 genotypes but not in the 3/3 genotype. Of note ApoE genotype was not available for one of the sAD astrocyte lines.

5.3.2 Astrocyte glycolytic and mitochondrial abnormalities are independent of ApoE genotype

A reduction in MSRC and MMP was seen in all sporadic ApoE genotypes, but no particular genotype showed a greater deficit than another. When comparing each separate group of sAD lines split by ApoE to controls no significant differences were seen. This is a similar finding to that seen in the sporadic fibroblast group as discussed in chapter 3 in sections 3.3.3 and 3.3.4 (Figures 5.11 B&C). Glycolysis markers were also investigated for differences based on ApoE genotype. No significant difference in sAD astrocyte glycolytic reserve was seen when lines were split via ApoE genotype (Figure 5.11D). This finding was the same in the sAD fibroblasts. When investigating extracellular lactate levels there was a significant reduction in extracellular lactate in the ApoE ϵ 4/4 genotype when compared to controls (75% reduction $p=0.0007$, see Figure 5.11E). All sAD ApoE genotypes showed a reduction in extracellular lactate levels in sAD astrocytes, with the ApoE ϵ 2/3 genotype having a similar reduction in extracellular lactate to that seen in the 4/4 genotype. No significant difference based on ApoE ϵ 3/4 or 3/3 genotype was seen in extracellular lactate in sporadic AD fibroblasts. Glycolysis rate was also investigated, but no difference in ApoE was seen (data not shown). Sporadic AD astrocyte groups split based on ApoE genotype were compared using a one-way ANOVA to look for genotype differences. No significant difference was seen between sporadic AD astrocytes with different ApoE genotypes, when compared to each other.

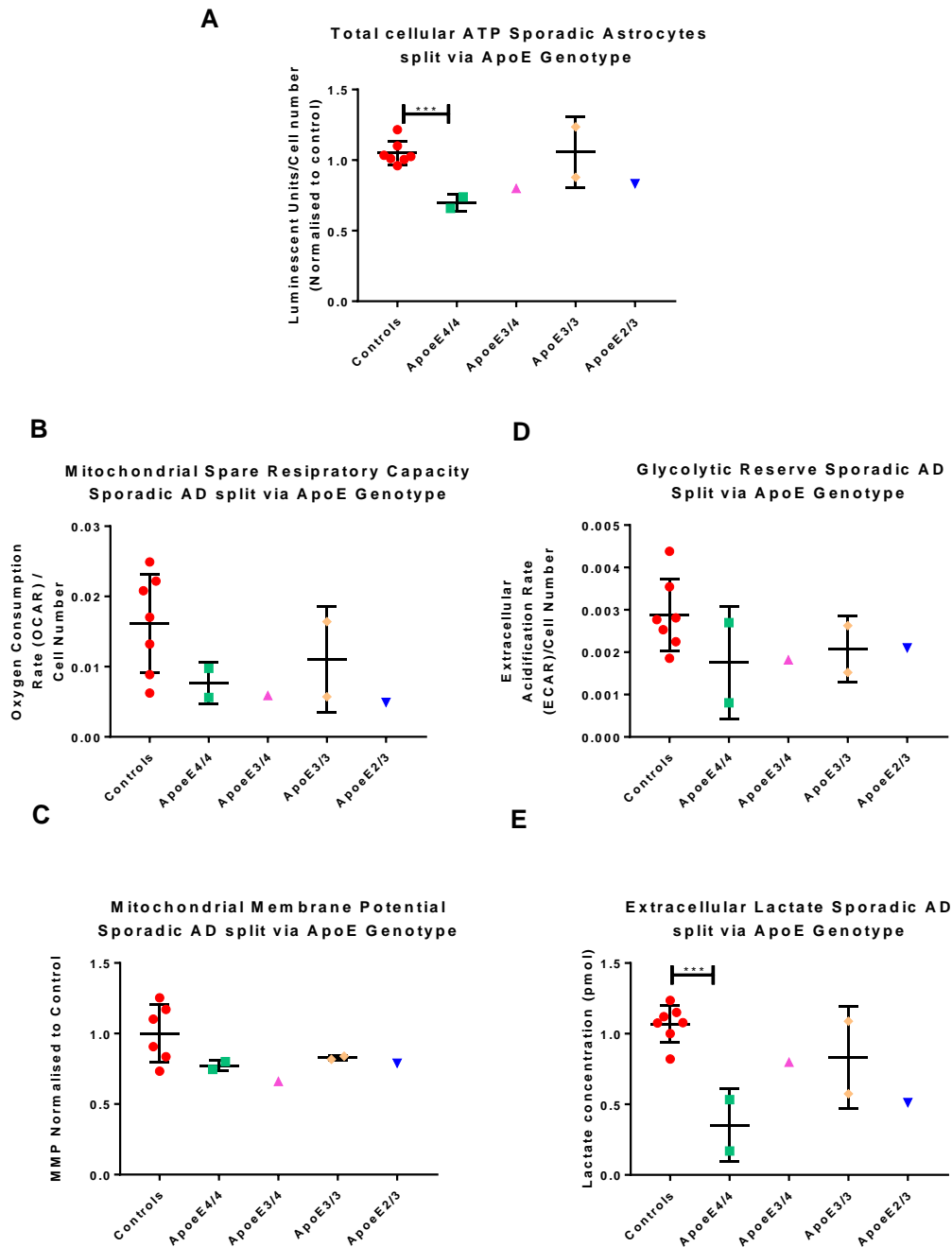


Figure 5.11| Astrocyte metabolic parameter split via sporadic Apoε genotype Figure displays total cellular ATP (Figure 5.1A), MSRC (Figure 5.1B), MMP (Figure 5.1C), Glycolytic reserve (Figure 5.1D) and extracellular Lactate (Figure 5.1E) with sporadic AD astrocyte line split based on ApoE genotype. ***=P<0.001. T-tests were performed for statistical comparisons. Red dots represent control astrocytes (n=7) of all ApoE genotypes, green dots represent sporadic AD astrocytes with an ApoE ε4/4 genotype(n=2), pink dots represent sporadic AD astrocytes with a 4/3 genotype (n=1), orange dots sporadic AD astrocytes with a ApoE ε3/3 genotype (n=2) and blue dots represent sporadic AD astrocytes with a ApoE ε2/3 genotype (n=1).

For control astrocytes the variance between different ApoE genotypes was assessed prior to investigating the effect of ApoE genotype on sporadic AD astrocytes. As with control fibroblasts, described in chapters 3&4, no significant difference between control astrocyte genotypes was seen when comparing ApoE groups. Figure 5.13 displays this data.

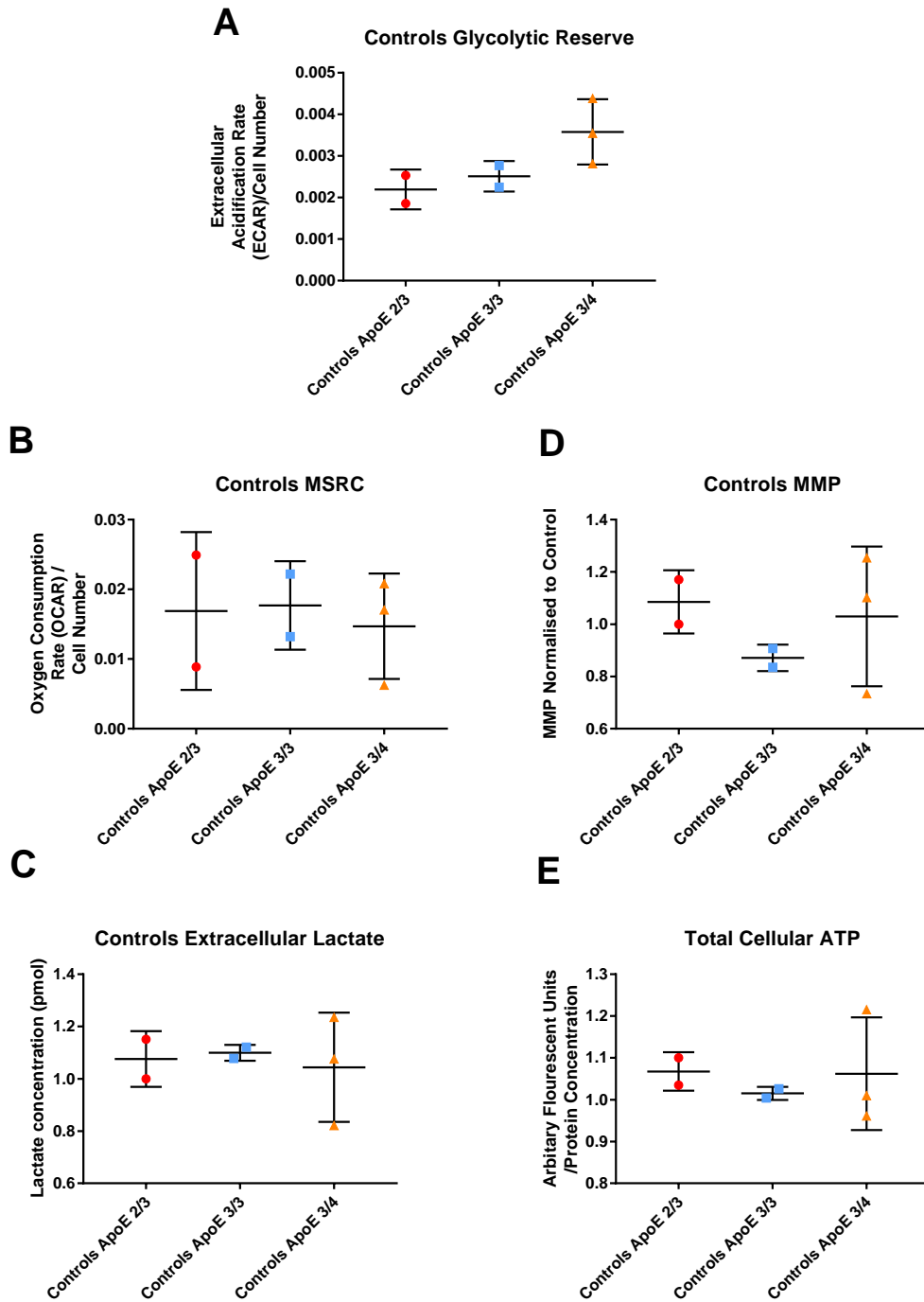


Figure 5.12 | Control Astrocytes separated based on ApoE status No difference was seen when the control cohort was split based on the astrocyte lines ApoE genotype for any of the five metabolic parameters assessed (Figures 5.12A-E). In each graph ApoE $\epsilon 2/3$ control fibroblasts are represented by red dots (n=2), ApoE $\epsilon 3/3$ controls represented by blue dots, (n=2) and ApoE $\epsilon 3/4$ controls represented by orange dots (n=3). A one-way ANOVA was performed to assess statistical significance for each morphological parameter.

5.3.3 Extracellular lactate levels correlate with DMN connectivity changes

DMN connectivity was investigated in the same way as previously described for fibroblasts detailed in chapter 4. MSRC, Glycolytic reserve and Extracellular Lactate were assessed for DMN correlations, as these parameters had correlations with neuropsychological parameters described in the chapter 5 paper. Bilateral prefrontal connectivity and right inferior parietal lobule connectivity were assessed for each metabolic parameter, as these connectivity areas showed positive correlations in fibroblasts. No significant correlations were seen between MSRC and bilateral frontal connectivity, or right inferior parietal lobule connectivity (Figures 5.13 A&B). No significant correlations were seen between glycolytic reserve and bilateral frontal connectivity, or right inferior parietal lobule connectivity (Figure 5.13 C&D). With extracellular lactate levels no significant difference was seen with and bilateral frontal connectivity, (Figure 5.13E), but a significant positive correlation was seen between extracellular lactate levels and right inferior parietal lobule connectivity ($R=0.788$, $p=0.001$ see Figure 5.13F).

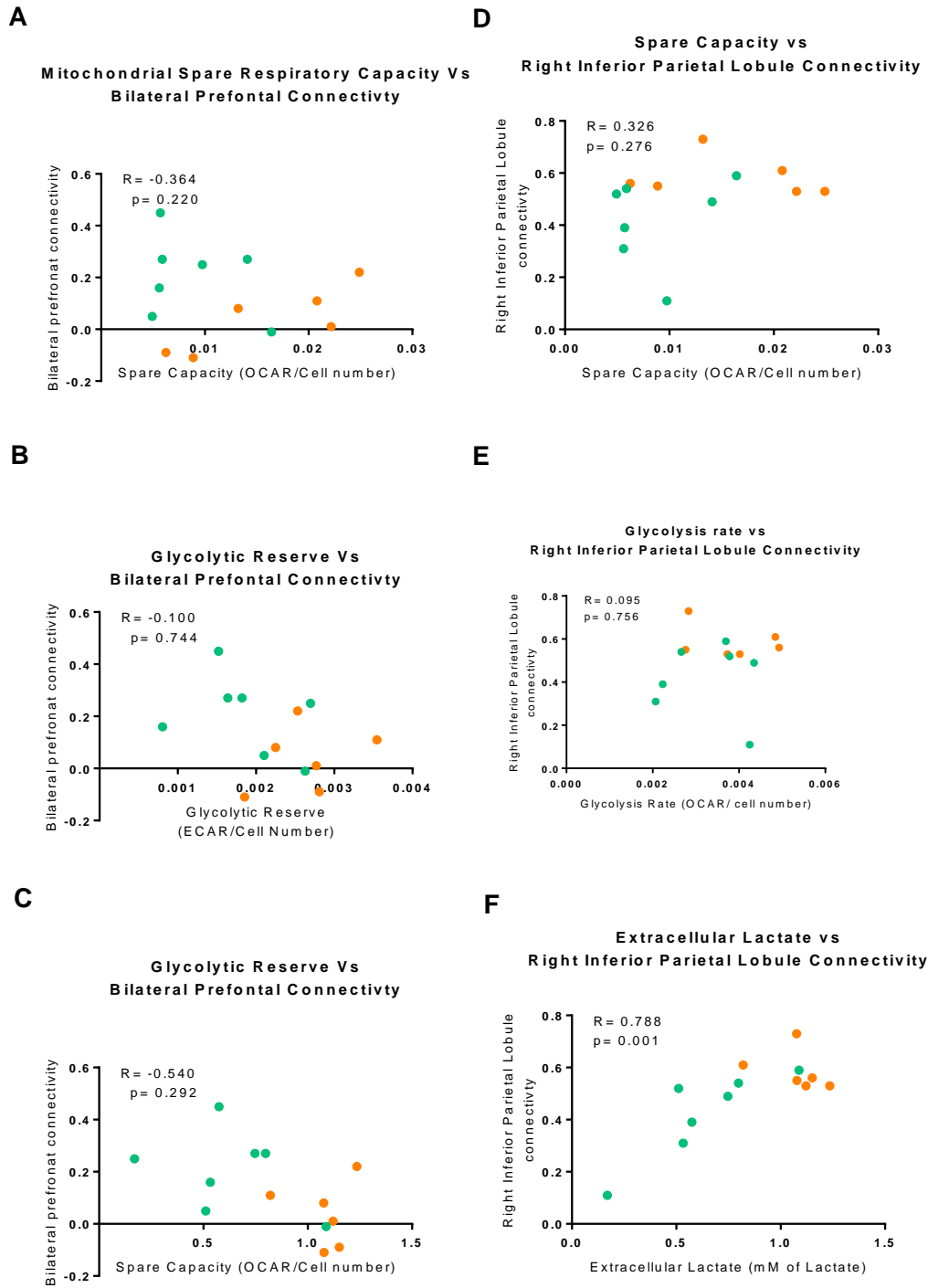


Figure 5.13 | Metabolic DMN correlations Figure displays correlations between bilateral frontal connectivity, or right inferior parietal lobule connectivity and MSRC (Figures A&B), Glycolytic Reserve (Figures C&D), and Extracellular Lactate Levels (Figures E&F). A Pearson’s correlation coefficient was used in each panel figure. Green dots represent sporadic AD astrocytes and orange dots represent control astrocytes.

5.3.4 Astrocytes derived using the iNPC method maintain an aged phenotype

To determine if astrocytes generated using the iNPC method displayed an aged phenotype, qPCR was performed on astrocytes of participants who were of 3 years old or younger (n=3) and participants who were over the age of 40 years old (n=3). Table 5.7 displays the cell lines used for this experiment and where they were sourced from. The work presented here contributed to a larger paper currently under review investigating the maintenance of the aged phenotype in iNPC derived astrocytes using this reprogramming method [496]. Fibroblasts samples taken from participants under the age of 3, i.e., below the age of consent were taken from established tissue banks (Coriell Institute).

Cell Line	Age	Source
Young 1	5 Months	Coriell (GMO8680)
Young 2	3 Years	Coriell (GMO0498)
Young 3	3 Years	Coriell (GMO3813)
Old 1	56 Years	Sheffield Cohort (Control 4)
Old 2	55 Years	Sheffield MND Cohort (3050)
Old 3	42 Years	Sheffield MND Cohort (155)

Table 5.7 | Ageing qPCR cell lines: This table displays the lines used in the aging qPCR experiments.

The expression of three genes described in the chapter introduction that have been shown to decrease with age (RanBP17, LAMA3, and TERF2) were assessed. Fibroblasts and astrocytes from each of the 6 lines highlighted above had RNA levels of the 3 proteins measured. All three proteins in both fibroblasts and astrocytes showed decreased expression with age (Figures 5.14A-C). A significant reduction was seen in RanBP17 levels in older fibroblasts (50% reduction, $p=0.0280$) when compared to young fibroblasts. The same change was seen in RanBP17 in old astrocytes (95% reduction, $p=0.0029$) when compared to young astrocytes. TERF2 was reduced in both old fibroblasts (50% reduction, $p=0.05$) and old astrocytes (76% reduction, $p=0.0065$) when compared to controls as well. LAMA3 was reduced in both old astrocytes and fibroblasts when compared to controls, but only a significant reduction was seen in old fibroblasts (80% reduction, $p=0.0113$), see figures 5.14A-C).

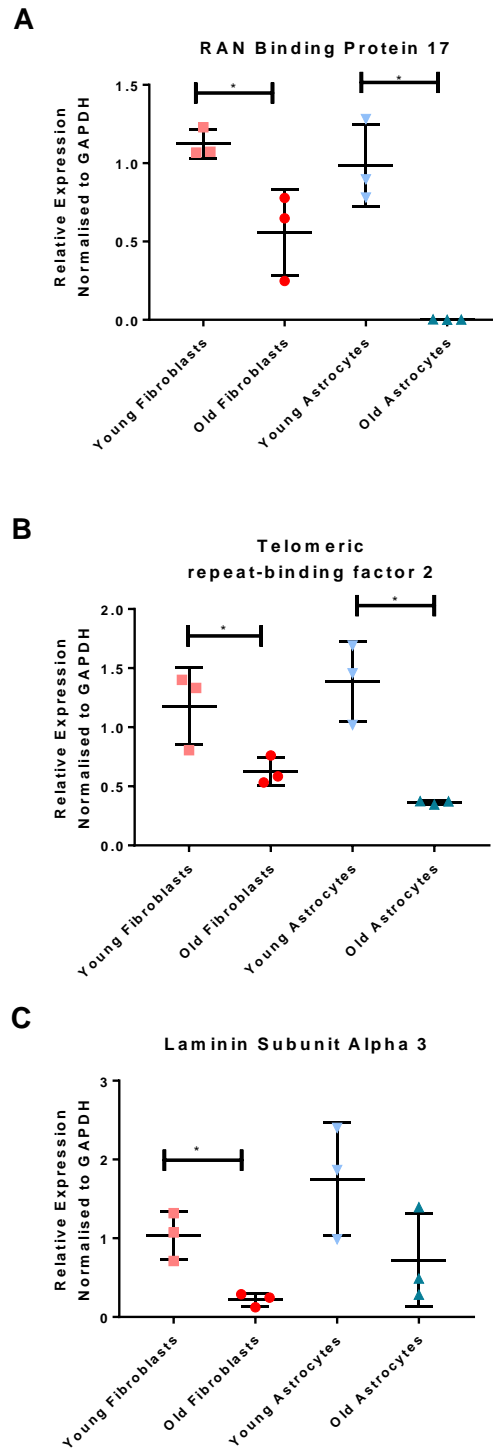


Figure 5.14 | qPCR data for ageing related gene expression The figures show RNA levels for RAN binding Protein 17 (Figure 5.14A), Telomeric receptor-binding factor 2 (Figure 5.14B) and Laminin Subunit alpha 3 (Figure 5.14C). For each panel data is displayed for young fibroblasts (pink), old fibroblasts (red), young astrocytes (pale blue) and old astrocytes (dark blue). All three genes show lower expression levels in older fibroblasts and astrocytes. *= $p < 0.05$. T-tests were performed for statistical comparisons.

5.4 Discussion

In this chapter astrocytes derived from patients with both sporadic and familial AD have been metabolically characterized. The astrocytes were derived using iNPC technology. The astrocytes were shown to have deficits in mitochondrial function, form and glycolysis when compared to controls in both AD disease types. The main deficits appeared to be in glycolysis, which was shown to be the main metabolic pathway used by astrocytes to produce ATP. Astrocytes had a reduced capacity to perform both OxPHOS and glycolysis in both types of AD. These metabolic deficits correlated with neuropsychological changes seen early in AD, and the reduced total ATP seen in the AD astrocytes could be corrected by compounds that have a mechanism of action that can alter both glycolysis and OxPHOS. This is one of the first studies to show metabolic deficits in astrocytes derived from patients with sporadic and familial AD. The rest of the chapter discussion will mainly focus on the extra chapter results.

5.4.1 ApoE genotype does not differentiate all metabolic abnormalities in AD sporadic Astrocytes, but may influence ATP levels

As with sporadic AD fibroblasts, sporadic AD astrocytes with the $\epsilon 4/4$ ApoE genotype appear to have more of a total cellular ATP deficit than AD astrocytes with other ApoE genotypes. This is an interesting finding and consistent with the idea that the ApoE $\epsilon 4/4$ causes metabolic deficits [422, 425]. As already mentioned though, separate ApoE genotype groups are very small in this study, and the study was not powered to identify metabolic deficits in specific ApoE genotypes in AD. Interestingly, the majority of other metabolic markers shown to be effected on a group level in sporadic AD, except for extracellular lactate, did not show a disease effect of ApoE $\epsilon 4/4$ genotype. Sample size could be the reason for this, but it should also be considered that the metabolic deficits are independent of ApoE genotype, and may be a separate contributing factor to the development of AD when investigating metabolic change in astrocytes.

Both MSRC and extracellular lactate levels in sporadic AD astrocytes showed the greatest reductions when compared to controls, in the ApoE $\epsilon 4/4$ and $2/3$ genotypes. Having a ApoE $\epsilon 2$ allele has been shown to be protective against AD in many studies, so this is an interesting finding [509, 510]. This may be further evidence that ApoE does not cause all the metabolic changes seen in AD but may also be a consequence of having allele heterogeneity. The ApoE $\epsilon 3$ allele may be driving the reduced metabolic function in the ApoE $\epsilon 2/3$ genotype, but a caveat to this idea is that the ApoE $\epsilon 3/3$ genotype appears to be least effected in regard to both MSRC and extracellular lactate. In this study fatty acid metabolism, and lipid transport have not been studied, which are the main effector sites for the ApoE gene [422]. To understand the interaction between ApoE and metabolism, further work

in bigger cohorts of sporadic AD patients controlled for ApoE genotype, which also investigates lipid metabolism, is required.

5.4.2 Extracellular lactate levels correlate with connectivity of the DMN

Of all the metabolic markers shown to be abnormal in AD astrocytes extracellular lactate level was the only marker that correlated with connectivity within the DMN. A strong positive correlation was seen between extracellular lactate levels and the connectivity within the inferior right parietal lobule. The inferior right parietal lobule is a component of the posterior DMN, an area of the DMN shown to be effected the most by the progression of AD [453, 511, 512]. As glucose metabolism alterations are one of the changes seen in the posterior DMN in AD, this may explain why extracellular lactate levels correlated with this DMN area. As already discussed, lactate is a major metabolic substrate produced by the astrocyte that is exported to the neuron. It would therefore be logical that astrocyte extracellular lactate levels would correlate with a marker of neuronal activity. PM studies investigating the expression of LDH and PK, enzymes involved with the metabolism of glucose to lactate, show increased levels of these enzymes in frontal and temporal regions but not in parietal regions in the AD brain [278]. This may highlight that the parietal lobe has an inability to increase lactate production in patients with AD when compared to frontal and temporal lobes, and may be the reason for the correlation between DMN connectivity and extracellular lactate levels. This relationship between extracellular lactate level and DMN connectivity could be studied further by investigating glucose metabolism, and other metabolic pathways in this particular area of the brain using PM AD samples.

5.4.3 Astrocyte deficits are more pronounced in galactose-based media

In the case of both OxPHOS and glycolysis assessment in this study, a more pronounced metabolic deficit was seen in galactose based media than a glucose based one. This would be expected with the OxPHOS deficits, as the metabolism of galactose consumes as much ATP as it generates, therefore cellular ATP demands rely more on OxPHOS. The experiments that investigated glycolysis in a glucose based media, were more variable than the glycolysis experiments performed in a galactose based media. This finding may be explained by the diverse nature of glucose metabolic fates in astrocytes. When an astrocyte is grown in an abundance of glucose it has several different sources of glucose that can be metabolised to meet the energy requirements of the cell. These include the media glucose, glucose stored as glycogen within the astrocyte, and lactate generated from neurotransmitter turnover and the PPS. In a galactose based media, the media galactose will not contribute to ATP output of the astrocytes, and so it will rely on other glucose sources. This may reduce variability when investigating glycolysis as the glucose sources that can be drawn upon have been decreased. As the most significant deficit in glycolysis in the galactose based media was a

reduction in glycolytic reserve this may also suggest that the AD astrocytes have a reduced storage capacity for glucose, and the reduction in reserve may be driven by either decreased glycogen stores or deficits in neurotransmitter metabolism. Further work investigating glycogen storage in astrocytes in a glucose and galactose based media would help answer this question.

5.4.4 Astrocytes have an aged phenotype based on RNA expression

One of the benefits of using a direct reprogramming method is that differentiated cells maintain an aged phenotype. The differentiation protocol used in this study produces astrocytes that maintain an aged phenotype evidenced by the fact that qPCR identified 3 genes (RanBP17, LAMA3 and TRF2) that have reduced expression as we age. This is consistent with literature of other direct reprogramming techniques which shows that RanBP17 and LAMA3 both have reduced expression in cells derived from older individuals [393], and that reduced telomere length, a sign of ageing, is to a certain extent, controlled by the expression of TRF2 [473]. Although these gene expression changes are a compelling argument of the retained aged phenotype of the astrocytes further investigation of the aged phenotype is warranted. Unpublished work from another group member has shown that astrocytes derived using this technique have altered nuclear compartmentalization, changes to nucleocytoplasmic shuttling properties, increased oxidative stress response and DNA damage response [496]. These are all features of cellular change seen in ageing.

Using a model system with an aged phenotype is important for this particular study as the metabolism of glucose changes as we age [480, 513]. Mitochondrial function is also known to change with the ageing process, with reduced ETC efficiency, increased mitochondrial DNA mutations, and decreased quality control all reported [514]. The fact that we have seen abnormalities in astrocyte function when AD lines have been compared to aged-matched controls shows that metabolism changes identified are likely to be a factor independent of the changes to metabolism seen during ageing.

5.5 Chapter limitations

Although powered to show group level differences in glycolysis and OxPHOS, a larger sample size to that studied here is needed to fully understand relationship between AD, ApoE, and metabolism changes. As stated in chapter 3 the study is underpowered to fully understand the relationship between apo ϵ expression and cellular metabolic changes. It is not debated however that astrocytes express the Apo ϵ , unlike in fibroblasts, so further work with an increased sample size split based on Apo ϵ status would be of merit. An increased sample size would also help to develop the understanding of the DMN correlations seen in this study. As discussed in chapter 4 when the same correlations were performed in fibroblasts, this element of the study should be considered a proof

of principle analysis, with further work needed in different model systems to link metabolism dysfunction to neuropsychological deficits more convincingly. As both mitochondrial and glycolytic deficits have now been identified, further work is needed to understand the mechanistic side to these changes in metabolism. This would include interrogation of the function of each of the separate ETC complexes in the mitochondria to identify the cause for the reduced MSRC and MMP. Further work needs to be performed on mitochondrial dynamics, with investigation of the proteins that control mitochondrial fission in particular. Investigation of glucose uptake into astrocytes via understanding of glucose transporter expression, and further characterisation of the different metabolic pathways involved in glucose metabolism is needed. This should include the investigation of glycogen storage, function of the PPS, and glycolysis enzyme activity.

Although astrocytes derived from patients with AD clearly have significant deficits in metabolic function, important future work would need to focus on how these astrocytic metabolic changes effect neuron support in co-culture, and if the drugs that improve ATP production in astrocytes effect this co-culture support relationship.

5.6 Chapter Conclusions

1. Astrocytes derived from sporadic and familial AD patients have reductions in total cellular ATP when compared to controls and are more reliant on glycolysis than OxPHOS for total cellular ATP.
2. Astrocytes derived from both sporadic and familial AD patients have reductions in MSRC when compared to controls.
3. Sporadic AD astrocytes have a reduction in MMP whereas familial AD astrocytes have an increase in MMP when compared to controls
4. Both sporadic and familial AD astrocytes have a more interconnected mitochondrial network, with longer mitochondria when compared to controls.
5. Both sporadic and familial AD astrocytes have reductions in glycolytic reserve and extracellular lactate when compared to controls.
6. Total cellular ATP and extracellular lactate levels may be affected by the ApoE ϵ 4/4 genotype, with sporadic AD astrocytes displaying this phenotype having greater deficits compared to controls.
7. MSRC, glycolytic reserve and extracellular lactate levels correlate with neuropsychological tests which show changes early in the course of AD
8. Extracellular lactate levels correlate with changes in DMN connectivity seen in AD.
9. 8 different drugs assessed could correct total cellular ATP deficits in both familial and sporadic AD astrocytes and alter mitochondrial morphology to a less diseased state.

10. Astrocytes derived using this reprogramming method maintain the expression of genes known to decrease with aging.

Chapter 6 Discussion

The aim of this PhD thesis was to characterize deficits in glycolysis, mitochondrial structure and function in fibroblasts and astrocytes derived from patients with both sporadic and familial AD. Secondary aims were to investigate if highlighted metabolic abnormalities correlated with established clinical biomarkers of AD, and whether the deficits identified could be corrected with drugs known to improve mitochondrial ATP production.

I have shown that deficits in glycolysis and mitochondrial function are present in the astrocytes and fibroblasts from patients with sAD and fAD (PSEN1 mutations). Specifically, the work in the thesis shows the capacity of the mitochondrial ETC and glycolysis are affected in both fibroblasts and astrocytes, with correlations between MSRC, glycolytic reserve, extracellular lactate production and neuropsychological tests shown to be abnormal early in AD identified. This research identifies that mitochondrial and glycolytic abnormalities in both astrocytes and fibroblasts from patients with AD are a potential future biomarker.

Mitochondrial functional and structural abnormalities identified in AD fibroblasts were corrected with the application of the drug UDCA. When AD astrocytes were treated with UDCA and an expanded cohort of compounds known to improve mitochondrial function, deficits in total cellular ATP and mitochondrial functional and structural abnormalities were also restored. This highlights how the metabolic deficits identified in this thesis have the capacity to be restored using small molecule treatments and are therefore potential therapeutic targets.

In the following sections these metabolic abnormalities will be discussed in greater detail.

6.1 Fibroblasts and Astrocytes have similar mitochondrial and glycolytic abnormalities in sporadic and familial AD

The abnormal metabolic profile is similar across both fibroblasts and astrocytes from both sAD and fAD patients, but difference in each cell group are present. Mitochondrial and glycolytic changes in the AD fibroblast groups were not as pronounced as those seen in the astrocytes. Defects common to both sporadic fibroblasts and astrocytes included reduced MSRC, an elongated, more interconnected mitochondrial network, and reduced glycolytic reserve. Familial fibroblasts and astrocytes showed similar changes but MSRC was not reduced in fAD fibroblasts. The markers of abnormal mitochondrial function and glycolysis common to both fibroblasts and astrocytes reflect deficits in the reserve capacity of mitochondrial function, and the reserve capacity of the glycolysis pathway. This appears not to affect the fibroblasts significantly, as without the presence of a known modulator of metabolic function (ApoE ϵ 4/4) no reduction in total cellular ATP is seen. It could be

postulated that the deficits in mitochondrial and glycolytic reserve capacity seen in fibroblasts and astrocytes are likely to reflect a reduced ability to manage metabolic stress, this could explain why the astrocytes which are a more metabolically active cell type than the fibroblasts, start to develop group level reductions in total cellular ATP that are independent of ApoE allele status. It has been shown in fibroblasts from patients with late-onset AD that deficits in mitochondrial OxPHOS are compensated for by increasing glycolytic function which increases fibroblast glycolytic capacity [207]. Astrocyte glycolysis is also known to be increased when astrocytes are exposed to amyloid [322]. Both these studies show how in AD cellular glycolytic capacity needs to increase to manage the metabolic cellular demand caused by increased amyloid presence and reduced mitochondrial efficiency. Although not direct evidence these studies do highlight how a reduced glycolytic reserve may affect cellular glycolytic capacity and therefore impair cellular responses to metabolic stress. The results from both AD fibroblasts and astrocytes suggest that deficits in metabolic capacity are common to both peripheral non-neuronal and CNS cells, which may be evidence that dysfunctional metabolism affects the whole body and not just the CNS in AD. This theory is supported by other studies that have shown mitochondrial and glycolytic changes in multiple cell types in AD [184, 204, 206, 207], but may also be supported by the fact that patients with AD are more prone to systemic infections [515] and have a reduced risk of developing certain malignancies [516]. MSRC reductions have been linked to an increased risk of developing infection [517], and established malignant cells are shown to have high glycolysis rates when compared to other cell types [518]. Therefore, deficits in glycolysis may protect an organ from malignancy developing, but deficits in MSRC may predispose to infection.

sAD fibroblasts and astrocytes both had a reduction in MMP, but fAD astrocytes had an increase and fAD fibroblasts had a decrease in MMP. This difference between the two AD cohorts may be explained by calcium concentration within the mitochondria. As the Presenilin mutations have been shown to increase mitochondrial calcium content [227-229], this potentially would increase the polarity of the mitochondria, which may lead to increased TMRM signal. Due to the changes to glycolysis and mitochondrial function in fAD astrocytes they may not be able to maintain calcium homeostasis as well as fAD fibroblasts due to the increased metabolic demand. This may explain why only fAD astrocytes had a raised MMP. Another discrepancy seen between fAD astrocytes and fibroblasts was the OCR. Sporadic and familial astrocytes had a decreased OCR when compared to controls, whereas fAD fibroblasts had significant increase in OCR when compared to control fibroblasts. The familial fibroblasts may be able to redirect substrates for metabolism via OxPHOS which would normally be consumed in glycolytic pathways, which may increase the OCR rate. As astrocytes have a greater metabolic demand than fibroblasts, and so greater need for glycolytic

substrates they may not be able to devote substrates common to both metabolic processes away from glycolysis utilization, and therefore have a lower OCR when compared to controls. fAD fibroblasts appear to have less efficient mitochondria when considering total cellular ATP as fAD have lower total cellular ATP levels, but higher OCR consumption when compared to control fibroblasts this relationship is also seen in fAD astrocytes. As fibroblasts need less ATP than astrocytes the inefficiencies of the OxPHOS pathway will have less energetic consequences and so the fibroblast cell can tolerate the reduced OxPHOS efficiency better than the astrocyte.

As both mitochondrial ETC function and glycolysis are interlinked metabolic pathways it has to be considered that the deficits seen in sporadic and familial AD may be a combination of deficits in both metabolic pathways, or that changes in one pathway lead to the deficits in capacity seen in the other. It is very likely that both astrocytes and fibroblasts have a primary deficit in glycolysis, as this metabolic pathway is upstream of mitochondrial OxPHOS, and hence the glycolysis deficits identified in this thesis are unlikely to be caused by the changes seen in mitochondrial function. The mitochondrial deficits on the other hand could be caused by the glycolysis changes. MSRC and MMP are determined by the function of ETC complexes I, III, & IV pumping protons across the inner mitochondrial membrane. In chapter 5 it was identified that astrocytes have a deficit in total cellular ATP when supplied with complex I substrates which suggests a complex I deficit. Complex I requires NADH to pump protons across the inner mitochondrial membrane. NADH can be sourced from both glycolysis and the TCA. Therefore, the deficits seen could be caused by a true complex I deficit or due to a reduced supply of NADH to complex I from either glycolysis or the TCA cycle. The fact that the assessment of complex I activity performed in this study uses an experimental paradigm where cells are supplied with an excess of complex I substrates points towards a glycolysis independent mechanism for the changes seen in OxPHOS.

Observing changes in fibroblasts metabolic function that correlate with changes in astrocyte metabolic function, which may lead to a drop in ATP levels, allows for the promotion of fibroblasts from patients with AD to be used as both a drug screening model, and a model for identify metabolic functional changes which may be important in AD. Using fibroblasts would be more cost effective than reprogramming the same number of astrocytes lines to test a hypothesis. When a drug target has been identified in the fibroblast lines this would then allow for further experimental work of target suitability to be performed in the reprogrammed astrocytes.

6.2 Astrocyte changes seen in other iNPC/iPSC models of neurodegenerative disease

Altered mitochondrial function and glycolysis has been reported in other iPSC models of neurodegenerative diseases. In both sporadic and familial MND a reduction in metabolic flexibility of astrocytes has been reported [396]. In this study the ability of astrocytes to create NADH when supplied with one of 91 different substrates was assessed. Astrocytes from sporadic and familial MND patients had a reduced number of substrates that they could create NADH from (10 vs 16). This was thought in the familial MND lines to be due to the C9orf72 protein expansion reducing the permeability of the cell membrane, but deficits in glycogen and fructose metabolism were also reported. The same group has also suggested that this lack of metabolic flexibility may be secondary to a deficit in adenosine deaminase in MND astrocytes [395]. Both these studies suggest that mitochondrial and glycolytic dysfunction may be a consequence of reduced supply of substrates to produce ATP. A deficit in MSRC is corrected and increased glycolysis are reported in C9orf72 familial MND lines when the effects of adenosine deaminase are by-passed [395]. Potentially the changes seen in this thesis in the function of astrocytes in sAD and fAD could be explained by a lack of metabolic flexibility with regard to the substrates that AD astrocytes can use to generate ATP. Performing similar experiments assessing the ability for AD astrocytes to use metabolic substrates would allow for comparison between different neurodegenerative conditions looking for common and unique metabolic signatures. These studies have not investigated if mitochondria from MND astrocytes have deficits in function or structure which might predispose them to have less metabolic flexibility. These studies have shown that astrocytes from the familial MND group have a normal expression of astrocyte glucose transporters, which would suggest against a lack of supply of glucose to the astrocyte causing the deficits seen in glycolytic rate. Interestingly, these studies look for the same metabolic changes in the fibroblasts for patient with C9orf72 mediated MND and find that the metabolic characterization of the fibroblasts is not as distinct as what is seen in the astrocytes, further showing the importance of cell specific study in neurodegenerative disease.

Mid-brain astrocytes derived from patients with familial mutations causing PD have been shown to have a more fragmented mitochondrial network, excess mitochondrial calcium release and a reduced MSRC [519]. In this study 3 familial forms of PD were studied, but only 2 showed reductions in MSRC, in this thesis a reduction in MSRC was seen in both sAD and fAD astrocytes, which is suggests that reduced MSRC is a common abnormality seen in astrocytes in several neurodegenerative diseases. Whether the cause of the reduction in MSRC is caused by a common pathway between both disease states is unknown and needs further investigation. There is a possibility that the mitochondrial deficits seen in a particular neurodegenerative disease are caused

by astrocyte reliance on specific metabolic substrates which non-neurodegenerative disease astrocytes do not depend on as much.

Work that has investigated astrocytes in co-culture with a human neuronal model of PD potentially highlights how abnormal metabolism in an astrocyte may propagate pathology in neurons. It has been shown that complex I and IV of the ETC have functional deficits in a PD neuronal model which can be corrected when co-cultured with iPSC astrocytes derived from a control cell lines [520]. The mechanism by which the astrocytes improve the PD neuron mitochondrial function is thought to be related to the astrocytes reducing the level of ROS present within the neuron. How the astrocyte performs this role may be by providing metabolic substrates to the astrocyte that bypass the function of the mitochondria and therefore reduce ROS production, or provide the neuron with antioxidant molecules such as glutathione, which remove the ROS generated. In either case, both processes are dependent on both astrocyte mitochondrial function and glycolysis performing within a boundary that allows for the energy demands of the astrocyte and neuron to be met. In this thesis it has been shown that both mitochondrial function and glycolysis are abnormal, which as shown in this PD model could worsen neuronal functional deficits.

These studies together show that similarities in astrocyte metabolic disturbance are seen across multiple neurodegenerative diseases, but potentially a specific pattern of metabolite usage may provide a disease specific signature. Limited numbers of studies have investigated human astrocyte metabolism across multiple diseases, which the above studies and this thesis highlight would be beneficial for understanding pathogenic metabolic mechanisms.

6.3 Mitochondrial dysfunction and its importance to AD

In both astrocytes and fibroblasts changes to the mitochondrial network are seen in this study. They include elongated mitochondria that are more interconnected, and are more focused around the cell nucleus. These changes in the structure of the mitochondria suggest that the cell is under metabolic stress, which is evidenced by the low ATP and MMP reported. A stressed mitochondrial network is more likely to produce ROS which can cause further stress and damage to the mitochondrial network by increasing mitochondrial DNA mutations. The particular changes in network structure may also have implications for cells with long projections, as the contraction of the mitochondrial network towards the nucleus may lead to these projections becoming devoid of mitochondria, or be left with not enough mitochondria to meet local cellular energy demands. The mitochondrial network changes may be caused by a changes in mitochondrial fission and fusion proteins, as described in chapter 3, which may mean that the pathology driving the change in network shape is protein expression abnormality as opposed to an inability of the mitochondrial network to maintain

cellular energy demands. Potentially both these explanations could be the reason for the change seen in mitochondrial network structure, as both decreased ATP demands and altered mitochondrial dynamics have both been reported in AD [418, 420, 479, 521].

The changes seen in MMP in this study are consistent with results from previous work on fibroblasts in both sporadic and familial AD, and astrocytes exposed to A β [522]. A reduced MMP could have significant implications for astrocytes as it will affect the ability of the mitochondria to buffer calcium currents produced in the astrocyte in response to several key physiological roles such as blood flow diversion, neurotransmitter metabolism and synaptic plasticity [523]. Altered blood flow and decreased synaptic plasticity are both seen in AD, and are potentially related to astrocyte mitochondrial dysfunction. A high MMP was seen in the fAD astrocytes, but if as hypothesised this is a consequence of already increased mitochondrial calcium concentrations, then the buffering capacity of the mitochondrial would be similarly affected to a state in which a low MMP is seen. Although astrocytes were shown in this study to be mainly dependent on glycolysis for total cellular ATP levels, it is also very likely that a reduction in MMP would contribute to this decreased ATP seen, which could compound the problems that a reduced mitochondrial calcium buffering capacity can cause, as ATP available for active pumping is reduced.

The cause for the reduced MMP seen in the sAD astrocytes in this study is likely related to the activity of the ETC complexes. It was shown in chapter 5 that sAD and fAD astrocyte mitochondria produce less ATP when supplied with complex I of the ETC substrates, suggesting a deficit in complex I function. Decreased expression of the mitochondrial subunits of complex I has been previously reported in the AD literature in PM specimens [175, 176], but by far more commonly reported are changes in the activity of complex IV [181-186]. Further work is needed to determine if the fibroblasts and astrocytes in this study have a complex IV deficit. Complex I activity deficits may drive reductions in MMP in astrocytes but not neurons and other brain cell types. As most data looking at complex activity comes from PM samples or studies focused on neurons, this deficit may have been missed. Further work is needed to clarify what the mechanism is that leads to the reduction in ATP production seen in AD astrocyte mitochondria in this thesis. This could be done by performing complex assays measuring the function of the ETC complexes separately. This would also reveal if the astrocytes used in this thesis have a complex IV deficit, as complex IV activity was not directly measured. If no deficit was found in ECT complex activity then this would also help develop our understanding of the mitochondrial deficits seen in AD astrocytes. Normal ETC function, and the already identified reduction in ATP production when cells are examined in complex I substrate excess may suggest that the intermediate metabolites passed between complexes are not in high enough supply.

It is possible that the changes to mitochondrial structure and function seen in this study are also seen in neurons from patients with AD. If neurons were shown to have the same mitochondrial deficits highlighted here in astrocytes and fibroblasts, then this would have a significant effect on their function as the main source of energy production in neurons is OxPHOS. Having a reduced MMP, and decreased MSRC would expose the neuron to increased ROS due to the need to divert glucose metabolites to OxPHOS to maintain ATP production. ROS production would increase as PPS metabolism would likely reduce. Therefore, the mitochondrial changes identified in the study are likely to have varying degrees of impact depending on cell type that they are expressed in.

6.4 Glycolytic dysfunction and its importance to AD

Impairments in glucose metabolism were seen in all cell types in this study. Glycolytic reserve and extracellular lactate levels were shown to be reduced in fibroblasts and astrocytes from both sporadic and fAD patients. Astrocytes from both sporadic and fAD patients also had deficits in basal glycolysis rate and glycolytic capacity, although not all these reductions were significant when compared to the astrocytes from healthy controls. Glucose is the main metabolite of the brain with astrocyte metabolism known to account for a large proportion of its utilization, therefore any reduction in the ability to metabolise glucose by the brain is likely to have functional implications. As already mentioned, astrocyte glucose metabolism has been shown to have a role in learning and memory [311, 312, 340], the results of this study suggest a decreased efficiency for glucose metabolism in astrocytes, which may have the consequence of making memory acquisition more difficult. Memory retrieval is also dependent, to a certain extent, on increased blood flow to particular brain areas [524]. As both blood redirection and glucose metabolism decrease during the course of AD, this could be explained by the glycolytic deficits seen here in astrocytes. If the same deficits were seen in neurons as well, the risk of neuronal oxidative damage is likely to increase, potentially making the deficits seen here key to the pathogenesis of AD.

Astrocyte glycolytic dysfunction is likely to be compounded by other aspects of AD pathology as well. Astrocytes have been shown to uptake A β with the aim of metabolising the protein and excreting it from the brain [321, 525]. Astrocyte uptake of A β has been shown to both increase astrocyte glycolysis, and also have a detrimental effect to neurons when they are co-cultured with A β primed astrocytes [526, 527]. The glycolysis deficits identified in AD astrocytes in this thesis may impair astrocytic ability to metabolise A β secondary to not being able to upregulate glycolysis, as is seen when A β is added to non-AD astrocytes. Glycolysis is also upregulated in neurons exposed to A β [288, 528] which is presumed to be a response to the increase in ROS production by mitochondria when exposed to A β . If glycolytic deficits seen in fibroblasts and astrocytes in this study are also common to neurons, this will also exacerbate the effect A β has on this cell type. Potentially in an AD-

susceptible brain a situation arises where increased amyloid production occurs which leads to mitochondrial stress meaning the brain relies more on glycolysis for energy production. Alzheimer's disease may progress in people who have a reduced brain glycolytic efficiency; resulting in impaired or reduced astrocytic clearance of A β , leading to further accumulation of A β , and loss of homeostatic mechanisms that exacerbates the effect A β has on mitochondrial function, and other neuronal processes. This hypothesis, whereby glycolysis efficiency determines A β mediated pathophysiology may explain why brain amyloid burden (as measured by amyloid PET scan or reduced CSF A β) does not correlate with the stage of Alzheimer's disease or predict disease progression. A brain with effective and efficient glycolysis would cope with the increased demand associated with increased A β levels in the brain better than in a brain with less efficient glycolysis (of whatever aetiology). The idea that glycolysis efficiency is key in the pathogenesis of AD is also supported by the fact that FDG-PET imaging data show areas of the brain at risk of developing early AD pathology, and loss of DMN connectivity, are the same brain areas that have the highest glycolysis requirements [452]. In the study by Buckner et al 2005 [452], the link between glycolysis demand and amyloid deposition was made by showing that areas of the brain with high glucose requirements in young people, are the same areas of the brain that develop amyloid deposition early in more elderly participants. This is a particularly good methodology to show this correlation, as normal ageing also reduces the brain glucose uptake [274]. Cell models of AD also suggest that glycolytic capacity may be protective against the negative effect of amyloid. When B12 and PC12 cell lines are grown in an amyloid rich media the cells that are able to utilize glycolysis better have greater survival than those that depend more on OxPHOS [288]. Animal models of AD also suggest that glycolysis is increased in response to amyloid build up [286], and evidence also exists which suggests that tau deposition in the human brain is increased in areas of lower aerobic glycolysis [483], adding further weight to the idea the glycolytic capacity and efficiency are a key mediator of AD pathology. In this study brain imaging of glucose usage, oxygen consumption and tau deposition was measured showing areas with low aerobic glycolysis had increased amounts of tau aggregation, [483]. Although glycolytic capacity has been shown to be important in all the above studies, a causal relationship between amyloid and tau deposition and glycolytic capacity is yet to be developed. To understand if brain glycolytic capacity is a protective factor against AD or a consequence of amyloid deposition is still to be established, but several points of evidence, including the results of this thesis point towards the importance of glycolytic capacity in AD.

6.5 ApoE genotype may contribute to mitochondrial and glycolytic impairment in AD

All three results chapters in this thesis have looked at the effect ApoE allele frequency has on mitochondrial and glycolytic function in AD. In sAD fibroblasts the mitochondrial structural changes appeared to be exacerbated by ApoE ϵ 4/4 genotype, but the same effect was not seen in the mitochondrial markers shown to be statistically different from controls in sAD astrocytes. The relationship between ApoE genotype, metabolism and AD has not been fully identified by this thesis, but there is a suggestion that certain metabolic changes seen in both AD fibroblasts and astrocytes, such as MSRC and glycolytic reserve, are independent of the effect of ApoE.

Understanding how metabolism and ApoE interact is important for sporadic AD as it is very likely several different physiological changes occur in cells to propagate the pathology of AD.

Understanding if ApoE and cellular metabolism each have a separate influence on the development of AD will allow for further development of the idea that sporadic AD is a group of diseases in which different physiological parameters, such as increased A β production, the ApoE ϵ 4/4 genotype or the presence of deficits in metabolic capacity, combine to cause the disease. In one group of at-risk patients metabolism change may be the main driver of AD, whereas increased A β production may be the main driver in another group. This research is vital in order to progress a personalised-medicine approach to diagnosing and treating people with AD; in order to test new therapies in more homogeneous groups with rational drug design. This study was not able to answer the question about the effects of ApoE on metabolism but future work should control for ApoE genotype (and potentially other genetic risk factors for sporadic AD) when studying metabolism in AD.

6.6 Developing a metabolic biomarker for AD

A biomarker is defined as a biological parameter which can be objectively measured to characterise a normal or pathological biological process [529]. When studying disease, or in the clinical realm biomarkers can be used to identify a condition, track a disease response to intervention, or help to prognosticate the eventual outcome of a patient with a particular condition. As deficits in mitochondrial function and glycolysis seem to be common to several cell types and present in both sporadic and familial AD there is potential that a metabolic biomarker could be developed for AD which could be used in any of the three scenarios described above. In any of the three scenarios, the approach to developing a metabolic biomarker could be done by taking a particular marker of mitochondrial function, or glycolysis and investigating if this is affected in large cohorts of AD patients. MSRC, or glycolytic reserve would be appropriate choices for the development of this type of biomarker, as deficits in both these parameters were present in fibroblasts and astrocytes, suggesting a deficit common to several cell types. A common metabolic deficit is particularly

important when developing a metabolic biomarker of AD, as a systemic change in metabolism must reflect a change in the CNS that leads to disease. If a biomarker can be developed through taking peripheral samples this would be beneficial over sampling tissue or fluid from the CNS. A difficulty with using either or both of these particular parameters of metabolic function when developing a biomarker would be the way each parameter is measured. Assessment of MSRC and glycolytic reserve performed in this thesis required several weeks of processing of biological samples from patients. This would be both expensive and time consuming on a large scale, making the development of a practical widely available biomarker difficult. If metabolic dysfunction did however improve the specificity of AD diagnosis or provide a robust marker of treatment response then this may be an appropriate time frame to wait. The time needed to process samples and certain elements of cost could be reduced if peripheral blood mononuclear cells were used to assess reserve metabolic capacity as opposed to fibroblasts. Previous research has shown that from fresh samples peripheral blood mononuclear cell MSRC and glycolytic reserve can be measured using the same techniques that have been used in this thesis [530].

Alternatively, measuring expression within the blood of a protein marker known to cause the abnormalities in either MSRC or glycolytic reserve could be developed into a surrogate metabolic biomarker. In chapter 5 data from astrocytes suggested that the activity complex I of the ETC may be reduced, potentially being the cause the deficit in MSRC. Complex I protein expression could be measured, although this would not be a direct measure of function or MSRC. An alternative measurement could be to investigate the NADH/NAD⁺ ratio in different systemic cells as this also may play a role in determining MSRC. Measurement of complex II levels may also be a useful surrogate marker of MSRC, as complex II activity has been shown to be directly linked to MSRC [433].

Determining a biomarker for glycolytic reserve is also likely to be difficult, as multiple enzyme functions in several glycolysis pathways are likely to contribute to the glycolytic reserve of a cell. One technique that may be able to deliver a relatively quick way to measure glycolytic reserve would be metabolomics analysis [531]. Further work would be needed to find the metabolic blueprint that corresponds to a low glycolytic reserve, but once found this could potentially provide a relatively quick measurement technique. To develop a biomarker based on a functional change in glycolysis or mitochondria function requires further work to determine a physical property of either pathway (such as enzyme protein content reduction) which causes the observed functional deficit.

Another approach to develop the changes in glycolysis and mitochondrial function seen in this study into a future biomarker would be to include mitochondrial or glycolytic assessment as part of a

battery of biomarkers for AD. This methodology would include performing multiple tests of metabolism in AD patient cells to define an AD metabolic phenotype. In chapters 4&5 it was shown that MSRC, glycolytic reserve and extracellular lactate levels correlate with neuropsychological testing affected early in AD, which suggests this is a feasible assessment. The clinical biomarker system referred to as the “ATN” system has been developed to help characterize people with a diagnosis of AD [97]. As discussed in chapter 1, this system is based on the presence or absence of amyloid (A), tau (T) or signs of neuronal injury (N) on brain imaging or CSF testing. Since the development of the ATN system it has been applied to patients with MCI with the aim of assessing progression to developing AD [80]. By adding metabolic assessment to the ATN biomarker system, this may increase the reliability of an Alzheimer disease diagnosis at the prodromal or preclinical stage when therapeutic engagement may be more effective at halting disease progression. Potentially adding cellular metabolic assessment to the biomarkers performed in MCI patients may help to predict which patients, and at what time point they will develop dementia. There is already evidence that combining different biomarkers of AD increases the accuracy of diagnosis [532], therefore an assessment in another biological property of people with AD may further improve this.

Understanding the full range of metabolic abnormalities that are common to all cell types in AD may also be a way to develop metabolic functional assessment into risk stratification tool for people known to be at risk of AD. ApoE ϵ 4/4 genotype [533] and CSF amyloid and tau levels [534, 535] can predict to a certain extent progression to AD in cognitively normal subjects. Performing a full metabolic assessment of peripheral cells in people who are at risk of AD may again be able to improve diagnostic accuracy.

Before peripheral assessment of metabolic function can be developed into a clinically useful diagnostic test much larger patient cohorts are needed to validate the findings of this thesis and other papers in the field that have shown metabolic compromise in AD. Very few papers that study metabolism in AD have a large cohort of patients sampled, therefore further investigation of metabolism on a large scale is needed to identify deficits that are common to the majority of AD patients.

6.7 Metabolism as a target for therapeutic intervention in AD

Having identified deficits in both mitochondrial function and glycolysis it has to be considered if these metabolic changes can be utilized as drug targets for therapeutics in AD. In Chapter 5 it was shown that compounds known to modulate the function of mitochondria can improve total cellular ATP in sAD and fAD astrocytes, and in chapter 3 UDCA was shown to improve fibroblast mitochondrial function in both sporadic and familial disease.

Targeting metabolic function has already been attempted in AD therapeutic development with both metformin and insulin shown to improve cognition in patients with AD and MCI in phase 1&2 clinical trials [536-538]. Interestingly the potential effects of metformin may be mediated through improving glycolysis in astrocytes, with studies in animal models shown to increase astrocyte glycolytic flux and lactate production [539, 540]. Insulin may have an effect on glucose uptake by the brain, but insulin-independent glucose uptake is present throughout the brain so this may not be how insulin improves cognitive performance [541]. Insulin can impair tau phosphorylation, which may be the method of action in decreasing cognitive impairment [542]. In this thesis glycolysis has been shown to be impaired in astrocytes in patients with AD, which may be of importance when considering using insulin as a treatment for AD. Astrocytic insulin release in the hypothalamus has been shown to reduce systemic blood glucose levels [543]. If astrocytes are effectively starved of glucose because of their glucose insensitivity, then this may lead to a reduction in astrocyte insulin release, which would allow for a higher blood glucose, making more available for insulin-independent glucose uptake. This highlights the importance of time of intervention of a therapy in a long-term condition. Insulin as a therapeutic may have very different effects on the progression of AD, if administered during different disease stages.

This should be also considered when developing new therapeutics targeting metabolism in AD. In the development of any therapy the timing on intervention, and cohort targeted is key for success. Metabolism changes are seen early in AD, [41] but may not drive disease progression when tau and amyloid pathology is established. Therefore, intervention may have to be in the prodromal stage or earlier to be effective. This is where the development of metabolic deficits into a biomarker of AD would be beneficial. It must also be considered that metabolism deficits may not drive disease in all patients with AD so applying a personalized medicine approach would again be important when designing a metabolic therapy for AD. Using a personalized medicine approach in AD treatment is likely to involve screening patients with either MCI, or even cognitively normal adults who are at risk of AD. Cellular metabolic function would be assessed, as would amyloid and tau burden, brain vascular damage and presence of dementia risk factors such as diabetes and obesity. A personalised therapeutic regime would be then developed to address each of this AD contributing factors.

Another hurdle to the development of a metabolic therapeutic targeting the abnormalities identified in this study would be monitoring of drug effect in clinical trials. In chapters 4&5 the correlations between metabolic dysfunction and neuropsychological testing was described. This correlation potentially could be developed for use to monitor response to drug therapies targeted at metabolism in clinical trials. FDG-PET imaging would also be another potential method for tracking response to metabolic targeted drug therapies.

6.8 Further Directions

As discussed previously in the results chapters larger cohorts of cell lines are needed to explore the relationship between metabolism, ApoE genotype and AD. This thesis has shown though that elements of this investigation could be performed in fibroblasts from patients with AD as similar deficits are seen in both astrocytes and fibroblasts.

The functional changes seen in both mitochondria and glycolysis need to be understood on the enzymatic level. Interrogation of the different enzymes and receptors involved in the metabolism of glucose is needed to discover what causes the reduced glycolytic reserve and low extracellular lactate in AD cells. Individual assessment of ETC complex activities and distribution within the mitochondria needs to be performed to understand how MSRC and MMP are affected in AD. Further work is also needed to explore how mitochondrial dynamics in AD are affected, and if this is a potential therapeutic target of the future.

Astrocyte metabolism changes need to be understood in relationship to changes in metabolism in neurons from patients with AD, but also with regard to how astrocyte metabolism affects neuronal support. This can be done with co-culture work using the same iNPC technologies employed in this study. Co-cultures systems that combine the iNPC generated astrocytes discussed in this thesis with neurons derived from Lund human mesencephalic cells, or cells lines such as the PC12 line would also be useful to study the ability for astrocyte neuronal support.

As all dementia types can present very summarily at the beginning of disease, performing the same experiments described here in other dementia types, and in patients with prodromal dementia would answer the question as to whether the changes seen here are unique to AD or are a global feature of dementias and neurodegenerative disease. The in-depth metabolic assessment that has been employed in this study may highlight certain metabolic patterns that are specific to dementia subtypes. In addition to studying mitochondrial function and glycolysis, fatty acid and protein metabolism could be added to the experimental battery to characterize AD and dementia metabolic deficits further.

It would also be important to explore further if the clinical correlation work performed in this study could be developed into a biomarker for AD, or a way of tracking cellular metabolic function clinically. Performing these experiments in patients with MCI and who are cognitively normal would help address this.

Finally, the utility of exploiting the deficits in metabolic function identified in this study as targets for drug treatments needs to be assessed. Drug screening assays focusing on improving MSRC, glycolytic

reserve and extracellular lactate levels would be a logical way to develop disease modifying therapies for patients with AD.

6.9 Final Conclusion

This thesis has shown that mitochondrial function and glycolysis are abnormal in both sporadic and familial AD, and that these abnormalities are not confined to the central nervous system. The functional reserve capacity of both OxPHOS and glycolysis is impaired in multiple cell types in AD and this impairment correlates with scores on neuropsychological tests shown to be abnormal early in AD.

This is one of the first studies to show that human derived astrocytes from both sporadic and familial AD patients have metabolic deficits, and that the main pathway by which astrocytes produce ATP is impaired. Impaired astrocyte metabolism is likely to affect neuronal astrocytic support, synaptic plasticity and memory acquisition which makes this finding of key importance in the understanding of the pathology of AD.

Both astrocyte and fibroblast mitochondrial deficits can be corrected with the application of certain already developed therapeutics, which combined with the correlation data between neuropsychological biomarkers of AD and metabolic dysfunction, suggests that the abnormalities identified in this thesis could be used as both a therapeutic target for AD and the development of a metabolic biomarker.

This thesis has shown the importance of studying metabolism in AD, and has also highlighted that the astrocyte, a cell not always considered a key player in the pathology of AD potentially has an important role.

References

1. *Global, regional, and national burden of neurological disorders, 1990-2016: a systematic analysis for the Global Burden of Disease Study 2016.* Lancet Neurol, 2019. **18**(5): p. 459-480.
2. Wu, Y.T., et al., *The changing prevalence and incidence of dementia over time - current evidence.* Nat Rev Neurol, 2017. **13**(6): p. 327-339.
3. Prince, M. *World Alzheimer report 2015: the global impact of dementia.* 2015. 2015 [cited 2020 06/05/2020].
4. Association, A. *What is Dementia.* 2020 7/05/20]; Available from: <https://www.alz.org/alzheimers-dementia/what-is-dementia>.
5. Mukadam, N., et al., *Population attributable fractions for risk factors for dementia in low-income and middle-income countries: an analysis using cross-sectional survey data.* Lancet Glob Health, 2019. **7**(5): p. e596-e603.
6. Ferri, C.P. and K.S. Jacob, *Dementia in low-income and middle-income countries: Different realities mandate tailored solutions.* PLoS medicine, 2017. **14**(3): p. e1002271-e1002271.
7. Jonsson, L., et al., *Determinants of costs of care for patients with Alzheimer's disease.* Int J Geriatr Psychiatry, 2006. **21**(5): p. 449-59.
8. Livingston, G., et al., *Dementia prevention, intervention, and care.* Lancet, 2017. **390**(10113): p. 2673-2734.
9. Strassnig, M. and M. Ganguli, *About a peculiar disease of the cerebral cortex: Alzheimer's original case revisited.* Psychiatry (Edgmont (Pa. : Township)), 2005. **2**(9): p. 30-33.
10. Alzheimer, A., *Über eine eigenartige Erkrankung der Hirnrinde.* Zentralbl. Nervenhe. Psych., 1907. **18**: p. 177-179.
11. Perl, D.P., *Neuropathology of Alzheimer's disease.* The Mount Sinai journal of medicine, New York, 2010. **77**(1): p. 32-42.
12. Hardy, J. and D.J. Selkoe, *The Amyloid Hypothesis of Alzheimer's Disease: Progress and Problems on the Road to Therapeutics.* Science, 2002. **297**(5580): p. 353-356.
13. Hardy, J.A. and G.A. Higgins, *Alzheimer's disease: the amyloid cascade hypothesis.* Science, 1992. **256**(5054): p. 184-5.
14. Hardy, J. and D. Allsop, *Amyloid deposition as the central event in the aetiology of Alzheimer's disease.* Trends Pharmacol Sci, 1991. **12**(10): p. 383-8.
15. Selkoe, D.J., *The molecular pathology of Alzheimer's disease.* Neuron, 1991. **6**(4): p. 487-98.
16. Braak, H. and E. Braak, *Neuropathological staging of Alzheimer-related changes.* Acta Neuropathol, 1991. **82**(4): p. 239-59.
17. Terry, R.D., *The pathogenesis of Alzheimer disease: an alternative to the amyloid hypothesis.* J Neuropathol Exp Neurol, 1996. **55**(10): p. 1023-5.
18. Savva, G.M., et al., *Age, neuropathology, and dementia.* N Engl J Med, 2009. **360**(22): p. 2302-9.
19. Iacono, D., et al., *The Nun study: clinically silent AD, neuronal hypertrophy, and linguistic skills in early life.* Neurology, 2009. **73**(9): p. 665-673.
20. van Dyck, C.H., *Anti-Amyloid-beta Monoclonal Antibodies for Alzheimer's Disease: Pitfalls and Promise.* Biol Psychiatry, 2018. **83**(4): p. 311-319.
21. Gold, M., *Phase II clinical trials of anti-amyloid β antibodies: When is enough, enough?* Alzheimer's & dementia (New York, N. Y.), 2017. **3**(3): p. 402-409.
22. Le Couteur, D.G., S. Hunter, and C. Brayne, *Solanezumab and the amyloid hypothesis for Alzheimer's disease.* Bmj, 2016. **355**: p. i6771.
23. Grundke-Iqbal, I., et al., *Microtubule-associated protein tau. A component of Alzheimer paired helical filaments.* J Biol Chem, 1986. **261**(13): p. 6084-9.
24. Grundke-Iqbal, I., et al., *Abnormal phosphorylation of the microtubule-associated protein tau (tau) in Alzheimer cytoskeletal pathology.* Proc Natl Acad Sci U S A, 1986. **83**(13): p. 4913-7.

25. Wood, J.G., et al., *Neurofibrillary tangles of Alzheimer disease share antigenic determinants with the axonal microtubule-associated protein tau (tau)*. Proceedings of the National Academy of Sciences, 1986. **83**(11): p. 4040-4043.
26. Binder, L.I., et al., *Tau, tangles, and Alzheimer's disease*. Biochimica et Biophysica Acta (BBA) - Molecular Basis of Disease, 2005. **1739**(2): p. 216-223.
27. Ghoshal, N., et al., *Tau Conformational Changes Correspond to Impairments of Episodic Memory in Mild Cognitive Impairment and Alzheimer's Disease*. Experimental Neurology, 2002. **177**(2): p. 475-493.
28. Arriagada, P.V., et al., *Neurofibrillary tangles but not senile plaques parallel duration and severity of Alzheimer's disease*. Neurology, 1992. **42**(3 Pt 1): p. 631-9.
29. Mitchell, T.W., et al., *Parahippocampal tau pathology in healthy aging, mild cognitive impairment, and early Alzheimer's disease*. Ann Neurol, 2002. **51**(2): p. 182-9.
30. Hardy, J., et al., *Genetic dissection of Alzheimer's disease and related dementias: amyloid and its relationship to tau*. Nat Neurosci, 1998. **1**(5): p. 355-8.
31. Masliah, E., et al., *Immunohistochemical quantification of the synapse-related protein synaptophysin in Alzheimer disease*. Neuroscience Letters, 1989. **103**(2): p. 234-239.
32. Per Dahl, E., et al., *Synapsin I (protein I) in different brain regions in senile dementia of Alzheimer type and in multi-infarct dementia*. J Neural Transm, 1984. **60**(2): p. 133-41.
33. Davies, C.A., et al., *A quantitative morphometric analysis of the neuronal and synaptic content of the frontal and temporal cortex in patients with Alzheimer's disease*. J Neurol Sci, 1987. **78**(2): p. 151-64.
34. Spires-Jones, T.L. and B.T. Hyman, *The intersection of amyloid beta and tau at synapses in Alzheimer's disease*. Neuron, 2014. **82**(4): p. 756-771.
35. DeKosky, S.T. and S.W. Scheff, *Synapse loss in frontal cortex biopsies in Alzheimer's disease: correlation with cognitive severity*. Ann Neurol, 1990. **27**(5): p. 457-64.
36. Scheff, S.W., et al., *Hippocampal synaptic loss in early Alzheimer's disease and mild cognitive impairment*. Neurobiol Aging, 2006. **27**(10): p. 1372-84.
37. Selkoe, D.J., *Alzheimer's disease is a synaptic failure*. Science, 2002. **298**(5594): p. 789-91.
38. Hsia, A.Y., et al., *Plaque-independent disruption of neural circuits in Alzheimer's disease mouse models*. Proc Natl Acad Sci U S A, 1999. **96**(6): p. 3228-33.
39. Mucke, L., et al., *High-level neuronal expression of abeta 1-42 in wild-type human amyloid protein precursor transgenic mice: synaptotoxicity without plaque formation*. J Neurosci, 2000. **20**(11): p. 4050-8.
40. Chen, G., et al., *A learning deficit related to age and beta-amyloid plaques in a mouse model of Alzheimer's disease*. Nature, 2000. **408**(6815): p. 975-9.
41. Vlassenko, A.G., et al., *Spatial correlation between brain aerobic glycolysis and amyloid-beta (Abeta) deposition*. Proc Natl Acad Sci U S A, 2010. **107**(41): p. 17763-7.
42. Vlassenko, A.G., et al., *Aerobic glycolysis and tau deposition in preclinical Alzheimer's disease*. Neurobiol Aging, 2018. **67**: p. 95-98.
43. Harris, J.J., R. Jolivet, and D. Attwell, *Synaptic energy use and supply*. Neuron, 2012. **75**(5): p. 762-77.
44. Akiyama, H., et al., *Inflammation and Alzheimer's disease*. Neurobiology of aging, 2000. **21**(3): p. 383-421.
45. Mandrekar-Colucci, S. and G.E. Landreth, *Microglia and inflammation in Alzheimer's disease*. CNS & neurological disorders drug targets, 2010. **9**(2): p. 156-167.
46. Broe, G.A., et al., *Anti-inflammatory Drugs Protect Against Alzheimer Disease at Low Doses*. Archives of Neurology, 2000. **57**(11): p. 1586-1591.
47. Mesulam, M.M., *Neuroplasticity failure in Alzheimer's disease: bridging the gap between plaques and tangles*. Neuron, 1999. **24**(3): p. 521-9.
48. Bliss, T.V. and G.L. Collingridge, *A synaptic model of memory: long-term potentiation in the hippocampus*. Nature, 1993. **361**(6407): p. 31-9.

49. Collingridge, G.L., et al., *Long-term depression in the CNS*. Nature Reviews Neuroscience, 2010. **11**(7): p. 459-473.
50. Shankar, G.M. and D.M. Walsh, *Alzheimer's disease: synaptic dysfunction and A β* . Molecular neurodegeneration, 2009. **4**: p. 48-48.
51. Miklossy, J., et al., *Curly fiber and tangle-like inclusions in the ependyma and choroid plexus--a pathogenetic relationship with the cortical Alzheimer-type changes?* J Neuropathol Exp Neurol, 1998. **57**(12): p. 1202-12.
52. Chow, V.W., et al., *An overview of APP processing enzymes and products*. Neuromolecular Med, 2010. **12**(1): p. 1-12.
53. Tanabe, C., et al., *ADAM19 is tightly associated with constitutive Alzheimer's disease APP alpha-secretase in A172 cells*. Biochem Biophys Res Commun, 2007. **352**(1): p. 111-7.
54. Fahrenholz, F., et al., *Alpha-secretase activity of the disintegrin metalloprotease ADAM 10. Influences of domain structure*. Ann N Y Acad Sci, 2000. **920**: p. 215-22.
55. Vassar, R., et al., *Beta-secretase cleavage of Alzheimer's amyloid precursor protein by the transmembrane aspartic protease BACE*. Science, 1999. **286**(5440): p. 735-41.
56. Wu, Z., et al., *Cathepsin B plays a critical role in inducing Alzheimer's disease-like phenotypes following chronic systemic exposure to lipopolysaccharide from Porphyromonas gingivalis in mice*. Brain, Behavior, and Immunity, 2017. **65**: p. 350-361.
57. Iwatsubo, T., *The gamma-secretase complex: machinery for intramembrane proteolysis*. Curr Opin Neurobiol, 2004. **14**(3): p. 379-83.
58. Hernández, F. and J. Avila, *The role of glycogen synthase kinase 3 in the early stages of Alzheimers' disease*. FEBS Letters, 2008. **582**(28): p. 3848-3854.
59. Cross, D.A., et al., *Inhibition of glycogen synthase kinase-3 by insulin mediated by protein kinase B*. Nature, 1995. **378**(6559): p. 785-9.
60. Aberle, H., et al., *beta-catenin is a target for the ubiquitin-proteasome pathway*. Embo j, 1997. **16**(13): p. 3797-804.
61. Patrick, G.N., et al., *Conversion of p35 to p25 deregulates Cdk5 activity and promotes neurodegeneration*. Nature, 1999. **402**(6762): p. 615-622.
62. Tamagno, E., et al., *H2O2 and 4-hydroxynonenol mediate amyloid beta-induced neuronal apoptosis by activating JNKs and p38MAPK*. Exp Neurol, 2003. **180**(2): p. 144-55.
63. Karran, E. and B. De Strooper, *The amyloid cascade hypothesis: are we poised for success or failure?* J Neurochem, 2016. **139 Suppl 2**: p. 237-252.
64. Elliott, C., et al., *A role for APP in Wnt signalling links synapse loss with β -amyloid production*. Translational psychiatry, 2018. **8**(1): p. 179-179.
65. Dolan, P.J. and G.V.W. Johnson, *The role of tau kinases in Alzheimer's disease*. Current opinion in drug discovery & development, 2010. **13**(5): p. 595-603.
66. Rumble, B., et al., *Amyloid A4 protein and its precursor in Down's syndrome and Alzheimer's disease*. N Engl J Med, 1989. **320**(22): p. 1446-52.
67. Das, B. and R. Yan, *A Close Look at BACE1 Inhibitors for Alzheimer's Disease Treatment*. CNS drugs, 2019. **33**(3): p. 251-263.
68. Patzward, G.A. and S.C. Wildt, *The use of convent archival records in medical research: the School Sisters of Notre Dame archives and the nun study*. Am Arch, 2004. **67**(1): p. 86-106.
69. Citron, M., et al., *Mutant presenilins of Alzheimer's disease increase production of 42-residue amyloid β -protein in both transfected cells and transgenic mice*. Nature Medicine, 1997. **3**(1): p. 67-72.
70. Lewis, J., et al., *Neurofibrillary tangles, amyotrophy and progressive motor disturbance in mice expressing mutant (P301L) tau protein*. Nat Genet, 2000. **25**(4): p. 402-5.
71. McKhann, G.M., et al., *The diagnosis of dementia due to Alzheimer's disease: recommendations from the National Institute on Aging-Alzheimer's Association workgroups on diagnostic guidelines for Alzheimer's disease*. Alzheimers Dement, 2011. **7**(3): p. 263-9.

72. Aronoff, J.M., et al., *Information content versus relational knowledge: semantic deficits in patients with Alzheimer's disease*. *Neuropsychologia*, 2006. **44**(1): p. 21-35.
73. Weintraub, S., A.H. Wicklund, and D.P. Salmon, *The neuropsychological profile of Alzheimer disease*. Cold Spring Harbor perspectives in medicine, 2012. **2**(4): p. a006171-a006171.
74. Luppá, M., et al., *Prediction of institutionalisation in dementia. A systematic review*. *Dement Geriatr Cogn Disord*, 2008. **26**(1): p. 65-78.
75. Kai, K., et al., *Relationship between eating disturbance and dementia severity in patients with Alzheimer's disease*. *PloS one*, 2015. **10**(8): p. e0133666-e0133666.
76. Brookmeyer, R., et al., *Survival following a diagnosis of Alzheimer disease*. *Arch Neurol*, 2002. **59**(11): p. 1764-7.
77. Lopez, O.L., *Mild cognitive impairment*. Continuum (Minneapolis, Minn.), 2013. **19**(2 Dementia): p. 411-424.
78. Langa, K.M. and D.A. Levine, *The diagnosis and management of mild cognitive impairment: a clinical review*. *JAMA*, 2014. **312**(23): p. 2551-2561.
79. Kelley, B.J. and R.C. Petersen, *Alzheimer's disease and mild cognitive impairment*. *Neurologic clinics*, 2007. **25**(3): p. 577-v.
80. Ekman, U., D. Ferreira, and E. Westman, *The A/T/N biomarker scheme and patterns of brain atrophy assessed in mild cognitive impairment*. *Scientific Reports*, 2018. **8**(1): p. 8431.
81. Bekris, L.M., et al., *Genetics of Alzheimer disease*. *Journal of geriatric psychiatry and neurology*, 2010. **23**(4): p. 213-227.
82. Chartier-Harlin, M.C., et al., *Early-onset Alzheimer's disease caused by mutations at codon 717 of the beta-amyloid precursor protein gene*. *Nature*, 1991. **353**(6347): p. 844-6.
83. Citron, M., et al., *Mutant presenilins of Alzheimer's disease increase production of 42-residue amyloid beta-protein in both transfected cells and transgenic mice*. *Nat Med*, 1997. **3**(1): p. 67-72.
84. Goate, A., et al., *Segregation of a missense mutation in the amyloid precursor protein gene with familial Alzheimer's disease*. *Nature*, 1991. **349**(6311): p. 704-6.
85. Mullan, M., et al., *A pathogenic mutation for probable Alzheimer's disease in the APP gene at the N-terminus of beta-amyloid*. *Nat Genet*, 1992. **1**(5): p. 345-7.
86. Murrell, J., et al., *A mutation in the amyloid precursor protein associated with hereditary Alzheimer's disease*. *Science*, 1991. **254**(5028): p. 97-9.
87. Bird, T., *Early-Onset Familial Alzheimer Disease*. 2012, University of Washington.
88. Campion, D., et al., *A novel presenilin 1 mutation resulting in familial Alzheimer's disease with an onset age of 29 years*. *Neuroreport*, 1996. **7**(10): p. 1582-4.
89. Duff, K., et al., *Increased amyloid-beta42(43) in brains of mice expressing mutant presenilin 1*. *Nature*, 1996. **383**(6602): p. 710-3.
90. Corder, E.H., et al., *Gene dose of apolipoprotein E type 4 allele and the risk of Alzheimer's disease in late onset families*. *Science*, 1993. **261**(5123): p. 921-3.
91. Ungar, L., A. Altmann, and M.D. Greicius, *Apolipoprotein E, gender, and Alzheimer's disease: an overlooked, but potent and promising interaction*. *Brain imaging and behavior*, 2014. **8**(2): p. 262-273.
92. Liu, C.-C., et al., *Apolipoprotein E and Alzheimer disease: risk, mechanisms and therapy*. *Nature reviews. Neurology*, 2013. **9**(2): p. 106-118.
93. Misra, A., S.S. Chakrabarti, and I.S. Gambhir, *New genetic players in late-onset Alzheimer's disease: Findings of genome-wide association studies*. *The Indian journal of medical research*, 2018. **148**(2): p. 135-144.
94. Johnson, K.A., et al., *Brain imaging in Alzheimer disease*. Cold Spring Harbor perspectives in medicine, 2012. **2**(4): p. a006213-a006213.
95. Niemantsverdriet, E., et al., *Alzheimer's disease CSF biomarkers: clinical indications and rational use*. *Acta neurologica Belgica*, 2017. **117**(3): p. 591-602.

96. Fleisher, A.S., et al., *Positron Emission Tomography Imaging With [18F]flortaucipir and Postmortem Assessment of Alzheimer Disease Neuropathologic Changes*. JAMA Neurology, 2020.
97. Jack, C.R., Jr., et al., *A/T/N: An unbiased descriptive classification scheme for Alzheimer disease biomarkers*. Neurology, 2016. **87**(5): p. 539-547.
98. Allegri, R.F., et al., *Prognostic value of ATN Alzheimer biomarkers: 60-month follow-up results from the Argentine Alzheimer's Disease Neuroimaging Initiative*. Alzheimer's & Dementia: Diagnosis, Assessment & Disease Monitoring, 2020. **12**(1): p. e12026.
99. Cummings, J.L. and C. Back, *The cholinergic hypothesis of neuropsychiatric symptoms in Alzheimer's disease*. Am J Geriatr Psychiatry, 1998. **6**(2 Suppl 1): p. S64-78.
100. Areosa, S.A., F. Sherriff, and R. McShane, *Memantine for dementia*. Cochrane Database Syst Rev, 2005(2): p. Cd003154.
101. Birks, J., *Cholinesterase inhibitors for Alzheimer's disease*. Cochrane Database Syst Rev, 2006(1): p. Cd005593.
102. Rinne, J.O., et al., *11C-PiB PET assessment of change in fibrillar amyloid-beta load in patients with Alzheimer's disease treated with bapineuzumab: a phase 2, double-blind, placebo-controlled, ascending-dose study*. Lancet Neurol, 2010. **9**(4): p. 363-72.
103. Sperling, R., et al., *Amyloid-related imaging abnormalities in patients with Alzheimer's disease treated with bapineuzumab: a retrospective analysis*. Lancet Neurol, 2012. **11**(3): p. 241-9.
104. Schneider, L., *A resurrection of aducanumab for Alzheimer's disease*. Lancet Neurol, 2020. **19**(2): p. 111-112.
105. Makin, S., *The amyloid hypothesis on trial*. Nature, 2018. **559**(7715): p. S4-s7.
106. Perrin, R.J., A.M. Fagan, and D.M. Holtzman, *Multimodal techniques for diagnosis and prognosis of Alzheimer's disease*. Nature, 2009. **461**(7266): p. 916-22.
107. Jansen, W.J., et al., *Prevalence of Cerebral Amyloid Pathology in Persons Without Dementia: A Meta-analysis*. JAMA, 2015. **313**(19): p. 1924-1938.
108. Selvackadunco, S., et al., *Comparison of clinical and neuropathological diagnoses of neurodegenerative diseases in two centres from the Brains for Dementia Research (BDR) cohort*. Journal of Neural Transmission, 2019. **126**(3): p. 327-337.
109. Grandal Leiros, B., et al., *Prevalence and concordance between the clinical and the post-mortem diagnosis of dementia in a psychogeriatric clinic*. Neurología (English Edition), 2018. **33**(1): p. 13-17.
110. Rasmusson, D.X., et al., *Accuracy of clinical diagnosis of Alzheimer disease and clinical features of patients with non-Alzheimer disease neuropathology*. Alzheimer Dis Assoc Disord, 1996. **10**(4): p. 180-8.
111. Lim, A., et al., *Clinico-neuropathological correlation of Alzheimer's disease in a community-based case series*. J Am Geriatr Soc, 1999. **47**(5): p. 564-9.
112. Mok, W., et al., *Clinicopathological concordance of dementia diagnoses by community versus tertiary care clinicians*. American journal of Alzheimer's disease and other dementias, 2004. **19**(3): p. 161-165.
113. Gauthreaux, K., et al., *Concordance of Clinical Alzheimer Diagnosis and Neuropathological Features at Autopsy*. Journal of Neuropathology & Experimental Neurology, 2020. **79**(5): p. 465-473.
114. Danner, D.D., D.A. Snowdon, and W.V. Friesen, *Positive emotions in early life and longevity: findings from the nun study*. J Pers Soc Psychol, 2001. **80**(5): p. 804-13.
115. Snowdon, D.A., *Healthy aging and dementia: findings from the Nun Study*. Ann Intern Med, 2003. **139**(5 Pt 2): p. 450-4.
116. Morgen, K. and L. Frolich, *The metabolism hypothesis of Alzheimer's disease: from the concept of central insulin resistance and associated consequences to insulin therapy*. J Neural Transm (Vienna), 2015. **122**(4): p. 499-504.

117. Johnson, E.C.B., et al., *Large-scale proteomic analysis of Alzheimer's disease brain and cerebrospinal fluid reveals early changes in energy metabolism associated with microglia and astrocyte activation*. *Nature Medicine*, 2020. **26**(5): p. 769-780.
118. Swerdlow, R.H. and S.M. Khan, A "mitochondrial cascade hypothesis" for sporadic Alzheimer's disease. *Med Hypotheses*, 2004. **63**(1): p. 8-20.
119. Youle, R.J. and A.M. van der Bliek, *Mitochondrial fission, fusion, and stress*. *Science (New York, N.Y.)*, 2012. **337**(6098): p. 1062-1065.
120. Friedman, J.R. and J. Nunnari, *Mitochondrial form and function*. *Nature*, 2014. **505**(7483): p. 335-343.
121. Stein, L.R. and S.-i. Imai, *The dynamic regulation of NAD metabolism in mitochondria*. *Trends in endocrinology and metabolism: TEM*, 2012. **23**(9): p. 420-428.
122. Kyriakouli, D.S., et al., *Progress and prospects: gene therapy for mitochondrial DNA disease*. *Gene Ther*, 2008. **15**(14): p. 1017-23.
123. Cadonic, C., M.G. Sabbir, and B.C. Albenisi, *Mechanisms of Mitochondrial Dysfunction in Alzheimer's Disease*. *Molecular Neurobiology*, 2016. **53**(9): p. 6078-6090.
124. Hames, B.D.H., N.M., *Instant notes in Biochemistry*, F. Kingston, Editor. 2000. p. 278-288.
125. Lenaz, G., et al., *Mitochondrial respiratory chain super-complex I-III in physiology and pathology*. *Biochimica et Biophysica Acta (BBA) - Bioenergetics*, 2010. **1797**(6): p. 633-640.
126. Diaz, F., et al., *Cytochrome c oxidase is required for the assembly/stability of respiratory complex I in mouse fibroblasts*. *Mol Cell Biol*, 2006. **26**(13): p. 4872-81.
127. Dencher, N.A., et al., *Proteome alterations in rat mitochondria caused by aging*. *Ann N Y Acad Sci*, 2007. **1100**: p. 291-8.
128. Tondera, D., et al., *SLP-2 is required for stress-induced mitochondrial hyperfusion*. *Embo j*, 2009. **28**(11): p. 1589-600.
129. Baker, M.J., T. Tatsuta, and T. Langer, *Quality control of mitochondrial proteostasis*. *Cold Spring Harbor perspectives in biology*, 2011. **3**(7): p. a007559.
130. Fukumitsu, K., et al., *Mitochondrial fission protein Drp1 regulates mitochondrial transport and dendritic arborization in cerebellar Purkinje cells*. *Mol Cell Neurosci*, 2016. **71**: p. 56-65.
131. van der Bliek, A.M., Q. Shen, and S. Kawajiri, *Mechanisms of mitochondrial fission and fusion*. *Cold Spring Harb Perspect Biol*, 2013. **5**(6).
132. Chan, D.C., *Mitochondrial Dynamics and Its Involvement in Disease*. *Annual Review of Pathology: Mechanisms of Disease*, 2020. **15**(1): p. 235-259.
133. Stauch, K.L., P.R. Purnell, and H.S. Fox, *Quantitative proteomics of synaptic and nonsynaptic mitochondria: insights for synaptic mitochondrial vulnerability*. *J Proteome Res*, 2014. **13**(5): p. 2620-36.
134. Kiebish, M.A., et al., *Lipidomic analysis and electron transport chain activities in C57BL/6J mouse brain mitochondria*. *J Neurochem*, 2008. **106**(1): p. 299-312.
135. Menacho, C. and A. Prigione, *Tackling mitochondrial diversity in brain function: from animal models to human brain organoids*. *The International Journal of Biochemistry & Cell Biology*, 2020. **123**: p. 105760.
136. Contreras, L., et al., *Mitochondria: The calcium connection*. *Biochimica et Biophysica Acta (BBA) - Bioenergetics*, 2010. **1797**(6): p. 607-618.
137. De Stefani, D., M. Patron, and R. Rizzuto, *Structure and function of the mitochondrial calcium uniporter complex*. *Biochimica et Biophysica Acta (BBA) - Molecular Cell Research*, 2015. **1853**(9): p. 2006-2011.
138. Kirichok, Y., G. Krapivinsky, and D.E. Clapham, *The mitochondrial calcium uniporter is a highly selective ion channel*. *Nature*, 2004. **427**(6972): p. 360-4.
139. Csordás, G., et al., *Calcium transport across the inner mitochondrial membrane: molecular mechanisms and pharmacology*. *Molecular and cellular endocrinology*, 2012. **353**(1-2): p. 109-113.

140. Perocchi, F., et al., *MICU1 encodes a mitochondrial EF hand protein required for Ca(2+) uptake*. *Nature*, 2010. **467**(7313): p. 291-296.
141. Mallilankaraman, K., et al., *MICU1 is an essential gatekeeper for MCU-mediated mitochondrial Ca(2+) uptake that regulates cell survival*. *Cell*, 2012. **151**(3): p. 630-44.
142. Denton, R.M., *Regulation of mitochondrial dehydrogenases by calcium ions*. *Biochim Biophys Acta*, 2009. **1787**(11): p. 1309-16.
143. Rizzuto, R., P. Bernardi, and T. Pozzan, *Mitochondria as all-round players of the calcium game*. *The Journal of Physiology*, 2000. **529**(1): p. 37-47.
144. Bernardi, P., *The mitochondrial permeability transition pore: a mystery solved?* *Frontiers in Physiology*, 2013. **4**(95).
145. Du, H. and S.S. Yan, *Mitochondrial permeability transition pore in Alzheimer's disease: cyclophilin D and amyloid beta*. *Biochim Biophys Acta*, 2010. **1802**(1): p. 198-204.
146. Murphy, M.P., *How mitochondria produce reactive oxygen species*. *The Biochemical journal*, 2009. **417**(1): p. 1-13.
147. Zorov, D.B., M. Juhaszova, and S.J. Sollott, *Mitochondrial reactive oxygen species (ROS) and ROS-induced ROS release*. *Physiological reviews*, 2014. **94**(3): p. 909-950.
148. Valko, M., et al., *Role of oxygen radicals in DNA damage and cancer incidence*. *Mol Cell Biochem*, 2004. **266**(1-2): p. 37-56.
149. Sena, Laura A. and Navdeep S. Chandel, *Physiological Roles of Mitochondrial Reactive Oxygen Species*. *Molecular Cell*, 2012. **48**(2): p. 158-167.
150. Marin-Hernandez, A., et al., *HIF-1alpha modulates energy metabolism in cancer cells by inducing over-expression of specific glycolytic isoforms*. *Mini Rev Med Chem*, 2009. **9**(9): p. 1084-101.
151. Johri, A. and M.F. Beal, *Mitochondrial dysfunction in neurodegenerative diseases*. *J Pharmacol Exp Ther*, 2012. **342**(3): p. 619-30.
152. Cecconi, F. and B. Levine, *The role of autophagy in mammalian development: cell makeover rather than cell death*. *Dev Cell*, 2008. **15**(3): p. 344-57.
153. De Duve, C. and R. Wattiaux, *Functions of lysosomes*. *Annu Rev Physiol*, 1966. **28**: p. 435-92.
154. Ding, W.-X. and X.-M. Yin, *Mitophagy: mechanisms, pathophysiological roles, and analysis*. *Biological chemistry*, 2012. **393**(7): p. 547-564.
155. Twig, G., et al., *Fission and selective fusion govern mitochondrial segregation and elimination by autophagy*. *Embo j*, 2008. **27**(2): p. 433-46.
156. Gomes, L.C. and L. Scorrano, *High levels of Fis1, a pro-fission mitochondrial protein, trigger autophagy*. *Biochim Biophys Acta*, 2008. **1777**(7-8): p. 860-6.
157. Gomes, L.C., G. Di Benedetto, and L. Scorrano, *During autophagy mitochondria elongate, are spared from degradation and sustain cell viability*. *Nat Cell Biol*, 2011. **13**(5): p. 589-98.
158. Rambold, A.S., et al., *Tubular network formation protects mitochondria from autophagosomal degradation during nutrient starvation*. *Proc Natl Acad Sci U S A*, 2011. **108**(25): p. 10190-5.
159. Narendra, D., et al., *Parkin is recruited selectively to impaired mitochondria and promotes their autophagy*. *J Cell Biol*, 2008. **183**(5): p. 795-803.
160. Lavie, J., et al., *Ubiquitin-Dependent Degradation of Mitochondrial Proteins Regulates Energy Metabolism*. *Cell Reports*, 2018. **23**(10): p. 2852-2863.
161. Ding, W.-X., et al., *Nix is critical to two distinct phases of mitophagy, reactive oxygen species-mediated autophagy induction and Parkin-ubiquitin-p62-mediated mitochondrial priming*. *The Journal of biological chemistry*, 2010. **285**(36): p. 27879-27890.
162. Halestrap, A.P., *What is the mitochondrial permeability transition pore?* *J Mol Cell Cardiol*, 2009. **46**(6): p. 821-31.
163. Kinnally, K.W., et al., *Is mPTP the gatekeeper for necrosis, apoptosis, or both?* *Biochimica et biophysica acta*, 2011. **1813**(4): p. 616-622.

164. Trushina, E., et al., *Defects in mitochondrial dynamics and metabolomic signatures of evolving energetic stress in mouse models of familial Alzheimer's disease*. PLoS One, 2012. **7**(2): p. e32737.
165. Bubber, P., et al., *Mitochondrial abnormalities in Alzheimer brain: mechanistic implications*. Ann Neurol, 2005. **57**(5): p. 695-703.
166. Trimmer, P.A. and M.K. Borland, *Differentiated Alzheimer's disease transmitochondrial cybrid cell lines exhibit reduced organelle movement*. Antioxid Redox Signal, 2005. **7**(9-10): p. 1101-9.
167. Wang, X., et al., *Amyloid-beta overproduction causes abnormal mitochondrial dynamics via differential modulation of mitochondrial fission/fusion proteins*. Proc Natl Acad Sci U S A, 2008. **105**(49): p. 19318-23.
168. Mastroeni, D., et al., *Nuclear but not mitochondrial-encoded oxidative phosphorylation genes are altered in aging, mild cognitive impairment, and Alzheimer's disease*. Alzheimers & Dementia, 2017. **13**(5): p. 510-519.
169. Chandrasekaran, K., et al., *Impairment in mitochondrial cytochrome oxidase gene expression in Alzheimer disease*. Brain Res Mol Brain Res, 1994. **24**(1-4): p. 336-40.
170. Hatanpää, K., et al., *No association between Alzheimer plaques and decreased levels of cytochrome oxidase subunit mRNA, a marker of neuronal energy metabolism*. Molecular Brain Research, 1998. **59**(1): p. 13-21.
171. Anderson, S., et al., *Sequence and organization of the human mitochondrial genome*. Nature, 1981. **290**: p. 457.
172. Cottrell, D.A., et al., *The role of cytochrome c oxidase deficient hippocampal neurones in Alzheimer's disease*. Neuropathol Appl Neurobiol, 2002. **28**(5): p. 390-6.
173. Simonian, N.A. and B.T. Hyman, *Functional Alterations in Alzheimer's Disease: Selective Loss of Mitochondrial-encoded Cytochrome Oxidase mRNA in the Hippocampal Formation*. Journal of Neuropathology & Experimental Neurology, 1994. **53**(5): p. 508-512.
174. Hirai, K., et al., *Mitochondrial abnormalities in Alzheimer's disease*. J Neurosci, 2001. **21**(9): p. 3017-23.
175. Manczak, M., et al., *Differential expression of oxidative phosphorylation genes in patients with Alzheimer's disease: implications for early mitochondrial dysfunction and oxidative damage*. Neuromolecular Med, 2004. **5**(2): p. 147-62.
176. Fukuyama, R., et al., *Gene expression of ND4, a subunit of complex I of oxidative phosphorylation in mitochondria, is decreased in temporal cortex of brains of Alzheimer's disease patients*. Brain Res, 1996. **713**(1-2): p. 290-3.
177. de la Monte, S.M., et al., *Mitochondrial DNA damage as a mechanism of cell loss in Alzheimer's disease*. Lab Invest, 2000. **80**(8): p. 1323-35.
178. Lin, F.H., et al., *Detection of point mutations in codon 331 of mitochondrial NADH dehydrogenase subunit 2 in Alzheimer's brains*. Biochem Biophys Res Commun, 1992. **182**(1): p. 238-46.
179. Linnane, A., et al., *MITOCHONDRIAL DNA MUTATIONS AS AN IMPORTANT CONTRIBUTOR TO AGEING AND DEGENERATIVE DISEASES*. The Lancet, 1989. **333**(8639): p. 642-645.
180. Griffiths, K.K. and R.J. Levy, *Evidence of Mitochondrial Dysfunction in Autism: Biochemical Links, Genetic-Based Associations, and Non-Energy-Related Mechanisms*. Oxidative Medicine and Cellular Longevity, 2017. **2017**: p. 4314025.
181. Chagnon, P., et al., *Distribution of brain cytochrome oxidase activity in various neurodegenerative diseases*. Neuroreport, 1995. **6**(5): p. 711-5.
182. Kish, S.J., et al., *Brain cytochrome oxidase in Alzheimer's disease*. J Neurochem, 1992. **59**(2): p. 776-9.
183. Mutisya, E.M., A.C. Bowling, and M.F. Beal, *Cortical cytochrome oxidase activity is reduced in Alzheimer's disease*. J Neurochem, 1994. **63**(6): p. 2179-84.

184. Parker, W.D., et al., *Electron transport chain defects in Alzheimer's disease brain*. Neurology, 1994. **44**(6): p. 1090-1096.
185. Parker, W.D. and J.K. Parks, *Cytochrome C Oxidase in Alzheimer's Disease Brain*. Purification and Characterization, 1995. **45**(3): p. 482-486.
186. Wong-Riley, M., et al., *Cytochrome oxidase in Alzheimer's disease: Biochemical, histochemical, and immunohistochemical analyses of the visual and other systems*. Vision Research, 1997. **37**(24): p. 3593-3608.
187. Hevner, R.F. and M.T. Wong-Riley, *Mitochondrial and nuclear gene expression for cytochrome oxidase subunits are disproportionately regulated by functional activity in neurons*. J Neurosci, 1993. **13**(5): p. 1805-19.
188. Wong-Riley, M.T., *Cytochrome oxidase: an endogenous metabolic marker for neuronal activity*. Trends Neurosci, 1989. **12**(3): p. 94-101.
189. Wong-Riley, M.T., et al., *Maintenance of neuronal activity by electrical stimulation of unilaterally deafened cats demonstrable with cytochrome oxidase technique*. Ann Otol Rhinol Laryngol Suppl, 1981. **90**(2 Pt 3): p. 30-2.
190. Chandrasekaran, K., et al., *Evidence for Physiological Down-regulation of Brain Oxidative Phosphorylation in Alzheimer's Disease*. Experimental Neurology, 1996. **142**(1): p. 80-88.
191. Maynard, S., et al., *Defective mitochondrial respiration, altered dNTP pools and reduced AP endonuclease 1 activity in peripheral blood mononuclear cells of Alzheimer's disease patients*. Aging-U.S., 2015. **7**(10): p. 793-+.
192. Leuner, K., et al., *Peripheral mitochondrial dysfunction in Alzheimer's disease: focus on lymphocytes*. Mol Neurobiol, 2012. **46**(1): p. 194-204.
193. Coskun, P., et al., *Metabolic and Growth Rate Alterations in Lymphoblastic Cell Lines Discriminate Between Down Syndrome and Alzheimer's Disease*. Journal of Alzheimers Disease, 2017. **55**(2): p. 737-748.
194. Lunnon, K., et al., *Mitochondrial genes are altered in blood early in Alzheimer's disease*. Neurobiology of Aging, 2017. **53**: p. 36-47.
195. Fisar, Z., et al., *Mitochondrial Respiration in the Platelets of Patients with Alzheimer's Disease*. Current Alzheimer Research, 2016. **13**(8): p. 930-941.
196. Talib, L.L., H.P. Joaquim, and O.V. Forlenza, *Platelet biomarkers in Alzheimer's disease*. World J Psychiatry, 2012. **2**(6): p. 95-101.
197. Casoli, T., et al., *Release of beta-amyloid from high-density platelets: implications for Alzheimer's disease pathology*. Ann N Y Acad Sci, 2007. **1096**: p. 170-8.
198. Smith, C.C., *Stimulated release of the beta-amyloid protein of Alzheimer's disease by normal human platelets*. Neurosci Lett, 1997. **235**(3): p. 157-9.
199. Prestia, F.A., et al., *Platelets Bioenergetics Screening Reflects the Impact of Brain A β Plaque Accumulation in a Rat Model of Alzheimer*. Neurochemical Research, 2019. **44**(6): p. 1375-1386.
200. Parker, W.D., Jr., C.M. Filley, and J.K. Parks, *Cytochrome oxidase deficiency in Alzheimer's disease*. Neurology, 1990. **40**(8): p. 1302-3.
201. Valla, J., et al., *Impaired platelet mitochondrial activity in Alzheimer's disease and mild cognitive impairment*. Mitochondrion, 2006. **6**(6): p. 323-330.
202. Citron, M., et al., *Excessive production of amyloid beta-protein by peripheral cells of symptomatic and presymptomatic patients carrying the Swedish familial Alzheimer disease mutation*. Proceedings of the National Academy of Sciences of the United States of America, 1994. **91**(25): p. 11993-11997.
203. Gray, N.E. and J.F. Quinn, *Alterations in mitochondrial number and function in Alzheimer's disease fibroblasts*. Metabolic brain disease, 2015. **30**(5): p. 1275-1278.
204. Pérez, M.J., et al., *Mitochondrial Bioenergetics Is Altered in Fibroblasts from Patients with Sporadic Alzheimer's Disease*. Frontiers in neuroscience, 2017. **11**: p. 553-553.

205. Sorbi, S., et al., *Alterations in metabolic properties in fibroblasts in Alzheimer disease*. *Alzheimer Dis Assoc Disord*, 1995. **9**(2): p. 73-7.
206. Curti, D., et al., *Oxidative metabolism in cultured fibroblasts derived from sporadic Alzheimer's disease (AD) patients*. *Neurosci Lett*, 1997. **236**(1): p. 13-6.
207. Sonntag, K.-C., et al., *Late-onset Alzheimer's disease is associated with inherent changes in bioenergetics profiles*. *Scientific Reports*, 2017. **7**(1): p. 14038.
208. Swerdlow, R.H., J.M. Burns, and S.M. Khan, *The Alzheimer's disease mitochondrial cascade hypothesis*. *Journal of Alzheimer's disease : JAD*, 2010. **20 Suppl 2**(Suppl 2): p. S265-S279.
209. Yao, J., et al., *Mitochondrial bioenergetic deficit precedes Alzheimer's pathology in female mouse model of Alzheimer's disease*. *Proceedings of the National Academy of Sciences of the United States of America*, 2009. **106**(34): p. 14670-14675.
210. Chou, J.L., et al., *Early dysregulation of the mitochondrial proteome in a mouse model of Alzheimer's disease*. *Journal of Proteomics*, 2011. **74**(4): p. 466-479.
211. Hartl, D., et al., *Presymptomatic Alterations in Energy Metabolism and Oxidative Stress in the APP23 Mouse Model of Alzheimer Disease*. *Journal of Proteome Research*, 2012. **11**(6): p. 3295-3304.
212. Behbahani, H., et al., *Differential role of Presenilin-1 and -2 on mitochondrial membrane potential and oxygen consumption in mouse embryonic fibroblasts*. *J Neurosci Res*, 2006. **84**(4): p. 891-902.
213. Contino, S., et al., *Presenilin 2-Dependent Maintenance of Mitochondria! Oxidative Capacity and Morphology*. *Frontiers in Physiology*, 2017. **8**: p. 11.
214. Rhein, V., et al., *Amyloid- β and tau synergistically impair the oxidative phosphorylation system in triple transgenic Alzheimer's disease mice*. *Proceedings of the National Academy of Sciences*, 2009. **106**(47): p. 20057-20062.
215. Escobar-Khondiker, M., et al., *Annonacin, a natural mitochondrial complex I inhibitor, causes tau pathology in cultured neurons*. *J Neurosci*, 2007. **27**(29): p. 7827-37.
216. Eckert, A., et al., *Soluble beta-amyloid leads to mitochondrial defects in amyloid precursor protein and tau transgenic mice*. *Neurodegener Dis*, 2008. **5**(3-4): p. 157-9.
217. Eckert, A., K. Schmitt, and J. Götz, *Mitochondrial dysfunction - the beginning of the end in Alzheimer's disease? Separate and synergistic modes of tau and amyloid- β toxicity*. *Alzheimer's Research & Therapy*, 2011. **3**(2): p. 15.
218. Sanchez, M., et al., *Amyloid precursor protein drives down-regulation of mitochondrial oxidative phosphorylation independent of amyloid beta*. *Scientific Reports*, 2017. **7**: p. 10.
219. Cardoso, S.M., et al., *Functional mitochondria are required for amyloid beta-mediated neurotoxicity*. *Faseb Journal*, 2001. **15**(6): p. 1439-+.
220. Fleck, D., et al., *PTCD1 Is Required for Mitochondrial Oxidative-Phosphorylation: Possible Genetic Association with Alzheimer's Disease*. *The Journal of Neuroscience*, 2019. **39**(24): p. 4636-4656.
221. Gan, X.Q., et al., *Inhibition of ERK-DLP1 signaling and mitochondrial division alleviates mitochondrial dysfunction in Alzheimer's disease cybrid cell*. *Biochimica Et Biophysica Acta-Molecular Basis of Disease*, 2014. **1842**(2): p. 220-231.
222. Jadia, P., et al., *Impaired mitochondrial calcium efflux contributes to disease progression in models of Alzheimer's disease*. *Nature communications*, 2019. **10**(1): p. 3885-3885.
223. Mattson, M.P., et al., *beta-Amyloid peptides destabilize calcium homeostasis and render human cortical neurons vulnerable to excitotoxicity*. *The Journal of neuroscience : the official journal of the Society for Neuroscience*, 1992. **12**(2): p. 376-389.
224. Calvo-Rodriguez, M., et al., *Increased mitochondrial calcium levels associated with neuronal death in a mouse model of Alzheimer's disease*. *Nature Communications*, 2020. **11**(1): p. 2146.
225. Britti, E., et al., *Tau inhibits mitochondrial calcium efflux and makes neurons vulnerable to calcium-induced cell death*. *Cell Calcium*, 2020. **86**: p. 102150.

226. Pérez, M.J., C. Jara, and R.A. Quintanilla, *Contribution of Tau Pathology to Mitochondrial Impairment in Neurodegeneration*. *Frontiers in neuroscience*, 2018. **12**: p. 441-441.
227. Guo, Q., et al., *Alzheimer's presenilin mutation sensitizes neural cells to apoptosis induced by trophic factor withdrawal and amyloid beta-peptide: involvement of calcium and oxyradicals*. *J Neurosci*, 1997. **17**(11): p. 4212-22.
228. Guo, Q., et al., *Calbindin D28k blocks the proapoptotic actions of mutant presenilin 1: reduced oxidative stress and preserved mitochondrial function*. *Proc Natl Acad Sci U S A*, 1998. **95**(6): p. 3227-32.
229. Sarasija, S., et al., *Presenilin mutations deregulate mitochondrial Ca(2+) homeostasis and metabolic activity causing neurodegeneration in Caenorhabditis elegans*. *eLife*, 2018. **7**: p. e33052.
230. Begley, J.G., et al., *Altered calcium homeostasis and mitochondrial dysfunction in cortical synaptic compartments of presenilin-1 mutant mice*. *J Neurochem*, 1999. **72**(3): p. 1030-9.
231. Area-Gomez, E., et al., *Presenilins are enriched in endoplasmic reticulum membranes associated with mitochondria*. *Am J Pathol*, 2009. **175**(5): p. 1810-6.
232. Hedskog, L., et al., *Modulation of the endoplasmic reticulum-mitochondria interface in Alzheimer's disease and related models*. *Proc Natl Acad Sci U S A*, 2013. **110**(19): p. 7916-21.
233. Wang, X., et al., *Oxidative stress and mitochondrial dysfunction in Alzheimer's disease*. *Biochimica et Biophysica Acta (BBA) - Molecular Basis of Disease*, 2014. **1842**(8): p. 1240-1247.
234. Nunomura, A., et al., *Neuronal RNA oxidation in Alzheimer's disease and Down's syndrome*. *Ann N Y Acad Sci*, 1999. **893**: p. 362-4.
235. Simpson, J.E., et al., *Population variation in oxidative stress and astrocyte DNA damage in relation to Alzheimer-type pathology in the ageing brain*. *Neuropathol Appl Neurobiol*, 2010. **36**(1): p. 25-40.
236. Tayler, H., et al., *Oxidative balance in Alzheimer's disease: relationship to APOE, Braak tangle stage, and the concentrations of soluble and insoluble amyloid-β*. *J Alzheimers Dis*, 2010. **22**(4): p. 1363-73.
237. Wang, J., et al., *Increased oxidative damage in nuclear and mitochondrial DNA in Alzheimer's disease*. *J Neurochem*, 2005. **93**(4): p. 953-62.
238. Cecchi, C., et al., *Oxidative stress and reduced antioxidant defenses in peripheral cells from familial Alzheimer's patients*. *Free Radical Biology and Medicine*, 2002. **33**(10): p. 1372-1379.
239. Moreira, P.I., et al., *Lipoic acid and N-acetyl cysteine decrease mitochondrial-related oxidative stress in Alzheimer disease patient fibroblasts*. *J Alzheimers Dis*, 2007. **12**(2): p. 195-206.
240. Nunomura, A., et al., *Oxidative damage is the earliest event in Alzheimer disease*. *J Neuropathol Exp Neurol*, 2001. **60**(8): p. 759-67.
241. Odetti, P., et al., *Early Glycoxidation Damage in Brains from Down's Syndrome*. *Biochemical and Biophysical Research Communications*, 1998. **243**(3): p. 849-851.
242. Melov, S., et al., *Mitochondrial oxidative stress causes hyperphosphorylation of tau*. *PLoS one*, 2007. **2**(6): p. e536-e536.
243. Xie, H., et al., *Rapid cell death is preceded by amyloid plaque-mediated oxidative stress*. *Proc Natl Acad Sci U S A*, 2013. **110**(19): p. 7904-9.
244. Aksenov, M.Y., et al., *The expression of key oxidative stress-handling genes in different brain regions in Alzheimer's disease*. *J Mol Neurosci*, 1998. **11**(2): p. 151-64.
245. Santa-María, I., et al., *Quinones Facilitate the Self-Assembly of the Phosphorylated Tubulin Binding Region of Tau into Fibrillar Polymers*. *Biochemistry*, 2004. **43**(10): p. 2888-2897.
246. Kontush, A., et al., *Amyloid-β is an antioxidant for lipoproteins in cerebrospinal fluid and plasma*. *Free Radical Biology and Medicine*, 2001. **30**(1): p. 119-128.

247. Hensley, K., et al., *A model for beta-amyloid aggregation and neurotoxicity based on free radical generation by the peptide: relevance to Alzheimer disease*. Proc Natl Acad Sci U S A, 1994. **91**(8): p. 3270-4.
248. Lustbader, J.W., et al., *ABAD directly links Abeta to mitochondrial toxicity in Alzheimer's disease*. Science, 2004. **304**(5669): p. 448-52.
249. Yan, S.D. and D.M. Stern, *Mitochondrial dysfunction and Alzheimer's disease: role of amyloid-beta peptide alcohol dehydrogenase (ABAD)*. International journal of experimental pathology, 2005. **86**(3): p. 161-171.
250. Cai, Q. and Y.Y. Jeong, *Mitophagy in Alzheimer's Disease and Other Age-Related Neurodegenerative Diseases*. Cells, 2020. **9**(1).
251. Corsetti, V., et al., *NH2-truncated human tau induces deregulated mitophagy in neurons by aberrant recruitment of Parkin and UCHL-1: implications in Alzheimer's disease*. Hum Mol Genet, 2015. **24**(11): p. 3058-81.
252. Cummins, N., et al., *Disease-associated tau impairs mitophagy by inhibiting Parkin translocation to mitochondria*. The EMBO journal, 2019. **38**(3): p. e99360.
253. Hu, Y., et al., *Tau accumulation impairs mitophagy via increasing mitochondrial membrane potential and reducing mitochondrial Parkin*. Oncotarget, 2016. **7**(14): p. 17356-68.
254. Kerr, J.S., et al., *Mitophagy and Alzheimer's Disease: Cellular and Molecular Mechanisms*. Trends in Neurosciences, 2017. **40**(3): p. 151-166.
255. Martín-Maestro, P., et al., *Mitophagy Failure in Fibroblasts and iPSC-Derived Neurons of Alzheimer's Disease-Associated Presenilin 1 Mutation*. Frontiers in molecular neuroscience, 2017. **10**: p. 291-291.
256. Martín-Maestro, P., et al., *PARK2 enhancement is able to compensate mitophagy alterations found in sporadic Alzheimer's disease*. Hum Mol Genet, 2016. **25**(4): p. 792-806.
257. Monteiro-Cardoso, V.F., et al., *Cardiolipin profile changes are associated to the early synaptic mitochondrial dysfunction in Alzheimer's disease*. J Alzheimers Dis, 2015. **43**(4): p. 1375-92.
258. Moreira, P.I., et al., *Increased autophagic degradation of mitochondria in Alzheimer disease*. Autophagy, 2007. **3**(6): p. 614-5.
259. Ye, X., et al., *Parkin-mediated mitophagy in mutant hAPP neurons and Alzheimer's disease patient brains*. Human molecular genetics, 2015. **24**(10): p. 2938-2951.
260. Cataldo, A.M., et al., *Presenilin mutations in familial Alzheimer disease and transgenic mouse models accelerate neuronal lysosomal pathology*. J Neuropathol Exp Neurol, 2004. **63**(8): p. 821-30.
261. Ji, Z.S., et al., *Reactivity of apolipoprotein E4 and amyloid beta peptide: lysosomal stability and neurodegeneration*. J Biol Chem, 2006. **281**(5): p. 2683-92.
262. Pérez, M.J., et al., *Mitochondrial permeability transition pore contributes to mitochondrial dysfunction in fibroblasts of patients with sporadic Alzheimer's disease*. Redox Biol, 2018. **19**: p. 290-300.
263. Du, H., et al., *Cyclophilin D deficiency attenuates mitochondrial and neuronal perturbation and ameliorates learning and memory in Alzheimer's disease*. Nat Med, 2008. **14**(10): p. 1097-105.
264. Du, H., et al., *Cyclophilin D deficiency improves mitochondrial function and learning/memory in aging Alzheimer disease mouse model*. Neurobiol Aging, 2011. **32**(3): p. 398-406.
265. Mattson, M.P., J. Partin, and J.G. Begley, *Amyloid β -peptide induces apoptosis-related events in synapses and dendrites*. Brain Research, 1998. **807**(1): p. 167-176.
266. Correia, S.C., G. Perry, and P.I. Moreira, *Mitochondrial traffic jams in Alzheimer's disease - pinpointing the roadblocks*. Biochimica et Biophysica Acta (BBA) - Molecular Basis of Disease, 2016. **1862**(10): p. 1909-1917.
267. Smith, E.F., P.J. Shaw, and K.J. De Vos, *The role of mitochondria in amyotrophic lateral sclerosis*. Neuroscience Letters, 2019. **710**: p. 132933.

268. Saxton, W.M. and P.J. Hollenbeck, *The axonal transport of mitochondria*. Journal of Cell Science, 2012. **125**(9): p. 2095.
269. Pigino, G., et al., *Alzheimer's Presenilin 1 Mutations Impair Kinesin-Based Axonal Transport*. The Journal of Neuroscience, 2003. **23**(11): p. 4499-4508.
270. Mandelkow, E.M., et al., *Clogging of axons by tau, inhibition of axonal traffic and starvation of synapses*. Neurobiology of Aging, 2003. **24**(8): p. 1079-1085.
271. MacAskill, A.F., et al., *Miro1 Is a Calcium Sensor for Glutamate Receptor-Dependent Localization of Mitochondria at Synapses*. Neuron, 2009. **61**(4): p. 541-555.
272. Dashty, M., *A quick look at biochemistry: Carbohydrate metabolism*. Clinical Biochemistry, 2013. **46**(15): p. 1339-1352.
273. Diemel, G.A. and N.F. Cruz, *Aerobic glycolysis during brain activation: adrenergic regulation and influence of norepinephrine on astrocytic metabolism*. J Neurochem, 2016. **138**(1): p. 14-52.
274. Mosconi, L., et al., *Reduced hippocampal metabolism in MCI and AD: automated FDG-PET image analysis*. Neurology, 2005. **64**(11): p. 1860-7.
275. Goyal, M.S., et al., *Loss of Brain Aerobic Glycolysis in Normal Human Aging*. Cell Metab, 2017. **26**(2): p. 353-360.e3.
276. Marcus, C., E. Mena, and R.M. Subramaniam, *Brain PET in the diagnosis of Alzheimer's disease*. Clinical nuclear medicine, 2014. **39**(10): p. e413-e426.
277. Bigl, M., et al., *Changes of activity and isozyme pattern of phosphofructokinase in the brains of patients with Alzheimer's disease*. Journal of Neurochemistry, 1996. **67**(3): p. 1164-1171.
278. Bigl, M., et al., *Activities of key glycolytic enzymes in the brains of patients with Alzheimer's disease*. Journal of Neural Transmission, 1999. **106**(5-6): p. 499-511.
279. Hashimoto, M., et al., *Analysis of microdissected neurons by 18O mass spectrometry reveals altered protein expression in Alzheimer's disease*. Journal of Cellular and Molecular Medicine, 2012. **16**(8): p. 1686-1700.
280. Simpson, I.A., et al., *Decreased concentrations of GLUT1 and GLUT3 glucose transporters in the brains of patients with Alzheimer's disease*. Ann Neurol, 1994. **35**(5): p. 546-51.
281. Sorbi, S., et al., *ALTERED HEXOKINASE-ACTIVITY IN SKIN CULTURED FIBROBLASTS AND LEUKOCYTES FROM ALZHEIMERS-DISEASE PATIENTS*. Neuroscience Letters, 1990. **117**(1-2): p. 165-168.
282. Sonntag, K.C., et al., *Late-onset Alzheimer's disease is associated with inherent changes in bioenergetics profiles*. Scientific Reports, 2017. **7**: p. 13.
283. Kaminsky, Y.G., et al., *Age-Related Defects in Erythrocyte 2,3-Diphosphoglycerate Metabolism in Dementia*. Aging and Disease, 2013. **4**(5): p. 244-255.
284. Bigl, M., et al., *Cortical glucose metabolism is altered in aged transgenic Tg2576 mice that demonstrate Alzheimer plaque pathology*. Journal of Neural Transmission, 2003. **110**(1): p. 77-94.
285. Harris, R.A., et al., *Aerobic Glycolysis in the Frontal Cortex Correlates with Memory Performance in Wild-Type Mice But Not the APP/PS1 Mouse Model of Cerebral Amyloidosis*. Journal of Neuroscience, 2016. **36**(6): p. 1871-1878.
286. Andersen, J.V., et al., *Alterations in Cerebral Cortical Glucose and Glutamine Metabolism Precedes Amyloid Plaques in the APP^{swE}/PSEN1^{dE9} Mouse Model of Alzheimer's Disease*. Neurochemical Research, 2017. **42**(6): p. 1589-1598.
287. Atlante, A., et al., *A disease with a sweet tooth: exploring the Warburg effect in Alzheimer's disease*. Biogerontology, 2017. **18**(3): p. 301-319.
288. Soucek, T., et al., *The Regulation of Glucose Metabolism by HIF-1 Mediates a Neuroprotective Response to Amyloid Beta Peptide*. Neuron, 2003. **39**(1): p. 43-56.
289. Pereira, C., M.S. Santos, and C. Oliveira, *Involvement of oxidative stress on the impairment of energy metabolism induced by A beta peptides on PC12 cells: Protection by antioxidants*. Neurobiology of Disease, 1999. **6**(3): p. 209-219.

290. Wamelink, M.M., E.A. Struys, and C. Jakobs, *The biochemistry, metabolism and inherited defects of the pentose phosphate pathway: a review*. J Inherit Metab Dis, 2008. **31**(6): p. 703-17.
291. Martins, R.N., et al., *Increased Cerebral Glucose-6-Phosphate Dehydrogenase Activity in Alzheimer's Disease May Reflect Oxidative Stress*. Journal of Neurochemistry, 1986. **46**(4): p. 1042-1045.
292. Palmer, A.M., *The activity of the pentose phosphate pathway is increased in response to oxidative stress in Alzheimer's disease*. J Neural Transm (Vienna), 1999. **106**(3-4): p. 317-28.
293. Orešič, M., et al., *Metabolome in progression to Alzheimer's disease*. Translational Psychiatry, 2011. **1**(12): p. e57-e57.
294. Tiwari, V. and A.B. Patel, *Pyruvate Carboxylase and Pentose Phosphate Fluxes are Reduced in A β PP-PS1 Mouse Model of Alzheimer's Disease: A 13C NMR Study*. Journal of Alzheimer's Disease, 2014. **41**: p. 387-399.
295. Wang, C., et al., *Malate-aspartate shuttle mediates the intracellular ATP levels, antioxidation capacity and survival of differentiated PC12 cells*. International journal of physiology, pathophysiology and pharmacology, 2014. **6**(2): p. 109-114.
296. Fu, Y.-J., et al., *Quantitative proteomic analysis of mitochondria in aging PS-1 transgenic mice*. Cellular and molecular neurobiology, 2009. **29**(5): p. 649-664.
297. Xu, J., et al., *Graded perturbations of metabolism in multiple regions of human brain in Alzheimer's disease: Snapshot of a pervasive metabolic disorder*. Biochimica et Biophysica Acta (BBA) - Molecular Basis of Disease, 2016. **1862**(6): p. 1084-1092.
298. McKenna, M.C., et al., *Neuronal and astrocytic shuttle mechanisms for cytosolic-mitochondrial transfer of reducing equivalents: current evidence and pharmacological tools*. Biochem Pharmacol, 2006. **71**(4): p. 399-407.
299. Snowden, S.G., et al., *Association between fatty acid metabolism in the brain and Alzheimer disease neuropathology and cognitive performance: A nontargeted metabolomic study*. PLoS medicine, 2017. **14**(3): p. e1002266-e1002266.
300. Goozee, K., et al., *Alterations in erythrocyte fatty acid composition in preclinical Alzheimer's disease*. Scientific Reports, 2017. **7**(1): p. 676.
301. Montine, T.J. and J.D. Morrow, *Fatty acid oxidation in the pathogenesis of Alzheimer's disease*. The American journal of pathology, 2005. **166**(5): p. 1283-1289.
302. Attwell, D. and S.B. Laughlin, *An energy budget for signaling in the grey matter of the brain*. J Cereb Blood Flow Metab, 2001. **21**(10): p. 1133-45.
303. Magistretti, P.J., et al., *Energy on Demand*. Science, 1999. **283**(5401): p. 496-497.
304. Bélanger, M., I. Allaman, and Pierre J. Magistretti, *Brain Energy Metabolism: Focus on Astrocyte-Neuron Metabolic Cooperation*. Cell Metabolism, 2011. **14**(6): p. 724-738.
305. Hertz, L., L. Peng, and G.A. Dienel, *Energy metabolism in astrocytes: high rate of oxidative metabolism and spatiotemporal dependence on glycolysis/glycogenolysis*. J Cereb Blood Flow Metab, 2007. **27**(2): p. 219-49.
306. Sibson, N.R., et al., *Stoichiometric coupling of brain glucose metabolism and glutamatergic neuronal activity*. Proceedings of the National Academy of Sciences, 1998. **95**(1): p. 316-321.
307. Falkowska, A., et al., *Energy Metabolism of the Brain, Including the Cooperation between Astrocytes and Neurons, Especially in the Context of Glycogen Metabolism*. Int J Mol Sci, 2015. **16**(11): p. 25959-81.
308. Herrero-Mendez, A., et al., *The bioenergetic and antioxidant status of neurons is controlled by continuous degradation of a key glycolytic enzyme by APC/C-Cdh1*. Nat Cell Biol, 2009. **11**(6): p. 747-52.
309. Brooks, G.A., *Cell-cell and intracellular lactate shuttles*. J Physiol, 2009. **587**(Pt 23): p. 5591-600.

310. Pellerin, L. and P.J. Magistretti, *Glutamate uptake into astrocytes stimulates aerobic glycolysis: a mechanism coupling neuronal activity to glucose utilization*. Proceedings of the National Academy of Sciences, 1994. **91**(22): p. 10625-10629.
311. Gibbs, M.E., D.G. Anderson, and L. Hertz, *Inhibition of glycogenolysis in astrocytes interrupts memory consolidation in young chickens*. *Glia*, 2006. **54**(3): p. 214-22.
312. Suzuki, A., et al., *Astrocyte-neuron lactate transport is required for long-term memory formation*. *Cell*, 2011. **144**(5): p. 810-23.
313. Sofroniew, M.V. and H.V. Vinters, *Astrocytes: biology and pathology*. *Acta Neuropathol*, 2010. **119**(1): p. 7-35.
314. Suzuki, A., et al., *Astrocyte-Neuron Lactate Transport Is Required for Long-Term Memory Formation*. *Cell*, 2011. **144**(5): p. 810-823.
315. Belanger, M. and P.J. Magistretti, *The role of astroglia in neuroprotection*. *Dialogues Clin Neurosci*, 2009. **11**(3): p. 281-95.
316. Blackburn, D., et al., *Astrocyte function and role in motor neuron disease: a future therapeutic target?* *Glia*, 2009. **57**(12): p. 1251-64.
317. Nishida, H. and S. Okabe, *Direct astrocytic contacts regulate local maturation of dendritic spines*. *J Neurosci*, 2007. **27**(2): p. 331-40.
318. Pellerin, L. and P.J. Magistretti, *Glutamate uptake into astrocytes stimulates aerobic glycolysis: a mechanism coupling neuronal activity to glucose utilization*. *Proc Natl Acad Sci U S A*, 1994. **91**(22): p. 10625-9.
319. Garwood, C.J., et al., *Review: Astrocytes in Alzheimer's disease and other age-associated dementias: a supporting player with a central role*. *Neuropathol Appl Neurobiol*, 2017. **43**(4): p. 281-298.
320. Haass, C., A.Y. Hung, and D.J. Selkoe, *Processing of beta-amyloid precursor protein in microglia and astrocytes favors an internal localization over constitutive secretion*. *J Neurosci*, 1991. **11**(12): p. 3783-93.
321. Wyss-Coray, T., et al., *Adult mouse astrocytes degrade amyloid-beta in vitro and in situ*. *Nat Med*, 2003. **9**(4): p. 453-7.
322. Allaman, I., et al., *Amyloid-beta Aggregates Cause Alterations of Astrocytic Metabolic Phenotype: Impact on Neuronal Viability*. *Journal of Neuroscience*, 2010. **30**(9): p. 3326-3338.
323. DaRocha-Souto, B., et al., *Brain oligomeric beta-amyloid but not total amyloid plaque burden correlates with neuronal loss and astrocyte inflammatory response in amyloid precursor protein/tau transgenic mice*. *J Neuropathol Exp Neurol*, 2011. **70**(5): p. 360-76.
324. Gavillet, M., I. Allaman, and P.J. Magistretti, *Modulation of astrocytic metabolic phenotype by proinflammatory cytokines*. *Glia*, 2008. **56**(9): p. 975-89.
325. Zilberter, M., et al., *Dietary energy substrates reverse early neuronal hyperactivity in a mouse model of Alzheimer's disease*. *J Neurochem*, 2013. **125**(1): p. 157-71.
326. Habib, N., et al., *Disease-associated astrocytes in Alzheimer's disease and aging*. *Nature Neuroscience*, 2020. **23**(6): p. 701-706.
327. Garwood, C.J., et al., *Insulin and IGF1 signalling pathways in human astrocytes in vitro and in vivo; characterisation, subcellular localisation and modulation of the receptors*. *Mol Brain*, 2015. **8**: p. 51.
328. Moloney, A.M., et al., *Defects in IGF-1 receptor, insulin receptor and IRS-1/2 in Alzheimer's disease indicate possible resistance to IGF-1 and insulin signalling*. *Neurobiol Aging*, 2010. **31**(2): p. 224-43.
329. Simpson, J.E., et al., *Microarray analysis of the astrocyte transcriptome in the aging brain: relationship to Alzheimer's pathology and APOE genotype*. *Neurobiol Aging*, 2011. **32**(10): p. 1795-807.
330. Cabezas-Opazo, F.A., et al., *Mitochondrial Dysfunction Contributes to the Pathogenesis of Alzheimer's Disease*. *Oxid Med Cell Longev*, 2015. **2015**: p. 509654.

331. Ratcliffe, L.E., et al., *Loss of IGF1R in Human Astrocytes Alters Complex I Activity and Support for Neurons*. Neuroscience, 2018. **390**: p. 46-59.
332. Sekar, S., et al., *Alzheimer's disease is associated with altered expression of genes involved in immune response and mitochondrial processes in astrocytes*. Neurobiology of aging, 2015. **36**(2): p. 583-591.
333. Garwood, C., et al., *Calcium dysregulation in relation to Alzheimer-type pathology in the ageing brain*. Neuropathology and Applied Neurobiology, 2013. **39**(7): p. 788-799.
334. Wharton, S.B., et al., *Population variation in glial fibrillary acidic protein levels in brain ageing: relationship to Alzheimer-type pathology and dementia*. Dement Geriatr Cogn Disord, 2009. **27**(5): p. 465-73.
335. Pekny, M. and M. Pekna, *Reactive gliosis in the pathogenesis of CNS diseases*. Biochimica et Biophysica Acta (BBA) - Molecular Basis of Disease, 2016. **1862**(3): p. 483-491.
336. Simpson, J.E., et al., *A neuronal DNA damage response is detected at the earliest stages of Alzheimer's neuropathology and correlates with cognitive impairment in the Medical Research Council's Cognitive Function and Ageing Study ageing brain cohort*. Neuropathol Appl Neurobiol, 2015. **41**(4): p. 483-96.
337. Simpson, J.E., et al., *Neuronal DNA damage response-associated dysregulation of signalling pathways and cholesterol metabolism at the earliest stages of Alzheimer-type pathology*. Neuropathol Appl Neurobiol, 2016. **42**(2): p. 167-79.
338. Cataldo, A.M. and R.D. Broadwell, *Cytochemical identification of cerebral glycogen and glucose-6-phosphatase activity under normal and experimental conditions. II. Choroid plexus and ependymal epithelia, endothelia and pericytes*. J Neurocytol, 1986. **15**(4): p. 511-24.
339. Bak, L.K., et al., *Astrocytic glycogen metabolism in the healthy and diseased brain*. The Journal of biological chemistry, 2018. **293**(19): p. 7108-7116.
340. Newman, L.A., D.L. Korol, and P.E. Gold, *Lactate produced by glycogenolysis in astrocytes regulates memory processing*. PLoS One, 2011. **6**(12): p. e28427.
341. Hertz, L., et al., *Astrocytic glycogenolysis: mechanisms and functions*. Metab Brain Dis, 2015. **30**(1): p. 317-33.
342. Sickmann, H.M., et al., *Functional significance of brain glycogen in sustaining glutamatergic neurotransmission*. J Neurochem, 2009. **109 Suppl 1**: p. 80-6.
343. Huang, L., et al., *Accumulation of high-molecular-weight amylose in Alzheimer's disease brains*. Glycobiology, 2004. **14**(5): p. 409-16.
344. Byman, E., et al., *Brain alpha-amylase: a novel energy regulator important in Alzheimer disease?* 2018. **28**(6): p. 920-932.
345. Byman, E., et al., *A Potential Role for α -Amylase in Amyloid- β -Induced Astrocytic Glycogenolysis and Activation*. J Alzheimers Dis, 2019. **68**(1): p. 205-217.
346. Yip, J., et al., *Cerebral Gluconeogenesis and Diseases*. Frontiers in pharmacology, 2017. **7**: p. 521-521.
347. González-Domínguez, R., et al., *Metabolomic investigation of systemic manifestations associated with Alzheimer's disease in the APP/PS1 transgenic mouse model*. Mol Biosyst, 2015. **11**(9): p. 2429-40.
348. Vasile, F., E. Dossi, and N. Rouach, *Human astrocytes: structure and functions in the healthy brain*. Brain Structure and Function, 2017. **222**(5): p. 2017-2029.
349. Takahashi, K. and S. Yamanaka, *Induction of pluripotent stem cells from mouse embryonic and adult fibroblast cultures by defined factors*. Cell, 2006. **126**(4): p. 663-76.
350. Meyer, K., et al., *Direct conversion of patient fibroblasts demonstrates non-cell autonomous toxicity of astrocytes to motor neurons in familial and sporadic ALS*. Proc Natl Acad Sci U S A, 2014. **111**(2): p. 829-32.
351. Musunuru, K., et al., *Induced Pluripotent Stem Cells for Cardiovascular Disease Modeling and Precision Medicine: A Scientific Statement From the American Heart Association*. Circulation: Genomic and Precision Medicine, 2018. **11**(1): p. e000043.

352. Maepa, S.W. and H. Ndlovu, *Advances in generating liver cells from pluripotent stem cells as a tool for modeling liver diseases*. *STEM CELLS*, 2020. **38**(5): p. 606-612.
353. Ahmed, E., et al., *Differentiation of Induced Pluripotent Stem Cells (iPSC) into human bronchial epithelium from healthy and severe COPD patients*. *European Respiratory Journal*, 2018. **52**(suppl 62): p. OA504.
354. Devlin, A.-C., et al., *Human iPSC-derived motoneurons harbouring TARDBP or C9ORF72 ALS mutations are dysfunctional despite maintaining viability*. *Nature Communications*, 2015. **6**(1): p. 5999.
355. Schweitzer, J.S., et al., *Personalized iPSC-Derived Dopamine Progenitor Cells for Parkinson's Disease*. *New England Journal of Medicine*, 2020. **382**(20): p. 1926-1932.
356. Israel, M.A., et al., *Probing sporadic and familial Alzheimer's disease using induced pluripotent stem cells*. *Nature*, 2012. **482**(7384): p. 216-220.
357. Armijo, E., et al., *Increased susceptibility to A β toxicity in neuronal cultures derived from familial Alzheimer's disease (PSEN1-A246E) induced pluripotent stem cells*. *Neuroscience Letters*, 2017. **639**: p. 74-81.
358. Dashinimaev, E.B., et al., *Neurons Derived from Induced Pluripotent Stem Cells of Patients with Down Syndrome Reproduce Early Stages of Alzheimer's Disease Type Pathology in vitro*. *Journal of Alzheimer's Disease*, 2017. **56**: p. 835-847.
359. Koch, P., et al., *Presenilin-1 L166P mutant human pluripotent stem cell-derived neurons exhibit partial loss of γ -secretase activity in endogenous amyloid- β generation*. *Am J Pathol*, 2012. **180**(6): p. 2404-16.
360. Shi, Y., et al., *A human stem cell model of early Alzheimer's disease pathology in Down syndrome*. *Sci Transl Med*, 2012. **4**(124): p. 124ra29.
361. Arber, C., et al., *Familial Alzheimer's disease patient-derived neurons reveal distinct mutation-specific effects on amyloid beta*. *Molecular Psychiatry*, 2019.
362. Birnbaum, J.H., et al., *Oxidative stress and altered mitochondrial protein expression in the absence of amyloid- β and tau pathology in iPSC-derived neurons from sporadic Alzheimer's disease patients*. *Stem Cell Research*, 2018. **27**: p. 121-130.
363. Fang, E.F., et al., *Mitophagy inhibits amyloid- β and tau pathology and reverses cognitive deficits in models of Alzheimer's disease*. *Nature Neuroscience*, 2019. **22**(3): p. 401-412.
364. Duan, L., et al., *Stem cell derived basal forebrain cholinergic neurons from Alzheimer's disease patients are more susceptible to cell death*. *Molecular Neurodegeneration*, 2014. **9**(1): p. 3.
365. Choi, S.H., et al., *A three-dimensional human neural cell culture model of Alzheimer's disease*. *Nature*, 2014. **515**(7526): p. 274-278.
366. Gonzalez, C., et al., *Modeling amyloid beta and tau pathology in human cerebral organoids*. *Mol Psychiatry*, 2018. **23**(12): p. 2363-2374.
367. Sproul, A.A., et al., *Characterization and molecular profiling of PSEN1 familial Alzheimer's disease iPSC-derived neural progenitors*. *PloS one*, 2014. **9**(1): p. e84547-e84547.
368. Hossini, A.M., et al., *Induced pluripotent stem cell-derived neuronal cells from a sporadic Alzheimer's disease donor as a model for investigating AD-associated gene regulatory networks*. *BMC Genomics*, 2015. **16**(1): p. 84.
369. Meyer, K., et al., *REST and Neural Gene Network Dysregulation in iPSC Models of Alzheimer's Disease*. *Cell Rep*, 2019. **26**(5): p. 1112-1127.e9.
370. Kondo, T., et al., *Modeling Alzheimer's disease with iPSCs reveals stress phenotypes associated with intracellular A β and differential drug responsiveness*. *Cell Stem Cell*, 2013. **12**(4): p. 487-96.
371. Muratore, C.R., et al., *Cell-type Dependent Alzheimer's Disease Phenotypes: Probing the Biology of Selective Neuronal Vulnerability*. *Stem Cell Reports*, 2017. **9**(6): p. 1868-1884.

372. Ortiz-Virumbrales, M., et al., *CRISPR/Cas9-Correctable mutation-related molecular and physiological phenotypes in iPSC-derived Alzheimer's PSEN2N141Neurons*. Acta Neuropathologica Communications, 2017. **5**(1): p. 77.
373. Li, L., et al., *iPSC Modeling of Presenilin1 Mutation in Alzheimer's Disease with Cerebellar Ataxia*. Experimental neurobiology, 2018. **27**(5): p. 350-364.
374. Ochalek, A., et al., *Neurons derived from sporadic Alzheimer's disease iPSCs reveal elevated TAU hyperphosphorylation, increased amyloid levels, and GSK3B activation*. Alzheimer's research & therapy, 2017. **9**(1): p. 90-90.
375. Ovchinnikov, D.A., et al., *The Impact of APP on Alzheimer-like Pathogenesis and Gene Expression in Down Syndrome iPSC-Derived Neurons*. Stem Cell Reports, 2018. **11**(1): p. 32-42.
376. Woodruff, G., et al., *The presenilin-1 ΔE9 mutation results in reduced γ-secretase activity, but not total loss of PS1 function, in isogenic human stem cells*. Cell reports, 2013. **5**(4): p. 974-985.
377. Muratore, C.R., et al., *The familial Alzheimer's disease APPV717I mutation alters APP processing and Tau expression in iPSC-derived neurons*. Hum Mol Genet, 2014. **23**(13): p. 3523-36.
378. Yagi, T., et al., *Modeling familial Alzheimer's disease with induced pluripotent stem cells*. Hum Mol Genet, 2011. **20**(23): p. 4530-9.
379. Wu, J.W., et al., *Neuronal activity enhances tau propagation and tau pathology in vivo*. Nature neuroscience, 2016. **19**(8): p. 1085-1092.
380. Moreno, C.L., et al., *iPSC-derived familial Alzheimer's PSEN2 N141I cholinergic neurons exhibit mutation-dependent molecular pathology corrected by insulin signaling*. Molecular Neurodegeneration, 2018. **13**(1): p. 33.
381. Sun, L., et al., *Analysis of 138 pathogenic mutations in presenilin-1 on the in vitro production of Aβ42 and Aβ40 peptides by γ-secretase*. Proc Natl Acad Sci U S A, 2017. **114**(4): p. E476-e485.
382. Xia, D., et al., *Presenilin-1 knockin mice reveal loss-of-function mechanism for familial Alzheimer's disease*. Neuron, 2015. **85**(5): p. 967-81.
383. Foveau, B., et al., *Stem Cell-Derived Neurons as Cellular Models of Sporadic Alzheimer's Disease*. Journal of Alzheimer's Disease, 2019. **67**: p. 893-910.
384. Oka, S., et al., *Human mitochondrial transcriptional factor A breaks the mitochondria-mediated vicious cycle in Alzheimer's disease*. Scientific Reports, 2016. **6**(1): p. 37889.
385. Hou, Y., et al., *Permeability transition pore-mediated mitochondrial superoxide flashes mediate an early inhibitory effect of amyloid beta1-42 on neural progenitor cell proliferation*. Neurobiol Aging, 2014. **35**(5): p. 975-89.
386. Lee, J.K., et al., *Acid sphingomyelinase modulates the autophagic process by controlling lysosomal biogenesis in Alzheimer's disease*. J Exp Med, 2014. **211**(8): p. 1551-70.
387. Mairet-Coello, G., et al., *The CAMKK2-AMPK kinase pathway mediates the synaptotoxic effects of Aβ oligomers through Tau phosphorylation*. Neuron, 2013. **78**(1): p. 94-108.
388. Krencik, R., et al., *Specification of transplantable astroglial subtypes from human pluripotent stem cells*. Nature biotechnology, 2011. **29**(6): p. 528-534.
389. Oksanen, M., et al., *PSEN1 Mutant iPSC-Derived Model Reveals Severe Astrocyte Pathology in Alzheimer's Disease*. Stem Cell Reports, 2017. **9**(6): p. 1885-1897.
390. Shaltouki, A., et al., *Efficient generation of astrocytes from human pluripotent stem cells in defined conditions*. Stem Cells, 2013. **31**(5): p. 941-52.
391. Sullivan, S.E., et al., *Candidate-based screening via gene modulation in human neurons and astrocytes implicates FERMT2 in Aβ and TAU proteostasis*. Human molecular genetics, 2019. **28**(5): p. 718-735.
392. Zhao, J., et al., *APOE ε4/ε4 diminishes neurotrophic function of human iPSC-derived astrocytes*. Human molecular genetics, 2017. **26**(14): p. 2690-2700.

393. Mertens, J., et al., *Directly Reprogrammed Human Neurons Retain Aging-Associated Transcriptomic Signatures and Reveal Age-Related Nucleocytoplasmic Defects*. Cell stem cell, 2015. **17**(6): p. 705-718.
394. Mertens, J., et al., *Directly Reprogrammed Human Neurons Retain Aging-Associated Transcriptomic Signatures and Reveal Age-Related Nucleocytoplasmic Defects*. Cell Stem Cell, 2015. **17**(6): p. 705-718.
395. Allen, S.P., et al., *Astrocyte adenosine deaminase loss increases motor neuron toxicity in amyotrophic lateral sclerosis*. Brain, 2019. **142**(3): p. 586-605.
396. Allen, S.P., et al., *C9orf72 expansion within astrocytes reduces metabolic flexibility in amyotrophic lateral sclerosis*. Brain, 2019. **142**(12): p. 3771-3790.
397. Ferraiuolo, L., et al., *Oligodendrocytes contribute to motor neuron death in ALS via SOD1-dependent mechanism*. Proceedings of the National Academy of Sciences of the United States of America, 2016. **113**(42): p. E6496-E6505.
398. Glajch, K.E., et al., *MicroNeurotrophins Improve Survival in Motor Neuron-Astrocyte Co-Cultures but Do Not Improve Disease Phenotypes in a Mutant SOD1 Mouse Model of Amyotrophic Lateral Sclerosis*. 2016. **11**(10): p. e0164103.
399. Hautbergue, G.M., et al., *SRSF1-dependent nuclear export inhibition of C9ORF72 repeat transcripts prevents neurodegeneration and associated motor deficits*. 2017. **8**: p. 16063.
400. Varciana, A., et al., *Micro-RNAs secreted through astrocyte-derived extracellular vesicles cause neuronal network degeneration in C9orf72 ALS*. EBioMedicine, 2019. **40**: p. 626-635.
401. Schwartzenruber, A., et al., *Oxidative switch drives mitophagy defects in dopaminergic parkin mutant patient neurons*. bioRxiv, 2020: p. 2020.05.29.115782.
402. Song, S., et al., *Major histocompatibility complex class I molecules protect motor neurons from astrocyte-induced toxicity in amyotrophic lateral sclerosis*. Nat Med, 2016. **22**(4): p. 397-403.
403. McKhann, G.M., et al., *The diagnosis of dementia due to Alzheimer's disease: recommendations from the National Institute on Aging-Alzheimer's Association workgroups on diagnostic guidelines for Alzheimer's disease*. Alzheimer's & dementia : the journal of the Alzheimer's Association, 2011. **7**(3): p. 263-269.
404. Iannetti, E.F., et al., *Multiplexed high-content analysis of mitochondrial morphofunction using live-cell microscopy*. Nature Protocols, 2016. **11**: p. 1693.
405. Duchen, M.R., *Mitochondria in health and disease: perspectives on a new mitochondrial biology*. Molecular Aspects of Medicine, 2004. **25**(4): p. 365-451.
406. Nicholls, D.G. and M.W. Ward, *Mitochondrial membrane potential and neuronal glutamate excitotoxicity: mortality and millivolts*. Trends Neurosci, 2000. **23**(4): p. 166-74.
407. Diot, A., et al., *A novel quantitative assay of mitophagy: Combining high content fluorescence microscopy and mitochondrial DNA load to quantify mitophagy and identify novel pharmacological tools against pathogenic heteroplasmic mtDNA*. Pharmacol Res, 2015. **100**: p. 24-35.
408. Mortiboys, H., et al., *UDCA exerts beneficial effect on mitochondrial dysfunction in LRRK2(G2019S) carriers and in vivo*. Neurology, 2015. **85**(10): p. 846-52.
409. Manfredi, G., et al., *Measurements of ATP in mammalian cells*. Methods, 2002. **26**(4): p. 317-26.
410. Buckner, R.L., J.R. Andrews-Hanna, and D.L. Schacter, *The brain's default network: anatomy, function, and relevance to disease*. Ann N Y Acad Sci, 2008. **1124**: p. 1-38.
411. Greicius, M.D., et al., *Default-mode network activity distinguishes Alzheimer's disease from healthy aging: evidence from functional MRI*. Proc Natl Acad Sci U S A, 2004. **101**(13): p. 4637-42.
412. Weintraub, S., A.H. Wicklund, and D.P. Salmon, *The Neuropsychological Profile of Alzheimer Disease*. Cold Spring Harbor Perspectives in Medicine, 2012. **2**(4): p. a006171.

413. Clark, L.J., et al., *Longitudinal verbal fluency in normal aging, preclinical, and prevalent Alzheimer's disease*. Am J Alzheimers Dis Other Demen, 2009. **24**(6): p. 461-8.
414. Wang, X., et al., *The role of abnormal mitochondrial dynamics in the pathogenesis of Alzheimer's disease*. J Neurochem, 2009. **109 Suppl 1**(Suppl 1): p. 153-9.
415. Palmer, C.S., et al., *Adaptor proteins MiD49 and MiD51 can act independently of Mff and Fis1 in Drp1 recruitment and are specific for mitochondrial fission*. J Biol Chem, 2013. **288**(38): p. 27584-93.
416. Misgeld, T. and T.L. Schwarz, *Mitostasis in Neurons: Maintaining Mitochondria in an Extended Cellular Architecture*. Neuron, 2017. **96**(3): p. 651-666.
417. Mishra, P. and D.C. Chan, *Metabolic regulation of mitochondrial dynamics*. The Journal of cell biology, 2016. **212**(4): p. 379-387.
418. Wang, X., et al., *Dynamin-like protein 1 reduction underlies mitochondrial morphology and distribution abnormalities in fibroblasts from sporadic Alzheimer's disease patients*. The American journal of pathology, 2008. **173**(2): p. 470-482.
419. Wang, X., et al., *Impaired balance of mitochondrial fission and fusion in Alzheimer's disease*. The Journal of neuroscience : the official journal of the Society for Neuroscience, 2009. **29**(28): p. 9090-9103.
420. Cho, D.H., et al., *S-nitrosylation of Drp1 mediates beta-amyloid-related mitochondrial fission and neuronal injury*. Science, 2009. **324**(5923): p. 102-5.
421. Strittmatter, W.J., et al., *Apolipoprotein E: high-avidity binding to beta-amyloid and increased frequency of type 4 allele in late-onset familial Alzheimer disease*. Proc Natl Acad Sci U S A, 1993. **90**(5): p. 1977-81.
422. Yamazaki, Y., et al., *Apolipoprotein E and Alzheimer disease: pathobiology and targeting strategies*. Nature reviews. Neurology, 2019. **15**(9): p. 501-518.
423. Lin, Y.T., et al., *APOE4 Causes Widespread Molecular and Cellular Alterations Associated with Alzheimer's Disease Phenotypes in Human iPSC-Derived Brain Cell Types*. Neuron, 2018. **98**(6): p. 1141-1154.e7.
424. Deane, R., et al., *apoE isoform-specific disruption of amyloid beta peptide clearance from mouse brain*. J Clin Invest, 2008. **118**(12): p. 4002-13.
425. Wu, L., X. Zhang, and L. Zhao, *Human ApoE Isoforms Differentially Modulate Brain Glucose and Ketone Body Metabolism: Implications for Alzheimer's Disease Risk Reduction and Early Intervention*. J Neurosci, 2018. **38**(30): p. 6665-6681.
426. Simonovitch, S., et al., *The Effects of APOE4 on Mitochondrial Dynamics and Proteins in vivo*. J Alzheimers Dis, 2019. **70**(3): p. 861-875.
427. Picard, M., et al., *Mitochondrial morphology transitions and functions: implications for retrograde signaling?* American Journal of Physiology-Regulatory, Integrative and Comparative Physiology, 2013. **304**(6): p. R393-R406.
428. Nielsen, H.M., et al., *Peripheral apoE isoform levels in cognitively normal APOE ε3/ε4 individuals are associated with regional gray matter volume and cerebral glucose metabolism*. Alzheimers Res Ther, 2017. **9**(1): p. 5.
429. Tambini, M.D., et al., *ApoE4 upregulates the activity of mitochondria-associated ER membranes*. EMBO Rep, 2016. **17**(1): p. 27-36.
430. Schellenberg, G.D., et al., *Genetic linkage evidence for a familial Alzheimer's disease locus on chromosome 14*. Science, 1992. **258**(5082): p. 668-71.
431. St George-Hyslop, P., et al., *Genetic evidence for a novel familial Alzheimer's disease locus on chromosome 14*. Nat Genet, 1992. **2**(4): p. 330-4.
432. Flynn, J.M., et al., *Impaired spare respiratory capacity in cortical synaptosomes from Sod2 null mice*. Free Radic Biol Med, 2011. **50**(7): p. 866-73.
433. Pflieger, J., M. He, and M. Abdellatif, *Mitochondrial complex II is a source of the reserve respiratory capacity that is regulated by metabolic sensors and promotes cell survival*. Cell Death & Disease, 2015. **6**(7): p. e1835-e1835.

434. Quinn, C.M., et al., *Induction of fibroblast apolipoprotein E expression during apoptosis, starvation-induced growth arrest and mitosis*. The Biochemical journal, 2004. **378**(Pt 3): p. 753-761.
435. Atlas, T.H.P. <https://www.proteinatlas.org/ENSG00000130203-APOE/tissue/skin>. [Webpage] 2020 [cited 2020 09.12.20]; Available from: <https://www.proteinatlas.org/ENSG00000130203-APOE/tissue/skin>.
436. Scheltens, P.H., *Structural neuroimaging of Alzheimer's disease and other dementias*. Aging (Milano), 2001. **13**(3): p. 203-9.
437. Scahill, R.I., et al., *Mapping the evolution of regional atrophy in Alzheimer's disease: unbiased analysis of fluid-registered serial MRI*. Proc Natl Acad Sci U S A, 2002. **99**(7): p. 4703-7.
438. Scheltens, P., et al., *Atrophy of medial temporal lobes on MRI in "probable" Alzheimer's disease and normal ageing: diagnostic value and neuropsychological correlates*. J Neurol Neurosurg Psychiatry, 1992. **55**(10): p. 967-72.
439. Chan, D., et al., *Change in rates of cerebral atrophy over time in early-onset Alzheimer's disease: longitudinal MRI study*. Lancet, 2003. **362**(9390): p. 1121-2.
440. Mosconi, L., *Glucose metabolism in normal aging and Alzheimer's disease: Methodological and physiological considerations for PET studies*. Clinical and translational imaging, 2013. **1**(4): p. 10.1007/s40336-013-0026-y.
441. Suter, O.-C., et al., *Cerebral Hypoperfusion Generates Cortical Watershed Microinfarcts in Alzheimer Disease*. Stroke, 2002. **33**(8): p. 1986-1992.
442. Bannai, T., et al., *Chronic cerebral hypoperfusion shifts the equilibrium of amyloid β oligomers to aggregation-prone species with higher molecular weight*. Scientific Reports, 2019. **9**(1): p. 2827.
443. Squire, L.R. and S.M. Zola, *Episodic memory, semantic memory, and amnesia*. Hippocampus, 1998. **8**(3): p. 205-11.
444. Venneri, A., M. Mitolo, and M. De Marco, *Paradigm shift: semantic memory decline as a biomarker of preclinical Alzheimer's disease*. Biomarkers in Medicine, 2015. **10**(1): p. 5-8.
445. Welsh, K., et al., *Detection of abnormal memory decline in mild cases of Alzheimer's disease using CERAD neuropsychological measures*. Arch Neurol, 1991. **48**(3): p. 278-81.
446. Nebes, R.D., *Semantic memory in Alzheimer's disease*. Psychol Bull, 1989. **106**(3): p. 377-94.
447. Henry, J.D., J.R. Crawford, and L.H. Phillips, *Verbal fluency performance in dementia of the Alzheimer's type: a meta-analysis*. Neuropsychologia, 2004. **42**(9): p. 1212-22.
448. Hodges, J.R. and K. Patterson, *Is semantic memory consistently impaired early in the course of Alzheimer's disease? Neuroanatomical and diagnostic implications*. Neuropsychologia, 1995. **33**(4): p. 441-59.
449. Seeley, W.W., *The Salience Network: A Neural System for Perceiving and Responding to Homeostatic Demands*. The Journal of Neuroscience, 2019. **39**(50): p. 9878.
450. Yang, Y.-L., et al., *Brain functional network connectivity based on a visual task: visual information processing-related brain regions are significantly activated in the task state*. Neural regeneration research, 2015. **10**(2): p. 298-307.
451. Badhwar, A., et al., *Resting-state network dysfunction in Alzheimer's disease: A systematic review and meta-analysis*. Alzheimer's & Dementia: Diagnosis, Assessment & Disease Monitoring, 2017. **8**: p. 73-85.
452. Buckner, R.L., et al., *Molecular, structural, and functional characterization of Alzheimer's disease: evidence for a relationship between default activity, amyloid, and memory*. J Neurosci, 2005. **25**(34): p. 7709-17.
453. Greicius, M.D., et al., *Default-mode network activity distinguishes Alzheimer's disease from healthy aging: evidence from functional MRI*. Proceedings of the National Academy of Sciences of the United States of America, 2004. **101**(13): p. 4637-4642.

454. Greicius, M.D. and V. Menon, *Default-mode activity during a passive sensory task: uncoupled from deactivation but impacting activation*. J Cogn Neurosci, 2004. **16**(9): p. 1484-92.
455. Raichle, M.E., *The Brain's Default Mode Network*. Annual Review of Neuroscience, 2015. **38**(1): p. 433-447.
456. Damoiseaux, J.S., et al., *Consistent resting-state networks across healthy subjects*. Proceedings of the National Academy of Sciences, 2006. **103**(37): p. 13848-13853.
457. Gardini, S., et al., *Increased functional connectivity in the default mode network in mild cognitive impairment: a maladaptive compensatory mechanism associated with poor semantic memory performance*. J Alzheimers Dis, 2015. **45**(2): p. 457-70.
458. Pasquini, L., et al., *Individual Correspondence of Amyloid- β and Intrinsic Connectivity in the Posterior Default Mode Network Across Stages of Alzheimer's Disease*. J Alzheimers Dis, 2017. **58**(3): p. 763-773.
459. Sperling, R.A., et al., *Amyloid deposition is associated with impaired default network function in older persons without dementia*. Neuron, 2009. **63**(2): p. 178-88.
460. Hoenig, M.C., et al., *Networks of tau distribution in Alzheimer's disease*. Brain, 2018. **141**(2): p. 568-581.
461. Gusnard, D.A., M.E. Raichle, and M.E. Raichle, *Searching for a baseline: functional imaging and the resting human brain*. Nat Rev Neurosci, 2001. **2**(10): p. 685-94.
462. Minoshima, S., et al., *Metabolic reduction in the posterior cingulate cortex in very early Alzheimer's disease*. Ann Neurol, 1997. **42**(1): p. 85-94.
463. Raichle, M.E., et al., *A default mode of brain function*. Proc Natl Acad Sci U S A, 2001. **98**(2): p. 676-82.
464. Calhoun, V.D., et al., *A method for making group inferences from functional MRI data using independent component analysis*. Hum Brain Mapp, 2001. **14**(3): p. 140-51.
465. Tzourio-Mazoyer, N., et al., *Automated Anatomical Labeling of Activations in SPM Using a Macroscopic Anatomical Parcellation of the MNI MRI Single-Subject Brain*. NeuroImage, 2002. **15**(1): p. 273-289.
466. Keeney, J.T., S. Ibrahim, and L. Zhao, *Human ApoE Isoforms Differentially Modulate Glucose and Amyloid Metabolic Pathways in Female Brain: Evidence of the Mechanism of Neuroprotection by ApoE2 and Implications for Alzheimer's Disease Prevention and Early Intervention*. J Alzheimers Dis, 2015. **48**(2): p. 411-24.
467. Lu, H., et al., *Aberrant interhemispheric functional connectivity within default mode network and its relationships with neurocognitive features in cognitively normal APOE ϵ 4 elderly carriers*. Int Psychogeriatr, 2017. **29**(5): p. 805-814.
468. De Marco, M., et al., *Cognitive Efficiency in Alzheimer's Disease is Associated with Increased Occipital Connectivity*. J Alzheimers Dis, 2017. **57**(2): p. 541-556.
469. Bigl, M., et al., *Altered phosphofructokinase mRNA levels but unchanged isoenzyme pattern in brains from patients with Alzheimer's disease*. Brain Res Mol Brain Res, 2000. **76**(2): p. 411-4.
470. Bigl, M., et al., *Activities of key glycolytic enzymes in the brains of patients with Alzheimer's disease*. J Neural Transm (Vienna), 1999. **106**(5-6): p. 499-511.
471. Oberheim, N.A., et al., *Uniquely hominid features of adult human astrocytes*. The Journal of neuroscience : the official journal of the Society for Neuroscience, 2009. **29**(10): p. 3276-3287.
472. Godin, L.M., et al., *Decreased Laminin Expression by Human Lung Epithelial Cells and Fibroblasts Cultured in Acellular Lung Scaffolds from Aged Mice*. PLoS One, 2016. **11**(3): p. e0150966.
473. Martínez, P., et al., *Essential role for the TRF2 telomere protein in adult skin homeostasis*. Aging Cell, 2014. **13**(4): p. 656-68.
474. Webster, C.P., et al., *The C9orf72 protein interacts with Rab1a and the ULK1 complex to regulate initiation of autophagy*. The EMBO journal, 2016. **35**(15): p. 1656-1676.

475. Adams, C.P. and V.V. Brantner, *Estimating the cost of new drug development: is it really 802 million dollars?* Health Aff (Millwood), 2006. **25**(2): p. 420-8.
476. Xue, H., et al., *Review of Drug Repositioning Approaches and Resources*. International journal of biological sciences, 2018. **14**(10): p. 1232-1244.
477. Bell, S.M., et al., *Ursodeoxycholic Acid Improves Mitochondrial Function and Redistributes Drp1 in Fibroblasts from Patients with Either Sporadic or Familial Alzheimer's Disease*. J Mol Biol, 2018. **430**(21): p. 3942-3953.
478. Bell, S.M., et al., *Deficits in Mitochondrial Spare Respiratory Capacity Contribute to the Neuropsychological Changes of Alzheimer's Disease*. 2020. **10**(2).
479. Martín-Maestro, P., et al., *Slower Dynamics and Aged Mitochondria in Sporadic Alzheimer's Disease*. 2017. **2017**: p. 9302761.
480. Vlassenko, A.G. and M.E. Raichle, *Brain aerobic glycolysis functions and Alzheimer's disease*. Clinical and translational imaging, 2015. **3**(1): p. 27-37.
481. Cunnane, S., et al., *Brain fuel metabolism, aging, and Alzheimer's disease*. Nutrition (Burbank, Los Angeles County, Calif.), 2011. **27**(1): p. 3-20.
482. An, Y., et al., *Evidence for brain glucose dysregulation in Alzheimer's disease*. Alzheimers Dement, 2018. **14**(3): p. 318-329.
483. Vlassenko, A.G., et al., *Aerobic glycolysis and tau deposition in preclinical Alzheimer's disease*. Neurobiology of Aging, 2018. **67**: p. 95-98.
484. Kuijlaars, J., et al., *Sustained synchronized neuronal network activity in a human astrocyte co-culture system*. Scientific Reports, 2016. **6**(1): p. 36529.
485. Bosworth, A.P. and N.J. Allen, *The diverse actions of astrocytes during synaptic development*. Curr Opin Neurobiol, 2017. **47**: p. 38-43.
486. Weber, B. and L.F. Barros, *The Astrocyte: Powerhouse and Recycling Center*. Cold Spring Harb Perspect Biol, 2015. **7**(12).
487. Garwood, C.J., et al., *Insulin and IGF1 signalling pathways in human astrocytes in vitro and in vivo; characterisation, subcellular localisation and modulation of the receptors*. Molecular Brain, 2015. **8**(1): p. 51.
488. Jones, V.C., et al., *Aberrant iPSC-derived human astrocytes in Alzheimer's disease*. Cell Death Dis, 2017. **8**(3): p. e2696.
489. Oksanen, M., et al., *PSEN1 Mutant iPSC-Derived Model Reveals Severe Astrocyte Pathology in Alzheimer's Disease*. Stem Cell Reports, 2017. **9**(6): p. 1885-1897.
490. Fu, W., et al., *Bioenergetic mechanisms in astrocytes may contribute to amyloid plaque deposition and toxicity*. J Biol Chem, 2015. **290**(20): p. 12504-13.
491. Malik, N. and M.S. Rao, *A review of the methods for human iPSC derivation*. Methods in molecular biology (Clifton, N.J.), 2013. **997**: p. 23-33.
492. Nakagawa, M., et al., *Generation of induced pluripotent stem cells without Myc from mouse and human fibroblasts*. Nat Biotechnol, 2008. **26**(1): p. 101-6.
493. Takahashi, K., et al., *Induction of pluripotent stem cells from adult human fibroblasts by defined factors*. Cell, 2007. **131**(5): p. 861-72.
494. Baxter, M., et al., *Phenotypic and functional analyses show stem cell-derived hepatocyte-like cells better mimic fetal rather than adult hepatocytes*. Journal of hepatology, 2015. **62**(3): p. 581-589.
495. Mertens, J., et al., *Aging in a Dish: iPSC-Derived and Directly Induced Neurons for Studying Brain Aging and Age-Related Neurodegenerative Diseases*. Annual review of genetics, 2018. **52**: p. 271-293.
496. Gatto, N., et al., *Directly converted astrocytes retain the ageing features of the donor fibroblasts and elucidate the astrocytic contribution to human CNS health and disease*. Aging Cell, UNDER REVIEW.
497. Hassel, B., et al., *Glutamate uptake is reduced in prefrontal cortex in Huntington's disease*. Neurochem Res, 2008. **33**(2): p. 232-7.

498. Hedegaard, A., et al., *Pro-maturational Effects of Human iPSC-Derived Cortical Astrocytes upon iPSC-Derived Cortical Neurons*. Stem Cell Reports, 2020. **15**(1): p. 38-51.
499. Ferraiuolo, L., et al., *Dysregulation of astrocyte-motoneuron cross-talk in mutant superoxide dismutase 1-related amyotrophic lateral sclerosis*. Brain : a journal of neurology, 2011. **134**(Pt 9): p. 2627-2641.
500. Bell, S.M., et al., *Deficits in Mitochondrial Spare Respiratory Capacity Contribute to the Neuropsychological Changes of Alzheimer's Disease*. J Pers Med, 2020. **10**(2).
501. Nunomura, A., et al., *The earliest stage of cognitive impairment in transition from normal aging to Alzheimer disease is marked by prominent RNA oxidation in vulnerable neurons*. J Neuropathol Exp Neurol, 2012. **71**(3): p. 233-41.
502. Nunomura, A., et al., *RNA oxidation is a prominent feature of vulnerable neurons in Alzheimer's disease*. J Neurosci, 1999. **19**(6): p. 1959-64.
503. Konttinen, H., et al., *PPAR β / δ -agonist GW0742 ameliorates dysfunction in fatty acid oxidation in PSEN1 Δ E9 astrocytes*. Glia, 2019. **67**(1): p. 146-159.
504. Zhang, C., R.A. Rissman, and J. Feng, *Characterization of ATP alternations in an Alzheimer's disease transgenic mouse model*. Journal of Alzheimer's disease : JAD, 2015. **44**(2): p. 375-378.
505. Hansson, H.-A., *A histochemical study of retinal changes induced by treatment with colchicine*. Experimental Eye Research, 1971. **12**(2): p. 198-205.
506. Lu, J., et al., *Effect of cholinergic signaling on neuronal cell bioenergetics*. Journal of Alzheimer's disease : JAD, 2013. **33**(4): p. 1135-1146.
507. Rees, J.M., W.C. Ford, and M.G. Hull, *Effect of caffeine and of pentoxifylline on the motility and metabolism of human spermatozoa*. J Reprod Fertil, 1990. **90**(1): p. 147-56.
508. Ye, J.-H., et al., *Pentoxifylline ameliorates non-alcoholic fatty liver disease in hyperglycaemic and dyslipidaemic mice by upregulating fatty acid β -oxidation*. Scientific Reports, 2016. **6**(1): p. 33102.
509. Conejero-Goldberg, C., et al., *APOE2 enhances neuroprotection against Alzheimer's disease through multiple molecular mechanisms*. Molecular Psychiatry, 2014. **19**(11): p. 1243-1250.
510. Reiman, E.M., et al., *Exceptionally low likelihood of Alzheimer's dementia in APOE2 homozygotes from a 5,000-person neuropathological study*. Nature Communications, 2020. **11**(1): p. 667.
511. Palmqvist, S., et al., *Earliest accumulation of β -amyloid occurs within the default-mode network and concurrently affects brain connectivity*. Nature communications, 2017. **8**(1): p. 1214-1214.
512. Hodgetts, C.J., et al., *Increased posterior default mode network activity and structural connectivity in young adult APOE- ϵ 4 carriers: a multimodal imaging investigation*. Neurobiology of Aging, 2019. **73**: p. 82-91.
513. Hipkiss, A.R., *Aging, Alzheimer's Disease and Dysfunctional Glycolysis; Similar Effects of Too Much and Too Little*. Aging and disease, 2019. **10**(6): p. 1328-1331.
514. Sun, N., R.J. Youle, and T. Finkel, *The Mitochondrial Basis of Aging*. Molecular cell, 2016. **61**(5): p. 654-666.
515. Lim, S.L., C.J. Rodriguez-Ortiz, and M. Kitazawa, *Infection, systemic inflammation, and Alzheimer's disease*. Microbes and Infection, 2015. **17**(8): p. 549-556.
516. Driver, J.A., et al., *Inverse association between cancer and Alzheimer's disease: results from the Framingham Heart Study*. BMJ, 2012. **344**: p. e1442.
517. van der Windt, G.J.W., et al., *Mitochondrial respiratory capacity is a critical regulator of CD8+ T cell memory development*. Immunity, 2012. **36**(1): p. 68-78.
518. Ganapathy-Kanniappan, S. and J.-F.H. Geschwind, *Tumor glycolysis as a target for cancer therapy: progress and prospects*. Molecular Cancer, 2013. **12**(1): p. 152.
519. Barbuti, P.A., et al., *iPSC-derived midbrain astrocytes from Parkinson's disease patients carrying pathogenic <math>SNCA</math> mutations exhibit alpha-synuclein*

- aggregation, mitochondrial fragmentation and excess calcium release. *bioRxiv*, 2020: p. 2020.04.27.053470.
520. Du, F., et al., *Astrocytes Attenuate Mitochondrial Dysfunctions in Human Dopaminergic Neurons Derived from iPSC*. *Stem cell reports*, 2018. **10**(2): p. 366-374.
521. Baloyannis, S.J., *Mitochondrial alterations in Alzheimer's disease*. *J Alzheimers Dis*, 2006. **9**(2): p. 119-26.
522. Abramov, A.Y., L. Canevari, and M.R. Duchen, *Beta-amyloid peptides induce mitochondrial dysfunction and oxidative stress in astrocytes and death of neurons through activation of NADPH oxidase*. *J Neurosci*, 2004. **24**(2): p. 565-75.
523. Jackson, J.G. and M.B. Robinson, *Regulation of mitochondrial dynamics in astrocytes: Mechanisms, consequences, and unknowns*. *Glia*, 2018. **66**(6): p. 1213-1234.
524. Birdsill, A.C., et al., *Low cerebral blood flow is associated with lower memory function in metabolic syndrome*. *Obesity (Silver Spring, Md.)*, 2013. **21**(7): p. 1313-1320.
525. Pihlaja, R., et al., *Transplanted astrocytes internalize deposited beta-amyloid peptides in a transgenic mouse model of Alzheimer's disease*. *Glia*, 2008. **56**(2): p. 154-63.
526. Allaman, I., et al., *Amyloid-beta aggregates cause alterations of astrocytic metabolic phenotype: impact on neuronal viability*. *J Neurosci*, 2010. **30**(9): p. 3326-38.
527. Fu, W., et al., *Bioenergetic mechanisms in astrocytes may contribute to amyloid plaque deposition and toxicity*. *The Journal of biological chemistry*, 2015. **290**(20): p. 12504-12513.
528. Andersen, J.V., et al., *Alterations in Cerebral Cortical Glucose and Glutamine Metabolism Precedes Amyloid Plaques in the APP^{swe}/PSEN1^{dE9} Mouse Model of Alzheimer's Disease*. 2017. **42**(6): p. 1589-1598.
529. Mayeux, R., *Biomarkers: potential uses and limitations*. *NeuroRx : the journal of the American Society for Experimental NeuroTherapeutics*, 2004. **1**(2): p. 182-188.
530. Jones, N., et al., *Bioenergetic analysis of human peripheral blood mononuclear cells*. *Clinical and experimental immunology*, 2015. **182**(1): p. 69-80.
531. TeSlaa, T. and M.A. Teitell, *Techniques to monitor glycolysis*. *Methods in enzymology*, 2014. **542**: p. 91-114.
532. Humpel, C., *Identifying and validating biomarkers for Alzheimer's disease*. *Trends in biotechnology*, 2011. **29**(1): p. 26-32.
533. Bookheimer, S. and A. Burggren, *APOE-4 genotype and neurophysiological vulnerability to Alzheimer's and cognitive aging*. *Annual review of clinical psychology*, 2009. **5**: p. 343-362.
534. Hampel, H., et al., *Value of CSF beta-amyloid1-42 and tau as predictors of Alzheimer's disease in patients with mild cognitive impairment*. *Mol Psychiatry*, 2004. **9**(7): p. 705-10.
535. Bos, I., et al., *Amyloid- β , Tau, and Cognition in Cognitively Normal Older Individuals: Examining the Necessity to Adjust for Biomarker Status in Normative Data*. *Frontiers in aging neuroscience*, 2018. **10**: p. 193-193.
536. Chapman, C.D., et al., *Intranasal insulin in Alzheimer's disease: Food for thought*. *Neuropharmacology*, 2018. **136**: p. 196-201.
537. Koenig, A.M., et al., *Effects of the Insulin Sensitizer Metformin in Alzheimer Disease: Pilot Data From a Randomized Placebo-controlled Crossover Study*. *Alzheimer disease and associated disorders*, 2017. **31**(2): p. 107-113.
538. Luchsinger, J.A., et al., *Metformin in Amnestic Mild Cognitive Impairment: Results of a Pilot Randomized Placebo Controlled Clinical Trial*. *Journal of Alzheimer's disease : JAD*, 2016. **51**(2): p. 501-514.
539. Westhaus, A., E.M. Blumrich, and R. Dringen, *The Antidiabetic Drug Metformin Stimulates Glycolytic Lactate Production in Cultured Primary Rat Astrocytes*. *Neurochem Res*, 2017. **42**(1): p. 294-305.
540. Zhu, X., et al., *Metformin improves cognition of aged mice by promoting cerebral angiogenesis and neurogenesis*. *bioRxiv*, 2020: p. 2020.03.25.006767.

541. Blázquez, E., et al., *Insulin in the brain: its pathophysiological implications for States related with central insulin resistance, type 2 diabetes and Alzheimer's disease*. *Frontiers in endocrinology*, 2014. **5**: p. 161-161.
542. Morris, J.K. and J.M. Burns, *Insulin: an emerging treatment for Alzheimer's disease dementia?* *Current neurology and neuroscience reports*, 2012. **12**(5): p. 520-527.
543. García-Cáceres, C., et al., *Astrocytic Insulin Signaling Couples Brain Glucose Uptake with Nutrient Availability*. *Cell*, 2016. **166**(4): p. 867-880.